

DISSERTATION

**STRUCTURAL AND FUNCTIONAL STUDIES ON THE CHROMATIN
AND NUCLEOSOME BINDING PROTEINS**

Submitted by

Jayanth Velandy Chodaparambil

Department of Biochemistry and Molecular Biology

In partial fulfillment of the requirements
for the Degree of Doctor of Philosophy
Colorado State University
Fort Collins, Colorado
Summer 2007

UMI Number: 3279500

INFORMATION TO USERS

The quality of this reproduction is dependent upon the quality of the copy submitted. Broken or indistinct print, colored or poor quality illustrations and photographs, print bleed-through, substandard margins, and improper alignment can adversely affect reproduction.

In the unlikely event that the author did not send a complete manuscript and there are missing pages, these will be noted. Also, if unauthorized copyright material had to be removed, a note will indicate the deletion.

UMI[®]

UMI Microform 3279500

Copyright 2007 by ProQuest Information and Learning Company.

All rights reserved. This microform edition is protected against unauthorized copying under Title 17, United States Code.

ProQuest Information and Learning Company
300 North Zeeb Road
P.O. Box 1346
Ann Arbor, MI 48106-1346

COLORADO STATE UNIVERSITY

May 2nd 2007

WE HEREBY RECOMMEND THAT THE DISSERTATION PREPARED UNDER OUR SUPERVISION BY **JAYANTH VELANDY CHODAPARAMBIL** ENTITLED “**STRUCTURAL AND FUNCTIONAL STUDIES ON THE CHROMATIN AND NUCLEOSOME BINDING PROTEINS**” BE ACCEPTED AS FULFILLING IN PART REQUIREMENTS FOR THE **DEGREE OF DOCTOR OF PHILOSOPHY**.

Committee on Graduate Work



(Oren P. Anderson)



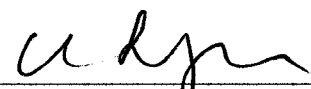
(Jeffrey C. Hansen)



(Paul J. Laybourn)



(Robert W. Woody)



Adviser (Karolin Luger)



Department Head (Marvin R. Paule)

ABSTRACT OF THESIS

“STRUCTURAL AND FUNCTIONAL STUDIES ON THE CHROMATIN AND NUCLEOSOME BINDING PROTEINS”

The approximately two meters of eukaryotic DNA are compacted within the confines of the nucleus by hierarchical packing with an equal amount of histone proteins to form chromatin. The nucleosome is the fundamental repeating structural unit of chromatin. Highly compacted DNA is very accessible to the transcription machinery. To understand the mystery behind the two opposing functions of the chromatin, it is essential for us to study nucleosome and chromatin structure in detail.

Higher order structure of chromatin has been an enigma for decades. Even though the nucleosome core particle has been intensively studied, the molecular mechanisms by which chromatin compaction takes place are poorly understood. One single nucleosome has a total accessible surface area of 28000\AA^2 . A single cell contains thousands of nucleosomes, which translates to abundant surface area (in square meters) for trans-acting proteins to interact with. An intriguing problem arises from the need to arrange these surfaces in a way that leaves them accessible to trans acting proteins while fitting them in the cell's nucleus that is only 10^{-6} m in diameter.

Using biophysical and biochemical techniques, we studied the mode of interaction of the trans acting Kaposi Sarcoma Herpes Virus protein LANA to the nucleosome. We show that a peptide derived from the very N-terminus of the ~ 1000 amino acid long LANA protein cannot bind to individual histones, but only binds to H2A-H2B dimers or fully intact nucleosomes. The dimerization of H2A-H2B histones within the nucleosome

leads to formation of a uniquely charged surface with which LANA interacts. This study thereby provides the first account of a protein directly and specifically interacting with the nucleosomal surface.

We further use the LANA and H4 tail peptides, which are both known to bind to the same surface of the nucleosome as molecular tools to show that the surface itself plays an important role in chromatin compaction. We show that a charged surface on the nucleosome acts as a repulsive domain that is modulated by tails and transacting proteins in chromatin compaction.

In an independent study, we investigate the histone chaperone nucleosome assembly protein 1 of yeast (yNAP1). We report three novel functions of this protein that are distinct from its histone chaperone function. Using biochemical techniques we show that yNAP1 can exchange histone dimers into preformed nucleosomes. During this process, yNAP1 can also slide nucleosomes assembled on longer DNA. We use a combination of analytical ultracentrifugation and atomic force microscopy to show that yNAP1 can facilitate the cleaning up of poorly assembled nucleosomal arrays. Using biochemical and biophysical techniques we show that the C-terminal acidic domain (CTAD) is essential for the ability of yNAP1 to remove histones from DNA and chromatin.

Jayanth V. Chodaparambil
Department of Biochemistry and Molecular Biology
Colorado State University,
Fort Collins, CO, 80523
Summer 2007.

Acknowledgements

From experience I know that the acknowledgement page would be one of the most read pages in a thesis. This page would give a good idea to the reader of how much sanity was still left in the student after his Ph.D. In my case, I still have a lot of sanity left thanks to working in a wonderful lab with some insanely wonderful lab mates and an equally great “boss”.

First off, I would like to thank my mentor Dr. Karolin Luger for her exceptional support and encouragement during my four years in her lab. The major reason I think I have been successful in working with Karolin is that she gave me an incredible amount of scientific freedom to think and design my own experiments. She also gave me a free hand in collaborating with other scientists in the department and also in other universities. This has given me a lot of confidence in building bridges and doing better science. Her work ethic is something I hope I will carry with me to make me a better scientist. She has always been there to discuss science and all other matters. Through the years she has not only been a wonderful mentor but also a great friend (whom I always loved to taunt).

I would like to thank my committee members Dr. Paul Laybourn, Dr. Jeffrey Hansen, Dr. Robert Woody and Dr. Oren Anderson who were always there for me to give me suggestions and criticisms. During committee meetings, they never had a dearth for ideas or experiments I could do. I immensely enjoyed interacting with them throughout my graduate career. I would also like to thank the other members of the faculty especially Dr. Olve Peersen who was very helpful with discussions about crystallography problems

and programs. I would also like to thank Dr. Steven McBryant who has been instrumental in helping me with the analytical ultracentrifuge.

I would also like to thank my collaborator Dr. Kenneth Kaye at Harvard Medical School and his graduate student Dr. Andrew Barbera who I consider the best collaborators I ever worked with.

No words can express my gratitude to my lab mates over the years that have made my life in this lab so wonderful. During my lab rotation I had the opportunity to work with Dr. Srinivas Chakravarthy who introduced me to the world of structural biology which led me to joining the lab in the first place. I am very grateful to have started working on my Ph.D. project with Dr. Young-Jun Park who gave me the much needed head start to my project. His mentorship and the long late-night discussions we used to have immensely helped me with my projects. When it was time for me to solve my first crystal structure, I had Dr. Rajeswari Edayathumangalam to teach me the ropes with data collection and the complex programs used. I would also like to thank my other seniors in the lab Dr. Yunhe Bao, Dr. Xu Lu and Dr. Uma Maheswari who were always there to help me with anything I wanted.

Through the years, I was lucky to have some great juniors like Vidya Subramanian, Mike Resch, Keely (lemon grass) Sudhoff, Chenghua Yang and Nick Clark. I am grateful that they have put up with all my usually “insane” antics. They always made the lab so lively and enjoyable.

I also had the opportunity to teach some wonderful undergrads. Robert Willingham, Tatsuya Sakurai and Karen Colbert were among the best students I have taught. Robert's and Tatsuya's contributions have helped the yNAP1 project immensely.

Special thanks are in order for Ms. Pam Dyer, the Luger lab manager a.k.a. "lab mom" who kept the lab running smoothly. I would also like to thank the other members of the lab: Ms. Kitty Brown, Ms. Beth Kasney, Dr. Mary Robinson, Dr. Andy Andrews and Dr Wayne Lilyestrom, Dr. Mark Van der Woerd and the undergrads Allie Voss, Chris Rothschild, Greg Downing and Allison White who all make the Luger lab such an exciting and enjoyable place to work.

Last but not the least; I would like to thank my family and friends who were always there for me when I needed them.

TABLE OF CONTENTS

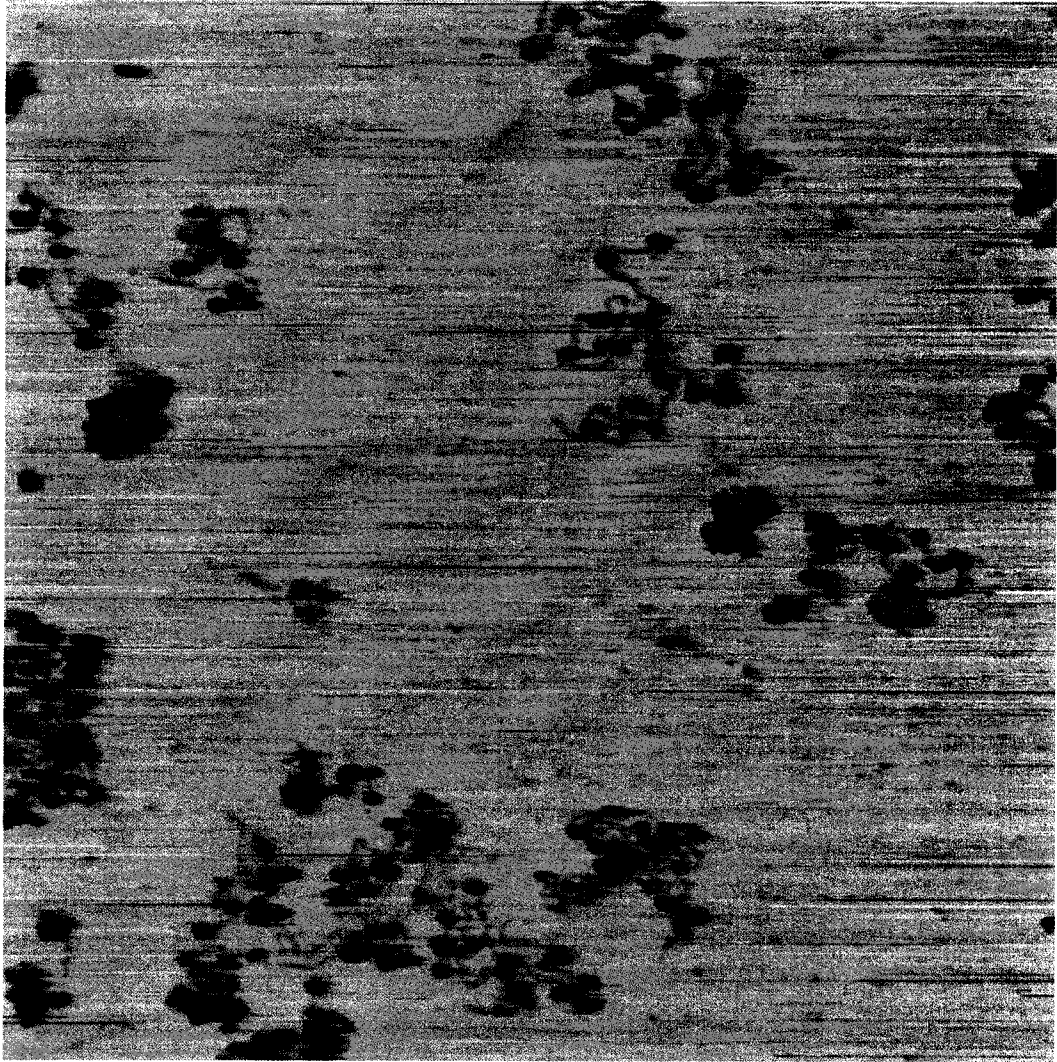
| | |
|--|----------|
| Title Page | i |
| Signature Page | ii |
| Abstract of Dissertation | iii |
| Acknowledgements | v |
| Table of Contents | viii |
| | |
| Chapter I: Review of Literature | 1 |
| | |
| 1.1 The Nucleosome..... | 2 |
| 1.2 Histone Variants..... | 7 |
| 1.3 Modulation of nucleosomal structure through histone tails and tail modification | 9 |
| 1.4 The Nucleosomal Surface | 14 |
| 1.5 Effect of trans acting proteins binding to the nucleosomal surface..... | 20 |
| 1.6 Chromatin structure beyond the nucleosome | 22 |
| 1.7 Histone tails and the 30nm fiber | 25 |
| 1.8 Yeast Nucleosome Assembly Protein 1 (yNAP1)..... | 26 |
| 1.9 Kaposi's Sarcoma Herpes Virus and Latency Associated Nuclear Antigen | 31 |
| 1.10 Specific aims and layout of the thesis | 36 |

| | |
|--|-----------|
| Chapter II: Nucleosomal surface as a docking station for Kaposi's | |
| Sarcoma Herpes Virus LANA. | 38 |
| 2.1 Abstract..... | 39 |
| 2.2 Introduction and Results..... | 40 |
| 2.3 Supporting materials..... | 63 |
| Chapter III: A charged and contoured surface of the nucleosome | |
| opposes tail dependent compaction | 75 |
| 3.1 Abstract..... | 76 |
| 3.2 Introduction and Results..... | 77 |
| 3.3 Materials and Methods | 93 |
| Chapter IV: Nucleosome Assembly Protein 1 exchanges histone | |
| H2A-H2B dimers and assists nucleosomal sliding | 95 |
| 4.1 Abstract..... | 96 |
| 4.2 Introduction | 97 |
| 4.3 Experimental Procedures | 100 |
| 4.4 Results..... | 103 |
| 4.5 Discussion..... | 125 |
| 4.6 Supplementary Figures | 132 |

| | |
|---|------------|
| Chapter V: The C-terminal acidic domain of yNAP1 is essential for | |
| Chromatin scavenging | 135 |
| 5.1 Introduction | 136 |
| 5.2 The CTAD of yNAP1 contributes to the binding affinity of yNAP1 for histones H2A/H2B | 138 |
| 5.3 The ability of yNAP1 to exchange histones into nucleosomes is a function of its affinity | 143 |
| 5.4 The CTAD contributes to the efficiency of chromatin assembly | 145 |
| 5.5 The CTAD is required for removal of non-specifically bound histones from DNA | 145 |
| 5.6 Discussion | 152 |
| 5.7 Materials and methods | 155 |
| | |
| Chapter VI: Contributions to Other Publications..... | 159 |
| | |
| Chapter VII: Future Considerations | 163 |
| | |
| Chapter VII: References | 169 |

CHAPTER I

Review of Literature



(Nucleosomal arrays visualized using an atomic force Microscope)

The fundamental blueprint for cell function in eukaryotes is encoded in double stranded DNA, which is around 2 meters long when stretched linearly. It is an ultimate engineering marvel through which nature compacts this 2 meter long DNA into a cell nucleus, which is approximately 10 μm in diameter. The DNA undergoes a compaction of about 20,000-fold to fit into the nucleus in the form of chromosomes. The initial step in DNA compaction involves wrapping the DNA around highly basic proteins called histones to form the single structural repeating unit of the chromosome called the nucleosome, leading to a seven-fold compaction. This forms the beads-on-a-string shaped 11nm fiber, which further compacts into the 30nm structure. The 30nm fiber then undergoes a 10,000-fold compaction to form the metaphase chromosome (Figure 1.1). This chapter will address nucleosomes and chromatin structure and how trans-acting proteins interact with chromatin to modulate chromatin function.

1.1 The nucleosome

The nucleosome core, the basic structural repeating unit of chromatin, contains 147 base pairs of DNA in 1.65 turns wrapped around a central histone octamer, consisting of two molecules each of the core histones (Histones H2A, H2B, H3, and H4) (Figure 1.2). In addition to the core histones, each nucleosome binds on average one single lysine-rich linker histone H1. Nucleosomes are spaced between 160 to 220 base pairs on genomic DNA and are connected by segments of DNA known as linker DNA. The crystal structures of nucleosomes from different organisms have been studied at atomic resolution (Davey and Richmond, 2002, Harp et al., 2000, White et al., 2001, Luger et al., 1997).

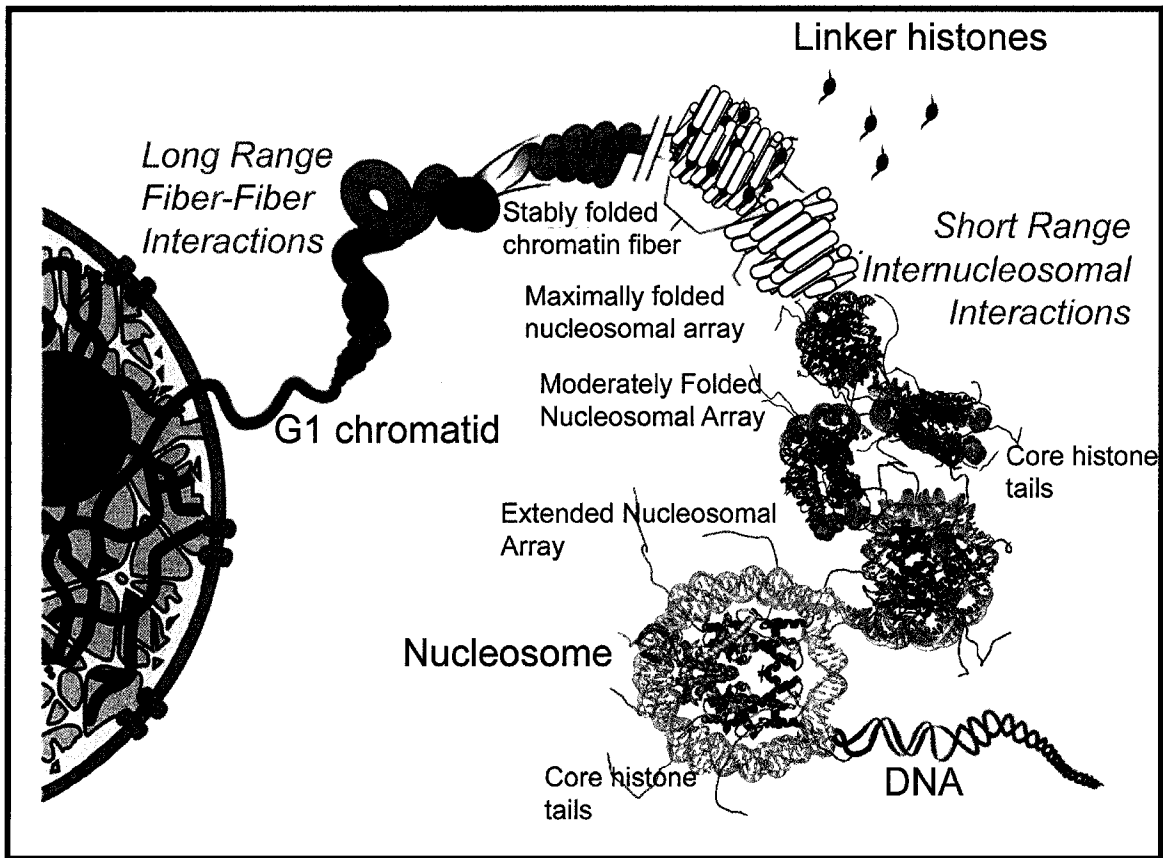


Figure 1.1: Levels of chromatin compaction. Adapted from (Hansen, 2002).

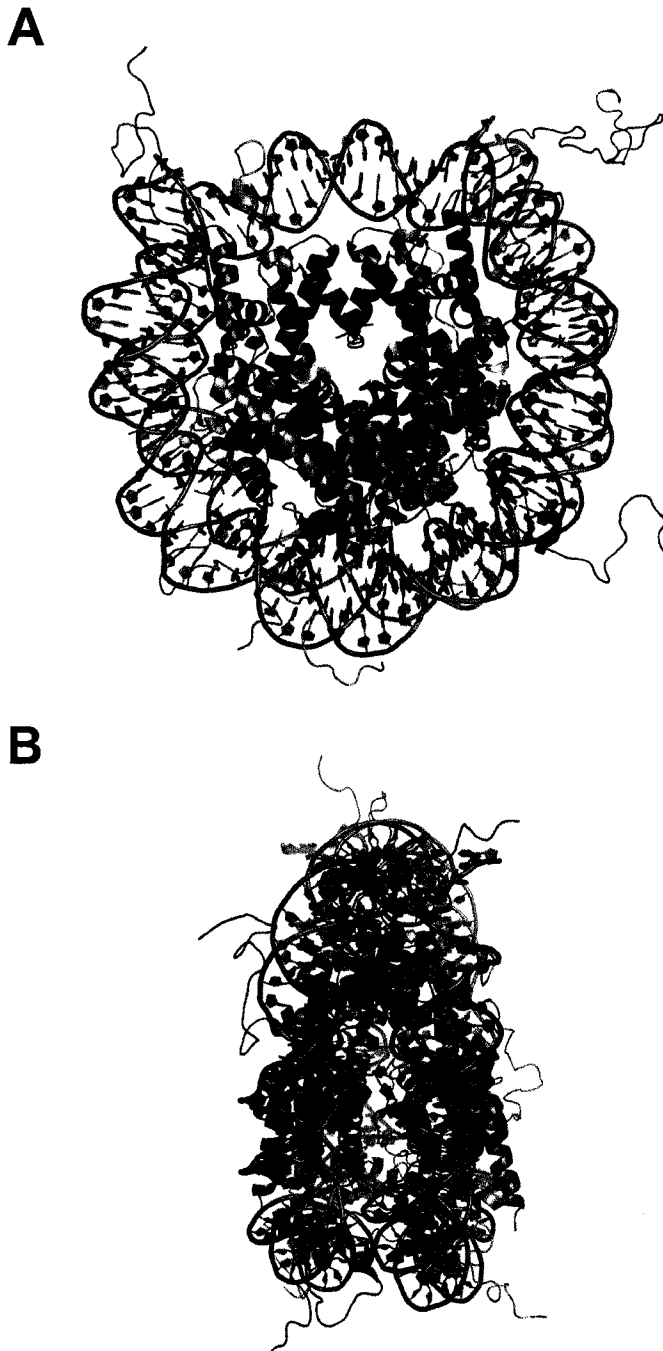


Figure 1.2: Structure of the nucleosome:

- A. Crystal structure of the nucleosome core particle. Histones H2A, H2B, H3 and H4 are shown in yellow, red, blue and green. DNA is seen in gray. The histone tails are seen protruding outwards from the structure.
- B. Side view of the nucleosome core particle. PDB code 1KX5.

Histone-histone interactions:

The four core histone (H2A, H2B, H3 and H4) sequences have been extraordinarily well conserved across species, indicating that there are strict structural constraints on histone function (Sullivan et al., 2000). Core histones are also structurally conserved through evolution (Arents and Moudrianakis, 1995).

Each of the core histones exists as part of a heterodimer, in which the two monomers are intimately associated in a head-to-tail manner in a so-called handshake motif. The histone fold motif consists of three α -helices ($\alpha 1$, $\alpha 2$ and $\alpha 3$) connected by short loops (L1 and L2) (Figure 1.3). The 10-14 residue helices ($\alpha 1$ and $\alpha 3$) flank the long 28-amino acid long central $\alpha 2$ helix. The histone-fold portion of each monomer is related to its partner in the dimer by an approximate two-fold axis. The (H3-H4) dimer through a four-helix bundle interaction, forms a (H3-H4)₂ tetramer, which is the stable entity at physiological ionic strength. Each H2A-H2B pair interacts with the tetramer through a second, homologous four-helix bundle between H2B and H4 histone folds. These heterodimers are stabilized through hydrophobic interfaces formed by the antiparallel arrangement of the helices.

The tetramer is involved in the initial step of nucleosome assembly and in determining octamer positioning on the DNA (Dong and van Holde, 1991). To the tetramer DNA complex, two H2A-H2B dimers are then added by histone chaperones, forming an octamer, around which 147 bp of DNA wraps, forming the nucleosome (Dong and van Holde, 1991) (Figure 1.2).

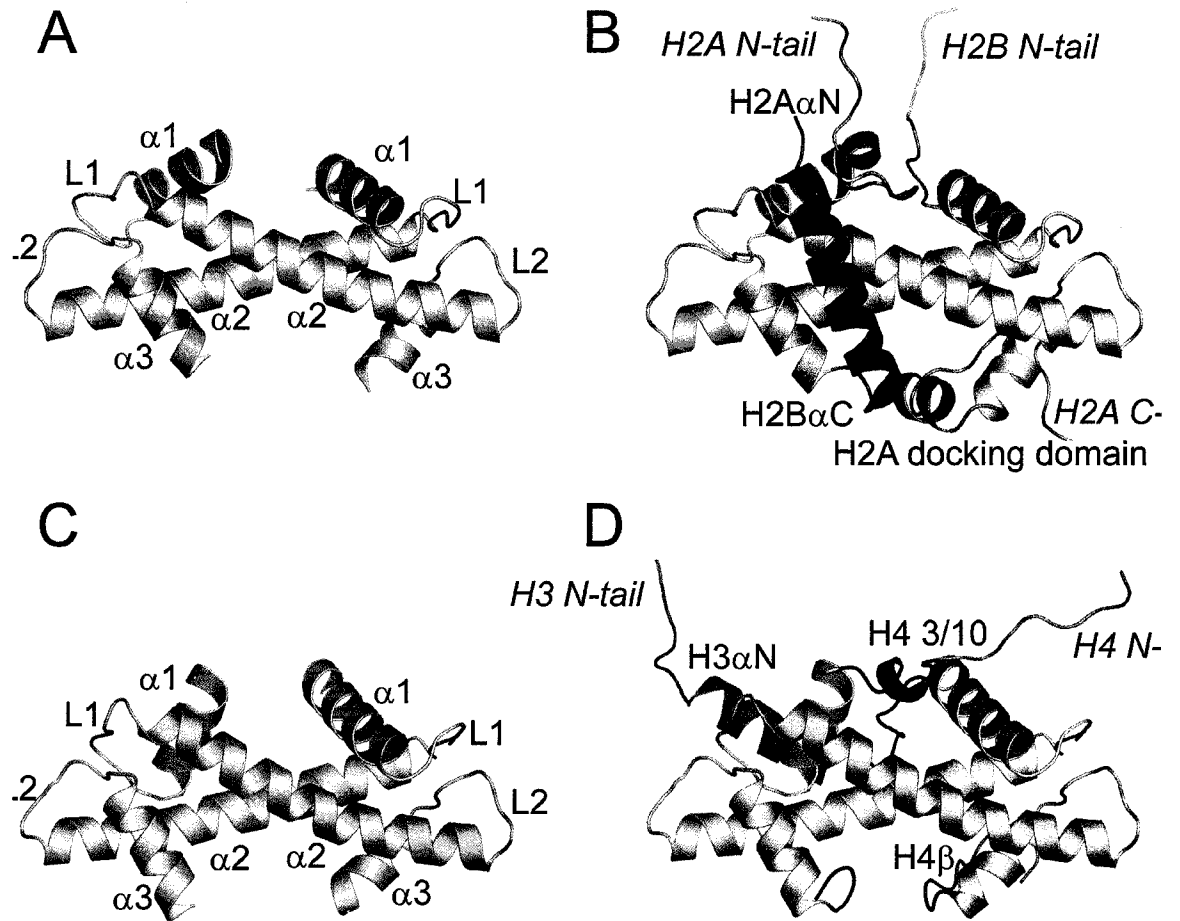


Figure 1.3: Structure of the histones in the nucleosome

The overall structure of individual histone fold pairs is remarkably similar. **A.** H2A-H2B, histone-fold region only (shown in light yellow and light red, respectively). **B.** H2A-H2B including histone-fold extensions (shown in yellow and red) and tails (shown in cyan). **C.** H3-H4 histone fold dimer, histone-fold region only (light blue and light green, respectively). **D.** H3-H4 including histone-fold extensions and tails, shown in dark blue and dark green, respectively; tails in cyan). Adapted from (Chodaparambil et al., 2006).

Histone-DNA interactions:

Each histone-fold dimer binds about 30 base pairs of DNA. The H2A-H2B dimer binds about 30 base pairs each and the H3-H4 tetramer binds about 80 base pairs of DNA. Interaction is primarily with the phosphodiester backbones of the DNA. One interesting aspect of the histone-DNA interaction is the arginine side chain from the histone core entering the minor groove of DNA. In four instances, the interaction between the minor groove of the DNA and the histones is at the histone tails.

Discussed below are some of the pathways through which the nucleosomal structure is modulated.

1.2 Histone Variants:

The nucleosome plays an important role in the regulation of transcriptional activity. One way this is achieved is by the incorporation of histone variants into the nucleosome core particle. Histones are among the slowest evolving proteins known, but a fraction of histones are non-allelic variants that have specific expression, localization, and species-distribution patterns (reviewed in Kamakaka and Biggins, 2005). The variants are usually present as single-copy genes and are not restricted in their expression to the S phase but are expressed throughout the cell cycle. The histone variants are incorporated into the nucleosome in a replication-independent manner. Unlike the major subtypes, the variant genes contain introns and the transcripts are often polyadenylated (Old et al., 1982).

Among the core histones, H2A has the largest number of variants, including H2A.Z (West and Bonner, 1980), MacroH2A (Pehrson and Fried, 1992), H2A-Bbd (Chadwick and Willard, 2001), and H2A.X (West and Bonner, 1980).

The crystal structures of some of the histone variant nucleosomes like H2A.Z containing nucleosome (Suto et al., 2000) , macro-H2A containing nucleosome (Chakravarthy et al., 2005) have been solved. Histone variants have distinct biophysical characteristics that are thought to alter the properties of nucleosomes and transcriptional behavior. H2A.Z has been linked to both transcriptional repression and activation. Recent results indicate that H2A.Z may be involved in heterochromatin organization. For H2A-Bbd, which lacks a significant C-terminal tail, it has been postulated that the lack of such a tail may destabilize the nucleosome, thus aiding in ease of nucleosome displacement during transcription (Gautier et al., 2004, Bao et al., 2004). The MacroH2A variant is thought to be involved in transcriptional repression. This variant localizes to the inactive X-chromosome in female mammals (Costanzi and Pehrson, 1998). H2AX has been determined to function as a DNA damage sensor. H2A.X is conserved in all organisms analyzed to date (Redon et al., 2002). Studies also indicate that changing the surface of the nucleosome through introduction of histone variants like H2A.Z (Fan et al., 2004) also changes chromatin compaction.

Histone H3 is the other histone for which diverse histone variants exist. Histone H3 variants include H3.3, CenH3 and H3.4. H3.3 is a histone variant that is not S-phase regulated and is found in transcriptionally active chromatin (Ahmad and Henikoff, 2002). H3.4 is a tissue-specific H3 variant found in primary spermatocytes (Albig et al., 1996, Witt et al., 1996). The CenH3 variant is localized in centromeric chromatin in all

eukaryotes; along with a difference in the histone-fold domain, their N-terminal tails are extremely divergent and share no sequence similarity with canonical H3 (Malik and Henikoff, 2003).

H3.3 and H3.4 are the least divergent variants, containing only four amino acid differences compared to H3.1 in *Drosophila*. The H3.3 histone variant also plays a role in transcription. One important feature of this variant is that it is constitutively expressed during the cell cycle and can be deposited into chromatin outside of S phase. In dividing cells, H3.3 is present at genes that are either poised for transcription, or are actively transcribed. Because the *Drosophila* H3.3 variant is deposited at transcriptionally active loci like the rDNA, outside of S phase (Ahmad and Henikoff, 2002), H3.3 may serve to replace H3 at active genes as nucleosomes re-form behind the transcribing polymerase.

1.3 Modulation of nucleosome structure through histone tails and tail modifications:

The N-terminal regions of the histones called the “histone tails” are intrinsically disordered, and are characterized by an abundance of highly basic amino acids. The histone tails are also the regions of highest sequence divergence among species (Sullivan et al., 2002). Even though the entire tail is not visible in the crystal structures, it is observed that the histone tails exit the nucleosome most frequently at the minor groove of the DNA (Figure 1.2). In solution, the basic regions of the histone tails could be bound weakly to DNA on the outside of the particle (Lee and Hayes, 1997). Even though the histone tails do not contribute significantly to the structure of individual nucleosomes or to their stability, they do play an essential role in controlling the folding of nucleosomal arrays into higher-order structures (Dorigo et al., 200, Shogren-Knaak et al., 2006). *In*

vitro removal of the histone tails results in nucleosomal arrays that cannot condense past the beads-on-a-string 10-nm fiber. Although the highly basic histone tails are generally viewed as DNA-binding modules, their essential roles in tail-mediated chromatin folding (compaction) also involve inter-nucleosomal histone–histone interactions. Enzymatic removal of H2A/H2B tails primarily decreased the strength of histone–DNA interactions located ± 36 bp from the dyad axis of symmetry, whereas removal of the H3/H4 tails affected the total amount of DNA bound (Brower-Toland et al., 2005). In the high-resolution crystal structure of the nucleosome (Luger et al., 1997), the H4 tail from the neighboring nucleosome interacts with the surface formed by H2A-H2B dimerization in the nucleosome. This was also confirmed through solution studies by Dorigo et al (Dorigo et al., 2004) who showed by cross-linking experiments that the H4 tail interacts with the H2A-H2B surface. Of the four histone tails, removal of H4 tail is the most deleterious to folding. Without the H4 tail, the inter-nucleosomal interactions are compromised, and the intra-fiber interactions are also hindered but not completely abolished, as the tails are additive and independent in function (Gordon et al., 2005).

Histone tails are subject to a large number of post-translational modifications and have emerged as critical determinants of chromatin dynamics. They play an integral role in chromatin-based processes like gene regulation. The ϵ -nitrogen of lysine and arginine amino acids is the substrate for many posttranslational modifications. These residues are modified through methylation, acetylation, sumoylation, ADP-ribosylation and ubiquitination. Serines and threonines can also be modified through phosphorylation (Figure 1.4).

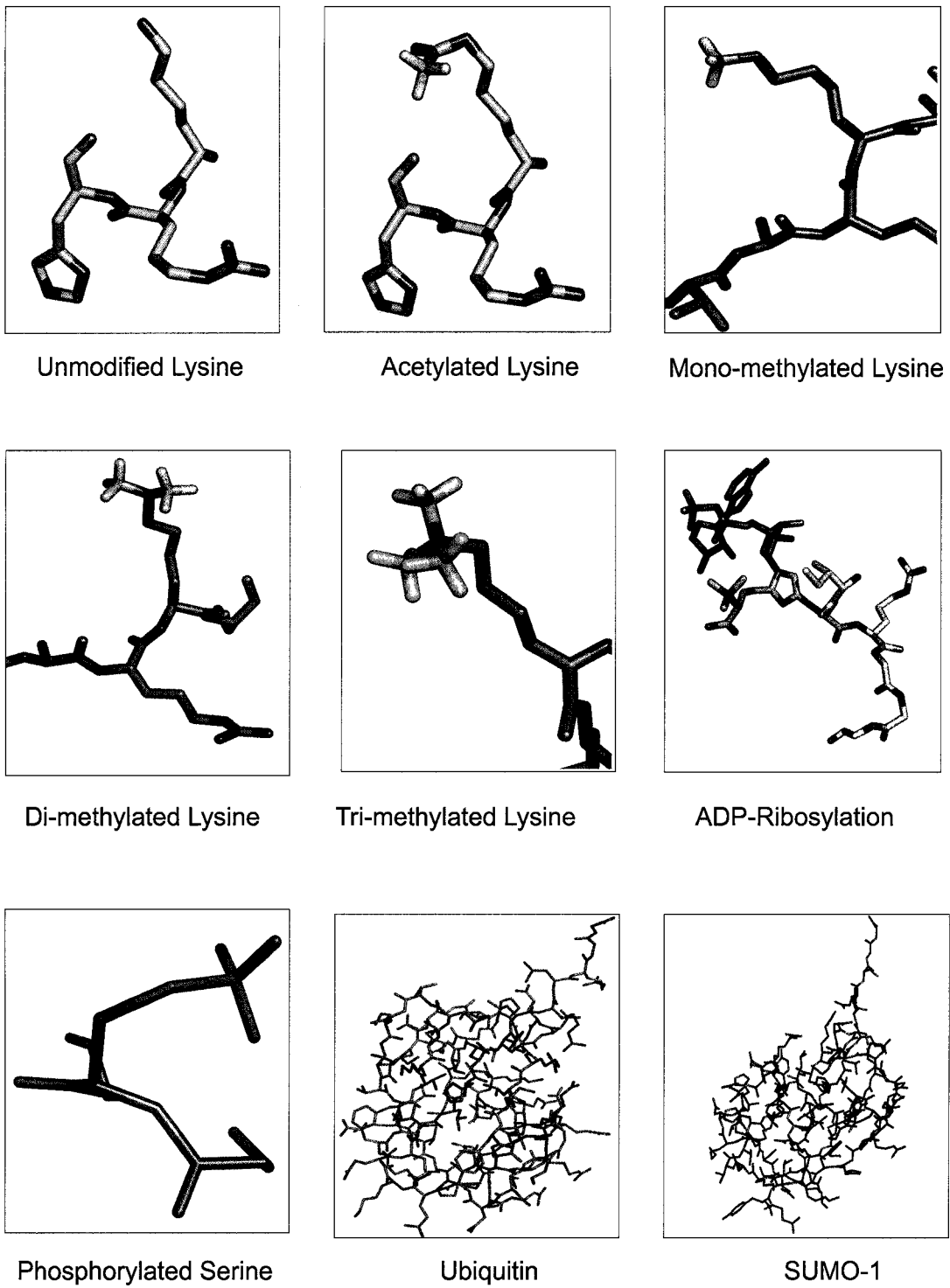


Figure 1.4: Post translational modifications

Examples of post translational modifications on histones.

These covalent modifications help establish global chromatin environments, which help distinguish between transcriptionally active and inactive chromatin regions by acting through mechanisms involving changing the structure of the nucleosomes, altering their ability to interact with other protein factors, modifying their propensity to fold into varying degrees of higher order structures (reviewed in Kouzarides, 2007). Some of the modifications are discussed below briefly.

Histone acetylation: Usually associated with activation of transcription. This is done by a subset of enzymes called acetyltransferases. Most of the acetylation is on lysines, and to date most of the acetylation sites are on the tails with the exception of H3 K56, which is a core-domain modification (Xu et al., 2005). Recent studies have shown that the K16 acetylation of the H4 tail, helps modulate chromatin folding *in vitro* (Shogren-Knaak et al., 2006). This modification can be reversed to modulate transcriptional repression through histone deacetylases.

Histone methylation: Histones may be methylated on either lysine or arginine residues. Lysine side chains may be mono-, di- or tri-methylated, whereas the arginine side chain may be mono-methylated or (symmetrically or asymmetrically) di-methylated (reviewed in (Margueron et al., 2005), (Bannister et al., 2002)). Histone methylation can lead to either activation or repression of a gene. Three methylation sites (H3K4, H3K36, and H3K79) are implicated in activation of transcription. On the other hand, lysine methylation of H3K9, H3K27 or H4K20 is connected to transcriptional repression. Until recently, histone methylation—unlike all other histone modifications was considered a

permanent mark. The discovery of a histone demethylase LSD1 (Shi et al., 2004), changed the outlooks thereby substantially increasing the complexity of histone modification pathways. A number of demethylases have been identified since then.

Histone ubiquitination: This is a modification found on human histones H2AK119 and H2BK29. This modification is mediated by the enzyme Bmi/Ring1A and also RNF20/RNF40 and is associated with transcriptional repression (Wang et al., 2006), (Zhu et al., 2005). This modification is also said to be involved in transcriptional elongation facilitated by histone chaperone FACT, but currently the molecular mechanism is unknown (Pavri et al., 2006). Two deubiquitinases have also been identified that are known to act on H2BK123 ubiquitination in yeast. The Ubp8 enzyme is required for transcriptional activation, whereas the enzyme Ubp10 is required in transcriptional silencing of heterochromatin sites (Emre et al., 2005), (Gardner et al., 2005).

Histone sumoylation: This is again a large modification like ubiquitination. Sumoylation can reverse the effects of acetylation and ubiquitination. Therefore this modification is usually seen accompanying transcriptional repression. All four histones can be modified at specific sites through this modification (Nathan et al., 2006).

Histone ribosylation: The function of this modification is still unclear. The modification is done by the enzyme MART (Mono ADP-ribosyltransferase) or PARP (Poly ADP-ribose polymerase) (reviewed in Hassa et al., 2006). It is known that PARP-1 enzyme is

activated during DNA double strand breaks and at sites where DNA repair is initiated (Ju et al., 2006).

Histone phosphorylation: The link between histone phosphorylation and gene expression is currently being studied at molecular detail. H3S10 is known to be phosphorylated during mitosis by the Aurora B kinase. This is known to activate NFkB-regulated genes like c-fos and c-jun (Macdonald et al., 2005). It is suggested that the phosphorylation of H3S10 leads to displacement of HP1 from H3K9me, which normally compacts chromatin (Fischle et al., 2005). A number of other phosphorylation sites have been identified in yeast.

Histone modifications and epigenetics: The protein component of the chromatin, just as DNA, is now being considered as an information carrier. It is also believed that the histone modifications mentioned above are benchmarks for information transfer. A number of phenotypes like X-chromosome inactivation, heterochromatin formation, reprogramming, gene silencing, etc. are transmitted hereditarily through these modifications. Further studies are being done in understanding these mechanisms, which will give us further insight into how the chromatin behaves.

1.4 The nucleosomal surface

The octamer has a total accessible surface area of $28,000\text{\AA}^2$. The octamer is usually shown as a “hockey puck” with a flat surface, which wraps 146bp of DNA and thereby forms chromatin. Contrary to this view, the octamer surface is a highly contoured

and charged surface, which could act as binding domains for proteins acting on the chromatin (Figure 1.5). With the dimerization of the histones H2A-H2B, a charged region is formed by a total of seven amino acids from both H2A and H2B (H2A E56, E61, E64, D90, E91, E92) and H2B (E110). The H4 tail from the adjacent nucleosome makes extensive contacts with this charged region of an adjacent particle. This interaction is considered important for chromatin compaction (Dorigo et al., 2004).

Using genetic screens, Park et al (Park et al., 2002) showed that a particular region on the surface is critically involved in silencing of gene expression. This surface is located at a H3/H4 histone-fold. The side chains, identified from the mutants, were centered around Lys79 of histone H3, a residue methylated by the yeast Dot1 protein. This surface flanks a large protuberance made up of several residues from the L1 loop of histone H3. This surface and the adjacent surface of histone H2B make a deep groove that is wide enough to accommodate a peptide, possibly an N-terminal histone peptide. Trimethylation of Lys79 would create substantial steric hindrance within this groove.

Some of the LRS (loss of rDNA silencing) mutations, such as those resulting in the Arg83Ala and Arg83Ser substitutions, lie in amino acids whose side chains interact directly with DNA in the crystal structure and do not directly form part of this groove.

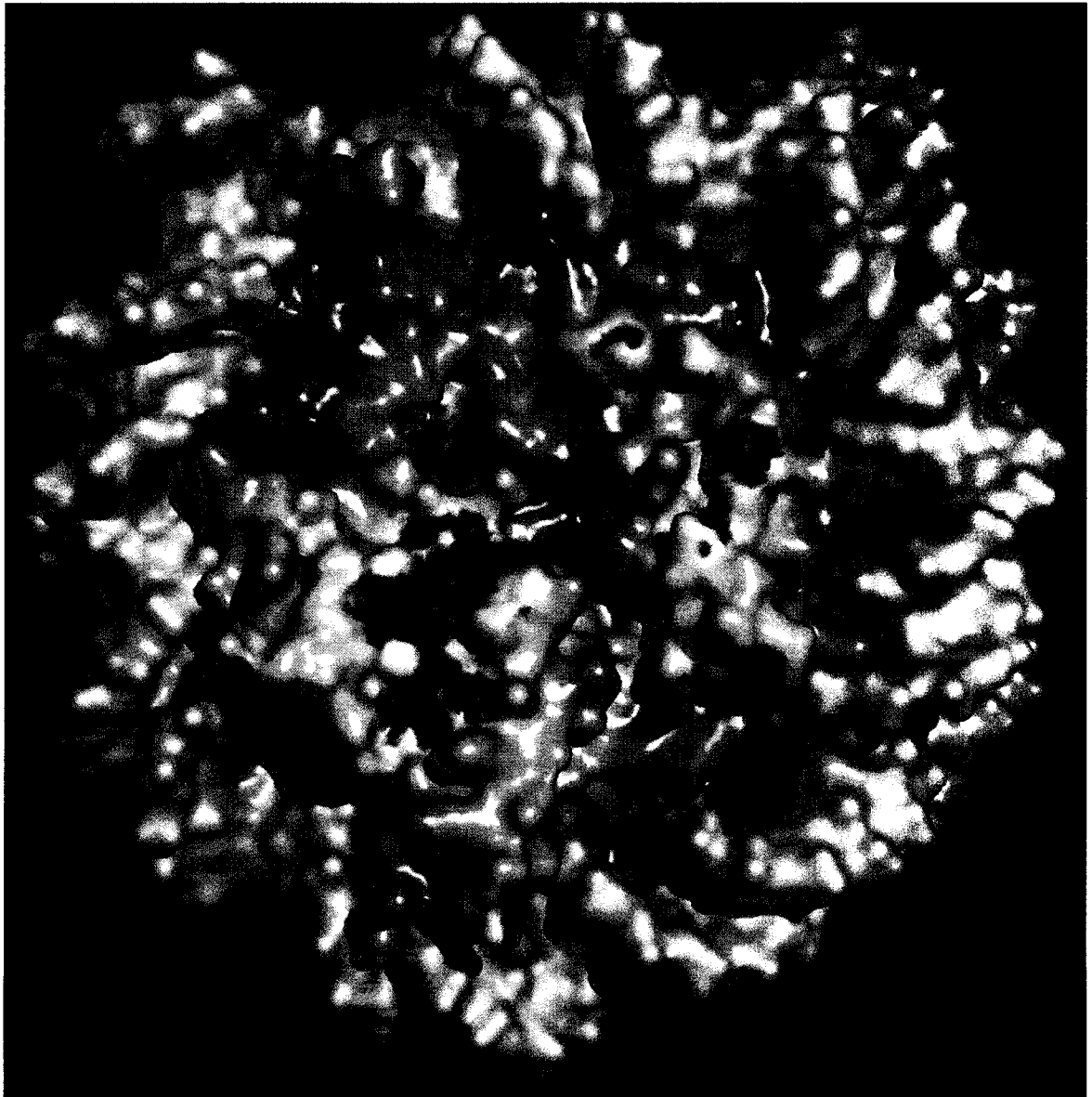


Figure 1.5: Surface of the nucleosome:

The nucleosome core particle exhibits a highly contoured and charged surface. Electrostatic potential of the nucleosome surface (red – negatively charged / blue – positively charged) were calculated with GRASP and rendered in PyMOL.

Apart from LRS mutants, mutations in the genes for histones H3 and H4 partially alleviate the transcription defects caused by the inactivation of the yeast chromatin-remodeling factor SWI/SNF (Kruger et al., 1995). These mutations are defined as the SIN mutants. Alterations in both the SIN and LRS domains disrupt telomeric silencing. It is also known that these domains are required for Sir2p and Sir4p (two components of the silencing machinery) binding to telomeric chromatin (Fry et al., 2006). These data show that the surface of the nucleosome is directly involved in chromatin function.

Nucleosomal surface modifications: The nucleosomal surface can also be modified through posttranslational modifications on the histone core. Parthun and colleagues (Mersfelder and Parthun, 2006) have used mass spectroscopic methods to identify histone modifications in the core of the nucleosomes. Similar to the situation observed with histone tail modifications, modifications located on the solvent accessible face of the nucleosome have the ability to alter higher-order chromatin structure and chromatin–protein interactions. Single amino acid substitutions of modifiable residues within the histone core have been shown to dramatically affect transcription, DNA damage repair, chromatin structure, chromatin assembly and heterochromatic gene silencing (Ng et al., 2002), (van Leeuwen et al., 2002, Xu et al., 2005, Hyland et al., 2005). Modifications to the nucleosomal face may function in much the same way as N-terminal tail modifications by controlling the ability of non-histone proteins to bind to the nucleosome (as in the case of Dot1p methyltransferase Lacoste et al., 2002, van Leeuwen et al., 2002), Sir2, Sir3 interaction (Strahl-Bolsinger et al., 1997)). Modifications to the nucleosome face may also have more direct structural effects by influencing nucleosome–nucleosome interactions that are thought to occur during the formation of 30 nm filaments.

Some of the modifications were mapped to residues that directly bind the DNA, while others were positioned in close proximity to the DNA (Freitas et al., 2004). Although the latter group does not make direct contact with DNA, these residues have the potential to influence the histone–DNA interface (Figure 1.6A,B and C).

The structure of the nucleosome is dependent upon specific histone–histone interactions that lead to the formation of the histone octamer. The use of post-translational modifications in these regions for the modulation of intra-nucleosomal histone–histone contacts may be an important mechanism for regulating chromatin structure. Mass-spectrometry analyses have revealed that a number of amino acids involved in making these histone-histone interactions that stabilize the histone octamer are posttranslationally modified (Cocklin and Wang, 2003, Zhang et al., 2003) (Figure 1.6D).

Point mutation analysis of the nucleosome surface: The core-domain modifications are conserved across a wide range of organisms. Any modifications or mutations in these residues can adversely affect the viability of the organism. Horikoshi and colleagues (Matsubara et al., 2007) have done studies where they mutated surface-exposed residues on the yeast nucleosome and looked at their phenotype under normal conditions. They used a site-directed mutagenesis approach, which allowed them to characterize particular residues in a system and then apply them generally to domains of interest. To evaluate the functional role of each amino acid that constitutes the core histones, they individually

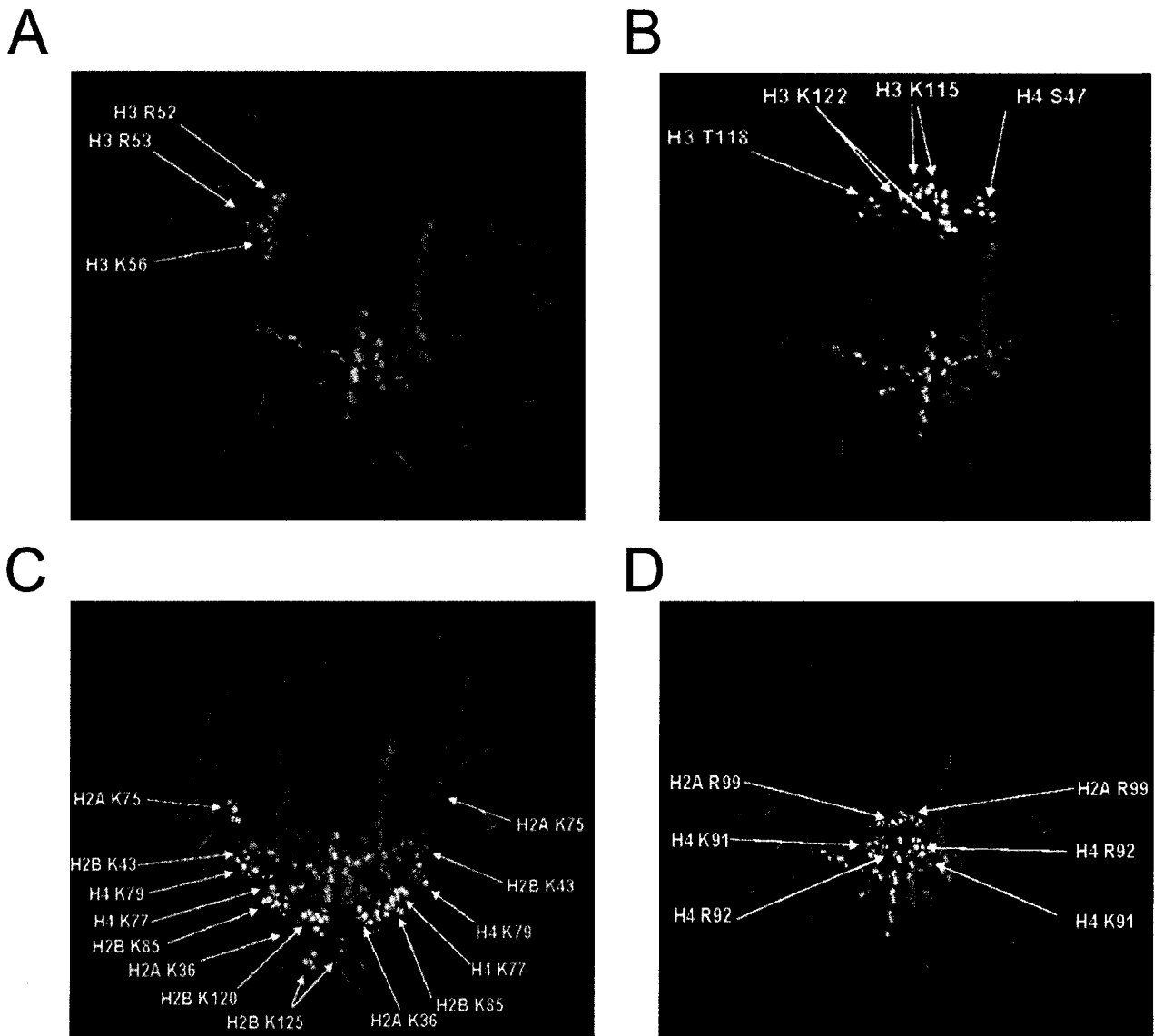


Figure 1.6: Post translational modifications on the nucleosomal surface.

A. Modifications located at the nucleosome dyad axis are modeled on the nucleosome crystal structure. **B.** Modifications near the DNA entry–exit points are highlighted on the nucleosome crystal structure. **C.** Additional modifications near site of histone–DNA contact are shown on the nucleosome crystal structure. **D.** Locations of modifications in regions of histone–histone interface are depicted on the crystal structure of the nucleosome. Adapted from Mersfelder et al. (Mersfelder and Parthun, 2006).

mutated each of the 320 residues in histones H2A, H2B, H3, and H4 to alanine, with the exception of endogenous alanine residues and those amino acids not located on the surface of the nucleosome. Even though there were phenotypic differences observed in these mutants, only eight mutations (H2A-Y58A, -E62A, -R82A, -D91A; H2B-L109A; H3-L48A, -I51A, and -Q55A) of the 320 amino acids were lethal. Interestingly, these are arranged in two regions. The first region encompasses H3-L48, -I51 -Q55 and H2A-R82, and these residues are linearly arranged on the nucleosome adjoining the C-terminal tail of H2A which make-up the docking domain. The second region is, composed of H2A-Y58, -E62, -D91 and H2B-L109 is located at the acidic patch formed by the H2A-H2B dimer interface (Figure 1.7). This patch is involved in making interactions with H4 tail from the neighboring nucleosome in the crystal lattice.

These studies show that the surface of the nucleosome is critical in mediating the formation of the higher order structure of chromatin. Current studies also indicate that trans-acting proteins can bind directly to the core of the nucleosome (Barbera et al., 2006).

1.5 Effects of trans-acting protein binding to the nucleosomal surface

Recently, there has been an increased interest in trans-acting proteins like transcriptional factors, viral proteins, and histone modifying enzymes using the nucleosome as a docking station. Recently, John Denu and colleagues have shown that the histone acetyl transferase (HAT) Piccolo-NuA4 complex, which acetylates the H4 tail, requires the histone-fold domain region; particularly residues 21-52 of H4, for tight binding and efficient tail acetylation (Berndsen et al., 2007).

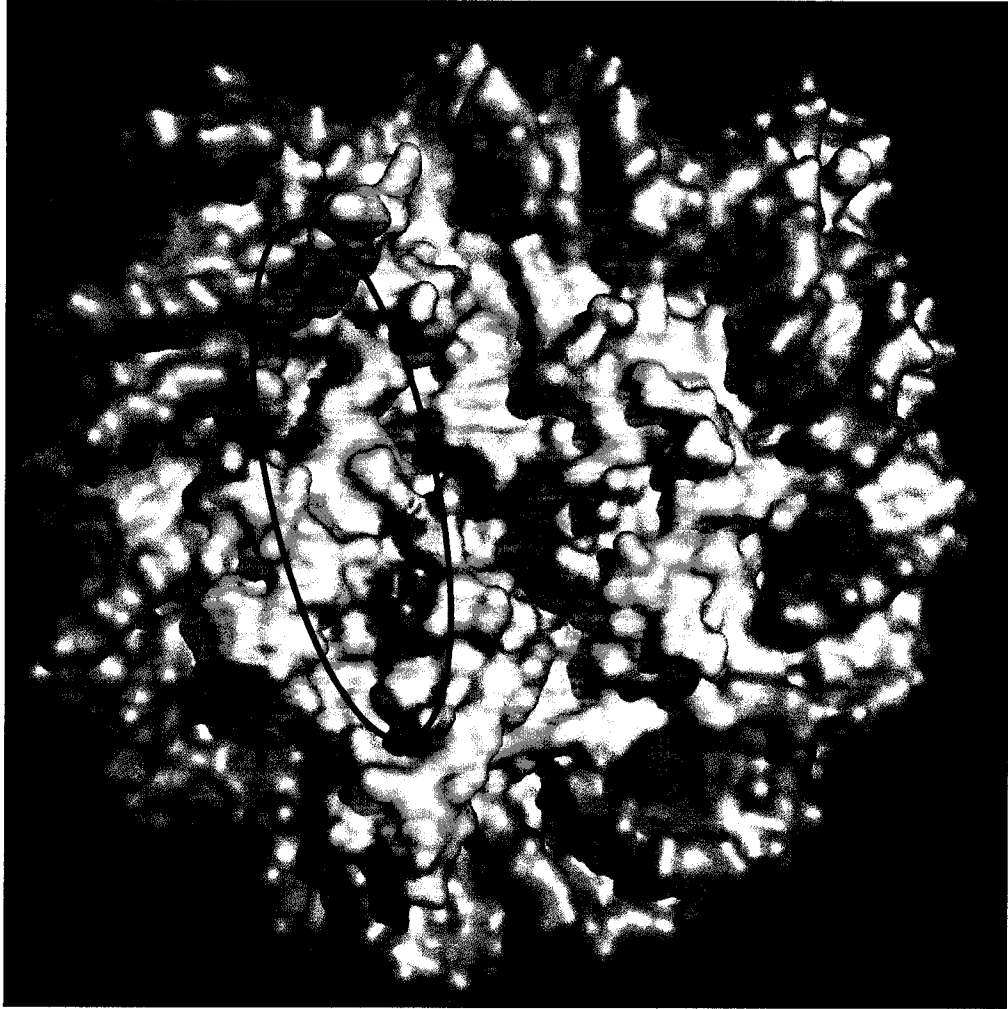


Figure 1.7: Surface modifications and lethal mutations:

Point mutation of amino acids leads to lethality. Colored amino acids show the eight point mutations which lead to lethality in yeast nucleosomes as described in Matsubara et al (Matsubara et al., 2007)

This shows that piccolo NuA4 recognizes the open surface of the nucleosome on which the histone-fold domain of H4 is located. This study directly links the crucial role of the surface in recruiting histone modifiers, which in-turn, further affects the chromatin higher order structure through modification of the histones.

1.6 Chromatin structure beyond the nucleosome:

To understand how the cell compacts and unravels the DNA during its cellular processes, it becomes essential to understand the structure of chromatin. The complexity of chromatin is the stumbling block to this quest, even after decades of research. Most of the research on higher order structure of chromatin has been focused on the “30-nm fiber” which is defined as the secondary folding motif of chromatin (Van Holde, 1988). The field is still divided about the models for the formation of the 30-nm fiber, the two most supported models are the solenoid model ((Finch and Klug, 1976, Robinson and Rhodes, 2006)) and the regularly spaced zig-zag model ((Horowitz et al., 1994, Schalch et al., 2005). In 2004, Richmond and colleagues showed, using electron microscopy and cross-linking studies that the 30-nm fiber exhibits a two-start helix (Dorigo et al., 2004). In 2005, the Richmond lab using the recombinant nucleosomal array approaches solved a 7.0Å structure of a tetra-nucleosome structure, which also exhibits a two-start helix structure (Schalch et al., 2005).

Further tertiary structures are formed through distant and local nucleosome-nucleosome interactions (Woodcock and Dimitrov, 2001, Hansen, 2002). Some evidence exists that indicates that the DNA loops of 30 to 90kb are anchored to scaffold proteins and this gives rise to scaffold-loops. In one of the models, called the radial loop model, it

is suggested that the scaffolds form a helically looped chromatin fiber of 200-300nm diameter, to which radially projecting loops of 30-nm fibers are anchored (Taniguchi and Takayama, 1986, Rattner and Lin, 1985). However, other studies counter that there is no radial organization; instead condensation may proceed through the association of linearly aligned bead-like aggregates of 200-500 nm known as chromomeres (Harauz et al., 1987, Mullinger and Johnson, 1987). Studies also show that there are non-histone proteins like condensins (Hirano and Mitchison, 1994) that are involved in chromatin condensation. Data has shown that condensins are actively involved in condensation by constraining chromatin into a coiled conformation (Swedlow and Hirano, 2003). However (Hudson et al., 2003) contend that the primary role of condensin is to promote correct association of non-histone proteins to mitotic chromosomes. In all, the chromatin community is still divided about a structural model for chromosome condensation.

Exploring the 30-nm fiber

Since the 30-nm fiber itself is a complex entity, its study in vitro can be simplified by using defined nucleosomal arrays. A nucleosomal array can be defined as any piece of DNA that is >300bp in length that is complexed with two or more core histone octamers (Fletcher and Hansen, 1996). One of the very well characterized DNA sequences used for making defined nucleosomal array is the 208-12mer DNA, which was derived from tandem repeats of the *Lytechinus* 5S rDNA (Simpson et al., 1985). Earlier studies using chicken erythrocytes by Lewis et al., (1976) showed that nucleosomal arrays formed compact structures in the presence of NaCl. Thoma et al., 1979, using electron microscopy, further studied the salt-dependent nucleosomal array folding in the presence

of the monovalent cation and the divalent cation salts. They showed that at >60mM NaCl or at >0.5mM MgCl₂, all H1-containing chromatin fragments folded to form highly condensed chromatin fibers. Since these chromatin fibers were extracted from cells, the lack of saturation of these arrays was an obstacle to getting accurate results. The use of the 208-12mer DNA alleviated this difficulty and refined the study of chromatin compaction *in vitro*. Using this DNA, Hansen et al., 1989, using analytical ultracentrifugation techniques, determined that the homogenous 29S “beads-on-a-string” structure seen at low salt concentrations was converted to a heterogeneous population of structures ranging from 29S to 40S with increasing NaCl salt concentrations. They also saw that in the presence of the linker histone H1, the arrays formed the stable 55S structures, which is considered to be the 30-nm fiber. The 55S particles can also be observed at 1-2mM MgCl₂ (Schwarz and Hansen, 1994). With divalent cation concentrations >3mM MgCl₂, the arrays exhibit an S value ranging from 55S to >100-120S. These particles are arrays undergoing long-range nucleosome-nucleosome interactions (termed “self-association” of nucleosomal arrays). All the above-observed data are very much relevant biologically because the whole process is reversible (Hansen et al., 1991). Removal of the salts brings the arrays back to the 29S beads-on-a-string-like structure. Further, Garcia-Ramirez et al., (1992) purified a homogenous preparation of native 12-mer nucleosomal array from chicken erythrocytes. Using both analytical ultracentrifugation and electron microscopy, they observed folding and self-association behavior of these arrays identical to those of the recombinantly assembled 208-12mer nucleosomal arrays. Taken together, these data support the conclusion that folding of 5S nucleosomal arrays reflects the folding behavior of native nucleosomal arrays.

1.7 Histone tails and the 30-nm fiber

The self-association behavior of these arrays changes in the absence of the tails, indicating that the salt-mediated compaction of the nucleosomal arrays is also dependent on the histone tails. More importantly, the histone tails play a very important role in chromatin compaction. Dorigo et al (Dorigo et al., 2003) showed that if the H4 tail is removed, chromatin compaction is adversely affected. Even though these studies showed that the H4 tail is the most important for chromatin compaction, Gordon et al., (2005) has shown that all the histone tails are important for chromatin compaction. They also show that all the tails act independently and additively in mediating chromatin compaction. Interactions of the tails on the nucleosomal core has being studied through cross-linking experiments (Dorigo et al., 2004, Kan et al., 2007) which have shown that the H3 tail domain performs multiple functions during chromatin condensation via distinct molecular interactions that can be differentially regulated by acetylation or binding of linker histones. It is still not clear whether the tails help physically “tether” nucleosomes together or whether the interaction of the tail with the nucleosomal surface leads to a change in the surface charge or contour which leads to chromatin compaction. It has been shown that the histone variant H2A.Z, which exhibits an extended acidic patch, can fold into secondary structures that are more compacted than H2A arrays both with and without HP1 α (Fan et al., 2004).

Chapter III of this thesis concentrates more on understanding the effects of the surface of the nucleosome on the 30-nm fiber, which is the secondary structure of chromatin compaction.

Nucleosome interacting proteins.

In this section we look at two different proteins which interact with the histones.

1.8 Yeast Nucleosome Assembly Protein 1 (yNAP1)

During DNA replication, histones are deposited onto the newly replicated DNA with the aid of chromatin assembly factors (reviewed in Krude and Keller, 2001), and further assembly and spacing of nucleosomes is facilitated by ATP-dependent chromatin assembly and spacing factor. Several chromatin assembly factors have been identified, such as CAF-1 and RCAF-1 (Mello et al 2001), ACF (Tyler et al., 1999), CHRAC and RSF (Verreault et al., 1996). The current model proposes that the first and probably rate-limiting step is the deposition of H3/H4 tetramers onto the DNA, followed by the rapid association of two H2A/H2B dimers. Both reactions are assisted by histone chaperones. Once nucleosomes have been assembled, spacing activities such as ACF, CHRAC, and RSF move the nucleosomes along the DNA to keep a regular spacing between nucleosomes (Ladoux et al., 2000, Ito et al., 2000). Other chaperone proteins are also needed during this process of assembly. One such protein involved in the assembly is the nucleosome assembly protein-1 (NAP1) (Ishimi et al., 1987)

NAP1 was first identified and isolated from HeLa cells by Ishimi et al., (1987). Homologues of NAP1 are present in different organisms including yeast (Ishimi and Kikuchi, 1991), *Drosophila* (Ito et al., 1996a), amphibians (Steer et al., 2003), and plants like tobacco and rice (Yoon et al., 1995). The importance of NAP1 is seen in the fact that in yeast, deletion of the yNAP1 gene leads to alterations in the gene expression of about 10% of the genome (Ohkuni et al., 2003). In *Drosophila*, it is more evident in the fact that

deletion of dNAP1 leads to embryonic lethality (Lankenau et al., 2003). NAP1 was determined to be an H2A-H2B dimer-specific chaperone through co-immunoprecipitation studies (Ito et al., 1996a). In physiological conditions, NAP1 is seen associated with histone H2A (Chang et al., 1997). In vitro, NAP1 binds preferentially to the (H3-H4)₂ tetramer. This preference is lost when the histone tails are deleted (McBryant et al., 2003). NAP1 is known to bind linker histone H1 (Kepert et al., 2005) and also interact with transcription factors like p300/CBP (Ito et al., 2000) and the kix domain of p300/CBP (Asahara et al., 2002). This interaction is modulated by core histones (Cairns et al., 1996) suggesting that NAP1 can serve as a bridging protein between transcriptional co-activators and the chromatin. This directly involves NAP1 in modulating access to the transcription machinery. NAP1 also plays an important role during the cell cycle through regulation of certain protein kinases (Altman and Kellogg, 1997). Also, several genes required for cell cycle regulation in yeast are up-regulated in Δ NAP-1 cells (Ohkuni et al., 2003). *Xenopus* NAP1 is known to interact with certain B-type cyclins during the cell cycle (Kellogg et al., 1995). Biochemical experiments demonstrate that cyclin B/p34cdc2 kinase complexes that control the transition between the S and G2 phases can phosphorylate purified NAP1 (Kellogg et al., 1995). *Drosophila* NAP1 and human NAP1 bind histones H2A and H2B in vivo and shuttle them from the cytoplasm to the nucleus as the cell progresses from the G1 to the S phase, concomitant with the activation of nucleosome assembly during DNA replication (Ito et al., 1996a, Rodriguez et al., 2000). This is mediated by the interaction of the NLS sequence of NAP1 with a karyopherin family of proteins called Kap114p (Miyaji-Yamaguchi et al., 2003). But the exact mechanism by which Nap1 is transported into the nucleus and back to the cytoplasm is

unclear. Kap114 Δ yeast still show import of NAP1 to the nucleus showing that there might be alternate pathways for this shuttling (Mosammaparast et al., 2002). yNAP1 can exchange histone-dimers into preformed nucleosomes (Park et al., 2005). It is also known to slide nucleosomes made on a longer DNA (Park et al., 2005) and chapter IV of this thesis).

One very well characterized NAP1 species is yeast NAP1 (yNAP1). yNAP1 is 417 amino acids in length and has a pI of 4.25 with a relative molecular mass of 48kDa. yNAP1 can be roughly divided into three domains. The N-terminal unstructured region comprises amino acids 1-74; the core domain makes up amino acids 74-365 and the C-terminal acidic domain makes up amino acids 365-417. Almost 21% of the 417 amino acids are either aspartic or glutamic acids. These acidic segments, which resemble the C-terminal acidic region of nucleoplasmin (Burglin and De Robertis, 1987, Dingwall et al., 1987), may be involved in the binding of histones, but further studies have shown that the largest acidic domain which makes the C-terminal tail is dispensable for its activity (Fujii Nakata et al., 1992, Fujii Nakata et al., 1992, McBryant et al., 2003). Studies have indicated that yeast NAP1 is an obligate dimer (McBryant et al., 2003). However, *in vitro* studies at lower salt concentrations (~100mM), NAP1 is seen to be an oligomer of the obligate dimers (McBryant and Peersen, 2004).

The crystal structure of yNAP1 was solved at a resolution of 3.0Å (Park and Luger, 2006b)(Figure 1.8A, B). This confirmed earlier data that yNAP1 is a homo dimer. Both the N-terminal region and the C-terminal acidic tail were absent from the structure because they were too disordered. A long α -helix is responsible for this dimerization. This also exhibited a novel non coiled-coil fold (Park and Luger, 2006b).

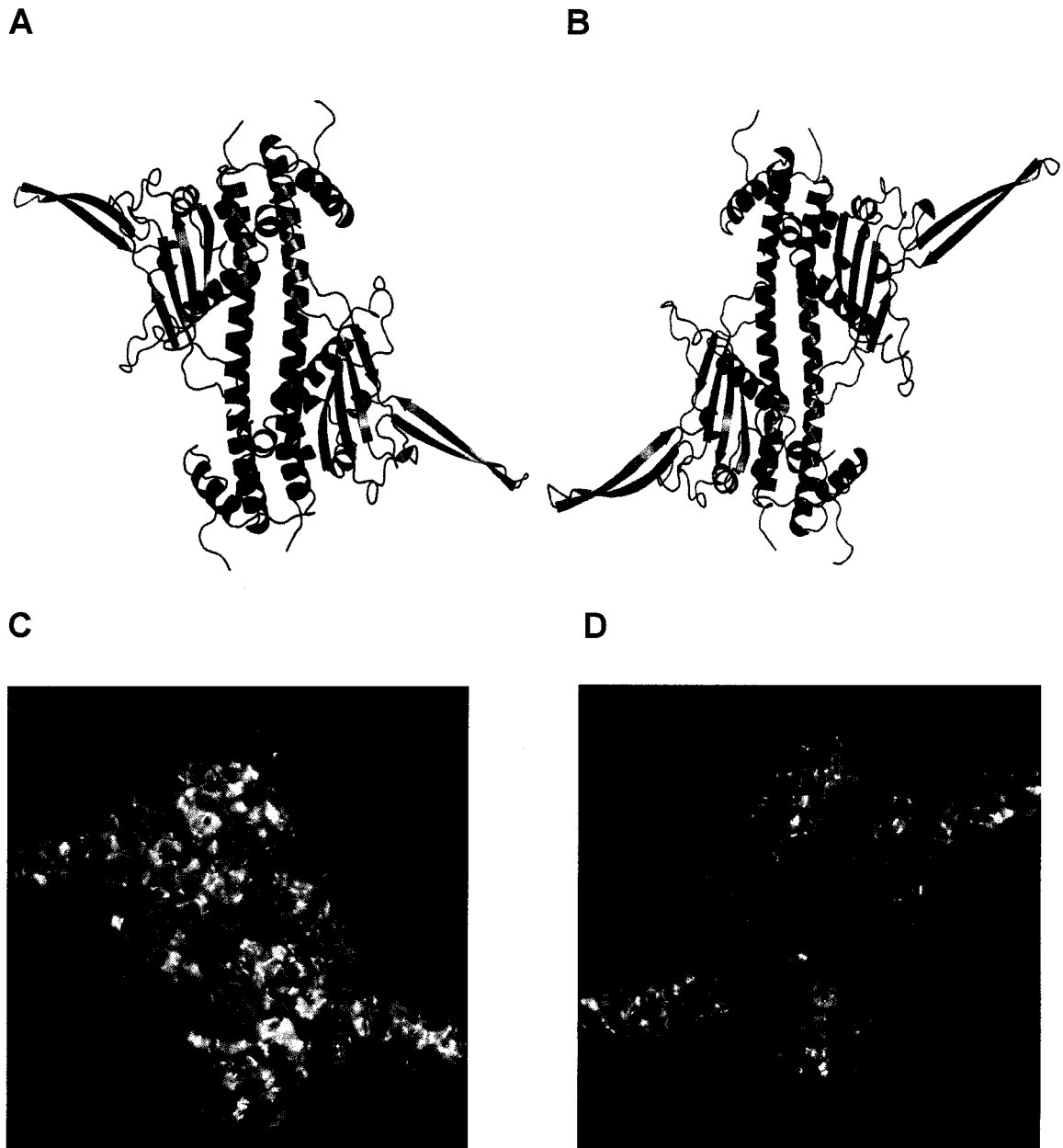


Figure 1.8: Structure of yNAP1

- A. Top view of yNAP1 shown in cartoon representation.
- B. Bottom view.
- C. Top surface representation of yNAP1. Electrostatic potential surfaces (red – negatively charged / blue – positively charged) were calculated in PyMOL.
- D. Bottom view of yNAP1.

A sub-domain C that is comprised of anti-parallel β -sheets is a critical domain in yNAP1. This domain exhibits some similarity to other histone chaperones, such as nucleoplasmin, ASF-1, and CAF-1. Residues 290–295 of yeast NAP form the NLS (Nuclear Localization Signal). These residues are part of a short antiparallel β -sheet formed by strands β 5 and β 6 that protrudes from the main structure. The surface representation of yNAP1 shows an interesting distribution of charge. The concave “bottom” side of yNAP1 is highly acidic (figure 1.8 C, D). This region might be involved in interacting with the positively charged histones or their tails.

The C-terminal acidic domain

The C-terminal acidic domain (CTAD) of yNAP1 is not necessary for yNAP1 to function in nucleosome assembly (Fujii Nakata et al., 1992), but our studies have shown that the CTAD is essential for histone exchange and nucleosome sliding (Park et al., 2005). Despite low levels of homology, all NAP1 species and other histone chaperones like ASF1, nucleoplasmin, etc. exhibit this acidic domain to a certain extent. In the case of *Drosophila* NAP1, the CTAD has more aspartates than glutamates, compared to yNAP1. Interestingly, *Drosophila* NAP1 can undergo a post-translational modification of the tail called polyglutamylation wherein a stretch of 10-13 glutamates is added, thereby increasing the glutamate content of the tail. Chapter V of this thesis looks at the effect of the CTAD of yNAP1 on a novel function we refer here as the “scavenging activity” of yNAP1.

1.9 Kaposi's Sarcoma Herpes virus and Latency Associated Nuclear Antigen.

Kaposi Sarcoma

Kaposi's sarcoma (KS) is a cancer-like disease. It usually shows up on the skin, or in the linings of the mouth, nose, or eyes. KS can also spread to the lungs, liver, stomach, intestines, and lymph nodes. KS lesions contain tumor cells with a characteristic abnormal elongated shape, called spindle cells derived from endothelial origins (Boshoff and Weiss, 1997, Chang et al., 1994). The KS is a slowly progressing tumor, which has a low potential of being malignant in immuno-competent patients. However, in the case of immuno-suppressed patients this can be fatal (Ganem, 1997).

Kaposi Sarcoma associated Herpes Virus (KSHV)

The primary cause of KS is the herpes virus HHV-8, also referred to as Kaposi's sarcoma-associated herpes virus (KSHV). The KSHV is a member of the γ 2- herpes virus family with a 165-kb genome (Chang et al., 1994). The viral genome of KSHV consists of a 140kb-long unique coding region flanked by multiple GC-rich 800bp terminal repeats (TR). There are at least 90 ORFs. The function of many genes has been assigned based on the known roles of homologues in other herpes virus. Only very few genes are expressed during viral latency in tumor cells in vivo. These include LANA (latency associated nuclear antigen) and the D-type cyclins.

Latency Associated Nuclear Antigen (LANA)

LANA is a 234-kDa nuclear phosphoprotein (Kedes et al., 1997; Rainbow et al., 1997) that is seen associated with nuclear heterochromatin during interphase and with

chromosomes in the mitotic phase. Figure 1.9A shows the predicted folding index of the protein. The gene coding for LANA is expressed from the ORF 73 of the KSHV genome as a polycistronic mRNA coding for a cyclin homolog and FLIP along with LANA. LANA is localized to the nucleus, where it is distributed throughout the nucleoplasm, and also accumulates in speckles referred to as LANA bodies (Rainbow et al., 1997, Kellam et al., 1997, Renne et al., 2001)

To attain latency, KSHV has to undergo the following:

1. Ensure propagation of the viral genome
2. Suppress the lytic program
3. Stimulate host cell proliferation
4. Interfere with cellular tumor suppression functions and
5. Block pro-apoptotic pathways (Wong et al., 2004).

LANA has been implicated in all the above mentioned processes.

LANA can act as a transcriptional activator of certain promoters and as repressors of certain promoters. The mechanism and the specificity of repression and activation of genes are not yet clearly understood. One of the major roles though, is to tether the viral DNA to the mitotic chromosomes (Ballestas et al., 1999). This is achieved when LANA binds to two 17bp nucleotide motifs, LBS1 and LBS2, located in the Terminal Repeat (TR) region of the KSHV genome via its c-terminal domain. As stated earlier, LANA can activate or repress several cellular and viral promoters (Viejo-Borbolla et al., 2003). LANA can activate cellular transcription factors like CREB, CBP, SP1 (Krithivas et al., 2000, Lim et al., 2003, Radkov et al., 2000). At the same time, LANA has also been implicated in directly binding to p53 and also p53-dependent promoters and repressing

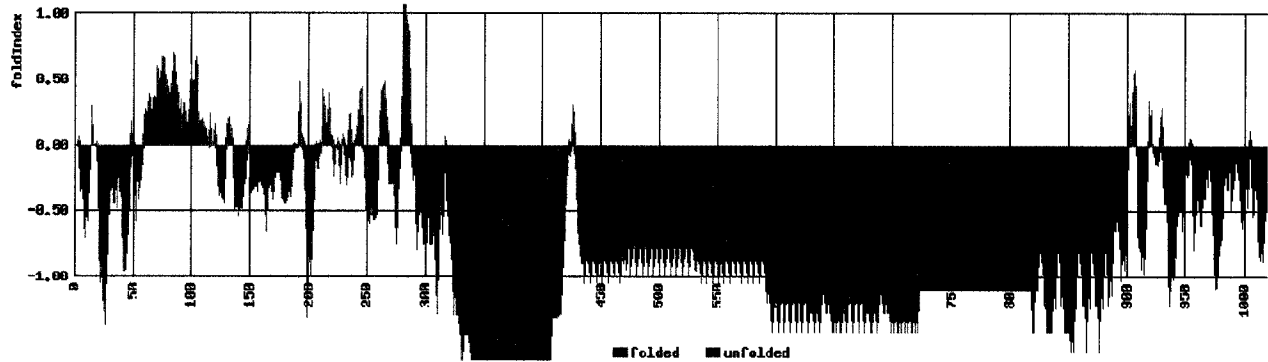
them (Friborg et al., 1999). Figure 1.9 B shows the binding sites for different nuclear proteins on LANA and other functionally important regions

LANA protein can be divided into 3 distinct domains:

1. The N-terminal 340 AA is extremely proline-rich and contains several PXXP motifs, which are potential binding sites for SH3 domain-containing proteins, a common domain seen in apoptosis-related proteins.
2. The central region contains three different highly repetitive blocks of acidic residues; similar domains often function in transcriptional activation in viral and cellular transcription factors.
3. The C-terminal domain contains a putative nuclear localization site, and partially overlapping with the central domain is a leucine zipper repeat motif.

The C-terminal region also acts as a multimerization domain, letting LANA form stable dimers. Both the N- and C-terminal regions have a putative NLS (nuclear localization sequences) and can independently localize to the nucleus (Piolot et al., 2001, Schwam et al., 2000). Amino acids 1-22 of LANA form what is called the chromosome-binding site (CBS). These 22 amino acids are essential for the interaction of LANA with the mitotic chromosomes. Their deletion inhibits the episomal maintenance of the oriP-based KSHV plasmid (Shinohara et al., 2002). Interestingly these two functions were rescued when full-length LANA was fused with H1. Mutation analysis by Barbera et al (2004) has also showed that amino acids 5 to 13 are sufficient for chromosome association.

A



B

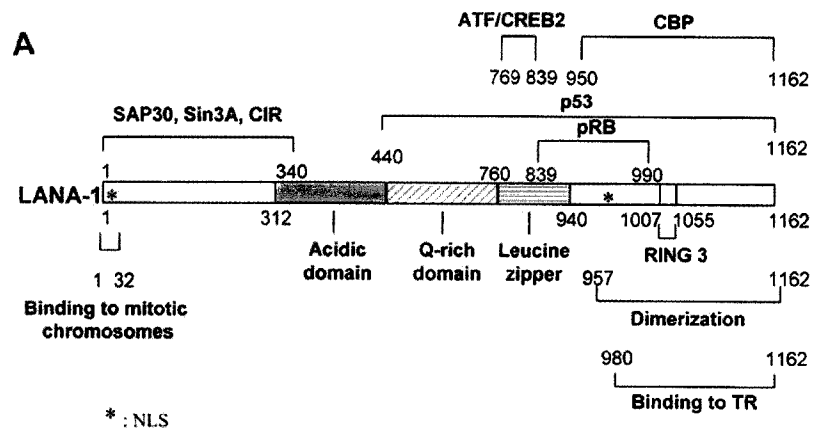


Figure 1.9: Latency Associated Nuclear Antigen.

- A. Fold-index plot (<http://bip.weizmann.ac.il/fldbin/findex>) of full-length LANA showing the folded (green) and unfolded (red) regions.
- B. Binding sites for different nuclear proteins on LANA. Adapted from (Viejo-Borbolla et al., 2003).

Residues 5 to 13 are also essential for LANA-mediated DNA replication since alanine substitutions for 5GMR7, 8LRS10, and 11GRS13 all abolished DNA replication (Barbera et al., 2004). LANA residues 5 to 13 likely associate with chromosomes via an interaction with a cell protein(s) associated with chromosomes. One of the proteins that has been proposed as a candidate cell protein through which the LANA N- terminus associates with chromosomes is MeCP2 (Krithivas et al., 2002).

Chapter II of this thesis describes a study of the binding of LANA to the nucleosome at a molecular level, and chapter III of this thesis deals with the effect of LANA binding on chromatin condensation.

1.10 Specific aims and layout of the thesis

The work outlined in this dissertation aims to investigate the structural and functional aspects of chromatin and nucleosome binding proteins. This dissertation has concentrated on studying the interaction of viral proteins like LANA and histone assembly factor like yNAP1 to mono-nucleosomes and its effect on chromatin compaction. We have used varied biophysical techniques like X-ray crystallography, analytical ultracentrifugation, fluorescence spectroscopy and atomic force microscopy to study these biological questions.

Chapter II analyzes, at molecular resolution, how the surface of the nucleosome can act as a docking station for the viral protein LANA. This chapter employs X-ray crystallography, biochemistry and cell biological techniques to determine the binding site for the viral protein. This chapter demonstrates the importance of the nucleosomal surface in chromatin compaction.

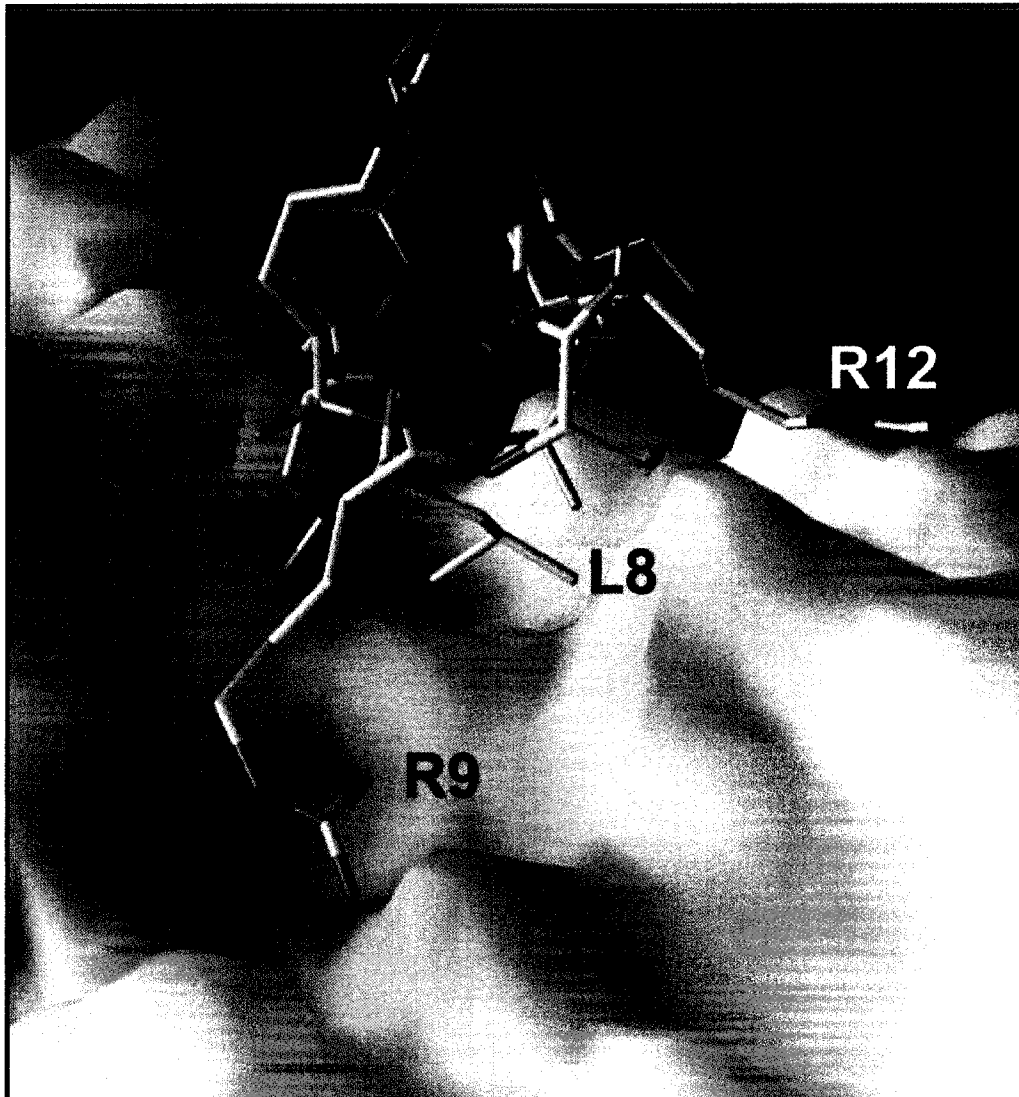
In Chapter III we used biochemical and biophysical techniques to determine the role of the nucleosomal surface in formation of higher order structures in chromatin. Using analytical ultracentrifugation and differential centrifugation studies on nucleosomal arrays, we show that changes in the nucleosomal surface either through point mutations or through binding of trans-acting proteins, leading to difference in chromatin compaction.

Chapters IV and V are directed to studying the effect of the histone chaperone yNAP1 on the nucleosomes and chromatin. In Chapter IV we show that yNAP1 can exchange histone dimers into preformed nucleosomes. We also demonstrate that yNAP1 can slide nucleosomes on a 196mer DNA from a centrally positioned to an end-

positioned state during this process. We show that the C-terminal tail of yNAP1 is essential for both these functions. We further study this C-terminal tail in detail in Chapter V where we show that this is essential for cleaning any misassembled mononucleosomes and chromatin using analytical ultracentrifugation and atomic force microscopy.

CHAPTER II

The nucleosomal surface as a docking station for Kaposi's sarcoma herpesvirus LANA



(LANA binding to the histone dimer)

This chapter was published in the journal *Science*. Andrew J. Barbera and Jayanth V. Chodaparambil were co-first authors. A.J.B. did all the cell biology and the pull-down experiments. J.V.C. did all the X-ray crystallography experiments.

ABSTRACT

Kaposi's sarcoma-associated herpesvirus latency-associated nuclear antigen (LANA) mediates viral genome attachment to mitotic chromosomes. We find that N-terminal LANA binds nucleosomes through the folded region of histones H2A-H2B. The same LANA residues were required for both H2A-H2B binding and chromosome association. Further, LANA did not bind *Xenopus* sperm chromatin, which is deficient for H2A-H2B. Binding was rescued after assembly of nucleosomes containing H2A-H2B. We also describe the 2.9 Å crystal structure of a nucleosome complexed with the first 23 LANA amino acids. The LANA peptide forms a hairpin that interacts exclusively with an acidic H2A-H2B region that is implicated in the formation of higher order chromatin structure. Our findings present a new paradigm for how nucleosomes may serve as binding platforms for viral and cellular proteins, and reveal a novel mechanism for KSHV latency.

Kaposi's sarcoma-associated herpesvirus (KSHV) has an etiological role in Kaposi's sarcoma (KS), the predominant AIDS malignancy, primary effusion lymphoma (PEL) and multicentric Castleman's disease (Cesarman et al., 1995; Chang et al., 1994; Moore and Chang, 1995; Soulier et al., 1995). KSHV persists as a multi-copy episome in latently infected tumor cells (Ballestas et al., 1999; Decker et al., 1996). Viral genomes lack centromeres, which govern faithful DNA partitioning in eukaryotic cells, and use a distinct segregation mechanism in which KSHV latency-associated nuclear antigen (LANA) tethers episomes to mitotic chromosomes. LANA is required for episome, and thus tumor, persistence and interaction with mitotic chromosomes is essential for its function. The first 22 residues comprise the dominant LANA-chromosome association region since the C-terminal domain is unable to rescue chromosome association in mutants that are deleted for or contain specific mutations within the N-terminal region (Barbera et al., 2004; Krithivas et al., 2002; Piolot et al., 2001; Shinohara et al., 2002). We therefore sought to determine the chromosome docking partner of the LANA N-terminus.

Genetic analysis of LANA's chromosome binding region was central to our strategy for characterization of putative docking partners. Transient assays have shown LANA_{5GMR7, 8LRS10}, and _{11GRS13} (Fig. 2.1A), lack chromosome association, and LANA_{14TG15}, may have reduced affinity for chromosomes (Barbera et al., 2004). To further investigate LANA_{14TG15}, we stably expressed these mutants in uninfected BJAB cells at levels similar to those of LANA in infected PEL cells. LANA (green) tightly associated with chromosomes (red) (overlay generates yellow) while LANA_{5GMR7, 8LRS10}, and _{11GRS13} (green) did not (Fig. 2.1B). LANA_{14TG15} (green) associated with

A

| | 1 | 23 | chromosome binding | episome persistence | H2A-H2B binding |
|---------|--|----|--------------------|---------------------|-----------------|
| | <p style="text-align: center;">chromosome binding</p> <p style="text-align: center;">MAPPGMRLRSGRSTGAPLTRGSC</p> | | + | + | + |
| 5GMR7 | — AAA — | | - | - | - |
| 8LRS10 | — AAA — | | - | - | - |
| 11GRS13 | — AAA — | | - | - | - |
| 14TG15 | — AA — | | +/- | +/- | +/- |
| 17PLT19 | — AAA — | | + | nd | + |
| 20RGS22 | — AAA — | | + | nd | + |

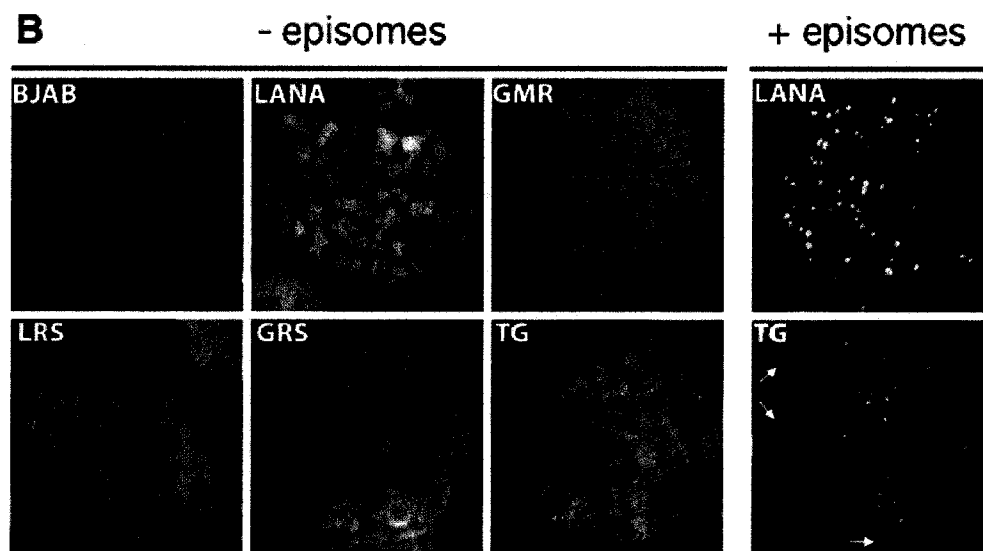


Figure 2.1. LANA N-terminus chromosome binding.

(A) LANA scanning alanine mutants with summaries for chromosome binding, episome persistence (Barbera et al., 2004), and H2A-H2B binding.

(B) Metaphase spreads of BJAB cells, and BJAB cells stably expressing LANA, LANA_{5GMR7}, -_{8LRS10}, -_{11GRS13}, or -_{14TG15}. Overlay of LANA (green) and chromosomes (red) generates yellow. Cells containing KSHV episomes are indicated. Arrows denote LANA_{14TG15} dots that have detached from chromosomes. (630X)

chromosomes (red) (overlay generates yellow), but also distributed between chromosomes, indicating weak association. We also investigated LANA_{14TG15} chromosome association in cells with KSHV episomes. In contrast to its broad distribution over chromosomes in the absence of KSHV episomes, LANA concentrates to dots along mitotic chromosomes at sites of episomes with iterated LANA binding sites, consistent with its role in tethering KSHV DNA to chromosomes (Ballestas et al., 1999; Cotter and Robertson, 1999). Although LANA dots always tightly associated with chromosomes, ~30% of mitotic cells had LANA_{14TG15} dots which were detached from chromosomes (Fig. 2.1B, arrows). Since LANA dots are sites of KSHV DNA, LANA_{14TG15} dots not associated with chromosomes indicate inefficient episome partitioning. This finding follows our previous observation that TG is deficient in supporting episome persistence (Barbera et al., 2004).

To identify N-terminal LANA's mitotic chromosome binding partner, we affinity purified interacting proteins. BJAB cells stably expressing GFP fused to LANA 1-32 (GFP LANA 1-32), or GFP fused with a nuclear localization signal (GFP NLS), were generated (Fig. 2.1C). GFP does not affect LANA's chromosome localization (Barbera et al., 2004) or its ability to mediate episome persistence (Tetsuka et al., 2004). Proteins that interacted specifically with GFP LANA 1-32 were identified by co-immune precipitation followed by mass spectrometry (Fig. 2.1D). These included large amounts of core histones H2A, H2B, H3, and H4, as well as Ku70, Ku80, PARP1, and BAB14565, a protein with high homology to the histone variant macroH2A. We determined, using knockout mouse embryo fibroblasts (MEFs), that Ku70, Ku80 and PARP1 do not mediate LANA chromosome association (Fig. S1, SOM text).

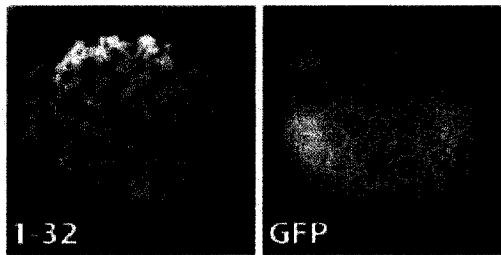
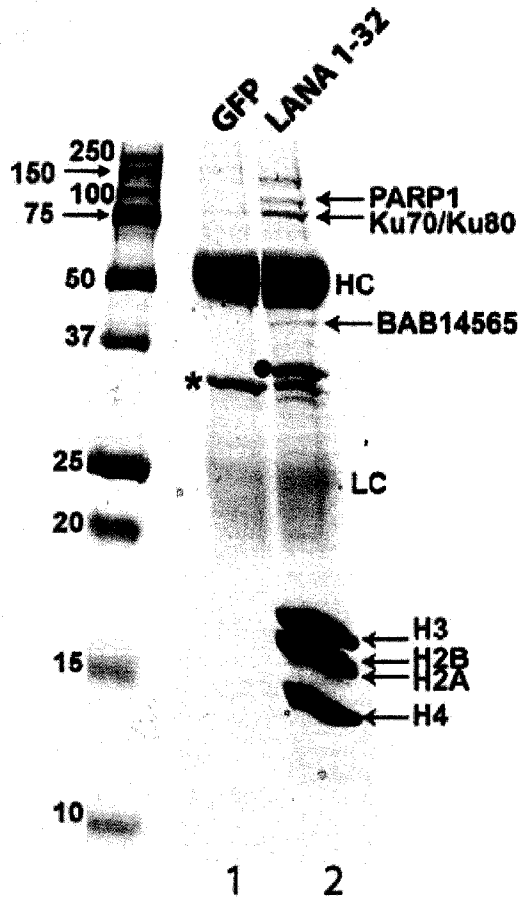
C**D**

Figure 2.1. LANA N-terminus chromosome binding.

(C) Metaphase BJAB cells stably expressing GFP NLS or GFP LANA 1-32. (630X)

(D) Proteins co-precipitating with GFP LANA 1-32 (lane 2) were identified after resolution in a 4-16% gradient gel. HC, heavy chain; LC, light chain; (*), GFP; (●), GFP LANA 1-32. The intense histone Coomassie staining is due to their arginine-rich nature and the stoichiometry of histones within nucleosomes.

The diffuse distribution of the LANA N-terminus over mitotic chromosomes and the efficient precipitation of core histones strongly suggested that core histones mediate LANA chromosome docking. To further investigate this possibility, we assayed whether N-terminal LANA bound histones during mitosis. GFP LANA 1-32 was immune precipitated from asynchronous cells (~5% mitotic) (Fig. 2.2A, lane 2), or from metaphase arrested cells (~85% mitotic) (Fig. 2.2A, lane 5). Despite the 17 fold difference in mitotic index, core histones precipitated similarly from asynchronous and metaphase-arrested cells. These results indicate LANA associates with core histones throughout most or all of the cell cycle.

We determined whether full-length LANA also associated with core histones. GFP LANA 1-32 and GFP LANA, but not GFP NLS, efficiently precipitated core histones after expression in COS cells (Fig. 2.2B). We also investigated LANA's association with core histones in KSHV-infected BCBL-1 PEL cells. After incubation with anti-LANA monoclonal antibody or polyclonal serum, histone H2B was precipitated from BCBL-1 cells, but not uninfected BJAB cells (Fig. 2.2C, D). Therefore, LANA interacts with core histones in KSHV-infected tumor cells.

We investigated whether the LANA N-terminus directly binds nucleosome core particles (NCPs), which consist of two copies each of core histones H2A, H2B, H3 and H4, organizing ~147 bp of DNA (Luger et al., 1997). GST LANA 1-23, but not GST, directly bound and precipitated purified nucleosomes (Fig. 2.2E). Further, GST LANA 1-23 supershifted recombinant nucleosomes in a native gel (Fig 2.2F).

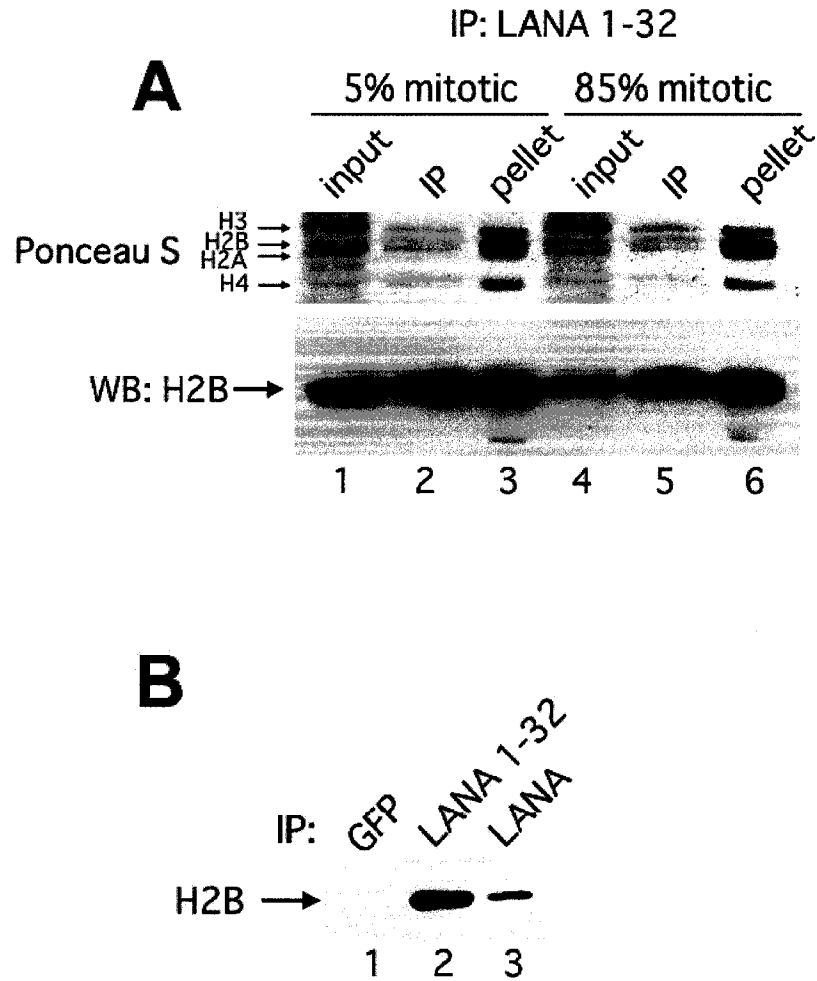


Figure 2.2. Core histones interact with residues critical for LANA chromosome binding.

(A) GFP LANA 1-32 was immune-precipitated from asynchronous or metaphase-arrested BJAB cells and proteins detected by Ponceau S (above) or H2B immunoblot (below). Input, 3%; Pellet, 10%.

(B) GFP NLS, GFP LANA 1-32, or GFP LANA were immune-precipitated from COS cells, and H2B detected by immunoblot. GFP LANA 1-32 is expressed at higher levels than GFP LANA, accounting for the greater amount of precipitated H2B in lane 2.

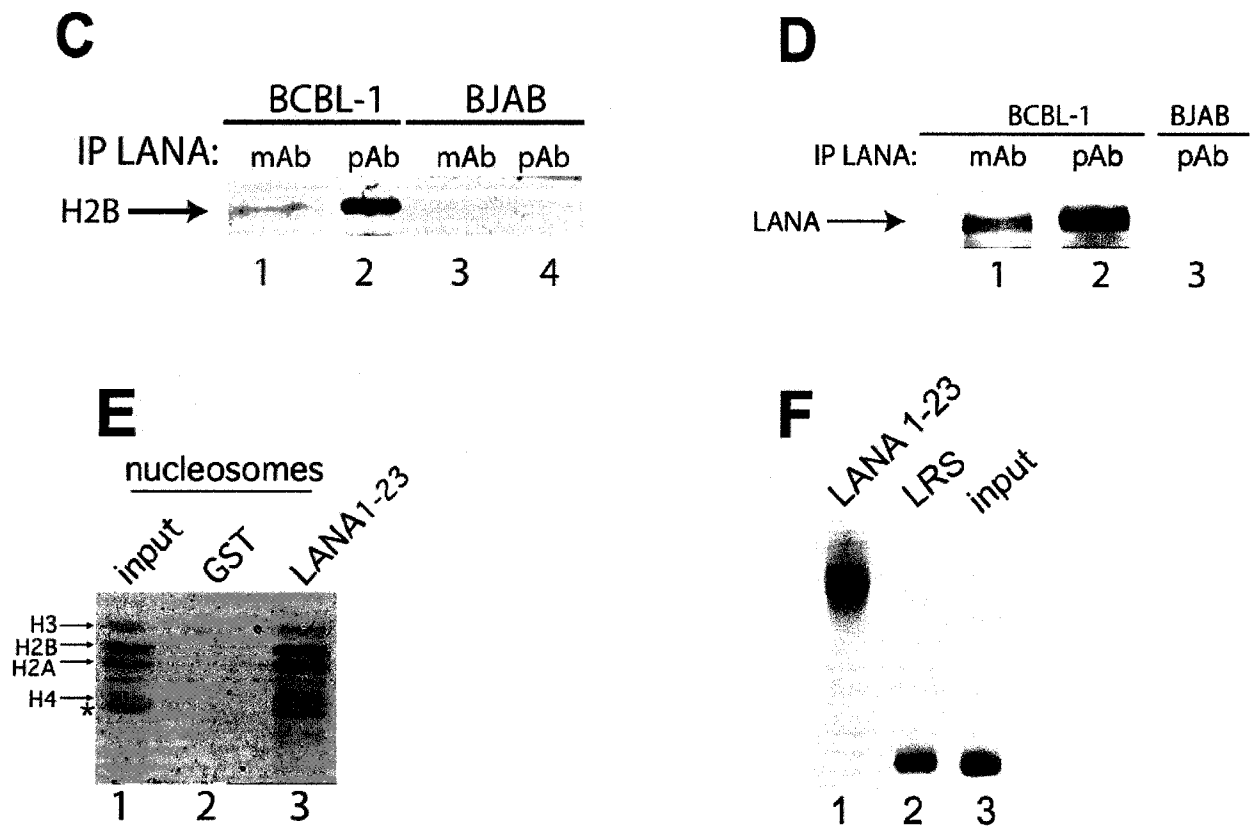


Figure 2.2. Core histones interact with residues critical for LANA chromosome binding.

(C) Immune precipitations were performed from KSHV-infected BCBL-1 or uninfected BJAB cells using anti-LANA monoclonal antibody (mAb) or polyclonal serum (pAb). H2B was detected by immunoblot. The increased H2B signal obtained with polyclonal serum was due to more efficient LANA precipitation with this antibody (D).

(D) LANA immunoblot of extracts from (C).

(E) H1-depleted nucleosomes were incubated with GST or GST LANA 1-23, and precipitated histones detected by Coomassie. Input, 30%.

(F) Nucleosomes were incubated with GST LANA 1-23 or GST LANA LRS, resolved by 5% native PAGE, and detected by Coomassie.

Experiments investigated whether core histones interact with LANA residues necessary for chromosome association. GFP LANA 1-32 and GFP LANA ₂₀RGS₂₂, which associate with chromosomes, precipitated core histones from COS cells, while GFP LANA ₅GMR₇, which does not associate with chromosomes, did not (Fig. 2.2G). Further, GST LANA 1-23 ₁₇PLT₁₉ and ₂₀RGS₂₂ bound purified nucleosomes and those from BJAB cell extracts (Figs. 2.2H, Fig. S2). In contrast, GST LANA 1-23 ₅GMR₇, ₈LRS₁₀, and ₁₁GRS₁₃, substituted at residues essential for chromosome binding, did not bind histones (Fig. 2.2F, 2.2H; Fig. S2). GST LANA 1-23 ₁₄TG₁₅ bound nucleosomes at a reduced level (Figs. 2.2H, Fig. S2), similar to the reduced chromosome binding with this mutation (Fig. 2.1B). Thus, the same LANA residues are critical for histone and chromosome binding, providing strong evidence that core histones mediate LANA chromosome attachment.

We next investigated through which histones the LANA N-terminal region binds nucleosomes. GST LANA 1-23 and GST were incubated with acid-extracted histones, which contain core histone H2A-H2B dimers and H3-H4 tetramers. GST LANA 1-23 precipitated histones H2A and H2B, but not H3 and H4 (Figure 2.3A). GST did not bind histones. Antibody that detects both histones H1 and H2B confirmed the H2B binding and demonstrated that GST LANA 1-23 does not bind linker histone H1 (Fig. 2.3B). Experiments also investigated whether LANA bound the tails or folded domain of H2A-H2B. GST LANA 1-23 precipitated both recombinant full-length H2A-H2B and tailless H2A-H2B (Fig. 2.3C). These results indicate that the LANA N-terminus specifically binds nucleosomes through the folded domain of H2A-H2B.

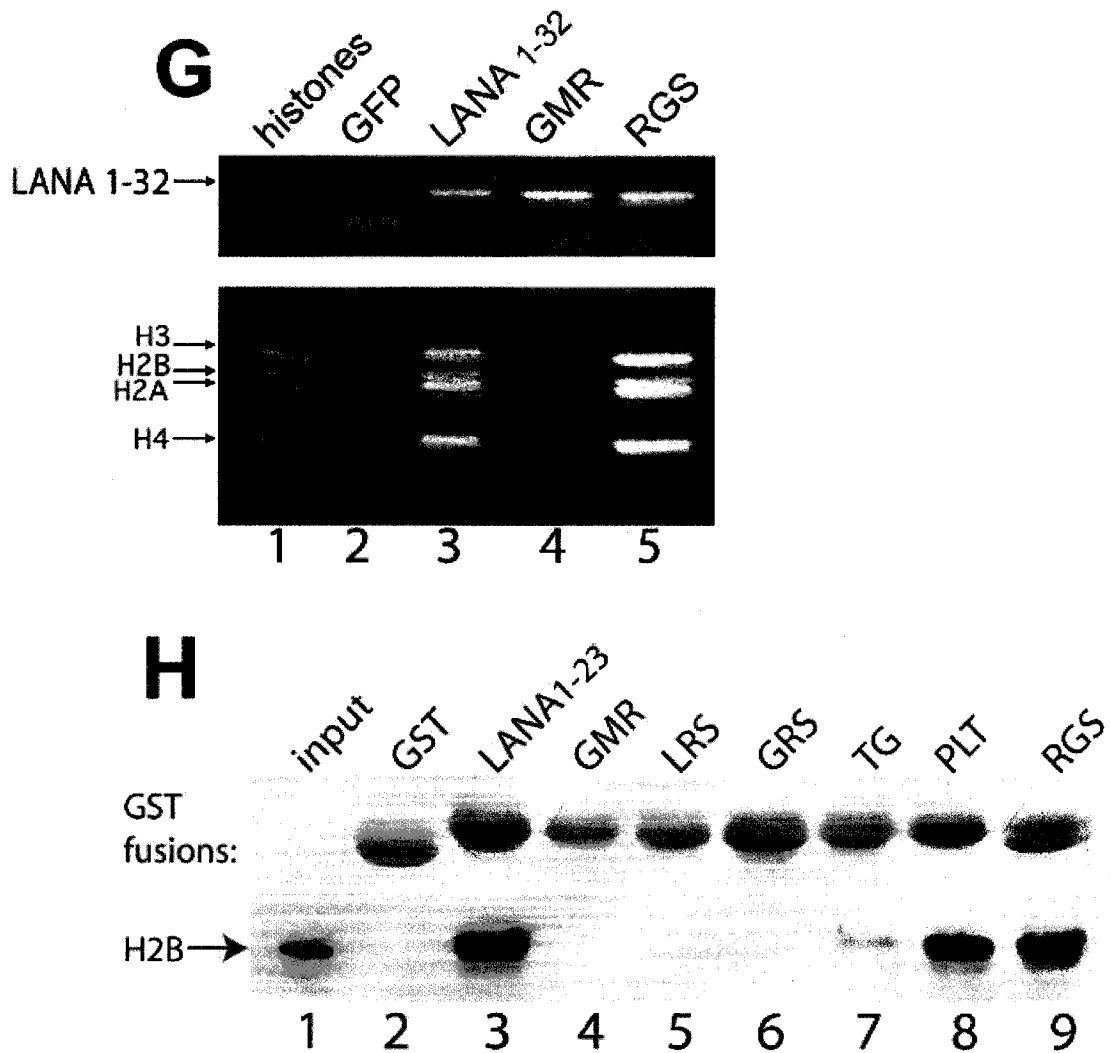


Figure 2.3 Core histones interact with residues critical for LANA chromosome binding.

(G) Proteins immune-precipitated by GFP or GFP fusions were detected by SYPRO Ruby. Lane 1, purified histones.

(H) GST fusion proteins were incubated with H1-depleted nucleosomes. GST fusions were detected by Coomassie, and precipitated H2B detected by immunoblot.

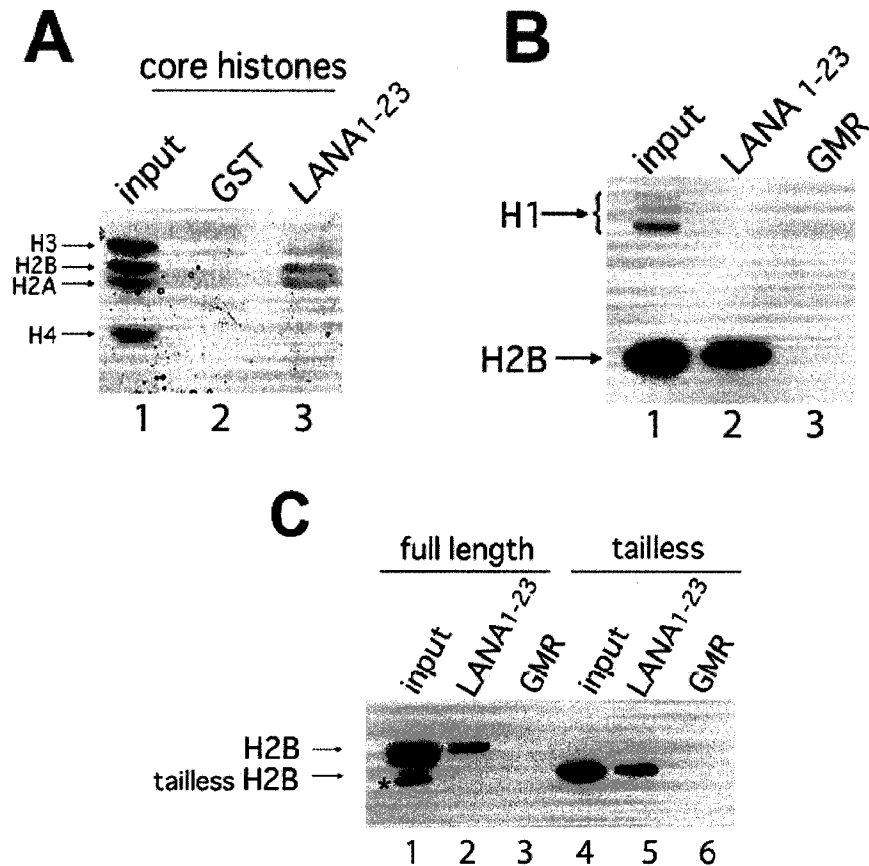


Figure 2.3 Histones H2A-H2B are essential for LANA N-terminal chromosome binding.

(A) GST or GST LANA 1-23 was incubated with purified histones, and bound histones detected by Coomassie. Lane 1, 30% input.

(B) GST LANA 1-23 or GST LANA 1-23 _{5GMR7} was incubated with purified histones, and precipitated H1 and H2B detected by immunoblot. Lane 1, 30% input.

(C) GST LANA 1-23 or GST LANA 1-23 _{5GMR7} was incubated with full-length or tailless H2A-H2B dimers, and precipitated H2B detected by immunoblot. Input, 30%.

(*), degradation product.

We wished to directly demonstrate that the LANA N-terminus uses H2A-H2B to bind chromosomes. We utilized Xenopus laevis sperm chromatin, which is naturally deficient in H2A-H2B, and instead contains sperm-specific basic proteins X and Y. In addition, Xenopus sperm lack H1 (Murray, 1991; Philpott and Leno, 1992; Philpott et al., 1991). Upon incubation with high speed supernatant (HSS) from Xenopus egg lysate, egg cell-derived nucleoplasmin protein mediates sperm chromatin decondensation and replacement of X and Y with egg H2A-H2B dimers. To verify LANA chromosome binding in this system, HSS-treated chromatin, which contains wild-type H2A-H2B dimers, was incubated with GST fusions. GST LANA 1-23 bound sperm chromatin that had undergone H2A-H2B deposition through HSS treatment, but GST LANA 1-23_{5GMR7} and GST did not (Fig. 2.3D). No LANA protein precipitated in the absence of chromatin. Therefore, N-terminal LANA binds Xenopus chromosomes after H2A-H2B deposition.

We wished to stringently assay whether H2A-H2B were required for LANA chromosome binding. HSS contains other factors in addition to H2A-H2B and nucleoplasmin. We therefore employed a purified system with nucleoplasmin and recombinant H2A-H2B dimers in place of HSS. GST LANA 1-23 did not bind H2A-H2B-deficient sperm chromatin that had been treated with buffer or with purified nucleoplasmin alone. However, after incubation with nucleoplasmin and recombinant histone H2A-H2B dimers, which allows for deposition of histones H2A-H2B into sperm chromatin, GST LANA 1-23 specifically bound sperm chromatin (Fig. 2.3E). Thus, H2A-H2B is essential for LANA chromosome binding.

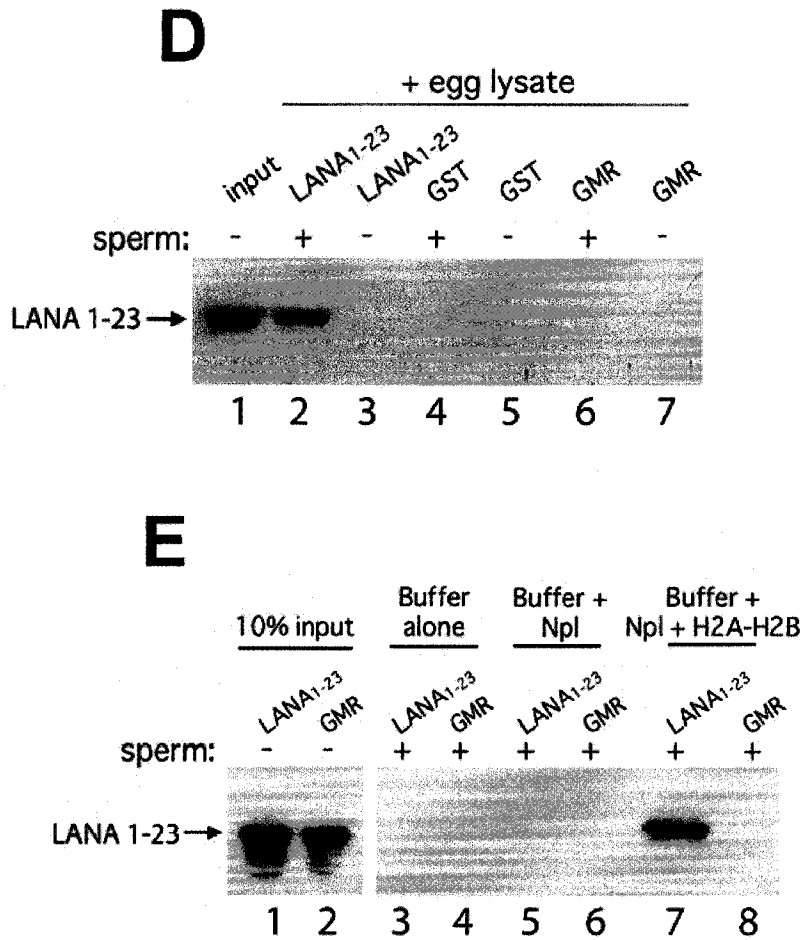


Figure 2.3 Histones H2A-H2B are essential for LANA N-terminal chromosome binding.

(D) GST, GST LANA 1-23, or GST LANA 1-23 ₅GMR₇, was incubated with or without *Xenopus* HSS-treated sperm chromatin, and chromatin-bound GST proteins detected by immunoblot. Input, 10%.

(E) GST LANA 1-23 or GST LANA 1-23 ₅GMR₇ was incubated with *Xenopus* sperm chromatin in buffer alone, with purified nucleoplasmin (Npl), or with nucleoplasmin plus H2A-H2B dimers. Chromatin-bound GST proteins were detected.

We solved the X-ray crystal structure of LANA residues 1-23 complexed with the NCP. Data collection and refinement statistics are summarized in Table S1. Fig. 2.4A shows a 2Fo-Fc map of the final model of the LANA peptide, contoured at 2σ . LANA forms a tight hairpin that is stabilized by five intra-molecular hydrogen bonds (three β -type interactions, and two side-chain/main chain interactions; Fig. 2.4A and C) and by numerous hydrogen bonds and van der Waals contacts with the nucleosomal surface (below).

Consistent with the biochemical experiments (Fig. 2.3A-C), the LANA peptide interacts exclusively with the H2A-H2B dimer within the nucleosome (Fig. 4B). Histone fold regions and extensions of H2A and H2B are implicated in the interaction, but not the flexible histone tails. The hairpin is wedged between the α C and α 1 helix of H2B (Fig. 2.4C); the turn of the hairpin abuts the H2A docking domain that forms a major interaction interface between the H2A-H2B dimer and the (H3-H4)₂ tetramer (Luger and Richmond, 1998b). The L1 loop of H2B as well as the α 2 and α 3 helices of H2A are also involved in LANA binding, consistent with the requirement for a folded (H2A-H2B) dimer for LANA binding. Molecular details of the interactions between LANA and the nucleosome are shown in Fig. S3 (SOM text). Substitution of individual LANA amino acids 5-16 demonstrated that residues important for chromosome association (Fig. S4, SOM text) have critical roles in the interaction between LANA and the NCP. Of note, the overall structure of the nucleosome is maintained upon LANA binding (Fig. 2.4B).

Table S1: X-ray refinement statistics

| | |
|-----------------------------------|-------------|
| Resolution (Å) | 50-2.9 |
| $R_{\text{work}}/R_{\text{free}}$ | 0.22 / 0.28 |
| Number of atoms | 12466 |
| Protein ^(a) | 5986 |
| DNA | 6272 |
| Ligand (LANA) ^(a) | 100 |
| Water | 66 |
| B-factors | |
| Protein | 39.4 |
| DNA | 89.6 |
| Ligand (LANA) | 76.1 |
| Water | 31.41 |
| R.m.s deviations | |
| Bond lengths (Å) | 0.013 |
| Bond angles (°) | 1.51 |

^(a) Residues included in each histone subunit: H3: 38 – 135, H3': 38-135, H4: 19-102, H4': 24-102, H2A: 14-120, H2A': 14-120, H2B: 30-122, H2B': 30-122, LANA: 4-17. The remaining histone tails and LANA regions were too disordered to be included in the final model.

A

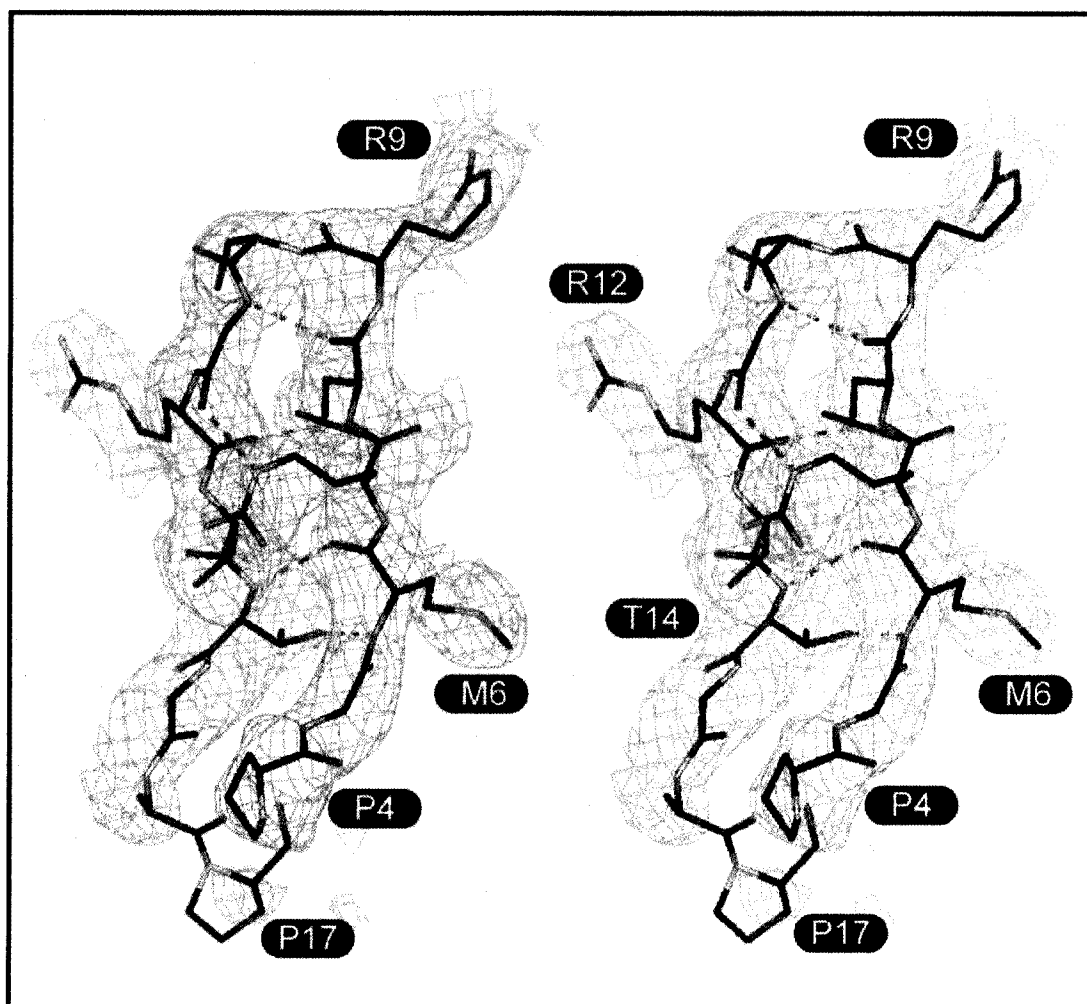


Figure 2.4 Structure of the LANA – nucleosome complex.

A) Stereo view of a section of the final 2fo-Fc electron density map calculated at 2.9 Å and contoured at 2 σ , depicting the LANA peptide. The intramolecular hydrogen bonds are represented as red dots.

B

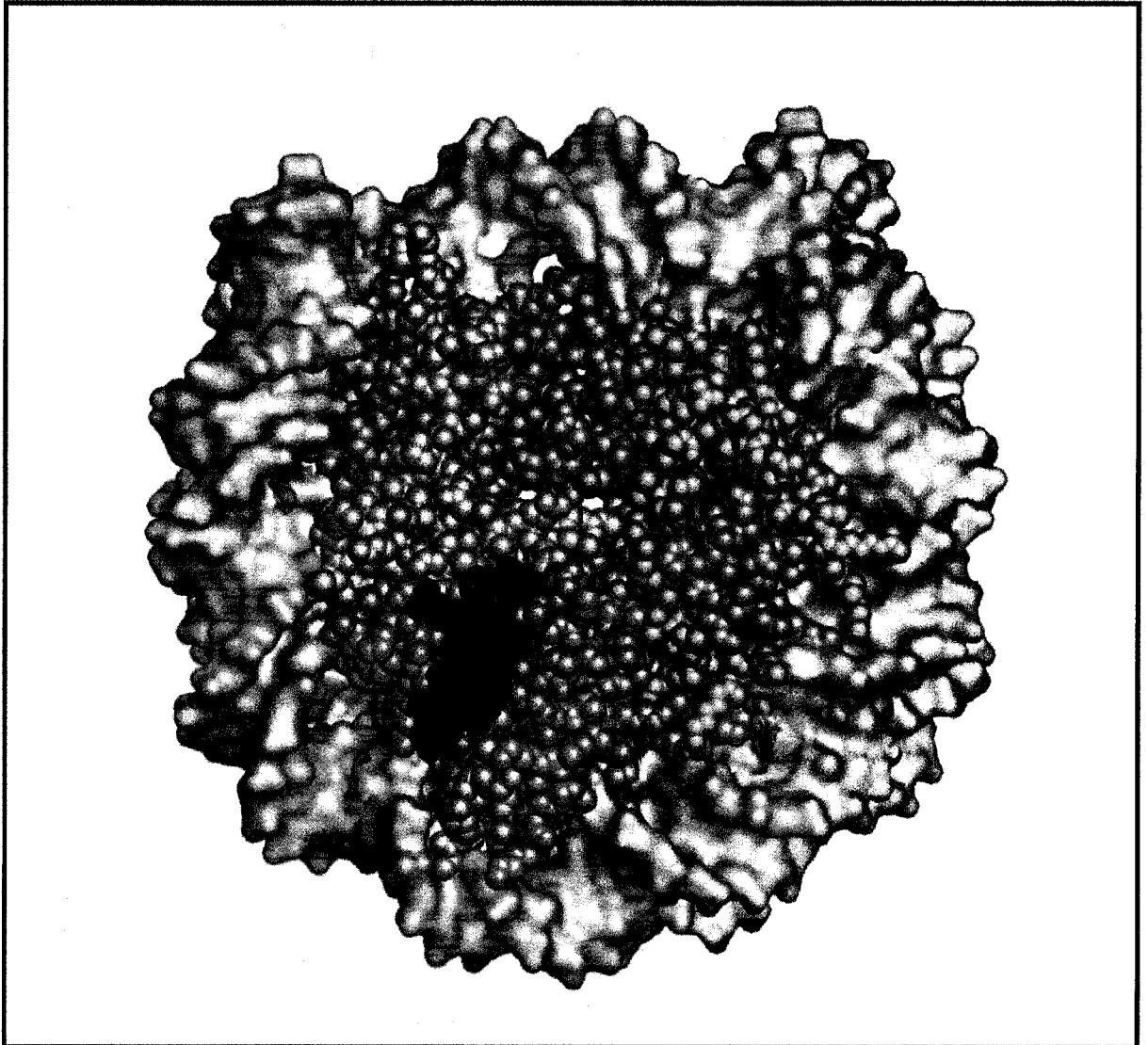


Figure 2.4 Structure of the LANA – nucleosome complex.

B) Space-filling representation of the nucleosome-LANA complex. H2A is shown in yellow, H2B in red, H3 in light blue, H4 in green and LANA in dark blue. DNA is silver.

Interactions of LANA with the NCP resemble those between the NCP and the H4 N-terminal tail from a neighboring nucleosome within the crystal lattice (Fig. 2.4D) (Davey et al., 2002). Both peptides interact with the same conserved acidic patch comprised of several residues from H2A and H2B on the highly contoured nucleosomal surface (Luger and Richmond, 1998a). Despite a lack of sequence homology between the LANA peptide and the N-terminal tail, many of the targeted residues in H2A and H2B are the same (see LANA Arg 9 and H4 Arg 19 in Fig. 2.4C and 2.4D, respectively). The interaction shown in Fig. 2.4D is essential for nucleosome crystallization (Luger et al., 1997), and biophysical experiments have indicated a unique role for the H4 tail and acidic patch interaction in the formation of chromatin higher order structure (Dorigo, 2003; Fan et al., 2004).

Analysis of the molecular surfaces of both the LANA peptide and the H2A-H2B dimer demonstrates excellent shape- and charge- complementarity (Fig. 2.4E), indicating that the LANA N-terminal region has evolved to recognize this region within the NCP with high specificity. LANA Arg 9 and Ser 10 point into the acidic pocket formed by H2A and H2B, and hydrophobic LANA residues are inserted deep into a cleft delineated by the α C helix of H2B (Fig. 2.4F). The LANA-peptide interaction buries 1340 \AA^2 , well within the range that is considered to be a stable interaction (Jones and Thornton, 1996), and which is significant considering that only fourteen residues of LANA contribute to the interaction. For comparison, the molecular surface buried by the H4 tail – NCP interaction (Fig. 2.4D) is only 680 \AA^2 and contains larger cavities.

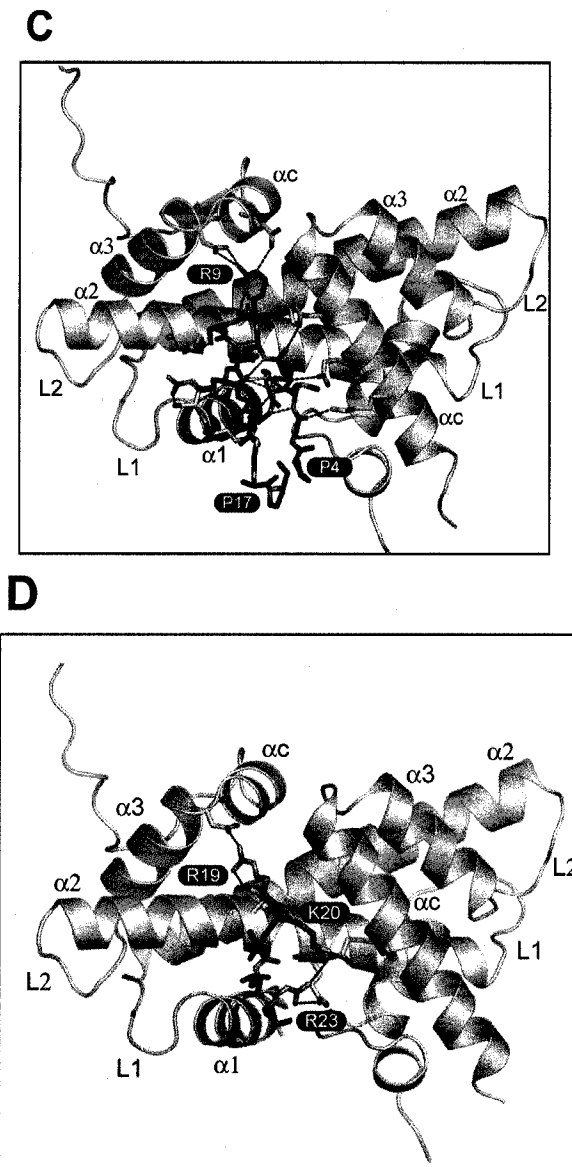


Figure 2.4 Structure of the LANA – nucleosome complex.

C) Overview of LANA interaction with the H2A-H2B dimer within the NCP. Only H2A (yellow ribbon), H2B (red ribbon), and LANA (blue sticks) are shown. Intramolecular and intermolecular bonds are shown as red and blue dashes, respectively. Secondary structural elements in the histones are indicated. D) Crystal contact between the H4 tail and the H2A-H2B dimer. Orientation and coloring of H2A and H2B is shown as in C), the H4 tail is shown in green.

E

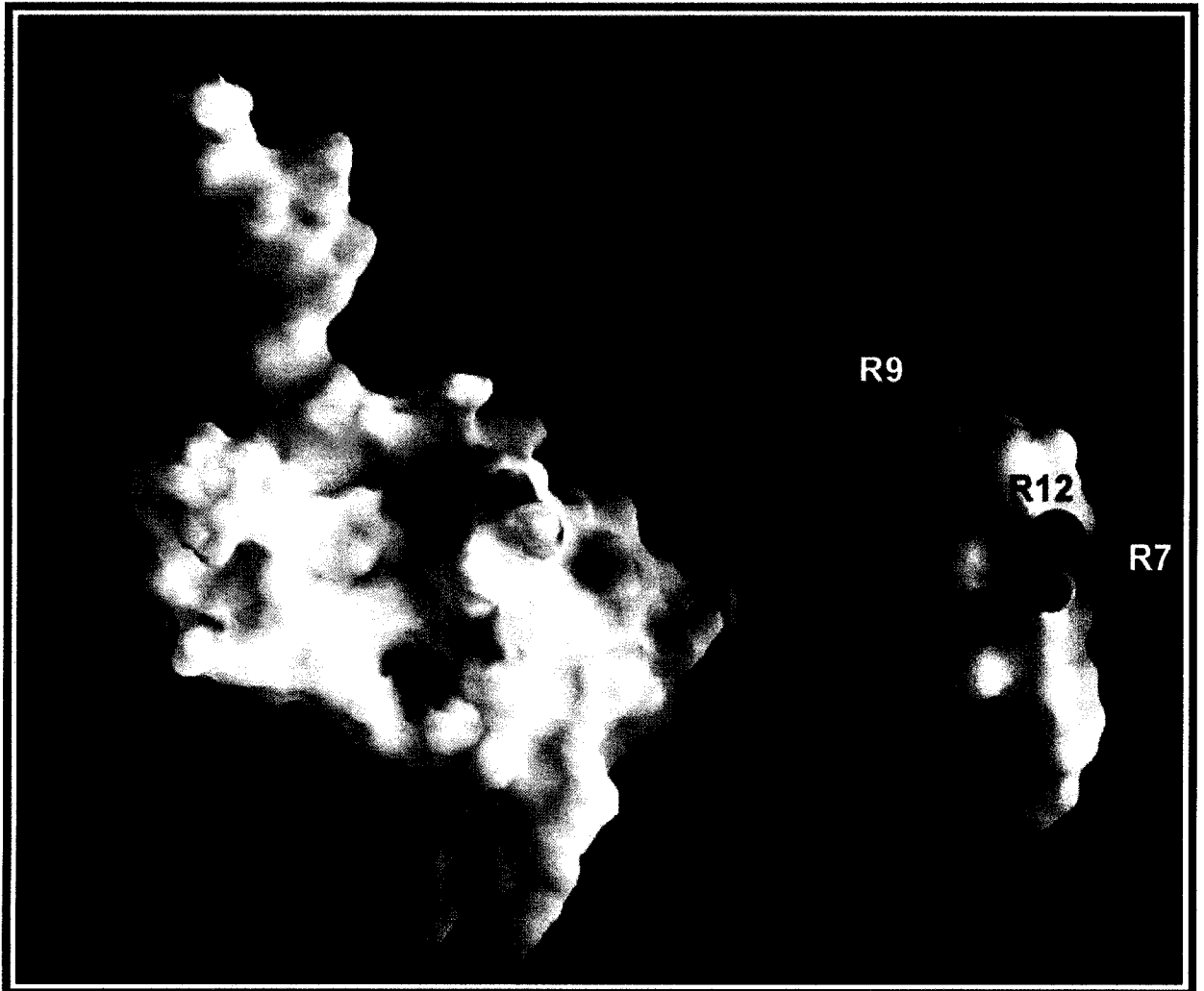


Figure 2.4 Structure of the LANA – nucleosome complex.

E) LANA recognizes distinct features of the nucleosomal surface. Charged surfaces (red – negatively charged / blue – positively charged) were calculated with GRASP (35). The H2A-H2B dimer (left) and LANA are shown individually; LANA has been rotated by 90° along the y axis. The H2A-H2B dimer is in approximately the same conformation as in Fig 4C.

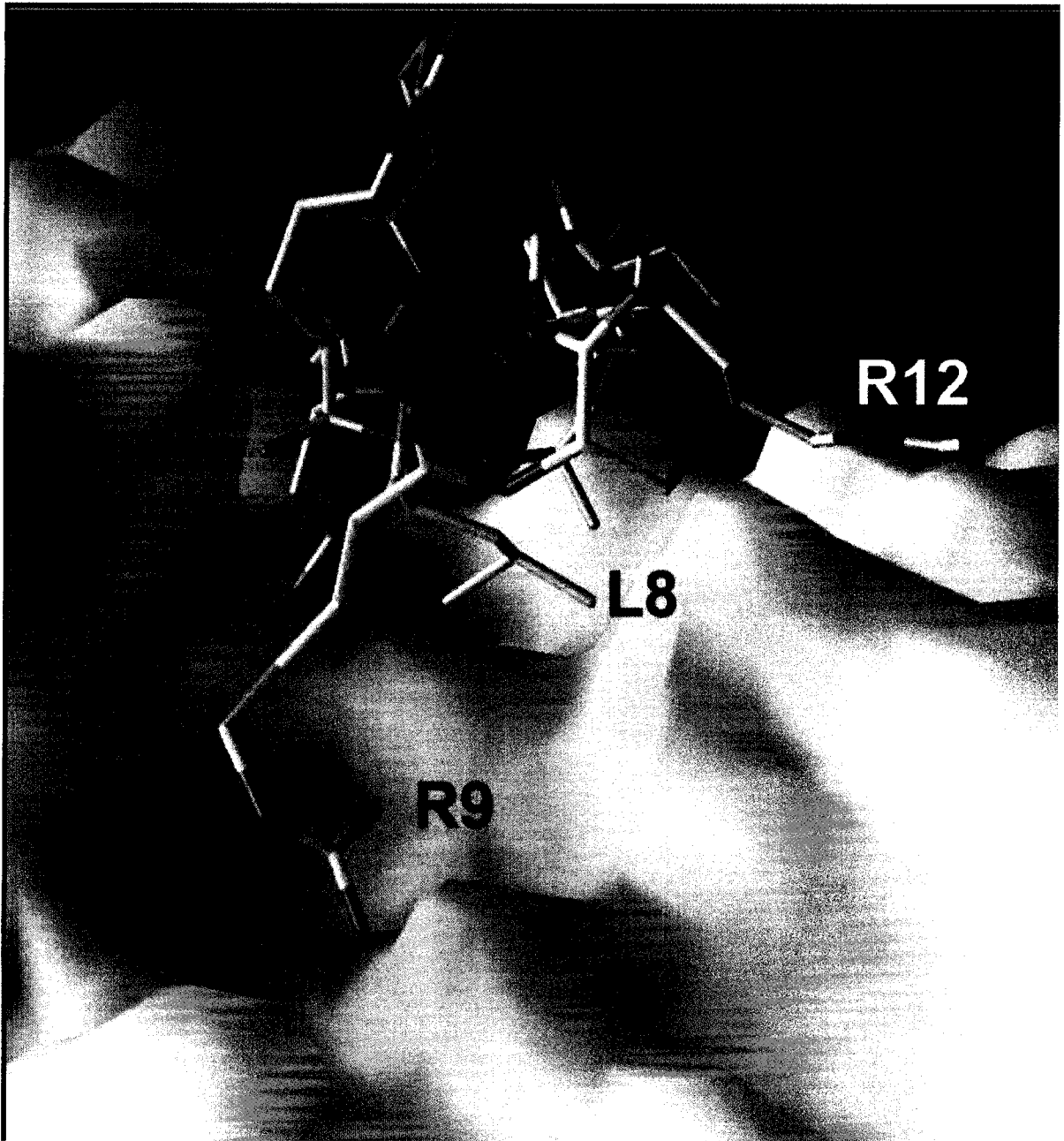


Figure 2.4 Structure of the LANA – nucleosome complex.

F) Top view of LANA bound to the histone dimer within the NCP (rotation by 90° around y , and 180° around x with respect to the view in E). Only the H2A-H2B dimer (charged surface) and LANA (stick model) are shown.

This work demonstrates that LANA's N-terminal chromosome association is mediated by H2A-H2B, and not by the earlier proposed candidates methyl-CpG binding protein 2 (MeCP2) or H1 (Cotter and Robertson, 1999; Krithivas et al., 2002). It was previously reported that LANA did not associate with murine chromosomes unless human MeCP2 was co-expressed (Krithivas et al., 2002). In contrast, we found that LANA bound murine chromosomes (Fig. S1); MeCP2 was not identified from our affinity purification. Histone H1 did not bind the LANA N-terminus, and was not required for LANA to bind *Xenopus* chromatin (Fig. 2.3B,E). These results also differ from proposed chromosome binding mechanisms for other episome maintenance proteins. Epstein-Barr virus EBNA1 binds chromosomes through the nucleolar EBP2 protein or AT hooks and bovine papillomavirus E2 through the bromodomain protein Brd4 (Kapoor et al., 2001; Sears et al., 2004; You et al., 2004).

This work may also link H2A-H2B binding to LANA's transcriptional regulatory effects (Krithivas et al., 2000; Renne et al., 2001). An intriguing possibility is that LANA may affect transcription by regulating transient H2A-H2B removal from nucleosomes through complexes such as FACT or NAP-1 (Orphanides et al., 1998; Park et al., 2004). Histone modifications regulate transcription and may also affect LANA's affinity for nucleosomes and effects on chromatin, although experiments with bacterially expressed protein (Figs. 2.2, 2.3, 2.4) indicate that histone modifications are not required for binding.

This work indicates a role for H2A-H2B in LANA-mediated DNA replication and episome persistence, since these functions are dependent on N-terminal LANA chromosome binding(Barbera et al., 2004). Interestingly, H1 in place of the LANA or EBNA1 chromosome association domain restored episome persistence, whereas H2B and H3, respectively, did not, perhaps due to positional restrictions related to the covalent linkage (Hung et al., 2001; Sears et al., 2004; Shinohara et al., 2002; Yates et al., 1985). Of note, LANA has a C-terminal chromosome association domain but it cannot rescue chromosome binding of N-terminal mutated LANA (Fig. 2.1B, (Barbera et al., 2004; Shinohara et al., 2002) and does not have a detectable role in episome persistence (manuscript in preparation). The distribution of H2A-H2B throughout chromosomes provides a platform through which LANA-tethered episomes can efficiently segregate to progeny nuclei. Strategies which interrupt the interaction between LANA and H2A-H2B may provide effective treatment and prevention of KSHV-associated diseases.

The x-ray crystal structure shows that a hairpin formed by KSHV LANA residues 5-13 interacts with eukaryotic chromatin by binding to an acidic patch formed by H2A-H2B within the nucleosome. Thus, LANA has evolved to utilize the differentially charged and contoured surface of the nucleosome as a “docking station” for episome attachment. The concept of the nucleosomal surface (as opposed to the flexible histone tails) as an interaction platform has been proposed earlier (Dorigo, 2003; Luger et al., 1997; Park et al., 2002; Suto et al., 2000; van Leeuwen et al., 2002); we now report the first structure of a protein complexed with the nucleosome. It appears that an important function of histones, in addition to maintaining interaction with other histones to form the octamer, and to compacting genomic DNA, is to maintain a distinct surface landscape

that is utilized as a docking platform by cellular and viral factors. Such interactions may locally affect nucleosome dynamics, and/or alter chromatin higher order structure, with profound implications for transcription of underlying DNA regions.

Acknowledgements

Hela nucleosomes were a gift of Xi He, Payo Pascual-Ahuir Giner, and Robert Kingston. PARP1 and Ku80 knockout MEFs were generously provided by Jae Jung and Andre Nussenzweig, respectively. We thank Pannyun Yiu for assistance with sperm chromatin experiments, Elliott Kieff for helpful discussions, Pamela Dyer and Olve Peersen for technical assistance, and Rajeswari Edayathumangalam and Srinivas Chakravarthy for help with data collection and structure determination. We thank Aaron Straight and Tim Mitchison for the plasmid encoding H2A-H2B used in the chromatin binding experiments. This work was supported by grant CA82036 (to KMK) from the National Cancer Institute, and grants GM067777 (to KL) and GM62267 (to JCW) from the National Institute of General Medical Sciences. Coordinates have been deposited at the PDB database (entry code 1ZLA).

Supporting Materials

2.3 Methods

Plasmids, cell lines, and microscopy. GFP NLS (Hung et al., 2001) has the green fluorescent protein (GFP) gene fused to a nuclear localization signal (NLS). GFP LANA 1-32 contains the indicated LANA amino acids downstream of GFP (Barbera et al., 2004). GST LANA 1-23 has the indicated LANA residues downstream of GST in the vector pGEX-KG (Guan and Dixon, 1991). Scanning alanine substitutions within GST LANA 1-23 were generated by PCR mutagenesis and sequence confirmed. Point mutations within LANA 1-32 were generated by QuickChange Mutagenesis II kit (Stratagene) and sequence confirmed. BJAB B lymphoma cells stably expressing GFP NLS or GFP LANA 1-32 were generated using neomycin. BJAB cells stably express FLAG epitope-tagged wild-type LANA (Ballestas et al., 1999) or LANA with alanine substitution mutants (Barbera et al., 2004). Ku80^{+/-}, Ku80^{-/-} (Nussenzweig et al., 1996), PARP1^{-/-} and PARP1^{+/+} (Gwack et al., 2003) MEFs were described. BJAB cells were transfected as described (Barbera et al., 2004) and adherent cells were transfected with Lipofectamine 2000 reagent (Invitrogen). Metaphase spreads and confocal microscopy were performed as described (Barbera et al., 2004), except cells were cytopun onto glass slides.

Immune precipitations and protein detection. For affinity purification, 1×10^9 BJAB cells expressing GFP LANA 1-32 or control GFP NLS were lysed in 40 mL of IP buffer (50 mM HEPES pH 7.2, 250mM NaCl, 10% glycerol, 2mM EDTA, 1% NP-40, 0.1 mM PMSF, 1 μ g/mL aprotinin, 1 μ g/mL leupeptin, and 0.7 μ g/mL pepstatin) at 4°C with brief

sonication. Protein was precipitated with anti-GFP polyclonal serum (Clontech) followed by protein G bead capture. Gel slices were analyzed by tandem mass spectrometry at Partners HealthCare Center for Genetics and Genomics (HPCGG).

Lysis for smaller scale immune precipitations was performed with IP buffer and lysates were supplemented with 5mM MgSO₄ and 2mM CaCl₂ and incubated with 50 µg DNase I (Sigma) at 4°C x 45 min, prior to the addition of antibody. DNase I treatment was again performed on collected protein G beads. DNase I cleaves DNA between nucleosomes but does not disrupt mononucleosomes, and limits nonspecific co-precipitations bridged by DNA. Anti-H2B (and anti-H1) antibody (Upstate) at 1:1000 dilution was used in conjunction with HRP-conjugated secondary antibodies (Southern Biotechnology) and ECL reagents (Perkin Elmer). Alternatively, protein was detected with Coomassie Brilliant Blue G250 or Sypro RUBY (Molecular Probes).

GST fusion protein binding assays. GST fusion proteins were expressed in *E. coli* and collected on glutathione sepharose beads (Amersham). Full-length H2A-H2B dimers and tailless H2A-H2B dimers (H2A, residues 13-118; H2B, residues 27-122) were purified from *E. coli* (Luger et al., 1999). GST precipitations were performed in precipitation buffer (150 mM NaCl, 50mM Tris-pH 7.5, 10% glycerol, 0.1% NP-40, 0.5 mM DTT, 1µg/mL aprotinin, 1 µg/mL leupeptin, and 0.7 µg/mL pepstatin) overnight at 4°C, and washed in above buffer supplemented to 250mM NaCl. For GST precipitations from cell extracts, BJAB cells were lysed in IP lysis buffer, pre-cleared with GST beads, and incubated overnight at 4°C with GST fusion proteins, with DNase treatment. For gel shift assays, recombinant NCPs, prepared as described (Dyer et al., 2004), were

incubated with 5-fold excess of GST fusion proteins for 10 hours at 4° C in buffer (20mM Tris pH 7.5, 1mM EDTA, 1mM DTT) and analyzed by 5% native PAGE.

Xenopus laevis sperm chromatin binding assays. Xenopus laevis sperm were obtained and demembrated nuclei prepared (Walter and Newport, 1997; Walter, 2000). Xenopus eggs were lysed and high speed supernatant (HSS) generated. Adenosine triphosphate (ATP)-regeneration system(Smythe and Newport, 1991), nocodazole (3µg/mL), and GST fusion proteins (30 ng/µl) were added to HSS and the extract was then clarified by centrifugation at 6000 x g for 5 minutes. Sperm chromatin was added to 10 µl of the clarified extract at a concentration of 5000 nuclei equivalents per µl and incubated for 30 minutes at 22°C. Chromatin was isolated through a sucrose cushion as described (Takahashi et al., 2004). GST was detected by immunoblot with anti-GST antibody (Covance).

For decondensation reactions using purified factors, sperm chromatin was incubated in Buffer D (50mM HEPES-KOH pH 7.8, 75 mM K-Acetate, 0.5 mM spermidine, 0.15 mM spermine, 1 mM EGTA) (Philpott and Leno, 1992) for 30 min. at 22°C. Where indicated, histone H2A-H2B dimers (40ng/µl) and nucleoplasmin (900ng/µl) purified from Xenopus laevis eggs were added. H2A-H2B dimers were expressed from a bicistronic vector in E. coli and purified using HiTrap SP FF columns (Pharmacia).

X-ray crystal structure. Crystals of the NCP reconstituted with a palindromic 146mer DNA fragment derived from human α -satellite DNA (Luger et al., 1997) were incubated

with chemically synthesized LANA 1-23 (₁MAPPGMRLRSGRSTGAPLTRGS₂₃). Nucleosomes were crystallized using salting in vapor diffusion at NCP concentrations ranging from 10-12 mg/ml with salt concentrations of 27.5 mM KCl and 35 mM of MnCl₂. The crystals were soaked in 24% 2-methyl, 2,4-pentanediol (MPD) containing 5% trehalose (Luger et al., 1997) and 5 mg/ml of LANA peptide. X-ray data were collected on a Rigaku RU-H3R rotating anode generator (1.5418Å Cu-K α radiation) with osmic confocal multilayer optics system, R-axis IV⁺⁺ image plate detector and an X-stream cryocooling system. The data was processed with Denzo and Scalepack (Otwinowski and Minor, 1997). PDB entry 1AOI was used as a search model for molecular replacement. Molecular replacement and further refinements were done using CNS (Rice et al., 1998). The model building was done using O (Jones et al., 1991). The fidelity of the model was checked using simulated annealing omit maps during early stages of the model building. The geometry of the final model was checked using a Ramachandran plot with 90% of the amino acids in the most favored region, 8.8% of the amino acids in the additionally allowed region, and 1.2% of the model lying in the generously allowed region. Figures 2.4A-D were made using PyMOL molecular graphics system (www.pymol.org). Figure 2.4E, F and occluded surface areas were done using GRASP (Nicholls et al., 1991).

Supporting Online Text

Ku70, Ku80, and PARP1 do not mediate LANA chromosome association. A role for Ku70, Ku80 and PARP1 in mediating LANA chromosome association was assessed using knockout mouse embryo fibroblasts (MEFs). GFP LANA 1-32 (green) tightly associated with chromosomes (red) (overlay generates yellow) both in the absence (Ku80^{-/-}) and presence (Ku80^{+/-}) of Ku80 (Fig. S1). The dramatic reduction of Ku70 expression in these cells (Nussenzweig et al., 1996) also did not affect GFP LANA 1-32's chromosome targeting. Further, GFP LANA 1-32 associated with chromosomes in the absence (PARP^{-/-}) and presence (PARP^{+/+}) of PARP1 (Fig S1). Therefore, neither Ku70, Ku80 nor PARP1 are the LANA N-terminal mitotic docking partner.

Interactions between LANA and the nucleosome. Details of the interaction between LANA and the nucleosome are shown in Fig. S3. The main chain of one side of the LANA hairpin (amino acids 5-8) makes three hydrogen bonds with three different amino acid side chains in H2B α C (Fig. S3A). The complex is further stabilized by the insertion of LANA Met 6 and Leu 8 into a hydrophobic region formed by the long α 2 helix of H2A (Figs.S3B and 4F respectively). Of all LANA residues, Arg 9 makes the most interactions with the H2A-H2B dimer: we count a total of five hydrogen bonds between the side chain of LANA Arg 9 and residues in H2A that form the acidic patch (H2A Glu 92, Glu 61, and Asp 90; Fig. S3C). Interactions with this particular region are enforced by a hydrogen bond between LANA Ser 10 and H2A Glu 64 (Fig. S3C), and between the main chain of LANA Arg 7 and H2B Glu 110. Thus, the LANA peptide interacts with five of the seven amino acids that form the acidic patch on the nucleosomal surface.

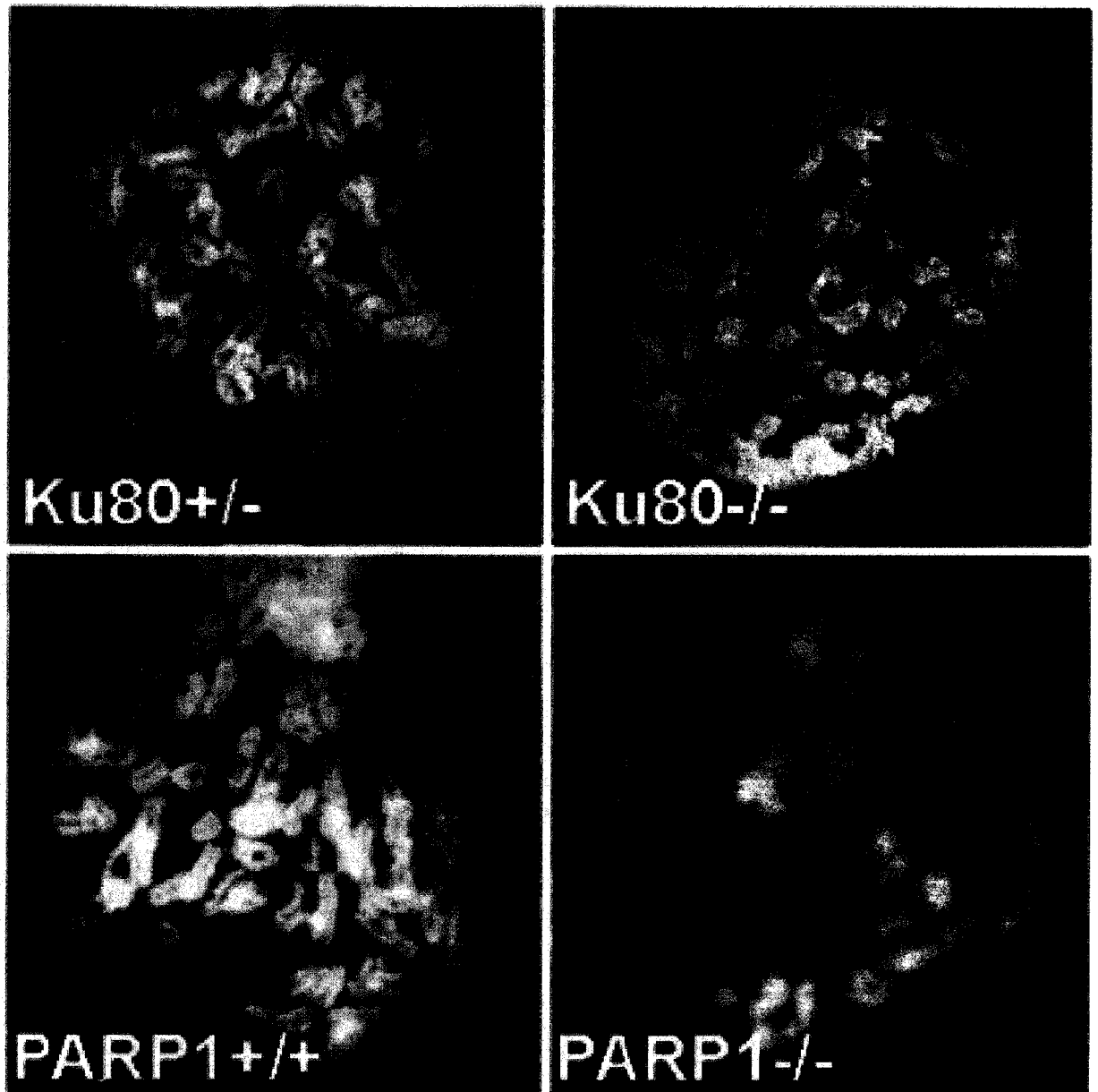


Figure S1. Ku70, Ku80, and PARP1 do not mediate LANA N-terminal chromosome association.

MEF cells expressing GFP LANA 1-32 (green) were metaphase arrested and DNA counterstained with propidium iodide (red) (overlay of green and red generates yellow). (630X)

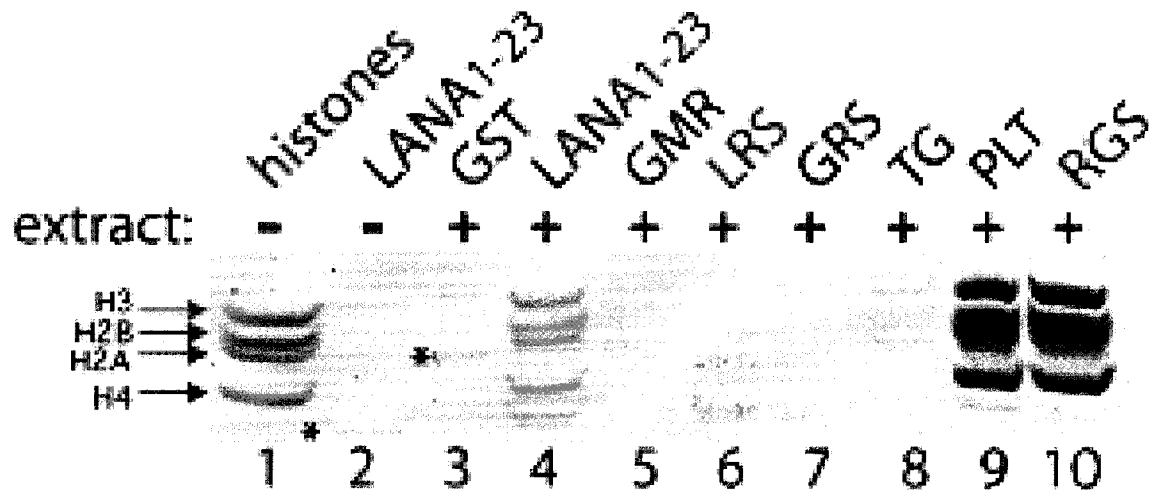


Figure S2. Bound histones were detected by Coomassie after incubation of bacterially expressed GST fusions with cell extract. Greater histone signal in lanes 9, 10 are due to ~50% more input GST fusion. (*), GST or GST fusion degradation products.

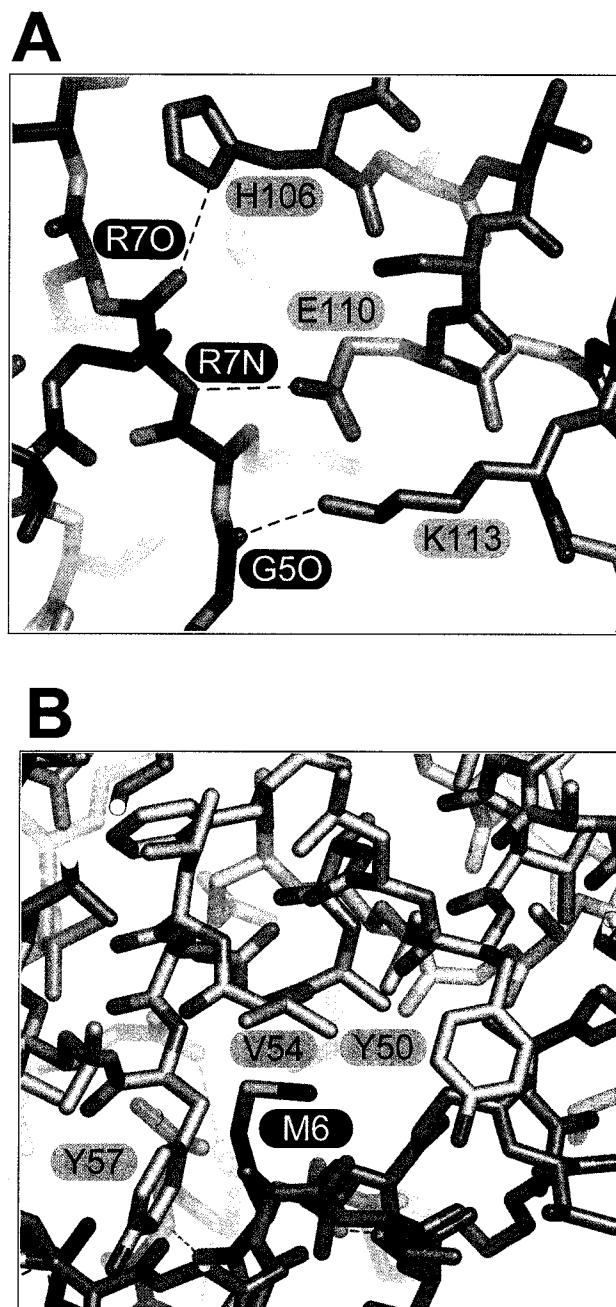


Figure S3. Details of the LANA – nucleosome interactions. Coloring of histones and LANA as in Fig. 2.4. Hydrogen bonds between LANA and histones are indicated by blue dashed lines.

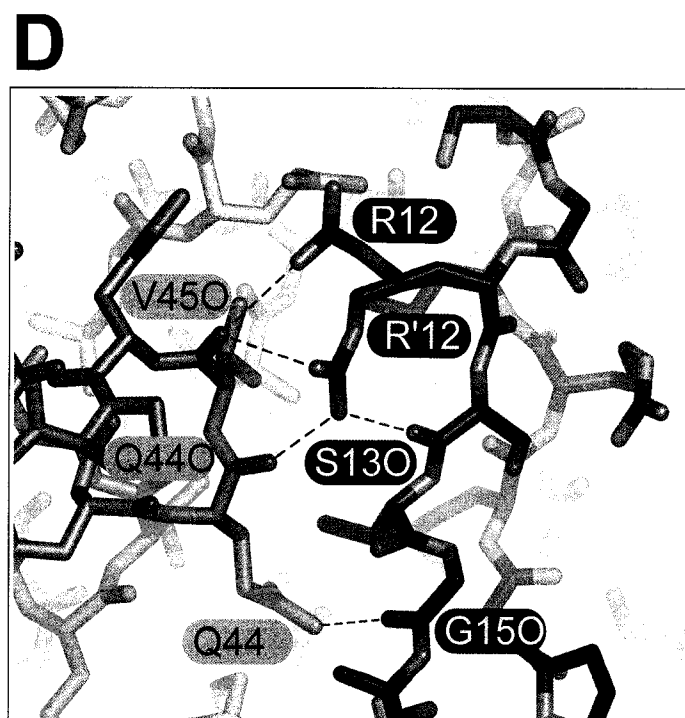
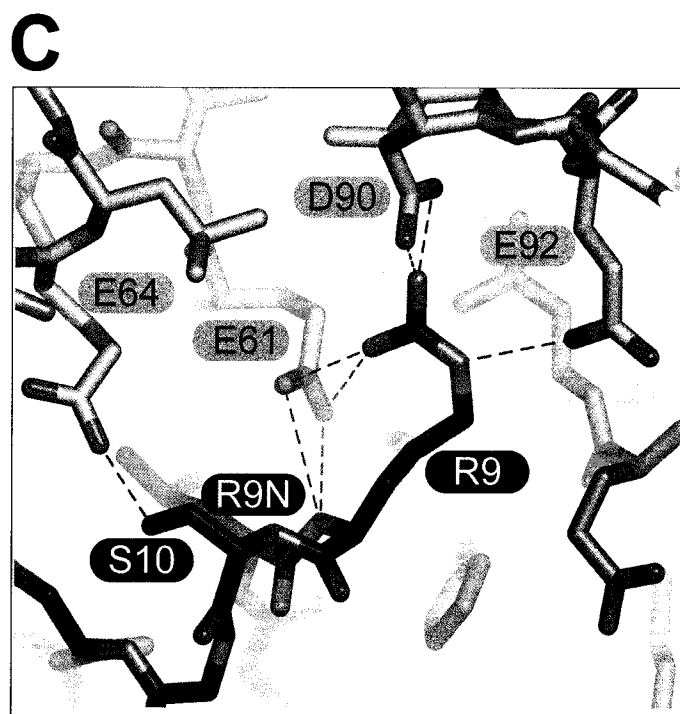


Figure S3. Details of the LANA – nucleosome interactions. Coloring of histones and LANA as in Fig. 2.4. Hydrogen bonds between LANA and histones are indicated by blue dashed lines.

Interactions between other LANA residues and the H2A-H2B dimer are less abundant, and engage the side chains of LANA residues Ser 10, Arg 12, and the main chain of Ser 13, Gly 15 (Fig. S3D). A glycine in position 11 maintains the β -turn. LANA residue Arg 12 assumes two alternative side chain conformations (Fig. S3D) that are both clearly visible in the original electron density map; both are involved in hydrogen bonding with the main chain of the α 1 helix of H2B. Nevertheless, this residue can be replaced with an alanine without significant reduction in LANA chromosome association, unlike other LANA residues involved in interactions with the nucleosome (Fig. S4).

Individual LANA residues critical for chromosome association. We investigated the importance of individual LANA residues for chromosome association since previous experiments used triple alanine substitutions. Residues Gly 5, Met 6, Leu 8, Arg 9, Ser 10, and Gly 11 were each essential for chromosome association since GFP fused to N-terminal LANA (GFP LANA 1-32 (green)) with alanine substitutions at these sites did not localize to chromosomes (red) (Fig. S4). In contrast, Arg 7, Arg 12, Ser 13, Gly 15, and Ala 16 were each dispensable for chromosome association since GFP LANA 1-32 (green) mutated at each residue diffusely painted chromosomes (red) (overlay of green and red generates yellow). Thr 14 had a role in chromosome association since GFP LANA 1-32 mutated at this site diffusely painted chromosomes but also distributed between them. These results are consistent with those of others who used point mutations to investigate LANA chromosome association (Lim et al., 2004; Sears et al., 2004).

¹MAPPGMRLRSGRSTGAPLTRGS²³

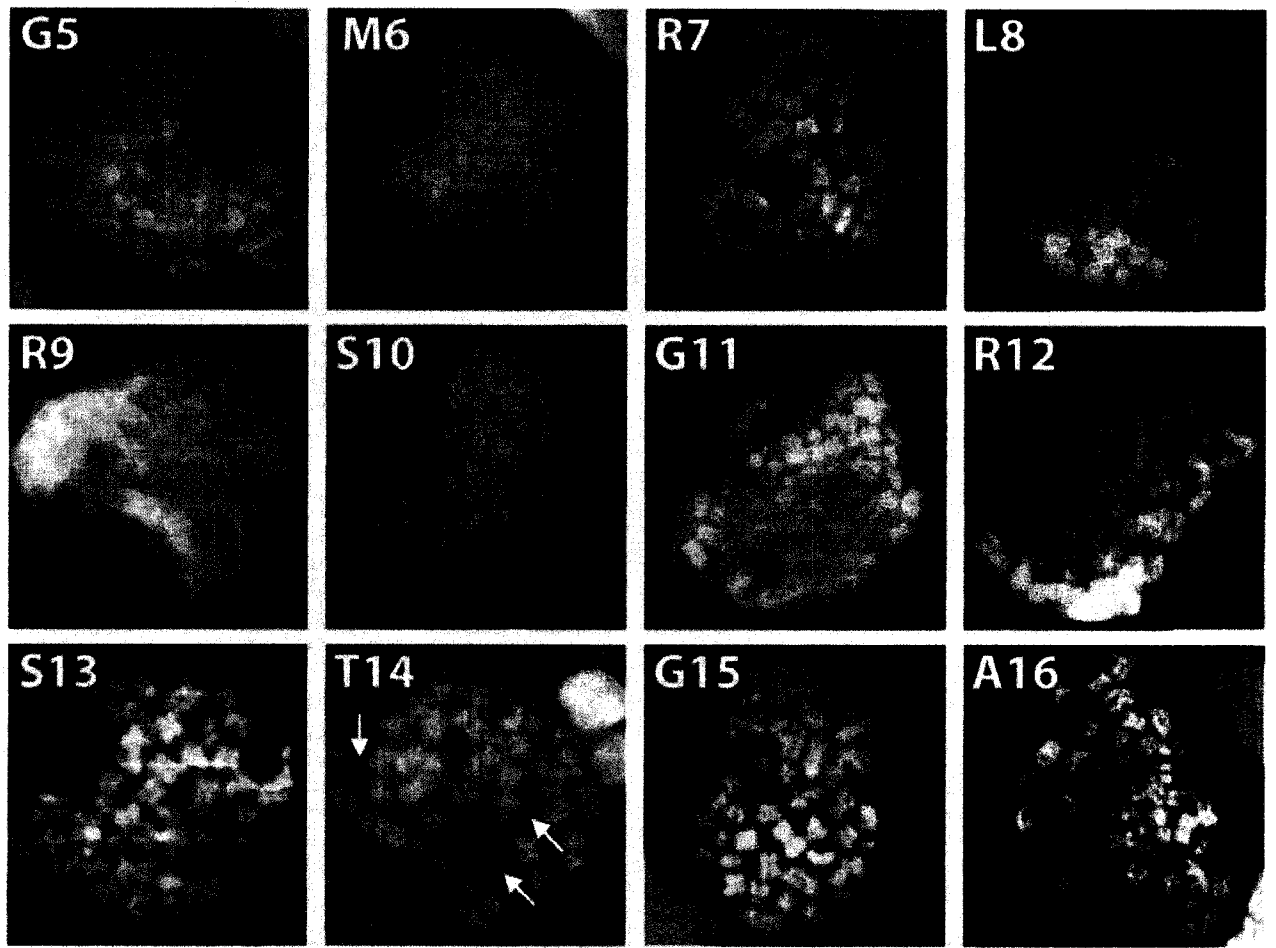


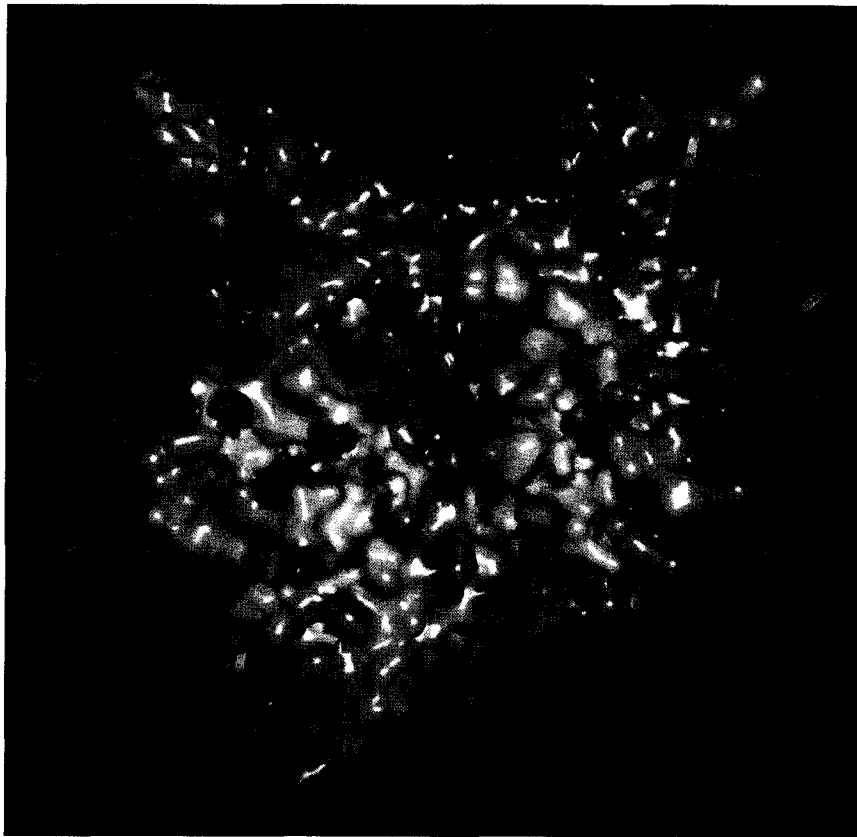
Figure S4. Point mutation analysis of the KSHV LANA N-terminal region. Residues essential for chromosome association are underlined at the top. Residues 5 through 15 were individually mutated to alanine. Alanine 16 was mutated to glycine. Panels are denoted by the mutated residue. Mutations were generated in the context of GFP LANA 1-32. Each mutant was expressed in BJAB cells. Overlay of GFP LANA 1-32 (green) and chromosomes (red) generates yellow. (630X)

This work demonstrates that with the exception of Arg 7 which points outwards, away from the H2A-H2B dimer, LANA residues 5 – 11 are each essential for binding of LANA to chromatin. The presence of the two glycine residues at strategic places appears to be essential to maintain the hairpin structure. The moderate importance of T14 is consistent with its role in stabilizing the lower portion of the hairpin via a hydrogen bond (Fig 2.4A).

CHAPTER III

A charged and contoured surface on the nucleosome opposes tail- dependent chromatin compaction

Jayanth V. Chodaparambil, Andrew J. Barbera, Xu Lu, Kenneth Kaye, Jeffrey C. Hansen,
and Karolin Luger



(Surface representation of LANA bound nucleosome)

This chapter has been submitted for publication. J.V.C did all the experiments. X.L and A.J.B. gave technical suggestions.

Abstract

Nucleosomes are dynamic nucleoprotein assemblages that play a central role in regulating genome structure and accessibility. In addition to maintaining the first level of DNA compaction, they participate in multiple reversible self-association interactions that govern chromatin fiber structure. Local nucleosome-nucleosome interactions in cis drive fiber folding, while interactions in trans lead to cooperative fiber-fiber oligomerization. The N-terminal tail domains of the core histones are essential for both types of interactions, functioning through largely unknown mechanisms. Here we demonstrate that peptides derived from the histone H4 tail and Kaposi's sarcoma herpesvirus LANA protein compete with and replace the endogenous H4 tails leading to folding and oligomerization of model nucleosomal arrays. Neutralization of an H4 tail/LANA binding site on the histone octamer surface via site-directed mutagenesis enhanced rather than abolished nucleosome-nucleosome interactions in cis and trans. These results imply that 'tethering' of nucleosomes via histone tail- nucleosome interactions is not an absolute requirement for folding and oligomerization and suggest that changes in the properties of the nucleosome surface (mediated either by histone tails, posttranslational modifications, or interacting proteins) can modulate higher order chromatin structure. We maintain that the contoured nucleosome surface is an abundant macromolecular binding interface that is centrally involved in regulating genome structure and function through complex interactions during chromatin condensation.

We have previously shown that a peptide spanning the N-terminal 23 amino acids of the viral LANA protein (LANA1-23) occupies the same negatively charged region on the nucleosomal surface as the H4 tail from a symmetry-related particle in the crystal lattice (Barbera et al., 2006). This same region has been implicated as an H4 tail binding site that mediates nucleosome-nucleosome interactions during chromatin folding and self-association (Dorigo et al., 2004). We hypothesized that if this charged nucleosome surface region is involved in H4 tail-dependent interactions, exogenous LANA1-23 would effectively compete with the H4 tail and bind to the nucleosome surface, thereby preventing H4-mediated chromatin condensation.

To test this hypothesis, we utilized a previously established model system reconstituted from recombinant histones (containing either full-length or tailless H4 (gH4) and full-length H3, H2A, and H2B) and a 12-mer repeat of a 208-bp DNA fragment derived from the 5S rRNA gene (Gordon et al., 2005) to yield wild type and gH4 nucleosomal arrays (wt-NA and gH4-NA). All arrays were carefully matched to contain 11 ± 2 octamers per 208-12mer DNA, to allow for direct comparison of folding and self-association (Figure S1A). Self-association, which is believed to mimic fiber-fiber interactions in cellular chromatin (Schwarz et al., 1996), was assayed by measuring the amount of monomeric nucleosomal arrays as a function of $MgCl_2$ concentration. The Mg_{50} value is defined as the concentration of $MgCl_2$ at which 50% of nucleosomal arrays are oligomerized and subsequently pellet upon centrifugation. Chromatin fiber folding was assayed using sedimentation velocity to monitor progression from a ~ 27 S 11nm fiber to the 40S intermediate and ~ 55 S “30nm” folded states under $MgCl_2$ conditions where the arrays

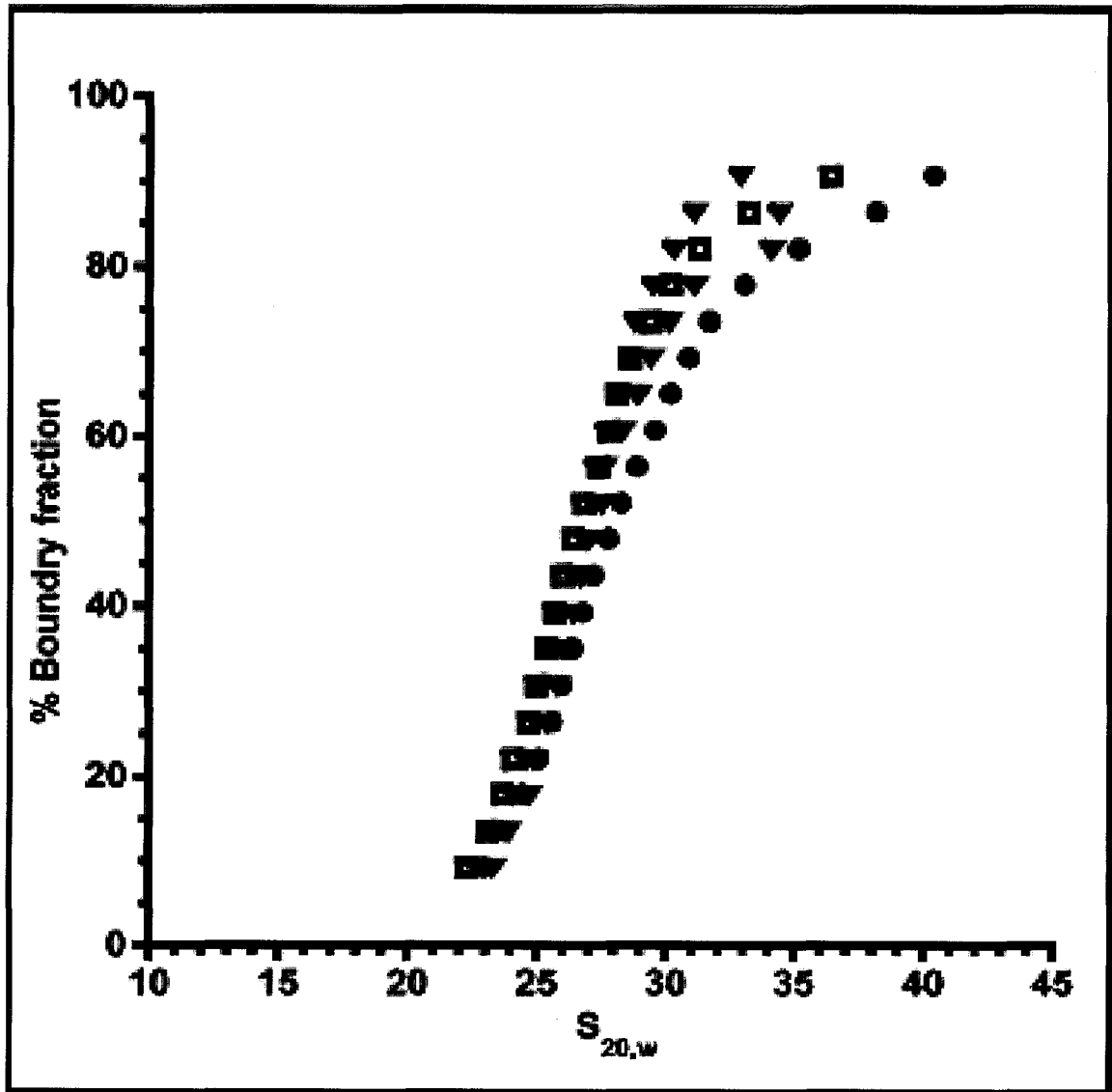
A

Figure S1: Normalization of nucleosomal arrays used. All nucleosomal arrays were adjusted to the same nucleosome occupancy. Using sedimentation velocity experiments we determined that all arrays used have an average S value of $\sim 27s$. The arrays represented here are wt-NA (□), GH4-NA (▼), nhs-NA (●), gh4-nhs-na (△).

B

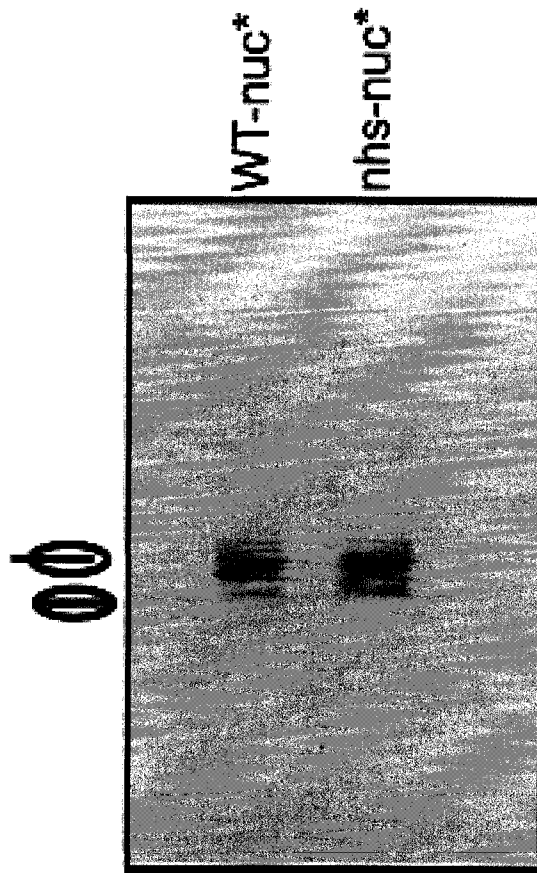


Figure S1: Normalization of nucleosomal arrays used. All (B) WT nucleosomes and nhs-nucleosomes are identical: WT nucleosomes and nhs-nucleosomes were assembled through salt gradient dialysis. The samples were run on a 5% native PAGE gel and visualized under UV at 365nm for observing the label.

were monomeric. Both assays are considered to be definitive (for example, (Fan et al., 2002, Shogren-Knaak et al., 2006)). Wild-type nucleosomal arrays were incubated with LANA1-23 at various molar ratios and the ability of the arrays to self-associate was measured as a function of MgCl_2 . A representative experiment is shown in Figure 3.1A. The curves are co-operative as expected (Figure 3.1A) and fully reversible upon removal of Mg^{2+} from solution (data not shown). Mg50 values from this experiment as a function of increasing amounts of LANA1-23 are plotted in Figure 3.1B. Contrary to our hypothesis, Figures 3.1A, 3.1B show that LANA1-23 significantly lowers the Mg50 needed for fiber-fiber self-association. This demonstrates that the binding of LANA1-23 to the nucleosomal surface as an untethered peptide promotes self association. This effect is saturable because the addition of excess LANA1-23 at >5 equivalents of LANA1-23 per nucleosome (or >2.5 per binding site) did not lower the Mg50 further. The effect is specific because a mutant of LANA1-23 (LRS) that has the same charge but is unable to bind to the nucleosomal surface (Barbera et al., 2006) is unable to induce self association (Figure 3.1B). Thus, LANA1-23 does not act as a polycationic salt, but instead appears to promote compaction through the specific interactions previously observed by crystallography (Barbera et al., 2006).

Compared to wild-type arrays, tailless H4 (gH4-NA) arrays require more MgCl_2 for self association (Dorigo et al., 2003) (Gordon et al., 2005). This reflects the independent and additive effect of the H4 tail to self association 3. LANA1-23 retains the ability to promote self association of nucleosomal arrays lacking the endogenous H4 tail (Figure 3.1C, D). In the presence of LANA (1:5), the Mg50 for gH4-NA drops to 2.5 mM, the same value observed for wt-NA in the absence of LANA. However, the Mg50 does not

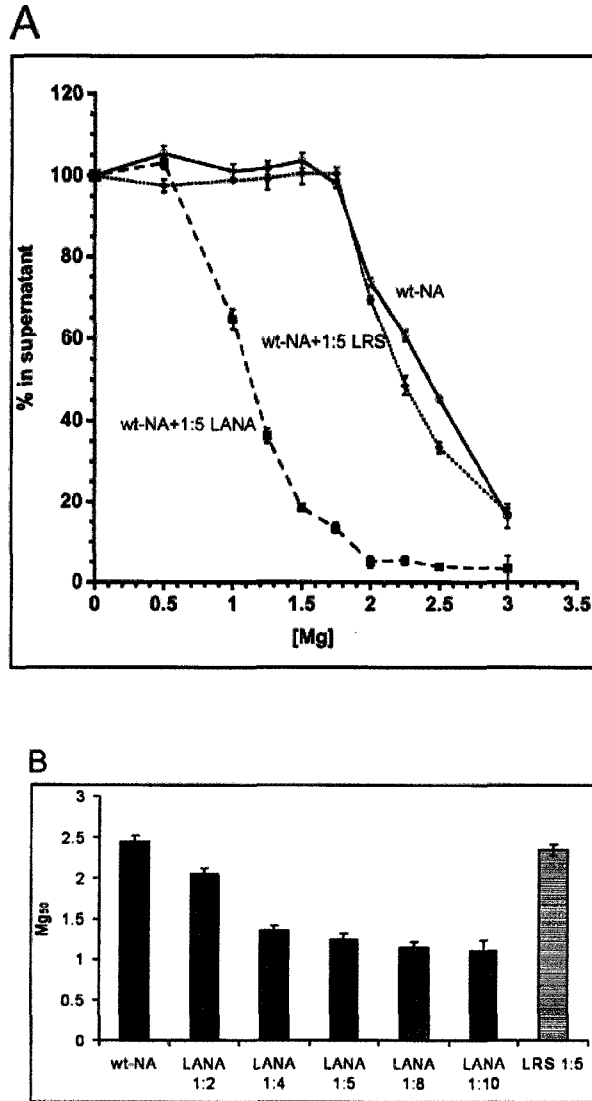


Figure 3.1: LANA1-23 promotes chromatin self-association. (A) Self-association of wild type nucleosomal arrays is plotted as a function of the $MgCl_2$ concentration (\square). (\blacksquare and \blacklozenge) were done in the presence of 5-fold excess of LANA1-23 or a triple alanine substitution of LANA1-23 (LRS) that abrogates binding to nucleosomes (Barbera et al., 2006). Note that each nucleosome has two charged surfaces and thus two binding sites for LANA1-23. (B) Mg_{50} values (obtained from experiments as shown in (A)) are plotted as a function of molar ratio of LANA1-23 to nucleosome in the array, assuming a saturation of 12.

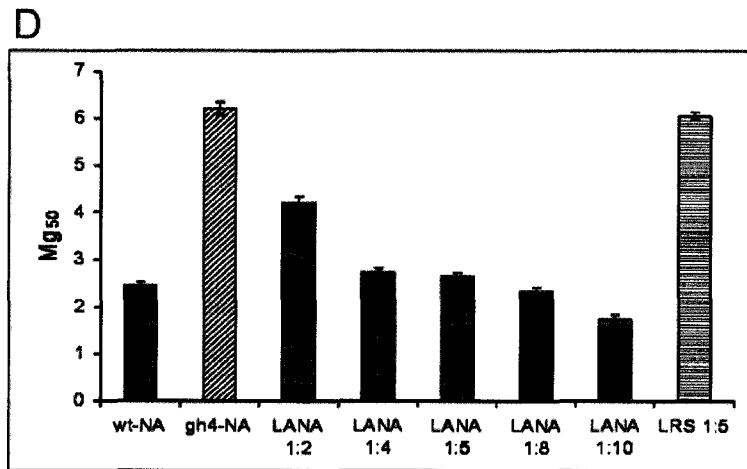
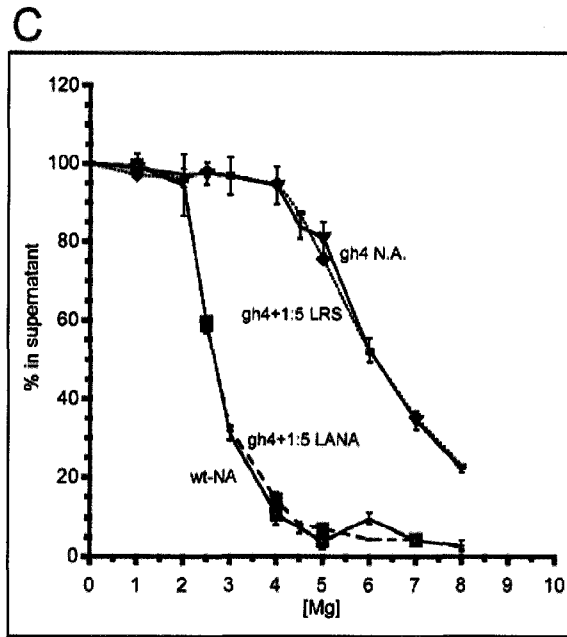


Figure 3.1: LANA₁₋₂₃ promotes chromatin self-association. (C) Self-association of gh4-NA is plotted as a function of the MgCl₂ concentration (▼). (■ and ◆) show gh4-NA in the presence of 5-fold molar excess of LANA₁₋₂₃ and a triple alanine substitution of LANA₁₋₂₃ (LRS). wt-NA is shown as (□). (D) Mg₅₀ values are plotted as a function of molar ratio of LANA₁₋₂₃ to gh4-nucleosome. For all experiments, error bars represent standard deviations from three separate experiments.

reach the low levels (1.2 mM) observed for wt-NA in the presence of LANA and the covalently attached H4 tail. Thus, we believe that LANA peptide can mimic some actions of the H4 tail, but not all. This in turn suggests there is one unique site for LANA and multiple binding sites for the H4 tail on the nucleosome. For example, we have shown that the H4 tail peptide, but not LANA1-23, binds to free DNA (Figure S2).

How does LANA influence self-association in the presence and absence of covalently attached H4 N-terminal domains? One possibility is that LANA binding to the nucleosomal surface neutralizes a negatively charged, 'repulsive' domain on the nucleosomal surface that may prevent the close association of nucleosomes (Figure 3.2A, B). Toward this end, we hypothesized that nucleosome-nucleosome interactions are mediated by a collection of opposing and attractive domains on the nucleosome surface. This yields a carefully balanced condensation equilibrium that can easily be regulated in either direction by environmental conditions and other chromatin-binding proteins. To test this hypothesis, we neutralized six out of the seven acidic surface residues that contribute to the LANA binding region by site-directed mutagenesis (H2A E56T, E61T, E64T, D90S, E91T, and E92T). The mutated H2A, together with the other three wild-type core histones, were renatured into histone octamers and assembled into nucleosome arrays that had partially neutralized histone surfaces (nhs-NA). Nucleosomes and nucleosomal arrays reconstituted with this histone mutant were indistinguishable from those reconstituted with wild type H2A, as judged by sedimentation velocity (Figure S1A) and 5% native gels (Figure S1B). Nhs-NAs required significantly less $MgCl_2$ compared to wt-NA for self association (Figure 3.2C), indicating that the charged and/or stereo-chemical character of this region indeed opposes the ability of wild-type arrays to

| | | | | | | | | | | |
|----------|---|---|---|---|---|---|---|---|---|----|
| GST | - | - | - | - | + | - | - | - | - | - |
| GST-LANA | - | - | - | - | - | + | + | + | + | - |
| GST-H4 | + | + | + | + | - | - | - | - | - | - |
| DNA | + | + | + | + | + | + | + | + | + | + |
| Lane No. | 1 | 2 | 3 | 4 | 5 | 6 | 7 | 8 | 9 | 10 |

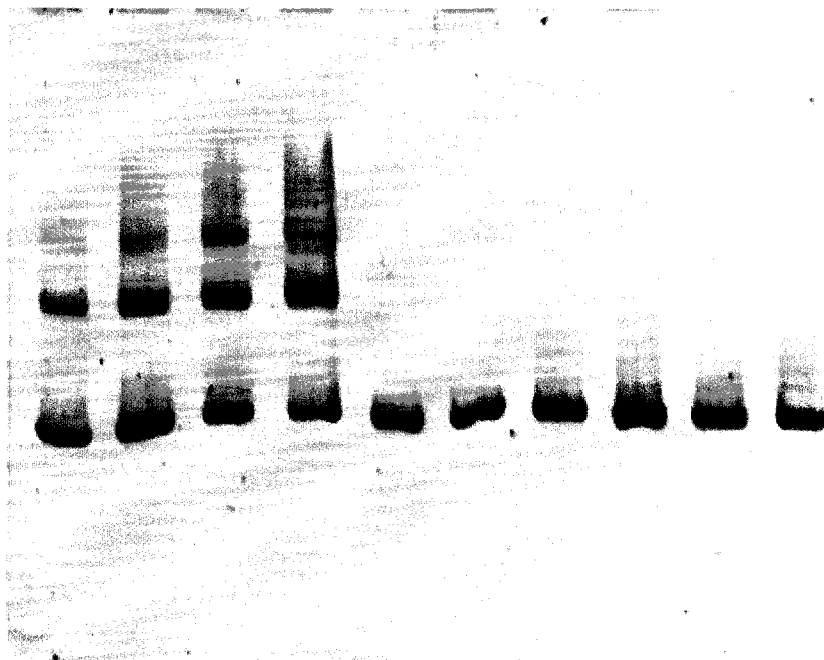


Figure S2: GST-H4 but not GST-LANA interacts with DNA. GST-H4 was incubated with increasing molar ratios of 146mer 5S DNA (lanes 1-4). Lane 5 shows GST incubated with DNA, lanes 6-9 show GST-LANA incubated with increasing molar concentrations of 146mer 5s DNA, lane 10 shows 5s 146mer DNA. A 5% native polyacrylamide gel was stained with ethidium bromide and the gel is shown in inverted color.

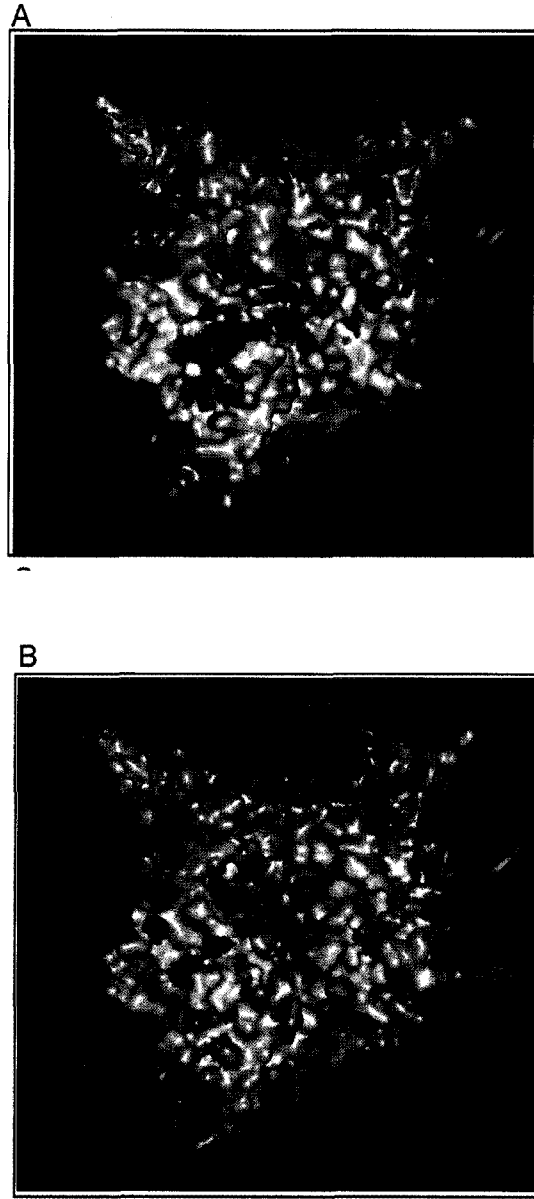


Figure 3.2: A negatively charged region on the surface of the nucleosome acts as a repulsive domain (A) Electrostatic potential surfaces for pdb entry 1zla (red, negatively charged; blue, positively charged) were calculated through Delphi / GRASP (Nicholls et al., 1991) and the figure was rendered in PyMol (DeLano, 2002). **(B)** Upon interaction with LANA1-23, the surface contours and charge of the nucleosomal region is altered.

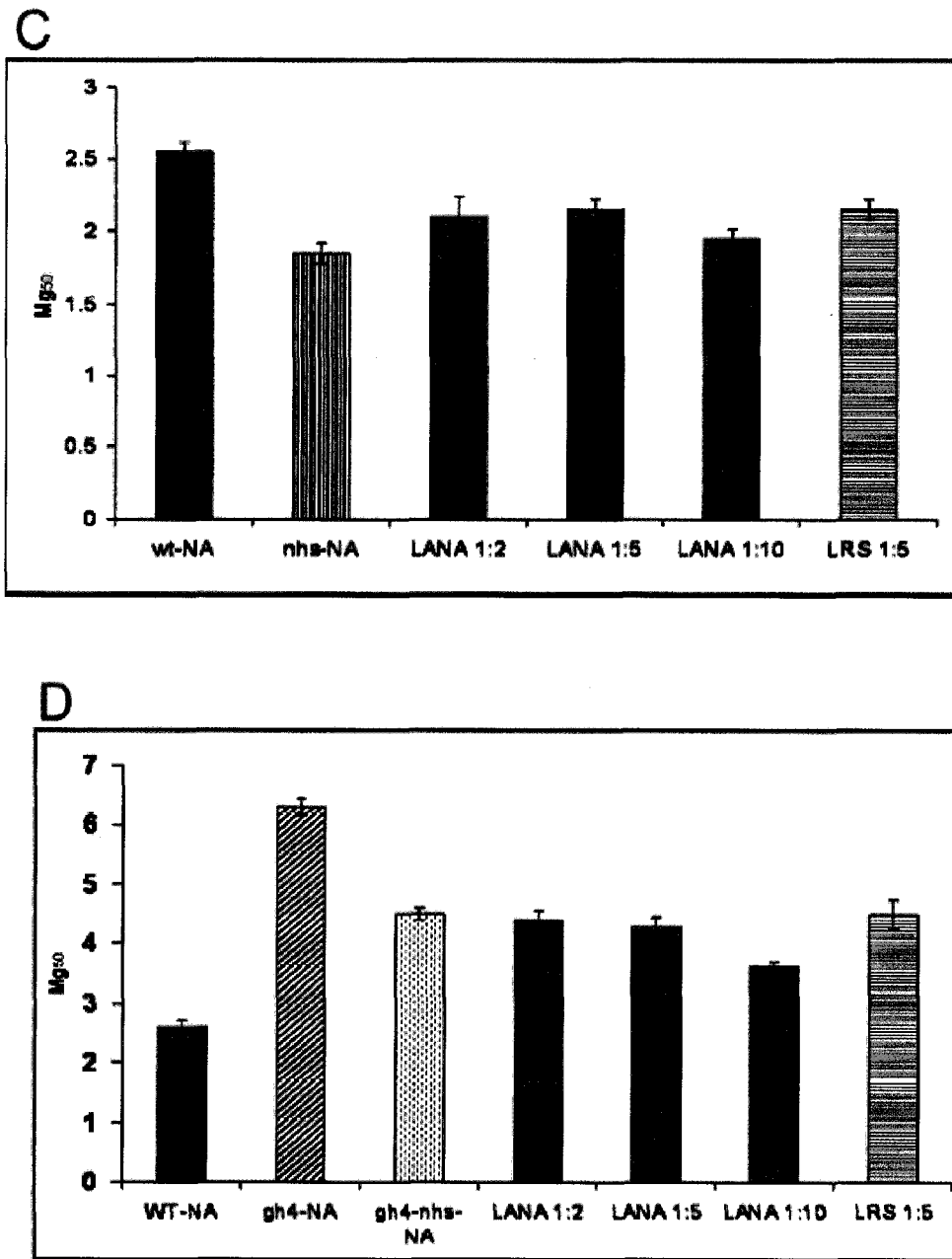


Figure 3.2: A negatively charged region on the surface of the nucleosome acts as a repulsive domain. (C) Mg50 values are plotted as a function of molar ratio of LANA1-23 to nhs-nucleosomes in the nhs-array. **(D)** Mg50 values are plotted as a function of molar ratio of LANA1-23 gh4-nhs-nucleosome. For all data shown, error bars represent standard deviation from three separate experiments.

self-associate. The addition of LANA1-23 or LRS had no little or no effect, likely due to the inability of either peptide to bind to the mutated histone surface (Figure 3.2C). As suggested by experiments described above, the endogenous H4 tail promotes self-association by binding to regions on the nucleosome that are at least in part distinct from that bound by LANA1-23. If this is the case, mutagenesis of the LANA-binding region should not completely compensate for the deletion of the H4 tail. We prepared nucleosomal arrays with histone octamers that had neither the H4 tail nor the charged region (gH4-nhs-NAs). Mg50 values for such arrays fall between those of wild type-NA and gH4-NA (Figure 3.2D), indicating that the H4 tail is at most only partially involved in neutralizing the region defined by crystallographic analysis (Luger et al., 1997). Again, addition of LANA1-23 had no effect, except at high concentrations, indicating non-specific interactions with regions usually occupied by the H4 tail.

We next wanted to test whether a synthetic H4 tail peptide could promote self-association when added exogenously, analogous to the experiments described above with LANA1-23. As with LANA1-23, the addition of H4 tail peptide to wild type nucleosomal arrays significantly lowers the Mg50 value (Figure 3.3A). However, the effect is non-saturable as molar ratios as high as 10- to 16-fold continue to lower Mg50 (Figure 3.3A, and data not shown). We speculate this is due to the presence of multiple H4 binding sites on nucleosomal arrays with overlapping affinities. We next tested whether the exogenous H4 tail peptide could replace the missing H4 tail in trans in gH4-NAs (Figure 3.3B), and in arrays carrying both neutralizing surface mutations and tail deletions (gH4-nhs-NA; Figure 3.3D). Arrays with a mutated charged region were used as a control (nhs-NA, Figure 3.3C). In all cases, addition of the H4 tail further promoted self-association, and in

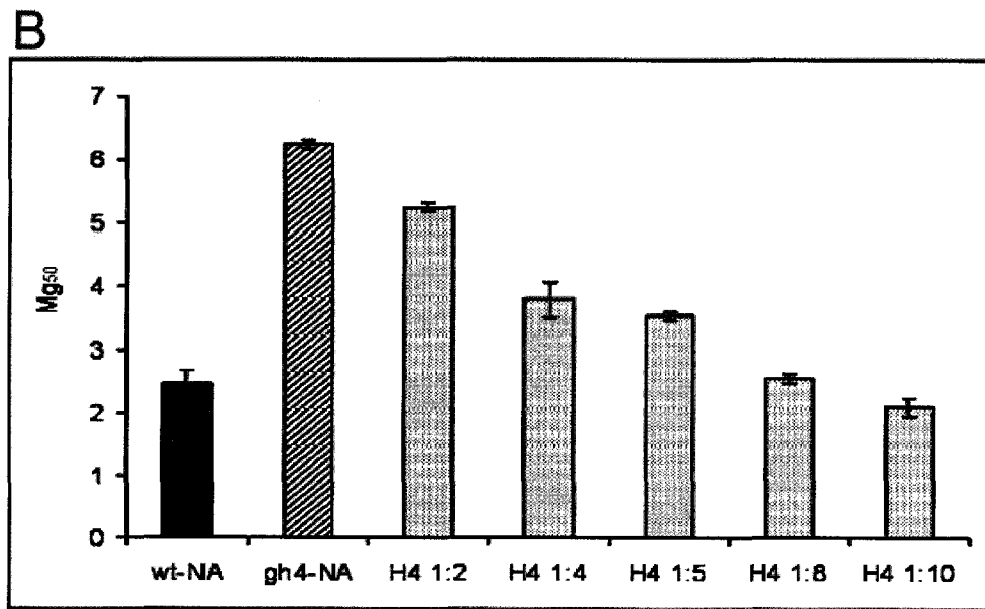
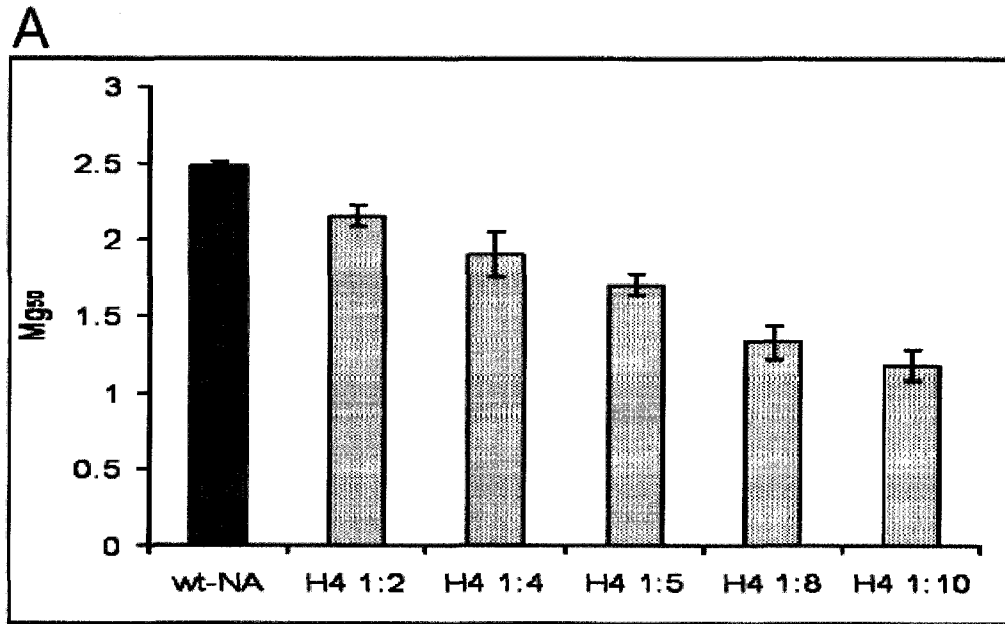


Figure 3.3: The H4 tail acts in trans to promote self-association. (A) Mg₅₀ values are plotted as a function of molar ratio of H4 tail peptide added to wt-nucleosome. (B) Mg₅₀ values are plotted as a function of molar ratio of H4 to gh4-nucleosome.

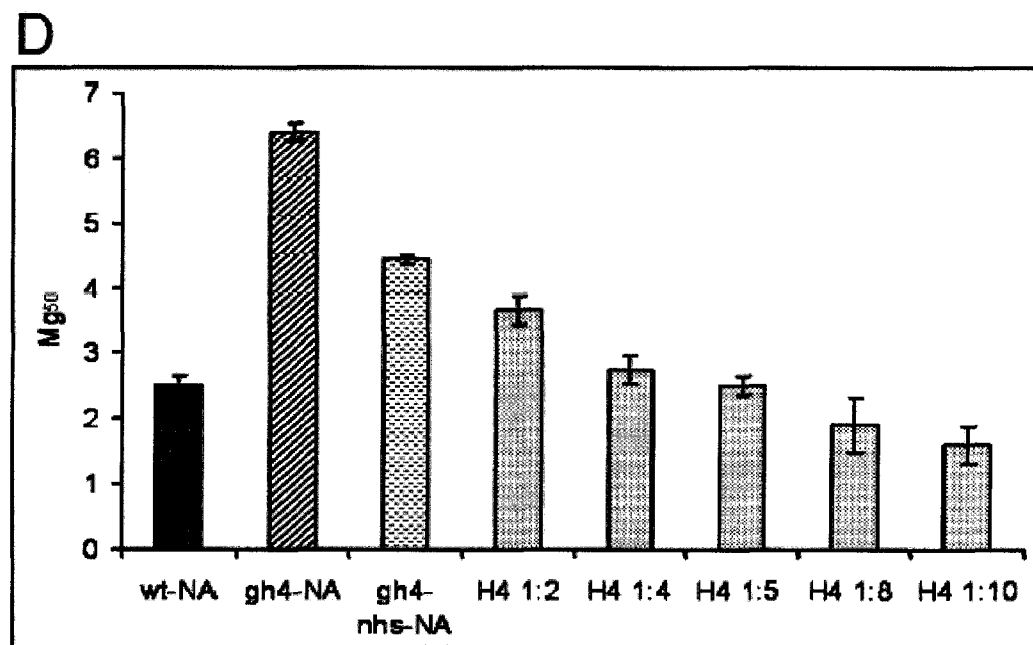
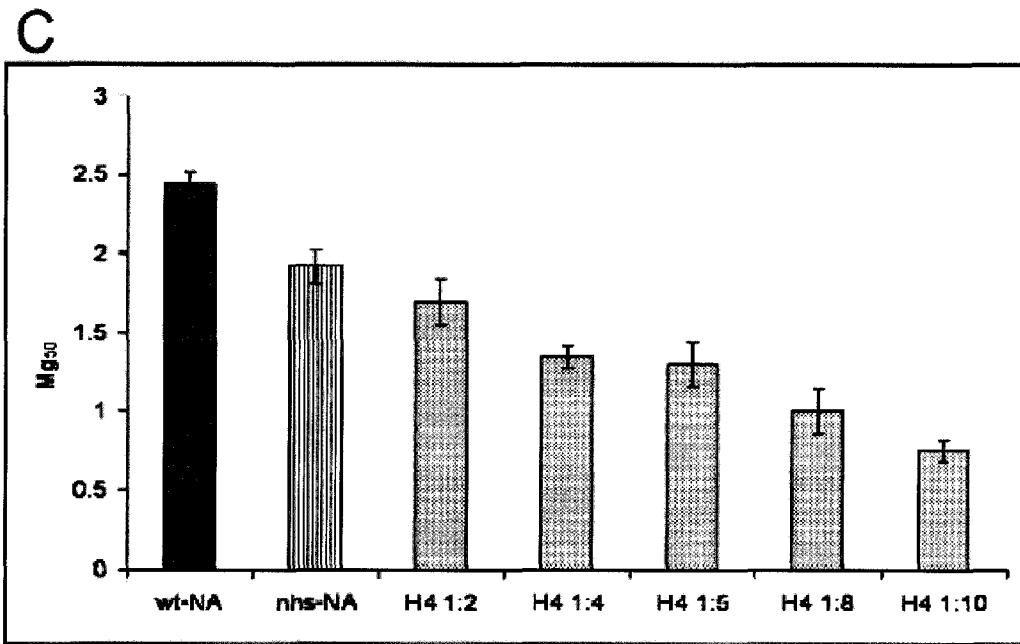


Figure 3.3: The H4 tail acts in trans to promote self-association. (C) Mg_{50} values are plotted as a function of molar ratio of H4 to nhs-nucleosome. (D) Mg_{50} values are plotted as a function of molar ratio of H4 to gh4-nhs-nucleosome. Error bars represent standard deviation from three separate experiments

all cases the addition of increasing amounts of H4 tail peptide resulted in further lowering the Mg50 values in a linear dependency. This data confirms that H4 tail binds to multiple binding sites on nucleosomal arrays (Figure S2) during self-association.

Chromatin folding into 30 nm fibers has been studied for over 30 years. It is a separate, mechanistically distinct process from self-association, although it also is mediated by tail-dependent nucleosome-nucleosome interactions (Dorigo et al., 2003, Shogren-Knaak et al., 2006), some involving the nucleosomal surface (Dorigo et al., 2003). We used sedimentation velocity to study the MgCl₂- dependent transition from the 27S 11-nm fiber to the 40S intermediate folded state, to the 55S 30-nm structure. wt-NA were incubated with LANA1-23, LRS, or buffer in the presence of 1.05 mM MgCl₂. Under these conditions, no self-association occurred and folding was limited to the 30 to 40S transition in the absence of LANA. However, a significant portion of the arrays sedimented between 40 to 55S upon the addition of a five-fold excess of LANA1-23, confirming that LANA1-23 promotes formation of a compact 30 nm conformation (Figure 3.4A). As with self-association, the effect is specific since LRS has no discernible effect on folding. In the absence of LANA, the same arrays required 1.75mM MgCl₂ to reach an equivalent level of folding (not shown). Mutagenesis of the histone surface (nhs-NA) also promoted folding of a significant portion of arrays into a 55 S species (Figure 3.4B). Consistent with earlier studies (Dorigo et al., 2003), we confirmed that arrays in which the H4 tail was deleted were incapable of forming 55 S structures in 1.9 mM or even 3.6 mM MgCl₂ (data not shown). However, at these salt concentrations, a significant percentage of arrays sedimented between 40-55S upon addition of a five-fold molar excess of LANA (data not shown). Thus, altering the charged surface region

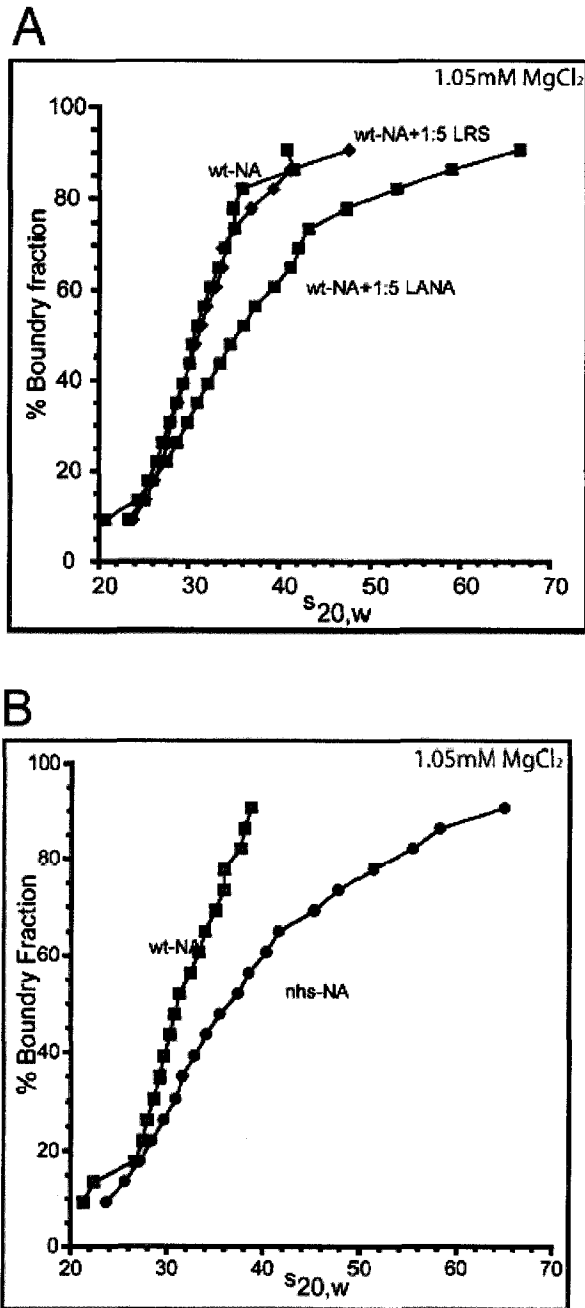


Figure 3.4: Changes in the nucleosomal surface via LANA₁₋₂₃ interactions or histone point mutations promote chromatin folding. (A) Folding of wt-NA at 1.05 mM $MgCl_2$ in the presence of either a five-fold excess of LANA over nucleosome (■), LRS (◆), or buffer (□). (B) Folding of wt-NA (□), nhs-NA (●) at 1.05 mM $MgCl_2$.

either by interaction with LANA1-23 or by mutation of selected charged residues in H2A has a profound effect on chromatin fiber folding. While we have shown that mutating seven of the acidic acid residues promotes folding, not all of these residues may be functionally equivalent because mutating a subset of these acidic residues can actually inhibit folding (David Tremethick, personal communication).

Therefore, the extent of chromatin compaction may be regulated by complex interplay between small regions on the surface of the nucleosome that promote or suppress the condensation process.

In conclusion, we have introduced evidence that the histone octamer surface of the nucleosome is a major player in the regulation of chromatin higher order structure(s). We maintain that the level of chromatin compaction results from the net effects of repulsive and attractive domains on the nucleosome surface. Its character may be individually and locally altered by unmodified histone tails, through posttranslational modification of the tails (Shogren-Knaak et al., 2006) and the structured region of the histones (Freitas et al., 2004), introduction of histone mutants (Park et al., 2002) (Matsubara et al., 2007), histone variants (Suto et al., 2000), or through the interaction with a multitude of chromatin architectural proteins such as H1, HP1, or MeCP2. By extension, we propose that there are many different ways in which nucleosomal surfaces interact to promote chromatin condensation, resulting in numerous interchangeable types of higher order structures of varying stability.

Materials and methods:

Reconstitution of nucleosomal arrays. 208-12 mer 5sDNA, histones, and histone octamers were prepared as described (Dyer et al., 2004, Gordon et al., 2005). DNA and histone octamers were mixed at an equimolar ratio of octamer to 208mer repeat at 2M NaCl, 10mM Tris pH 7.5 and 0.25 mM EDTA. The mixture was dialyzed against buffers containing 1M NaCl, 0.75M NaCl and 2.5mM NaCl (Hansen and Lohr, 1993).

EcoR I digestion. 1 μ g of nucleosomal array was treated with 20 units of EcoR I (NEBS) for 16h at room temperature. The digested samples were electrophoresed on a 1% agarose gel in 1xTAE. The ethidiumbromide-stained gel was imaged using a Bio-Rad Chemi-Doc XRS and the percentage of free DNA of each array sample was calculated from the integrated area under the peaks using Scion Image (www.scioncorp.com). In a fully saturated array, the amount of free DNA should be < 5% (all 12 positions are occupied by octamer). For further description see (Tse and Hansen, 1997).

Sedimentation velocity. Sedimentation velocity experiments were performed in a Beckman XLA ultracentrifuge. Data was analyzed using Van Holde-Weischet analysis (Ultrascan 7.3 software) (van Holde and Weischet, 1978, Demeler et al., 1997).

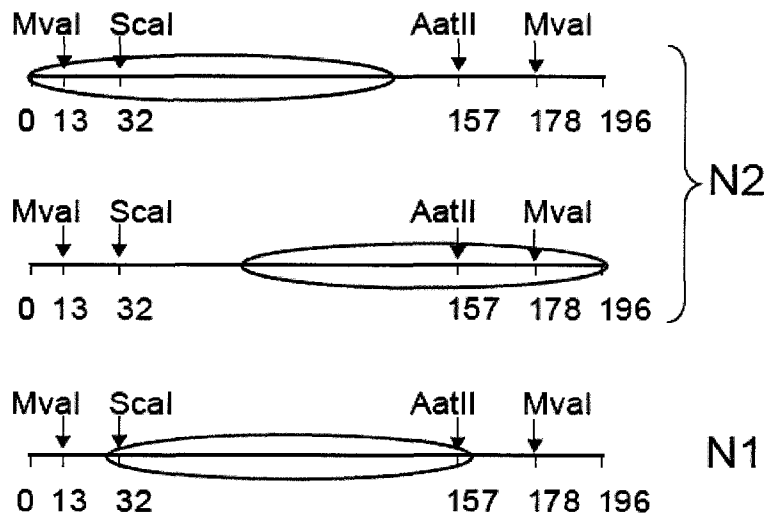
Self-association. 1.25 μ g array in 25 μ l were treated with indicated concentrations of MgCl₂ (Sigma) and incubated for 5 minutes at room temperature in an Eppendorf tube. Samples were centrifuged at 16,000 g for 5 minutes at room temperature. The absorbance of the supernatant was read at 260nm using a Beckman Coulter DU-800 UV/Vis

spectrophotometer. Reversibility experiments were done by removing the supernatant after the five-minute spin and treating the pellet with 2.5mM TEN containing 1mM EDTA. This was followed by a 16,000 g spin for five minutes at room temperature. The absorbance was measured as described above.

CHAPTER IV

Nucleosome assembly protein 1 exchanges histone H2A-H2B dimers and assists nucleosome sliding

Young-Jun Park, Jayanth V. Chodaparambil, Yunhe Bao, Steven J. McBryant, and
Karolin Luger



(Nucleosome sliding mapped by restriction digestion analysis)

This chapter was published in the *Journal of Biological Chemistry*. J.V.C. is the second author in this paper. The sliding experiments on the 196mer DNA were done by J.V.C. The exchange experiments were done by Y-J. P. Y.B and S.M. gave support and technical advice.

4.1 Abstract

Eukaryotic chromatin is highly dynamic and turns over rapidly even in the absence of DNA replication. Here we show that the acidic histone chaperone NAP1 from yeast reversibly removes and replaces H2A-H2B or histone variant dimers from assembled nucleosomes, resulting in active histone exchange. Transient removal of H2A-H2B dimers facilitates nucleosome sliding along the DNA to a thermodynamically favorable position. Histone exchange as well as nucleosome sliding is independent of ATP and relies on the presence of the C-terminal acidic domain of yeast NAP1, even though this region is not required for histone binding and chromatin assembly. Our results suggest a novel role for NAP1 (and perhaps other acidic histone chaperones) in mediating chromatin fluidity by incorporating histone variants and assisting nucleosome sliding. NAP1 may function either untargeted (if acting alone) or may be targeted to specific regions within the genome through interactions with additional factors.

4.2 Introduction

The organization of DNA into chromatin has profound consequences for all processes that involve the DNA template, and the biochemical makeup of the nucleosome has important regulatory functions. The nucleosome consists of an octamer of two copies each of the four histone proteins H2A, H2B, H3 and H4, around which 147 bp of DNA are wrapped in 1.65 superhelical turns (Luger et al., 1997). An (H3-H4)₂ tetramer organizes the central ~ 70 bp of DNA, and is flanked on either side by one H2A-H2B dimer that each organizes about 40 bp of DNA. Structural and functional variability is introduced by highly regulated reversible posttranslational modifications of individual histones and by the introduction of histone variants, in particular H2A and H3 variants, at specific regions in the genome (reviewed in (Khorasanizadeh, 2004; Malik and Henikoff, 2003)). Despite the high degree of DNA compaction, chromatin is surprisingly dynamic and fluidic, and its histone components are exchanged at a high rate in the absence of transcription and replication. Histone H2A-H2B dimers (and, to a certain extent, also (H3-H4)₂ tetramers), appear to be in rapid exchange in most regions of compacted chromatin (Jackson, 1990; Kimura and Cook, 2001), and histone variants are incorporated in replication-independent assembly pathways (e.g. Ahmad and Henikoff, 2002). ATP-dependent chromatin remodeling factors, in collaboration with histone modifying activities, further enhance chromatin fluidity (Flaus and Owen-Hughes, 2001); (Becker and Horz, 2002; Geiman and Robertson, 2002), with pronounced effects on gene expression patterns.

The transient removal of one or both H2A-H2B dimers from a nucleosome is involved in many vital cellular processes. For example, it has been known for over 20 years that transcriptionally active chromatin is depleted in H2A and H2B (Baer and Rhodes, 1983). The FACT complex is likely to be at least in part responsible (Belotserkovskaya et al., 2003). However, a possible role for the histone chaperone NAP1 has also been described recently (Levchenko and Jackson, 2004). RNA polymerase II alone is also able to displace H2A-H2B dimers during elongation *in vitro* (Kireeva et al., 2002). H2A/H2B destabilization occurs as a consequence of nucleosome sliding catalyzed by several chromatin remodeling complexes (Bruno et al., 2003). Finally, it was recently found that a specific ATP-dependent chromatin remodeling factor, Swr1, is responsible for the replication-independent incorporation of the histone variant H2A.Z into yeast chromatin (reviewed in Korber and Horz, 2004).

Histones are highly basic, and are usually found in complex with histone chaperones when not bound to DNA (reviewed in Loyola and Almouzni, 2004). These acidic proteins (several non-related families exist) are quite abundant in most eukaryotic cells, but their role in nucleosome turnover has not been thoroughly investigated (reviewed in Tyler, 2002; Akey and Luger, 2003). A renewal of interest has come with the recent discovery in yeast that the acidic histone chaperone NAP1 is found in association with an H2A.Z-H2B dimer *in vivo*. This NAP-Z complex is thought to supply H2A.Z-H2B dimers to the Swr1 complex (Krogan et al., 2003; Mizuguchi et al., 2004; Kobor et al., 2004) to promote assembly of H2A.Z-containing chromatin.

NAP1 is an average size (~ 400 amino acids) acidic protein of unknown structure with a relative molecular mass of ~ 47,000 Da and a pI of 4.25. Approximately 21% of

all amino acids are either aspartic or glutamic acid, clustered in several acidic stretches. The exact amino acid sequence of NAP1 is only moderately conserved between different organisms (Ito et al., 1996a); however, their character is maintained throughout most of its length. Although its roles in histone transport and nucleosome assembly are best characterized, NAP1 appears to have pleiotropic roles *in vivo*. In *Drosophila*, NAP1 is a part of the multi-factorial chromatin assembly machinery that mediates the ATP-facilitated assembly of regularly spaced nucleosomal arrays (Ito et al., 1996b; Ito et al., 1996a). NAP1 and other acidic histone chaperones were also shown to co-operate with SWI/SNF complexes in chromatin remodeling, and to facilitate transcription factor binding to nucleosomal DNA *in vitro* (Chen et al., 1994; Cote et al., 1994); Walter et al., 1995). Furthermore, direct functional and physical interactions between transcriptional activators and human NAP1 were reported (Asahara et al., 2002; Shikama et al., 2000; Rehtanz et al., 2004). Systematic deletion of the *NAP1* gene in yeast had no pronounced effect on yeast cells (Tong et al., 2004), suggesting redundancy in its function. However, genome-wide expression analysis of *NAP1* deletions in yeast has shown that the transcription level of ~10 % of all yeast open reading frames changed by at least two-fold (Ohkuni et al., 2003). Deletion of the *NAP1* gene in flies is lethal (Lankenau et al., 2003).

Analytical ultracentrifugation has shown that yeast NAP1 (yNAP1) exists as an obligate dimer in solution (McBryant and Peersen, 2004). Functional analysis of NAP1 *in vitro* is based primarily on its ability to introduce negative supercoils into relaxed circular DNA in the presence of core histones (Fujii Nakata et al., 1992), and to generate regularly spaced nucleosomes on salt-assembled chromatin (McQuibban et al., 1998), a quality which has been employed for *in vitro* nucleosome assembly reactions (Fyodorov

and Kadonaga, 2003). Using deletion analysis, it was also shown that residues 65 to 365 of yNAP1 were necessary and sufficient for histone binding and *in vitro* assembly reaction, and that a long negatively charged stretch at the C-terminus was dispensable for its assembly activity *in vitro* (Fujii Nakata et al., 1992; McBryant et al., 2003).

The functions described above can be ascribed to the well-characterized ability of NAP1 to specifically bind and sequester histone complexes (McBryant et al., 2003), and references therein). However, only a few studies address the interactions of NAP1 or any other chaperone with nucleosomes and chromatin, or its effect on chromatin structure and dynamics (Walter et al., 1995); (Ito et al., 2000; Bruno et al., 2004; Levchenko and Jackson, 2004). Here we study yNAP1 as a model system to investigate if and how histone chaperones contribute to dynamic histone exchange, a property that is emerging as an essential feature of eukaryotic chromatin. Using fluorescently labeled histones and nucleosomes we find that yNAP1 (in the absence of ATP or other protein factors) is capable of removing H2A-H2B dimers from folded nucleosomes, and actively exchanges histone dimers containing an H2A variant into completely assembled nucleosomes. We characterize the ability of yNAP1 to assist nucleosome sliding on DNA, and show conclusively that this activity requires the yNAP1 – dependent transient dissociation of H2A-H2B dimers from folded NCPs.

4.3 Experimental Procedures

Preparation of DNA, histones, yNAP1, and nucleosomes – a 146bp DNA fragment derived from a 5S rRNA gene (Simpson and Stafford, 1983) was prepared as described (Dyer et al., 2004). Both ends of the DNA were labeled with 7-diethylamino-3-(4'-

maleimidylphenyl)-4-methylcoumarin (CPM), (Park et al., 2004). To prepare the fluorescently labeled histones, H2B T112C and H4 T71C mutants were used (Park et al., 2004). Recombinant histones and histone H2A variants (H2A.Z, macroH2A histone domain, and H2A Bbd) were refolded to histone dimer or octamers. Nucleosomes were reconstituted by dialysis against decreasing salt concentration as previously described (Dyer et al., 2004), and analyzed by native PAGE on 5% polyacrylamide gels (acrylamide : bis-acrylamide 59 : 1) in 0.2 X Tris Borate EDTA. Full length yNAP1, GST-yNAP1, and truncated versions (yNAP1 Δ N and yNAP1 Δ NC) were expressed and purified as described (McBryant et al., 2003). The C-terminal domain (CTD, aa 302-417) of yNAP1 was purified over a nickel affinity resin. The his-tag was cleaved off with thrombin, followed by purification over a mono-Q column.

Detection of H2A-H2B dimer dissociation from the nucleosome – Nucleosomes containing fluorescently labeled histones or DNA were prepared as described above. 3.5 μ M CPM-labeled NCP was incubated with increasing molar ratios of yNAP1 at 4° C for 10 hours in buffer A (20 mM Tris/Cl, pH 7.5, 100 mM NaCl, 1 mM DTT). H2A-H2B dimer dissociation was analyzed by native PAGE as described above. Nucleosomal bands (N1, S1, S2, and S3) were electro-eluted from gel slices into 0.05 x TBE, and were analyzed by 15 % SDS-PAGE. As controls, fluorescently labeled NCP (as indicated) was incubated with a 4- to 24-fold molar excess of BSA (obtained from Sigma) under the same conditions.

Histone dimer exchange – 3.5 μ M unlabeled NCP was incubated with pre-incubated yNAP1– histone dimer mixtures (3.5 μ M H2A-H2B CPM dimer, and 3.5 μ M yNAP1 dimer) at 4 °C for 10 hours in buffer A). Nucleosomes containing fluorescently labeled

(H2A-H2BT112C) dimer were prepared as a control. The exchange of fluorescently labeled H2A-H2B dimer or (H2A.Z-H2B) dimer was analyzed by native PAGE as described above. Exchange was quantified by ImageQuant v5.1 (Amersham Biosciences). Gels were first photographed without staining to view fluorescence at 365nm, followed by staining with ethidium bromide and / or coomassie blue as indicated. Control experiments using fluorescently labeled (H3-H4)₂ tetramer were performed analogously.

Nucleosome sliding assay –Nucleosomes were assembled on a previously characterized 196-bp DNA fragment derived from the 5S rRNA gene (Simpson and Stafford, 1983; Dong et al., 1990). Nucleosomes located at the center (N1) or edge (N2) of the 196bp 5S DNA fragment were fractionated by preparative gel electrophoresis using Prep Cell (Bio-Rad Laboratories, Richmond, CA, U.S.A.), using methods previously described for 146-bp NCP (Dyer et al., 2004). Incubation in the presence or absence of yNAP1 was performed at 4°C for 10 hours in buffer A. 3.5 μM NCP was incubated with the indicated amounts of yNAP1. Samples were analyzed by native PAGE. Identical amount of N1 and N2 nucleosomes (~ 6μg of DNA) were digested with 3.0 units of MNase (Worthington) at 37°C (Bao et al., 2004). To analyze histone content, nucleosomes were first fractionated on a 5% native gel in 0.2 X TBE, and the nucleosome species were electro-eluted into 0.05 X TBE for 45 minutes at 150 W and 4° C. The eluate was concentrated and analyzed by 18% SDS-PAGE. MvaI (MBI Fermentas), ScaI and AatII (New England Bio Labs) were used for restriction enzyme protection assays. ~ 50 μM of NCP was digested with 10 units of enzyme for 4 hours at 37°C, using prescribed buffers. Samples were treated with proteinase K (Sigma-Aldrich)

at a concentration of 50 µg/ml (50° C, 3 hours). The digested DNA products were analyzed on a 10% acrylamide gel and were viewed by staining with ethidium bromide.

4.4 Results

yNAP1 removes H2A-H2B dimers from the nucleosome core particle

To investigate the structural changes in NCP structure resulting from yNAP1 action, we used native gel electrophoresis, a highly sensitive assay for nucleosome structure (Dyer et al., 2004), in conjunction with fluorescence labeling (Park et al., 2004). We verified that yNAP1 binding was not compromised (at least qualitatively) by addition of the label to H2B (supplemental Fig. 1B), and that a yNAP1 – H2A-H2B dimer complex was formed in solution (supplemental Fig. 1C). CPM-labeled H2B T112C was utilized in all subsequent experiments in which fluorescently labeled H2A-H2B or (H2A.Z-H2B) dimers were used. The stoichiometry of the yNAP1 – H2A-H2B dimer complex has been shown to be one yNAP1 dimer per histone fold dimer (McBryant et al., 2003). Molar ratios given throughout this manuscript take into account the dimeric nature of yNAP1 (McBryant and Peersen, 2004).

Upon incubation of purified NCP reconstituted with fluorescently labeled H2B with increasing amounts of yNAP1, two new bands were detected by native PAGE, and one additional band that is also present in the control significantly increased in intensity. Only two of these bands were visible without staining (Fig. 4.1A, upper panel, denoted with S1 and S2), demonstrating that only they contained H2B. One additional band, apparent at

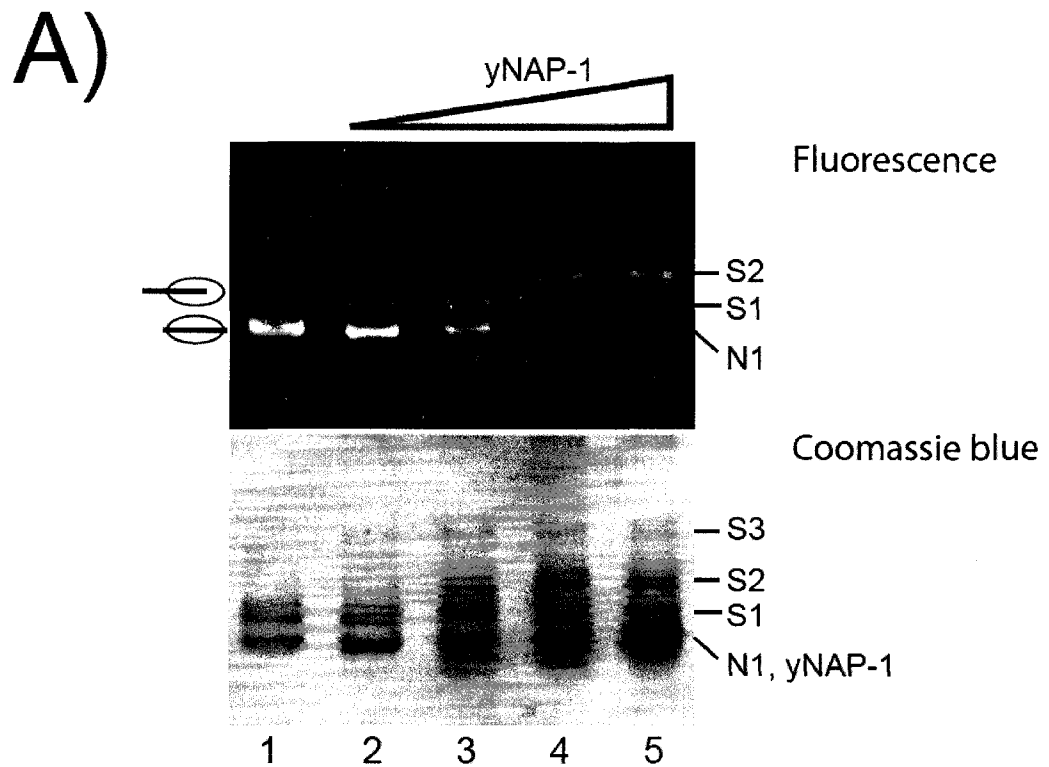


Figure 4.1 yNAP1 – induced H2A-H2B dimer dissociation from the NCP. (A) 3.5 μ M NCP, reconstituted with CPM-labeled H2A-H2B dimer was incubated with increasing molar ratios of yNAP1 (lane 1: no yNAP1, lanes 2-5: 0.5-, 1.5-, 3-, 4- fold molar ratio of yNAP1 dimer over NCP). Samples were incubated at 4° C for 10 hours and analyzed by native PAGE. The gel was first photographed without staining to view fluorescence (upper panel), then stained with coomassie blue (lower panel). The nucleosome and novel species are indicated with N1, S1, S2, and S3, respectively

higher yNAP1 to NCP ratios, is visible only after staining with ethidium bromide (not shown) and comassie brilliant blue (Fig. 4.1A, lower panel, S3).

Even at the largest excess of yNAP1 dimer over NCP (four-fold, lane 5), only very small amounts (< 2 %) of free DNA are released. The unstained gel was digitized under fluorescent light and the relative amounts of the nucleosomal bands (N1, S1 and S2) were plotted against the ratio of yNAP1 to NCP (Fig. 4.1B). This plot reveals that S1 is present in maximum amounts at a yNAP1 dimer to NCP ratio of ~1.5, and that S2 appears at the expense of N1 upon increasing yNAP1 / NCP ratios. S3 was too faint to be quantified.

To further investigate the composition of each band, we expanded the previous experiment and prepared NCPs in which either H2B, H4, or the DNA was fluorescently labeled as described earlier (Park et al., 2004). The purified NCPs were incubated with a two-fold molar excess of yNAP1 dimer over nucleosomes (refer to lane 3 in Fig. 4.1A), and the products were analyzed by native PAGE (Fig. 4.2A). The gels were analyzed without staining to visualize only fluorescent species. Importantly, we do not observe any detectable (H3-H4)₂ tetramer – yNAP1 complexes under moderate conditions (Fig. 4.2A, lanes 4 and 5); however, at higher temperature (37° C for 12 hours) and a large (12-fold) excess of yNAP1 over NCP, some dissociation of the (H3-H4)₂ tetramer from the DNA is observed (not shown). We show conclusively that N1 and S1 contain DNA, (H3-H4)₂ tetramer, and H2A-H2B dimers, since both of these bands light up if nucleosomes reconstituted with fluorescently labeled DNA (lane 3), H4 (lane 5), and H2B (lane 7) are used. S1 co-migrates with the off-centered NCP species that we routinely observe after salt-gradient reconstitution onto this particular DNA fragment, and is thus identified as a NCP with an altered translational position of the DNA with respect to the histone octamer

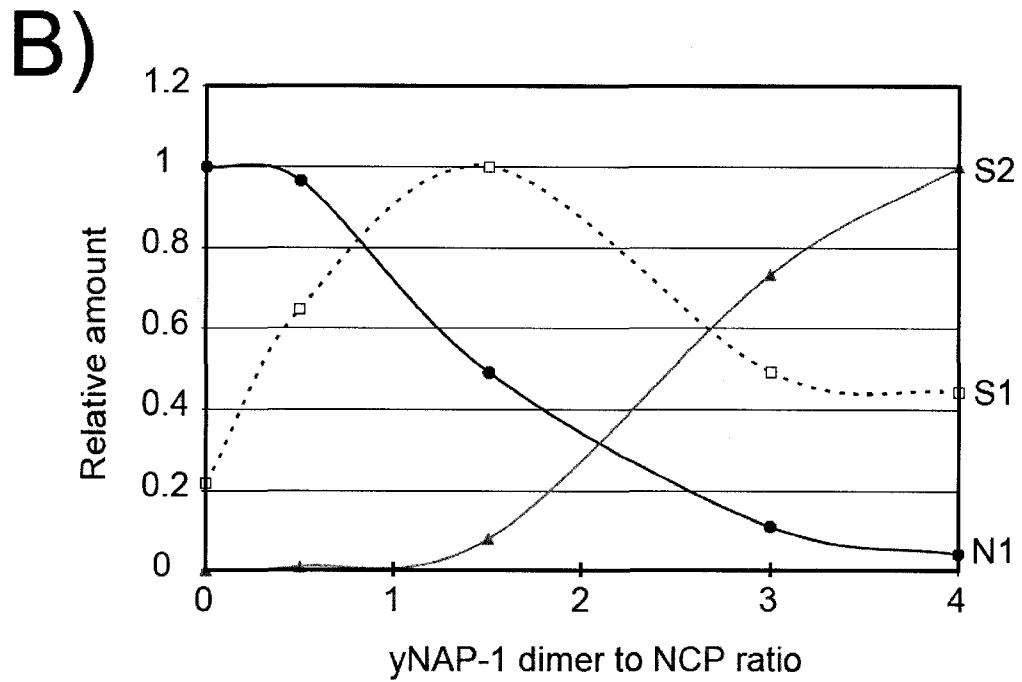


Figure 4.1 yNAP1 – induced H2A-H2B dimer dissociation from the NCP.

(B) Quantitation of the gel shown in (A). The lanes were scanned, and the intensity of the lanes was analyzed by ImageQuant v5.1 (Amersham Biosciences). Numbers were normalized in terms of ratio of N1, S1, or S2 species.

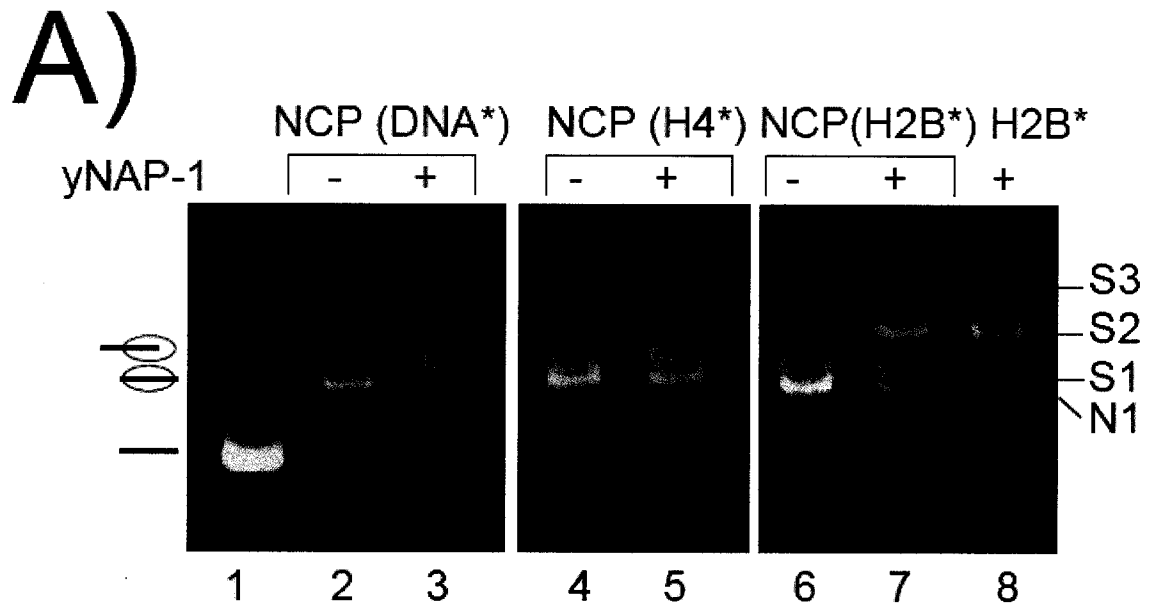


Figure 4.2 Analysis of novel nucleosomal species. (A) Nucleosomes (3.5 μ M) were incubated in the presence (+) or absence (-) of a 2-fold molar excess of yNAP1. Incubation and gel electrophoresis was done as in Fig. 4.1A. Lane 1: CPM-labeled DNA, lanes 2 and 3: DNA-labeled NCP in the absence and presence of yNAP1, lanes 4 and 5: H4-labeled NCP in the absence and presence of yNAP1, lanes 6 and 7: H2B-labeled NCP in the absence and presence of yNAP1; lane 8: CPM-labeled H2A-H2B dimer with yNAP1

(Flaus et al., 1996; Muthurajan et al., 2003). S3 only contains (H3-H4)₂ tetramer and DNA, but no H2A-H2B dimer (lanes 3 and 5), and is thus identified as a ‘tetrasome’ (a (H3-H4)₂ tetramer – DNA complex). S2 contains fluorescently labeled H2A-H2B dimer (lane 7), but no DNA or (H3-H4)₂ tetramer, and co-migrates with a H2A-H2B dimer – yNAP1 complex (lane 8).

To confirm that S2 contains yNAP1, we performed a similar experiment with GST-tagged yNAP1 and visualized its electrophoretic migration by fluorescence. GST-yNAP1 is just as efficient in converting N1 to S1 and S3, but only S2 is supershifted (Fig. 4.2B, lane 6). Consistent with the propensity of GST to dimerize, we observe an additional higher band on our native gels (denoted with 2GST-S2). Our experiments show no evidence of a stable yNAP1 – NCP complex, since the electrophoretic migration of N1 and S1 remains unchanged (Fig. 4.2B).

We next excised N1, S1, and S3 from a native gel and analyzed the protein content of these bands by SDS-PAGE (Fig. 4.2C). Consistent with our interpretation of the results shown above, we found that N1 and S1 contain stoichiometric amounts of the four histones. S3 contained only histone H3 and H4, confirming that at higher yNAP1 / NCP ratios, yNAP1 removes both H2A-H2B dimers from a folded NCP. Identical results were obtained using a GST fusion of yNAP1 (not shown). Using GST-yNAP1, we could also verify that S2 contained only H2A, H2B, and GST-yNAP1 (Fig. 4.2C).

Since yNAP1 is highly acidic, it is formally possible that the observed removal of H2A-H2B dimers from the NCP is a ‘salt effect’ due to competition between yNAP1 and DNA and for the histones. To evaluate the specificity of yNAP1 in H2A-H2B dimer

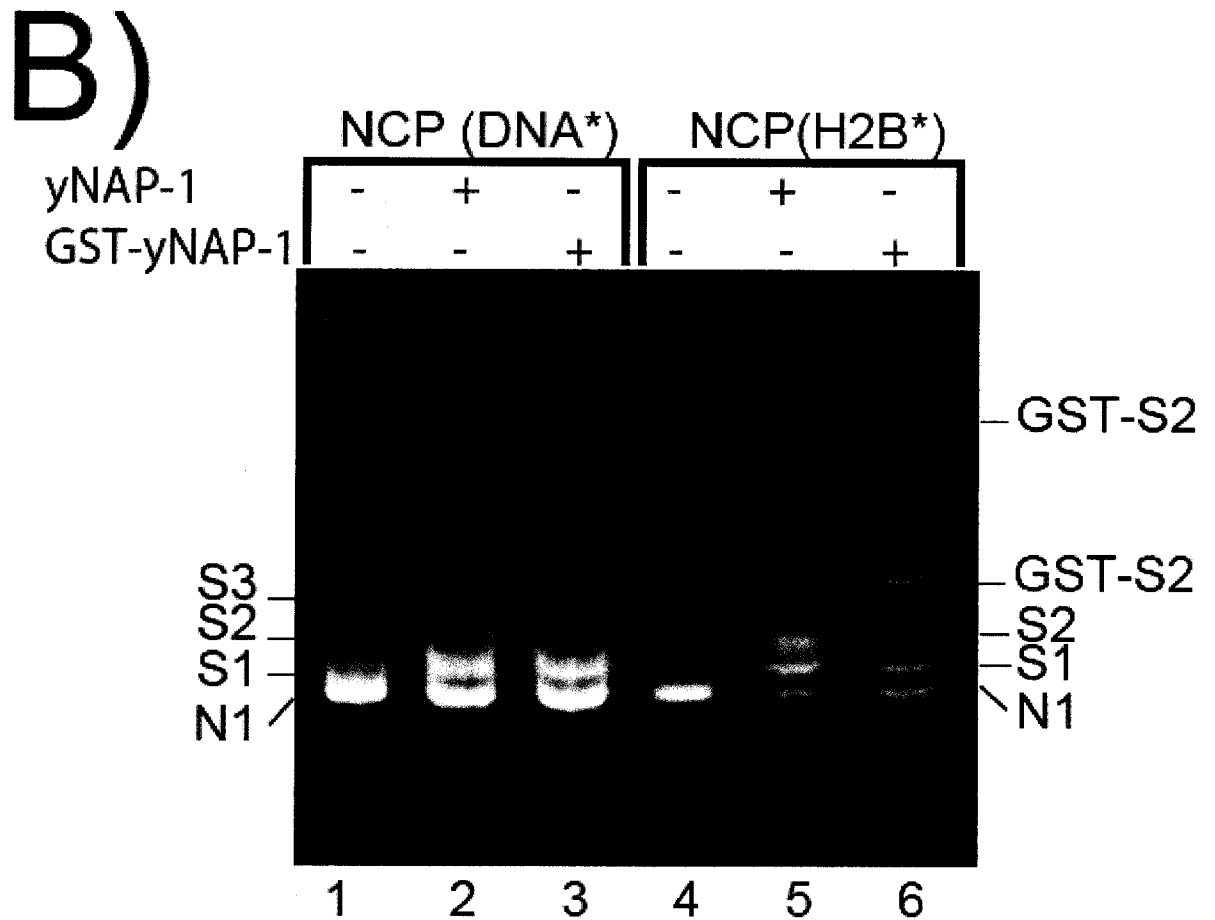


Figure 4.2 Analysis of novel nucleosomal species. (B) Analysis of yNAP1 – H2A-H2B complex (S2) was carried out by electromobility shift assay. Fluorescently labeled NCPs were incubated without yNAP1 (lane 1 and 4), with yNAP1(lane 2 and 5), or with GST-yNAP1 (lane 3 and 6). GST-yNAP1 – H2A-H2B dimer complex (GST-S2) is indicated.

C)

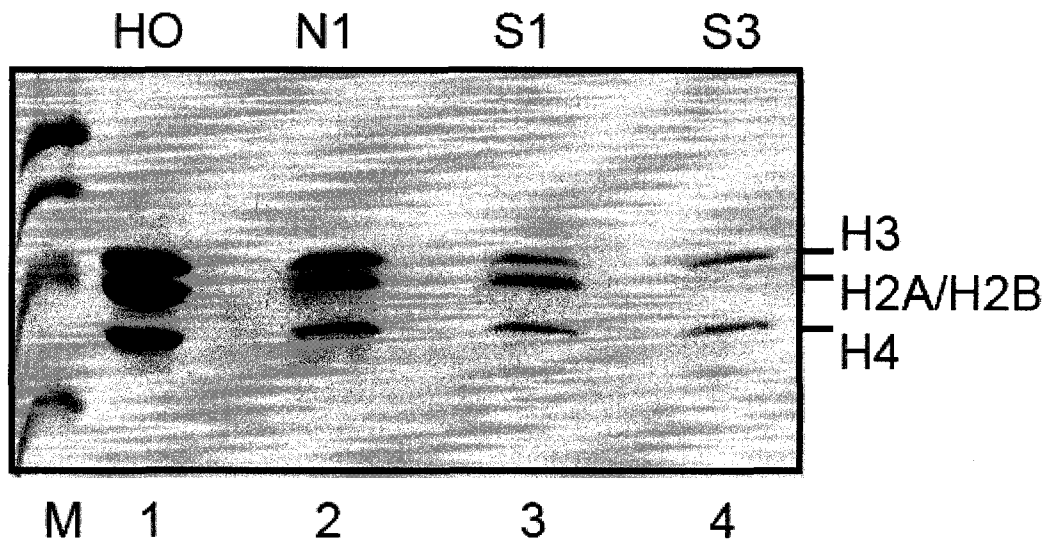


Figure 4.2 Analysis of novel nucleosomal species. (C) Analysis of the protein composition of yNAP1 – generated nucleosome species by 15% SDS PAGE. Lane 1-5: N1, S1, S3, GST-S2 (lower band) and 2GST-S2 (upper band). Nucleosome species were electro-eluted from 5% native gel slices (as seen in B). Lane 6: GST-NAP1. Lane 7: protein marker (M) 14.5, 21.5, 31, 45, 66.2, and 94.4 kDa.

dissociation, we compared the ability of yNAP1 and BSA to structurally alter the NCP, using gel shift assays. BSA is a protein of similar size and acidic pI. Unlike yNAP1, a four-fold molar excess of albumin had no effect on the nucleosomal band (Fig. 4.2D, compare lane 4 with 5, and 7 with 8). No H2A-H2B dimer dissociation or disruption of the NCP was observed upon addition of an up to 24-fold molar excess of albumin (data not shown).

The C-terminal acidic domain of yNAP1 is necessary for the dissociation of the H2A-H2B dimer from the NCP, although it is not required for histone binding

We and others have shown previously that the N-terminal domain (NTD, amino acids 1-73) and the C-terminal acidic domain (CTD, amino acids 366-417) of yNAP1 are not required for histone binding and nucleosome assembly (McBryant et al., 2003; Fujii Nakata et al., 1992). In order to test whether these regions of yNAP1 are required for the interactions with the nucleosome, we analyzed the ability of truncated yNAP1 constructs {lacking 73 amino acids from the N-terminus (yNAP1 Δ N), or the 73 N-terminal and 52 C-terminal amino acids (NAP1 Δ NC)} to remove H2A-H2B dimers from the folded NCP (Fig. 4.3). NAP1 Δ N retained the ability to dissociate H2A-H2B dimers from the NCP. In striking contrast, NAP1- Δ NC has completely lost the ability to structurally alter the NCP. This was shown conclusively using native PAGE of two different fluorescently labeled NCPs (Fig 4.3A, lanes 1-4 and 5-8). Importantly, the CTD alone (yNAP1 amino acids 302-417; pI 3.66) has no effect on the NCP (Fig. 4.3B), just as has been observed for BSA (Fig. 4.2D). It is however formally possible that the N-terminus can sustain activity in the absence of the C-terminal domain, and this possibility remains to be tested.

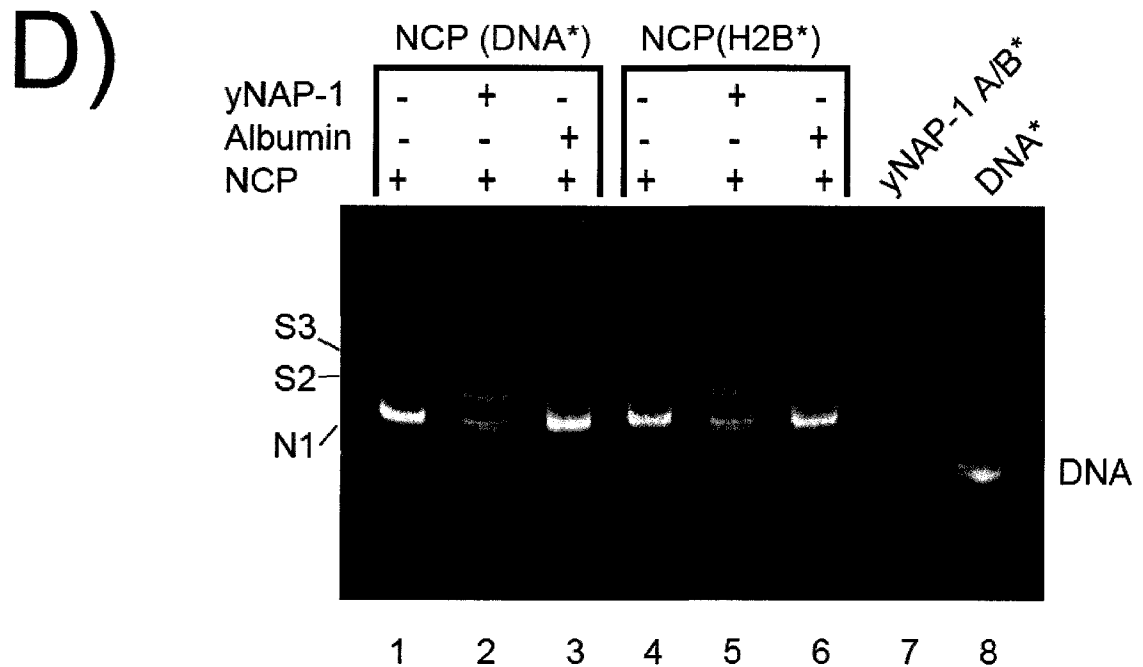


Figure 4.2 Analysis of novel nucleosomal species. (D) The observed effect is specific for yNAP1. NCP (3.5 μ M) containing fluorescently labeled H2A-H2B dimer or fluorescently labeled DNA was incubated with a 2-fold molar excess of yNAP1 or a 4-fold molar excess of BSA at 4°C for 10 hours. Lane 1: fluorescently labeled DNA; lane 2: fluorescently labeled (H2A-H2B) dimer with yNAP1 complex; lane 3 and 6: fluorescently labeled NCP without yNAP1 or BSA; lane 4-5 and 7-8: fluorescently labeled NCP was incubated with yNAP1 or BSA as indicated.

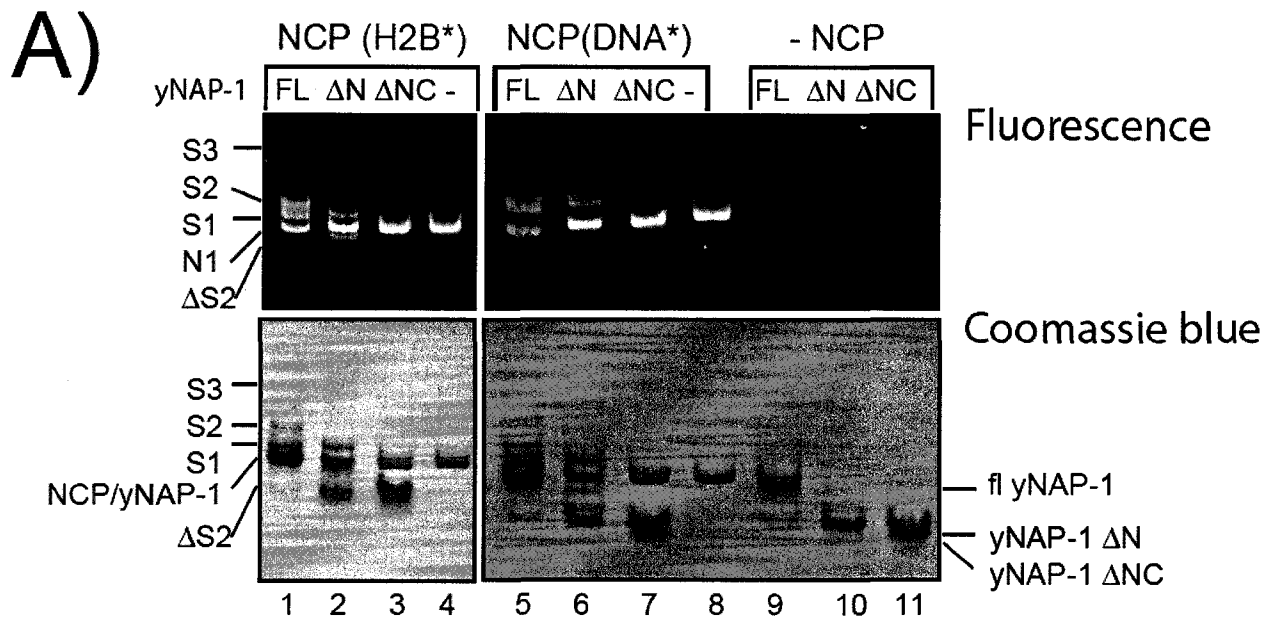


Figure 4.3 The C-terminal acidic domain (CTD) of yNAP1 is required for the dissociation of the H2A-H2B dimer. (A) NCP (3.5 μ M) containing fluorescently labeled H2A-H2B dimer (lanes 1-4) or fluorescently labeled DNA (lanes 5-8) was incubated with a 2-fold molar excess of full-length yNAP1 (lanes 1, 5, and 9), NAP1 ΔN (lanes 2, 6, and 10), or NAP1 ΔNC (lanes 3, 7, and 11). Full-length, NAP1 ΔN , and NAP1 ΔNC in the absence of NCP are shown in lanes 9-11. The gels were first photographed without staining to view fluorescence (upper panel), followed by staining with coomassie blue to visualize protein complexes (lower panel). The location of N1, S1-3, and the yNAP1 ΔN – H2A-H2B dimer complex ($\Delta S2$) is indicated.

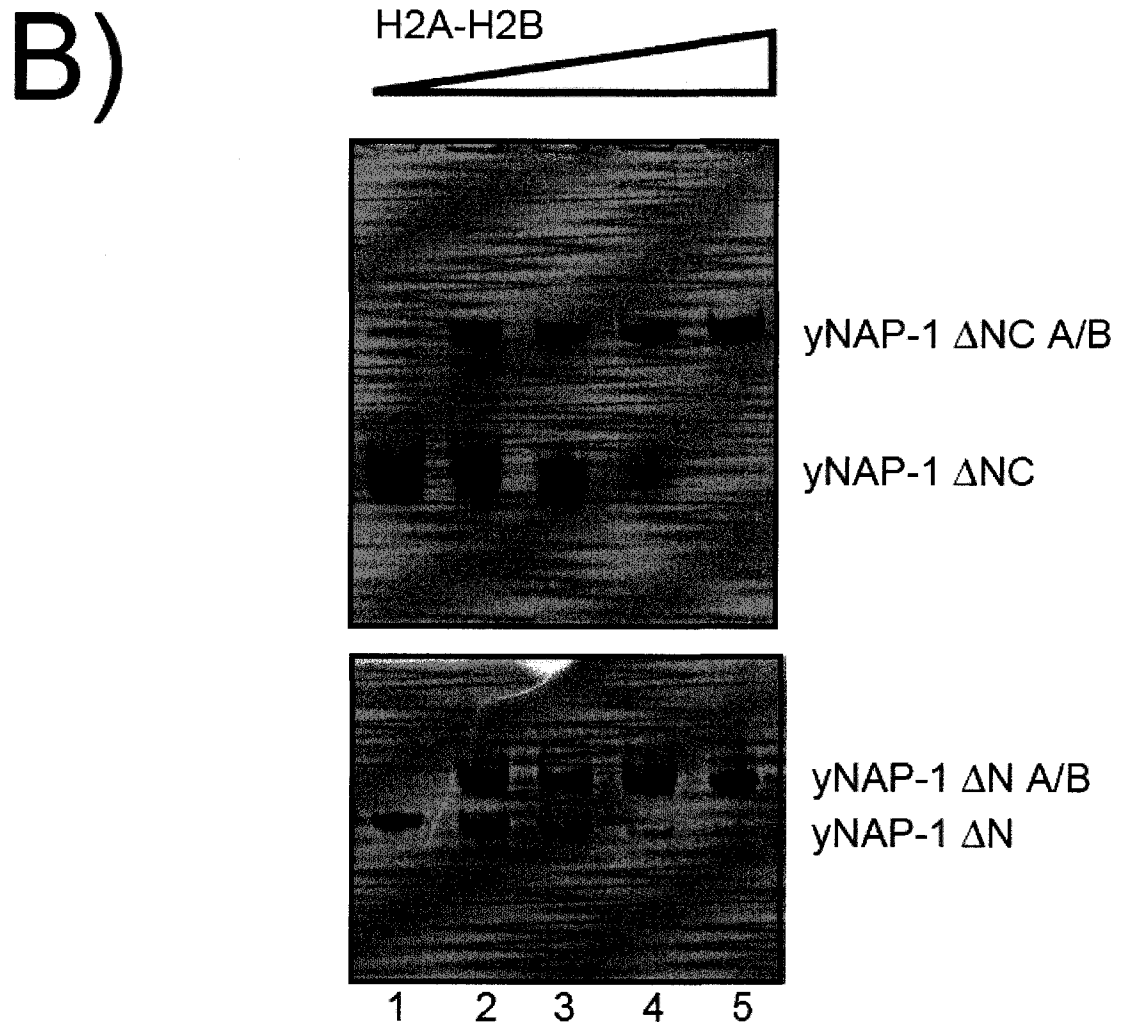


Figure 4.3 The C-terminal acidic domain (CTD) of yNAP1 is required for the dissociation of the H2A-H2B dimer. (B) NCP containing fluorescently labeled DNA (lane 1) incubated with full-length yNAP1 (lane 2) and the CTD of yNAP1 (lane 3). **(C)** Truncated versions of yNAP1 still form complexes with the H2A-H2B dimer. 10 μ M of NAP1 Δ N (74-417) or NAP1 Δ NC was incubated with H2A-H2B dimer (lanes 1-5: 1, 4, 6, 8, 10 μ M, respectively) at 4° C for 10 hours, and analyzed by native PAGE. yNAP1 – H2A-H2B dimer complexes are indicated.

Full length yNAP1, yNAP1 Δ N, and yNAP1 Δ NC are all capable of forming a complex with the H2A-H2B dimer (supplemental Fig. 1A, and Fig. 4.3C), confirming earlier data with GST-constructs of yNAP1 (McBryant et al., 2003). Thus, the core domain of yNAP1 is sufficient to bind the H2A-H2B dimer in solution, as well as to assemble chromatin from DNA and histone components. However, this core domain is not sufficient to remove H2A-H2B dimers once they are assembled into a functional NCP, but additionally requires the acidic C-terminal domain.

H2A-H2B dimers are exchanged in and out of nucleosomes by yNAP1

Having established that yNAP1 is capable of removing H2A-H2B dimers from a folded NCP, we wanted to investigate whether yNAP1 is capable of replacing one H2A-H2B dimer with another. To distinguish between the newly exchanged species and unaltered NCP, and to overcome the complication that yNAP1 co-migrates with the NCP in our gel system, we again exploited our library of fluorescently labeled histone subunits. A saturating amount of fluorescently labeled H2A-H2B dimer was pre-incubated with yNAP1 to allow complex formation under previously established conditions (see supplemental Fig. 1). Complexes (which do not contain free yNAP1) were incubated with previously assembled, unlabeled NCP preparations. The products were analyzed by native PAGE, and fluorescent species were visualized without staining (Fig. 4.4, upper panel). Exchange by yNAP1 in about 17 - 22 % of the nucleosome population (in four independent experiments) was observed, as evident in the appearance of a fluorescent NCP band (N1) when incubated with a preformed fluorescently labeled H2A-H2B dimer – yNAP1 complex, but not with dimer or yNAP1 alone (Fig. 4.4, upper panel, compare

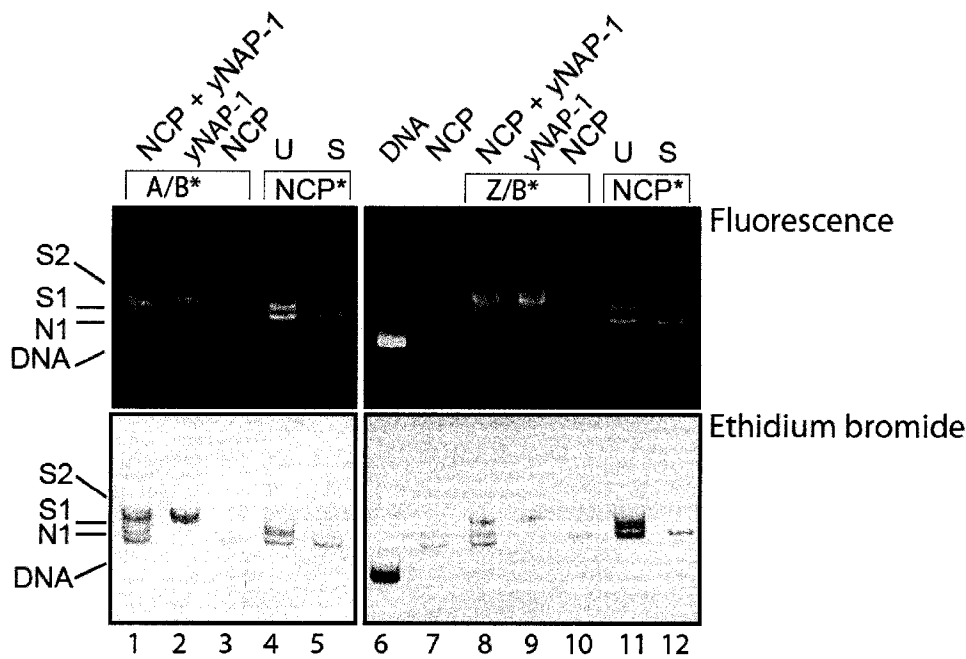


Figure 4.4. yNAP1-mediated exchange of canonical H2A-H2B dimer or histone variant (H2A.Z-H2B) dimer into nucleosomes. Unlabeled NCP was incubated with pre-formed yNAP1 – H2A-H2B dimer (or H2A.Z-H2B) dimer mixtures as indicated. Reconstituted nucleosomes were heat-shifted for 60 minutes at 37°C to obtain a unique species of nucleosome (shifted nucleosome). The gel was first photographed without staining to view fluorescence (upper panel), followed by staining with ethidium bromide (lower panel). 3.5 μ M NCP, 3.5 μ M yNAP1 with H2A-H2B or (H2A.Z-H2B) dimer complex were used. Lane 1: unlabeled NCP, yNAP1 and CPM-labeled H2A-H2B dimer. Lane 2: yNAP1 and CPM-labeled H2A-H2B dimer. Lane 3: unlabeled NCP, CPM-labeled H2A-H2B dimer. Lane 4 and 5: NCP containing CPM-labeled H2A-H2B dimers, unshifted (U) and shifted (S). Lane 6: CPM-labeled DNA. Lane 7: unlabeled NCP. Lane 8: unlabeled NCP, yNAP1 and CPM-labeled (H2A.Z-H2B) dimer. Lane 9: yNAP1 and CPM-labeled (H2A.Z-H2B) dimer. Lane 10: unlabeled NCP, CPM-labeled (H2A.Z-H2B) dimer. Lane 11 and 12: as lanes 4 and 5.

lanes 1-3). A strong fluorescent band corresponding to the γ NAP1 – H2A-H2B dimer complex (S2) is also observed in lanes 1 and 2. No significant amounts of free DNA are released in this process, as is shown in the ethidium bromide-stained gel (Fig. 4.4, lower panel). When nucleosomes were incubated with fluorescently labeled (H3-H4)₂ tetramer – γ NAP1 complex under identical conditions, no incorporation of fluorescently labeled (H3-H4)₂ tetramer into nucleosomes was observed (data not shown). When an H2A-H2B dimer – γ NAP1 complex was incubated with free DNA, no H2A-H2B – DNA complex or ternary DNA-H2A-H2B- γ NAP1 ternary complex was detected (data not shown; also see (Nakagawa et al., 2001). Together, these results demonstrate that γ NAP1 - mediated H2A-H2B dimer exchange does not occur by complete dissociation of the NCP, and that the exchange reaction is limited to the histone H2A-H2B dimer, despite the proven ability of γ NAP1 to bind the (H3-H4)₂ tetramer in solution with equal or higher affinity (McBryant et al., 2003).

We next examined whether γ NAP1 is capable of replacing major-type H2A-H2B dimer with a dimer containing an H2A variant. γ NAP1 does not display a markedly different ability to bind the major-type compared to several histone variant complexes (supplemental Fig. 1A). Upon incubation of unlabeled NCP with fluorescently labeled (H2A.Z-H2B) dimer, a fluorescent NCP species was observed (Fig. 4.4, lane 8). These experiments show conclusively that γ NAP1 mediates exchange of histone H2A-H2B dimers into folded nucleosomes. Our finding that histone variants are stably bound by γ NAP1 (supplemental Fig. 1A) and are readily utilized in this exchange reaction leads us to predict that not only H2A.Z, but other H2A histone variants in complex with H2B may be exchanged into assembled NCPs under physiological conditions.

yNAP1 facilitates nucleosome sliding

Upon incubation of yNAP1 with nucleosomes reconstituted on a 146-bp DNA fragment at 4° C, we reproducibly observe a second species (S1 in Fig. 1A and Fig. 4.4), which contains a full complement of histone proteins and DNA (Fig. 4.2C) and co-migrates with a well-characterized species that is routinely observed after salt-gradient reconstitution on this particular DNA fragment. This species represents an NCP in which the histone octamer is positioned asymmetrically on the DNA; it is stable over weeks at 4 °C, but can be converted into a thermodynamically more favorable species in which the DNA is placed symmetrically around the histone octamer by incubation at elevated temperatures (for example, Fig. 4.4, compare lanes 4 and 5). It appears that the significant energy barrier that exists towards repositioning of the histone octamer along the DNA is relieved by the transient yNAP1 – mediated removal of the H2A-H2B dimer.

To further investigate the possibility that yNAP1 facilitates nucleosome sliding, we reconstituted NCPs on a 196-bp DNA fragment derived from the 5S rRNA gene (Simpson and Stafford, 1983). Upon salt-gradient reconstitution, two major nucleosome species (N1 and N2) are routinely obtained (Fig. 4.5A, lane 1). These have been described earlier as nucleosomes with different translational positions (Dong et al., 1990). The two species were separated from each other by preparative gel electrophoresis (Fig. 4.5A, lanes 2-3). SDS-PAGE revealed that N1 and N2 contained an identical and stoichiometric composition of histones (Fig. 4.5B, compare lanes 1 and 3 with lane 5). Micrococcal nuclease treatment of the isolated species demonstrated that both protected ~ 146 bp of DNA (not shown).

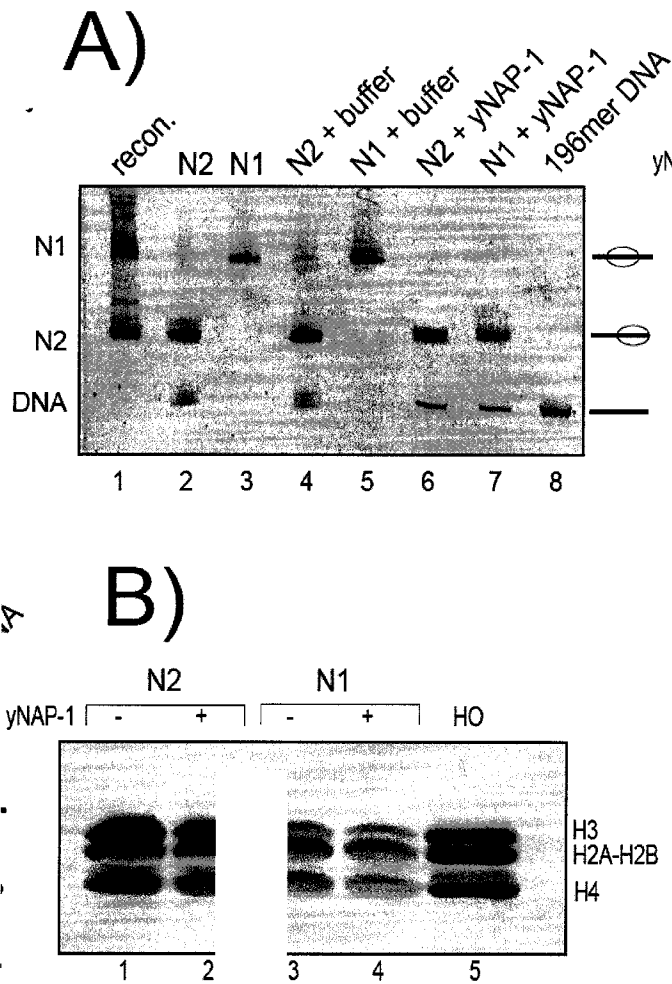


Figure 4.5. yNAP1-mediated nucleosome sliding on a 196-bp DNA fragment. (A) Effect of yNAP-1 on two nucleosomal species. Lane 1: nucleosomes after reconstitution; lanes 2 and 3: purified N2 and N1 bands; lanes 4 and 6: N2 in absence and presence of yNAP-1; lanes 5 and 7: N1 in absence and presence of yNAP-1. Lane 8: 196-bp DNA. N1 and N2 were incubated with NAP-1 for 10 hours at 4° C. **(B)** Histone composition of N1 (lanes 3 and 4) and N2 (lanes 1 and 2) in the absence and presence of yNAP-1, as indicated. Lane 5 shows purified histone octamer (HO).

Purified N1 and N2 were incubated independently with yNAP1. Intriguingly, N1 was transformed completely into N2 in the presence of equimolar amounts of yNAP1 dimer and NCP (Fig. 4.5A, lane 7). The same phenomenon was observed at yNAP1 to NCP ratios as low as 0.15 : 1 (not shown), indicating that yNAP1 acts catalytically. In contrast, yNAP1 had no effect on the electrophoretic mobility of N2 (lane 6). Incubation in the absence of yNAP1 at elevated temperatures (37 and 45 °C) had no effect on the electrophoretic mobility of either N1 or N2. Importantly, the histone composition of both nucleosomal species (Fig. 4.5B) and the amount of DNA that is protected against digestion with micrococcal nuclease (not shown) remains unchanged upon yNAP1 incubation.

To investigate whether treatment of N1 with yNAP1 results in true nucleosome sliding, it was necessary to characterize the position of the histone octamer with respect to the DNA in N1 and N2 before and after yNAP1 addition, using restriction enzyme protection assays in conjunction with micrococcal nuclease digestion. Sites for restriction enzymes MvaI, ScaI, and AatII in the 196-bp DNA fragment are depicted in Fig. 4.5C. In the absence of yNAP1, N2 is digested to about 30 - 50% with ScaI and AatII, and an apparent 100 % with MvaI (Fig. 4.5D). In this latter experiment, the two expected fragments of 178 and 183 base pairs in length cannot be distinguished. Nevertheless, this result strongly suggests that the regions of the DNA not occupied by nucleosomes is free of non-specifically bound histones. Together with the finding that 146 bp are protected from digestion with MNase (not shown), this is consistent with positions for N2 at either end of the nucleosomal DNA (Fig. 4.5C). N1 is cut to 100 % with MvaI, but is completely protected from digestion with AatII and ScaI.

C)

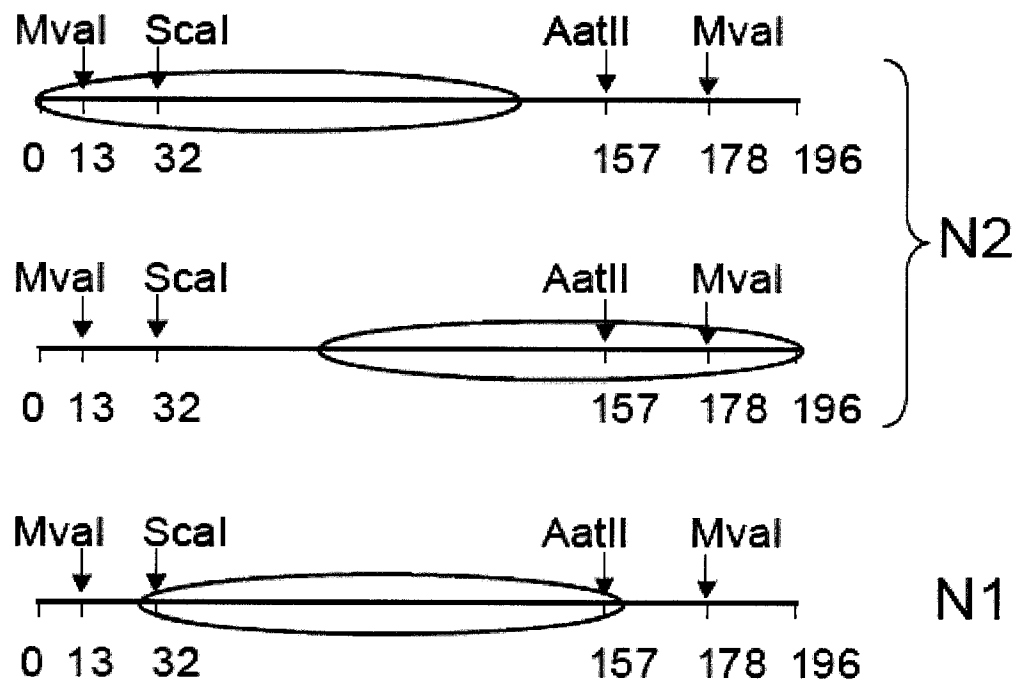


Figure 4.5 (C) Overview of nucleosome positions and restriction endonuclease sites used for nucleosome mapping

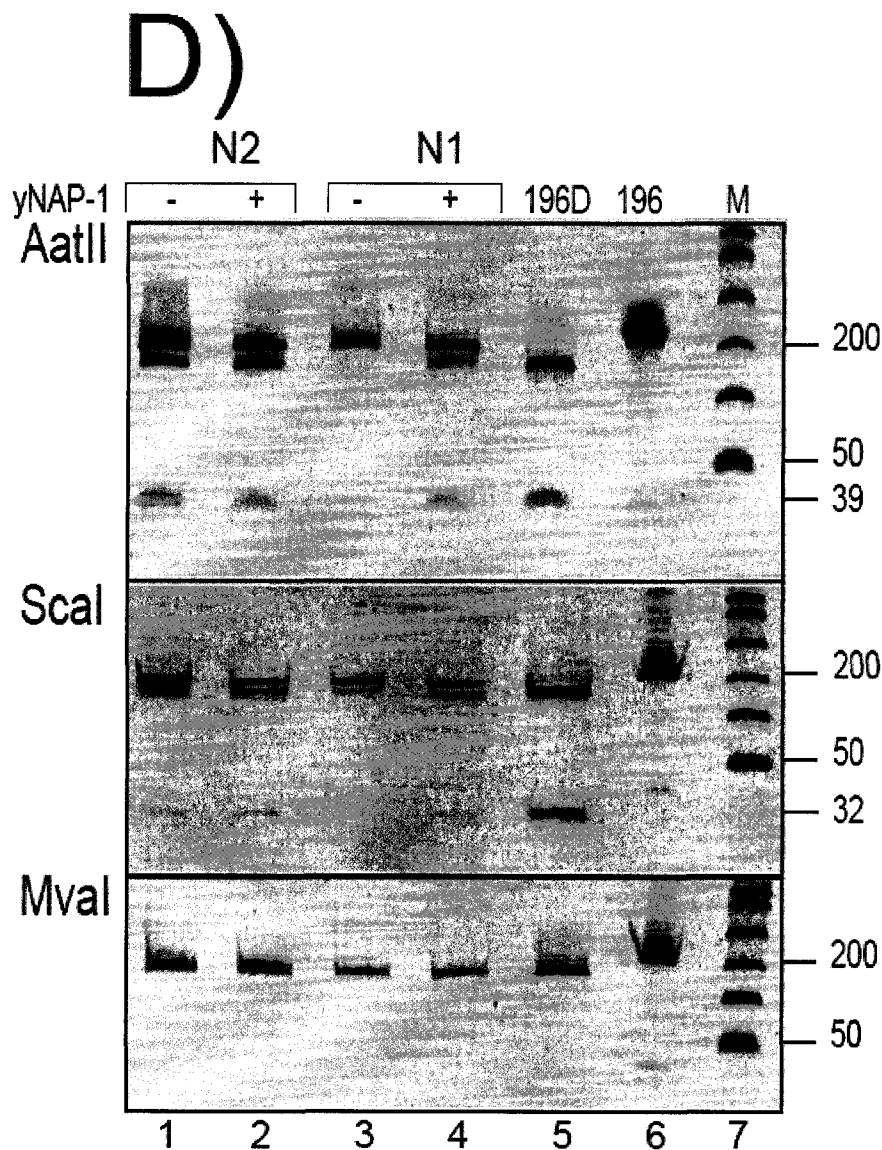


Figure 4.5 (D) Restriction endonuclease protection assays of N1 and N2 before and after yNAP-1 treatment, using AatII, ScaI, and MvaI. N1 (lanes 3 and 4) and N2 (lanes 1 and 2) were analyzed in the absence and presence of yNAP-1, as indicated. Lane 5 shows digestion of the free 196-bp DNA fragment, lane 6 is undigested DNA, and lane 7 a DNA ladder. Relative molecular masses of restriction products are indicated. 10 % polyacrylamide gels were stained with ethidium bromide, colors were reversed for clarity.

This places N1 between bp 32 and 157, which corresponds to the previously identified positioning sequence on this particular DNA fragment (Simpson et al., 1985).

Incubation with yNAP1 does not change the behavior of N2 in MNase (not shown) and restriction enzyme protection assays (Fig. 4.5D), consistent with the observation that yNAP1 has no effect on the electrophoretic behavior of N2. In contrast, N1 behaves like N2 after yNAP1 treatment in MNase and restriction endonuclease protection assays (Fig. 4.5D, compare lane 2 and 4), and contains a full complement of all four histones (Fig. 4.5B), confirming our interpretation that yNAP1 causes true nucleosome sliding.

We next investigated whether the ability of yNAP1 to exchange histone H2A-H2B dimers is required to facilitate nucleosome sliding. To this end, we exploited our earlier observation that a truncated version of yNAP1 (NAP1 Δ NC) was incapable of dissociating histone dimers from nucleosomes, although this yNAP1 mutant was perfectly capable of assembling chromatin and binding histone complexes. NAP1 Δ N and full-length yNAP1 were used as controls. Purified N1 was incubated with a 2-fold molar excess of different yNAP1 truncations under the same conditions as above, and examined by native PAGE. As shown in Figure 4.6 (upper panel), wild-type yNAP1 and yNAP1 Δ N were able to induce the redistribution of N1 nucleosomes to N2 (Fig. 4.6, lanes 3-5), concomitant with the formation of a H2A-H2B dimer – yNAP1 (or yNAP1 Δ N) complex (Fig. 4.6, lower panel, lanes 4 and 5). In striking contrast, no effect was observed in the presence of yNAP1 Δ NC (Fig. 4.6, lane 6), and no H2A-H2B dimer – yNAP1 Δ NC complex was observed. This finding demonstrates that transient H2A-H2B dimer dissociation from the NCP facilitates nucleosome sliding in the presence of yNAP1.

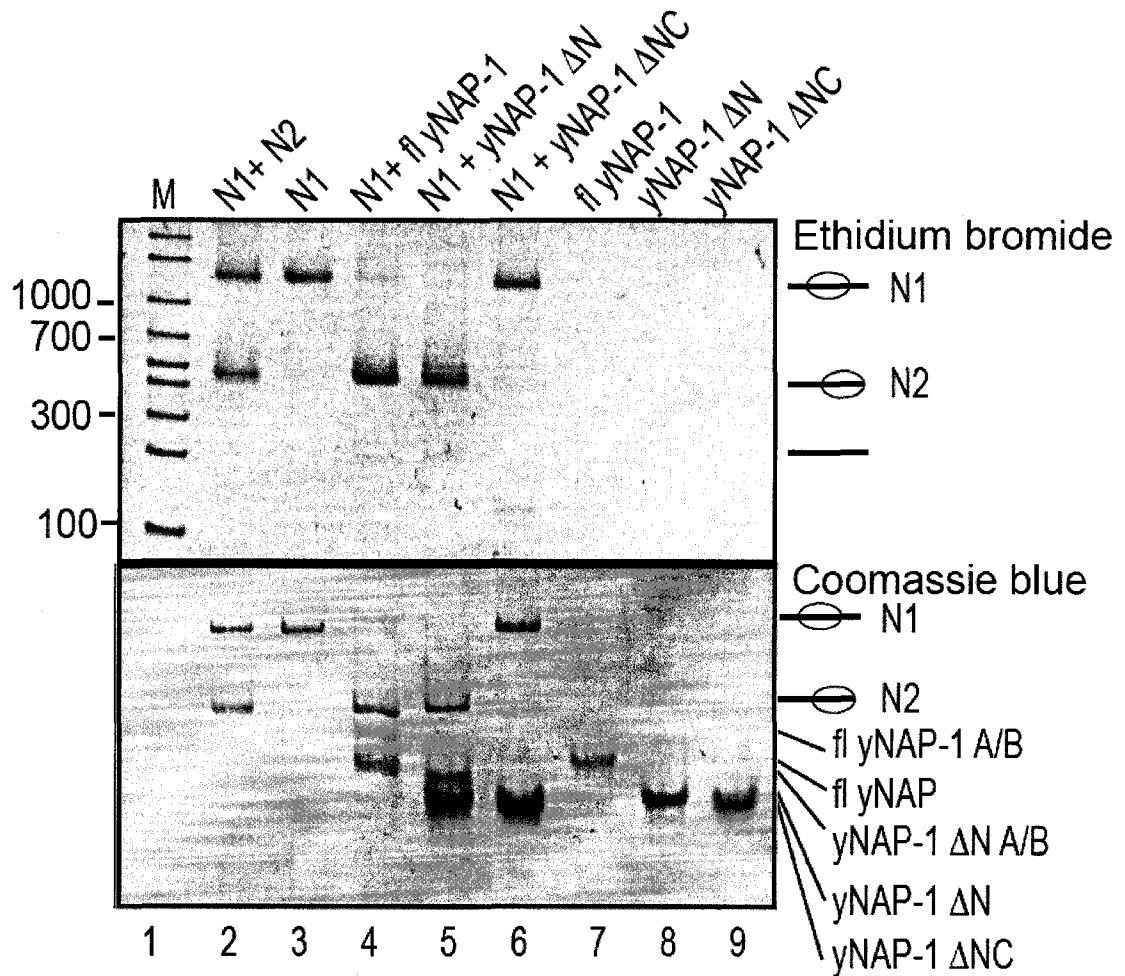


Figure 4.6. The C-terminal acidic domain of yNAP-1 is required for nucleosome sliding. 3.5 μ M NCP was incubated with a 2-fold molar excess of full-length yNAP-1 (1-417), yNAP-1 Δ N (74-417), or yNAP-1 Δ NC (74-365) for 10 hours at 4 $^{\circ}$ C. Samples were analyzed by native PAGE, and visualized by ethidium bromide (top panel) and coomassie blue staining (bottom panel). Lane 1: DNA marker (M), lane 2: N1 and N2 nucleosomes; lane 3: purified N1, lane 4: N1 with full-length yNAP-1, lane 5: N1 with yNAP-1 Δ N; lane 6: N1 nucleosome with yNAP-1 Δ NC; lanes 7-9: full-length yNAP-1, yNAP-1 Δ N, and yNAP-1 Δ NC as a control. The weak S3 band (lane 5) is indicated with an asterisk.

Under these conditions, only minimal amounts of free DNA are released and (H3-H4)₂ tetramer is not exchanged, indicating that nucleosome sliding occurs without complete nucleosome dissociation. As was the case with nucleosome core particles reconstituted on 146-bp DNA fragments, bands that were equivalent to S3 were observed in all cases (indicated by asterisks in Fig. 4.6).

4.5 Discussion

yNAP1 is an abundant, phylogenetically conserved acidic histone chaperone that has been shown to be involved primarily in histone transport and chromatin assembly. Here we have demonstrated that yNAP1 is also capable of transiently removing H2A-H2B dimers from a folded nucleosome. This results in the active exchange of H2A-H2B or histone variant dimers into nucleosomes in an ATP- and DNA replication-independent fashion, but also facilitates sliding of the nucleosome along the DNA to help it attain a thermodynamically more favorable position. These roles for yNAP1 are likely to be of biological significance, and may be a general characteristic of acidic histone chaperones.

yNAP1 facilitates the removal of one or both H2A-H2B dimers from a folded nucleosome at yNAP1 dimer to nucleosome stoichiometries of approximately 1:1, whereas the (H3-H4)₂ tetramer is removed only at much higher molar ratios. This is consistent with previous results (Ito et al., 2000), and with the observed rapid exchange of H2A-H2B dimers *in vivo* (Jackson, 1990; Kimura and Cook, 2001), and is expected if one considers the central position of the (H3-H4)₂ tetramer on the DNA (Luger et al., 1997). The removal of H2A-H2B dimers is likely to facilitate transcription (Levchenko and Jackson, 2004; Ito et al., 2000). This mechanism has also been recently attributed to

the FACT complex (Belotserkovskaya et al., 2003; also see Rhoades et al., 2004). Easier access of transcription factors to nucleosomal DNA in the presence of nucleoplasmin (an acidic histone chaperone with a different quaternary structure and no sequence homology to yNAP1) and yNAP1 has also been attributed to their ability to deplete mono-nucleosomes of H2A-H2B dimers (Chen et al., 1994; Walter et al., 1995). Complete nucleosome dissociation and reassembly has emerged as an important regulator of the PHO5 promoter (Reinke and Horz, 2003; Boeger et al., 2004). The recent finding that the H3/H4 histone chaperone Asf1p mediates nucleosome disassembly from the PHO5 promoter *in vivo* (Adkins et al., 2004) suggests that histone chaperones in general may have a more prominent role than previously assumed in promoting nucleosome dissociation during transcription.

Here we have shown that the ability of yNAP1 to remove a H2A-H2B dimer from a nucleosome depends on the C-terminal acidic region of yNAP1, which is dispensable for histone binding and nucleosome assembly (McBryant et al., 2003; and references therein). Therefore, histone removal from a folded nucleosome is not a simple reversal of the mechanism involved in histone deposition during nucleosome assembly. The extreme acidic character of the residues contained in the C-terminal domain (30 residues out of a total of 52 in the CTD are acidic, comprising one third of all acidic residues in the entire protein) may simply be required to compete with the DNA for the histone dimer, or it may contribute to histone removal via a more complex mechanism that remains to be elucidated. Interestingly, the acidic C-terminal region of the FACT subunit Spt16 is required for interaction with the nucleosome. However, unlike in case of yNAP1, it

appears to be required also for histone deposition onto DNA (Belotserkovskaya et al., 2003).

The removal of one or both H2A-H2B dimers from a mono-nucleosome is reversible, and can lead to an exchange reaction with histone dimers containing variants of histone H2A, such as H2A.Z (this study), and H2A.Bbd (Y. Bao and Y-J. Park, unpublished). We have also observed the reverse reaction in which a histone-variant containing nucleosome is converted into a canonical nucleosome (data not shown), demonstrating the lack of discrimination that yNAP1 has for various H2A-H2B dimers, both free in solution and when bound to a nucleosome. Importantly, yNAP1 – mediated histone exchange is independent of replication, does not require ATP, and does not result in the release of a significant amount of DNA or exchange of (H3-H4)₂ tetramer. This indicates that complete nucleosome disassembly and reassembly is not required.

yNAP1 alone is unlikely to target histone variants to specific regions within chromatin. However, it is possible that yNAP1 and other assembly proteins contribute to the incorporation of histone variants at specific regions within chromatin upon association with histone variant – specific chromatin assembly factors, such as the Swr1 complex that functions in conjunction with a yNAP1 – H2A.Z-H2B dimer complex (the ‘Nap-Z complex’; (Krogan et al., 2003; Kobor et al., 2004; Mizuguchi et al., 2004). The Swr1 complex catalyzes the exchange of an H2A-H2B dimer for an H2A.Z-H2B dimer in yeast in an ATP-dependent manner in both nucleosomal arrays and in mono-nucleosomes. Despite the presence of the Nap-Z complex, these authors see very little exchange in the absence of ATP, in contrast to the 20% efficiency of yNAP1 – dependent exchange of ~20% reported here.

Finally, we have shown conclusively that the ability of yNAP1 to transiently remove one or both H2A-H2B dimers from a nucleosome facilitates nucleosome sliding from a positioning sequence to an energetically more favorable end position. Our data indicate that yNAP1 functions in a catalytic manner, independent of ATP. A truncated version of yNAP1 lacking the acidic C-terminal domain, which is capable of binding histones and assembling chromatin, but has lost its ability to extract a H2A-H2B dimer from the NCP, is incapable of promoting this sliding reaction although we still do not exclude the possibility that the C-terminal and N-terminal domains are redundant. Repositioning is directional in that no yNAP1 – mediated nucleosome movement from the end-position to the central position is observed. In this, yNAP1 functions like the ATP-dependent remodeling factor dMi-2 and its recombinant ATPase subunit ISWI, which also moves centrally positioned nucleosomes to an end-position, but is unable to facilitate movement from the end to the center of the DNA (Langst and Becker, 2001). Intriguingly, it has been found earlier that yNAP1 and nucleoplasmin increase the stimulation of Gal4 binding to mono-nucleosome brought upon by the SWI/SNF complex, indicating that histone chaperones and remodeling factors may act synergistically (Cote et al., 1994).

While the net effect of yNAP1 and ATPases such as ISWI is similar, the mechanism by which these factors act is likely to be distinct. First, yNAP1-dependent nucleosome-sliding depends completely on its ability to remove and subsequently replace one or both H2A-H2B dimers. In contrast, in the presence of ATP-dependent remodelers, dimer exchange occurs subsequent to the movement of nucleosomes away from their initial locations coincident with and subsequent to the arrival of nucleosomes at positions at and beyond DNA ends, suggesting that H2A/H2B destabilization is not an obligate step in

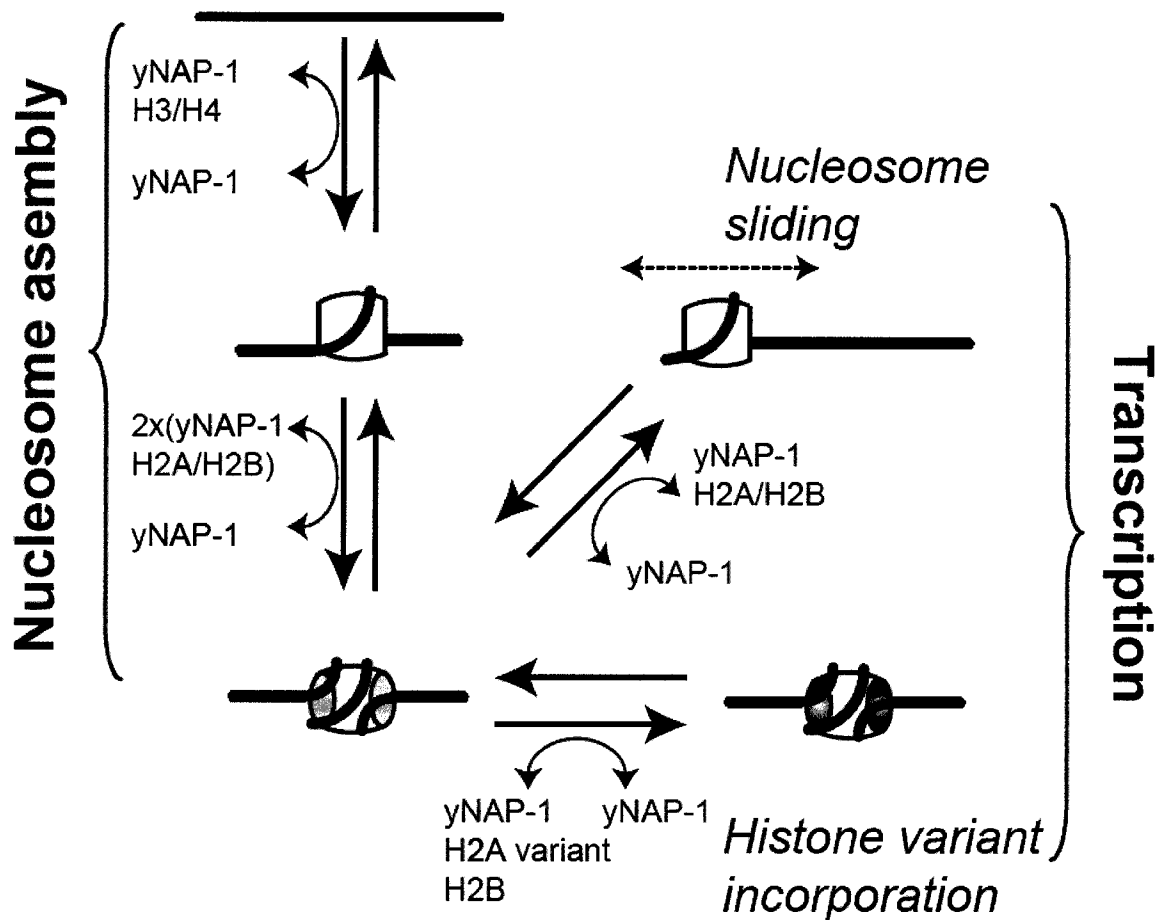


Figure 4.7. The multiple faces of yNAP-1. yNAP-1 is capable of stepwise assembly of nucleosomes *in vitro*, and appears to be involved in this process *in vivo*. An (H3-H4)₂ tetramer (white cylinder) is deposited on the DNA, followed by addition of two H2A-H2B dimers (grey ovals) to form a folded nucleosome. The reactions are reversible, resulting in transient H2A-H2B dimer removal leading to H2A/H2B exchange (and possibly the incorporation of histone variant dimers, dark grey ovals) and / or nucleosome sliding.

nucleosome movement (Bruno et al., 2003). Second, yNAP1 does not require energy from ATP hydrolysis to dissociate the histone dimer or to slide the nucleosome. Third, although apparently catalytic, yNAP1 is not a motor and therefore does not actively move nucleosomes along the DNA, but rather appears to lower the energy barrier that normally prohibits spontaneous nucleosome sliding to energetically favorable positions.

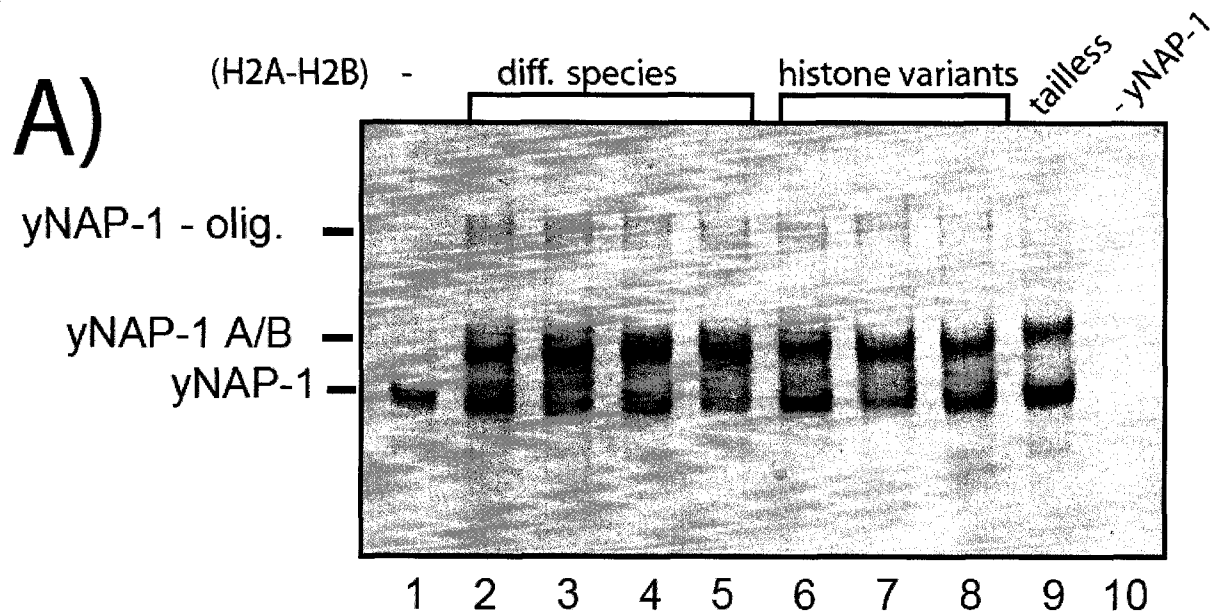
Since members of the class of acidic histone chaperones (of which yNAP1 is just one representative) are very abundant in the cell, their *in vivo* role may well be significant. For example, histone chaperones may play a role in introducing H2A variants into chromatin in a replication-independent manner, and in aiding nucleosome (re)-positioning along the DNA by lowering the significant energy barrier that must exist for nucleosome sliding. NAP1 may also contribute to the disassembly and reassembly of nucleosomes during transcription initiation and elongation, as discussed above (Fig. 4.7).

Overview of the role of NAP1 (and presumably that of other acidic histone chaperones) is clearly evolving, from being considered as a mere histone escort that manages histone transport into the nucleus before handing its precious cargo over to chromatin assembly and remodeling factors, to a much more glamorous role in maintaining chromatin and nucleosome fluidity and dynamics. Similarly, chromatin, once assembled, was once viewed as an ‘immovable object’ that only an advancing replication fork (and possibly an advancing RNA polymerase) can displace (Kornberg and Lorch, 1991). It is now perceived as a highly dynamic and malleable assembly that is capable of extensive cross-talk with the cellular machinery. Much remains to be learned on how this is achieved mechanistically, and doubtlessly many activities that are involved in this important aspect of chromatin metabolism remain yet to be discovered.

Acknowledgements

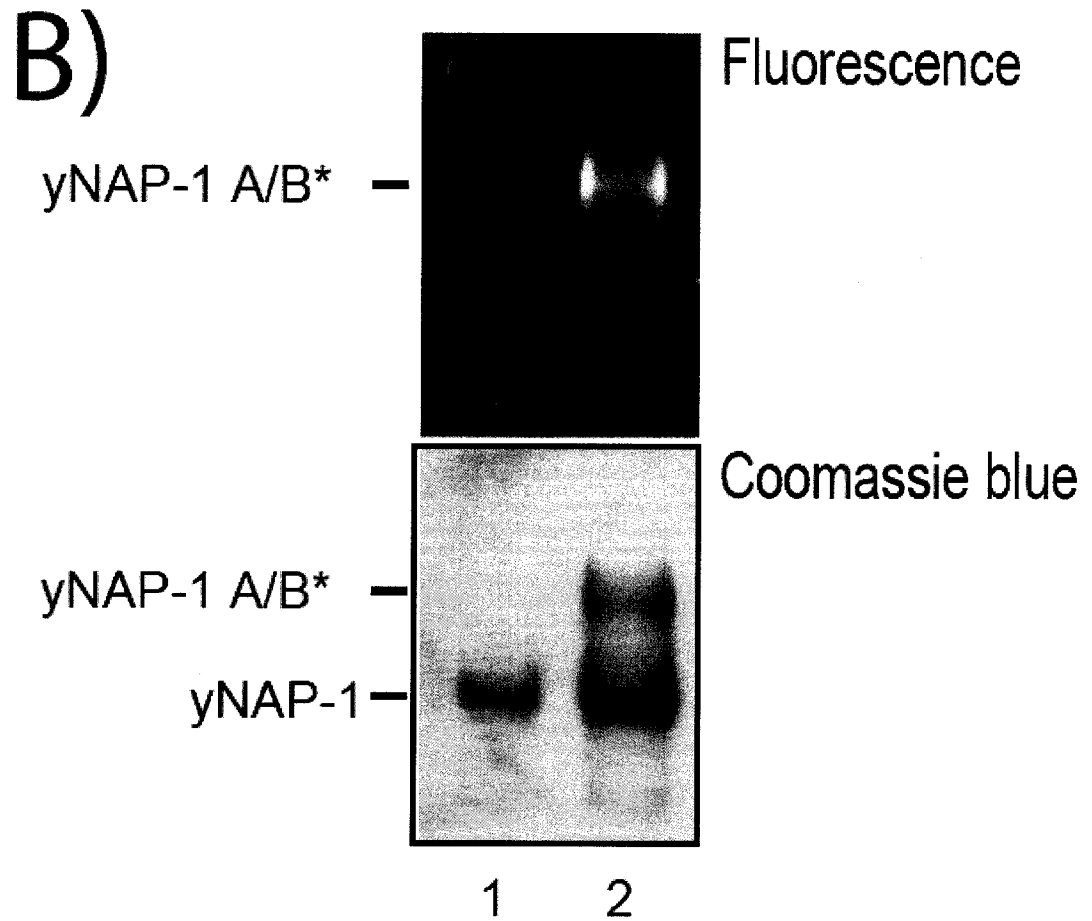
Supported by grants from the National Institutes of Health (GM561909 and GM067777)

4.6 Supplementary figures



Supplementary Figure 1A. Interaction of yNAP-1 with histone (H2A-H2B) dimer.

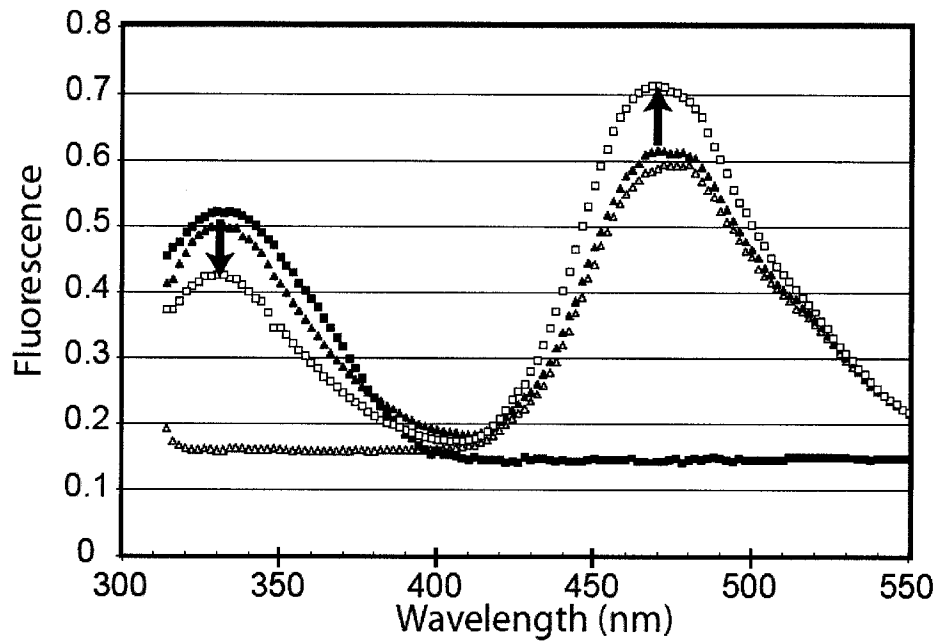
(A) 10 μ M yNAP-1 was incubated in the absence of (H2A-H2B) dimer (lane 1) or presence of 5 μ M (H2A-H2B) dimer derived from yeast (lane 2), *Xenopus laevis* (lane 3), mouse (lane 4) and drosophila (lane 5). Lanes 6-9 shows binding of yNAP-1 to 5 μ M dimers composed of human H2A Bbd and mouse H2B (lane 6), mouse H2A.Z and *Xenopus laevis* H2B (lane 7), human macroH2A histone domain and *Xenopus laevis* H2B (lane 8), and *Xenopus laevis* H2A and H2B in which the tails had been deleted (lane 9). Lane 10 shows *Xenopus laevis* (H2A-H2B) dimer in the absence of yNAP-1. Samples were incubated at 4 $^{\circ}$ C for 10 hours, and complex formation was analyzed by native PAGE. The position of yNAP-1 – (H2A-H2B) dimer complex (yNAP-1 A/B) and yNAP-1 are indicated, as is the oligomeric form of yNAP-1 that we sometimes observe.



Supplementary Figure 1B. Interaction of yNAP-1 with histone (H2A-H2B) dimer.

(H2A-H2B) dimer from *Xenopus laevis* was labeled with CPM at H2B T112C. 10 μ M yNAP-1 was incubated in the absence or presence of fluorescently labeled (H2A-H2B) dimer (A/B*; lane 1-2: 0 and 5 μ M). Incubation and gel electrophoresis were done as in (A). The gel was photographed without staining to view fluorescence (upper panel), then stained with coomassie blue (lower panel).

C)

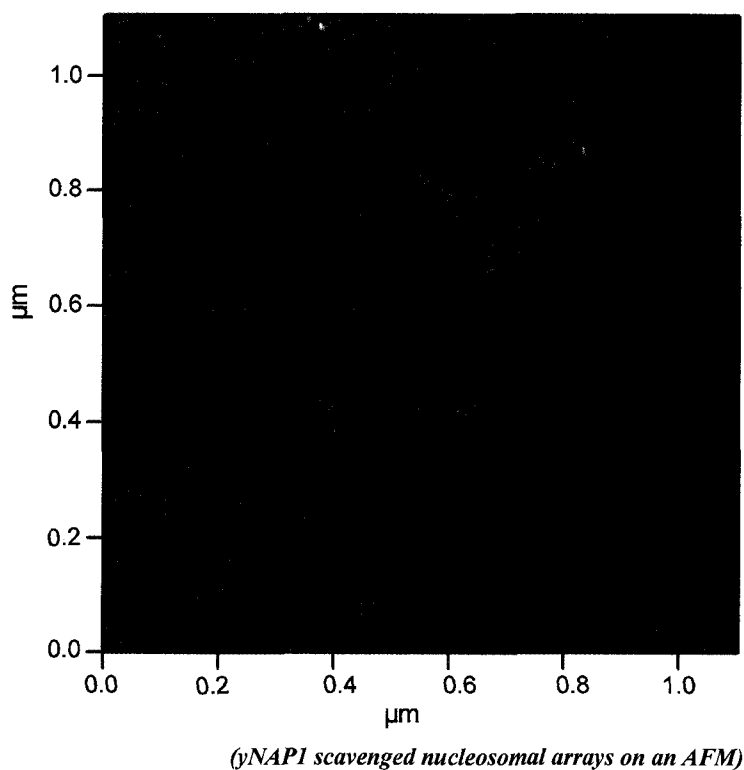


Supplementary Figure 1C. Interaction of yNAP-1 with histone (H2A-H2B) dimer. A complex of yNAP-1 with fluorescently labeled (H2A-H2B) dimer was prepared at a molar ratio of 1:1. Under these conditions, no free yNAP-1 is present. Tryptophan was excited at 300nm, and fluorescence of the complex was monitored. The same complex was analyzed at 1.25 M NaCl (▲). The emission spectrum of free (CPM-labeled H2A-H2B) dimer (Δ) and yNAP-1 (■) is shown as a control.

CHAPTER V

The C-terminal acidic domain of yNAP1 is essential for chromatin scavenging

Jayanth V. Chodaparambil, Tatsuya Sakurai, Robert Willingham, Jeffery C. Hansen, Karolin Luger



This chapter will be submitted for publication. J.V.C planned and did the experiments. T.S. performed the yNAP1 assembly, exchange experiments. R.W. made the yNAP1 constructs. J.C.H gave technical guidance for the sedimentation velocity experiments.

5.1 Introduction

Eukaryotic DNA is confined in the nucleus by a hierarchical scheme of folding and compaction into chromatin, a highly dynamic protein-DNA assembly. Chromatin is built from nucleosomes, which consist of an octameric histone core around which 147 base pairs of DNA are wrapped in 1.65 superhelical turns (Luger et al., 1997). The histone octamer itself is composed of two copies each of the four histone proteins H2A, H2B, H3, and H4 (reviewed in (Akey and Luger, 2003)). The formation and maintenance of functional chromatin is critical to cell survival. Histones, as the key components of nucleosomes, have a central and essential function in chromatin compaction, but due to their extreme charge can also interact nonspecifically with DNA and chromatin, potentially causing un-physiological and uncontrolled aggregation of nucleosomes and chromatin fibers. In most organisms, histone synthesis is tightly coupled to S-phase, and free histones are found in complex with histone chaperones that shield their charge and assist in their ordered deposition on DNA to form nucleosome (reviewed in (Loyola and Almouzni, 2004) (Akey and Luger, 2003)). Histones H3 and H4 form complexes with chromatin assembly factor (CAF-1) (Verreault et al., 1996), the Hir proteins (Kaufman et al., 1998). Histones H2A and H2B are also found in complex with histone chaperones, such as members of the nucleoplasmin and nucleosome assembly protein 1 (NAP1) families of proteins (Akey and Luger, 2003), and also interact with FACT. More recently, histone chaperones have been identified as players in regulating access of the transcription machinery to chromatin, and in the ordered exchange of histone variants into already assembled chromatin.

NAP1 is found in all eukaryotes (Park and Luger, 2006a), and its many functions have been reviewed recently (Park and Luger, 2006a, Zlatanova et al., 2007). First functional analysis of NAP1 *in vitro* was based on its ability to bind histones H3/H4 and H2A/H2B (Fujii Nakata et al., 1992) (Chang et al., 1997, McBryant et al., 2003)); its ability to introduce negative supercoils into relaxed circular DNA in the presence of core histones (chromatin assembly; (Fujii Nakata et al., 1992), and to generate regularly spaced nucleosomes (Ito et al., 1996). More recently, roles in histone removal and histone exchange have been discussed by several labs (including ours) as a mechanism to regulate DNA accessibility and to maintain chromatin integrity and fluidity (Levchenko and Jackson, 2004, Okuwaki et al., 2005, Park et al., 2005). New data implicate NAP1 (and several other H2A chaperones) in the replication-independent exchange of histone variants into assembled chromatin. NAP1 is also implicated in histone shuttling in a cell-cycle dependent manner (Kellogg and Murray, 1995, Mosammaparast et al., 2005).

The recently determined the crystal structure of yNAP1 (Park and Luger, 2006b) shows that the N-terminal 74 amino acids and a 50 amino acid long C-terminal acidic domain (CTAD) are disordered. A structure of the yNAP1 core domain (amino acids 74-365) is identical compared to full length yNAP1 (unpublished data), consistent with the earlier finding that the key functions of yNAP1 (histone binding and chromatin assembly) do not require the CTAD. In contrast, the more recently characterized ability of yNAP1 to disassemble nucleosomes, exchange histones, and promote nucleosome sliding *in vitro* have an absolute requirement for the CTAD (Park et al., 2005).

Here we test the hypothesis that the CTAD contributes to the affinity of yNAP1 for histones. This additional affinity is not required for histone binding and deposition on the

DNA, but is absolutely necessary for the removal of histones already bound to DNA or to nucleosomes. By testing several C-terminally truncated versions of yNAP1, we demonstrate that these functions are directly related to the length and charge of the CTAD.

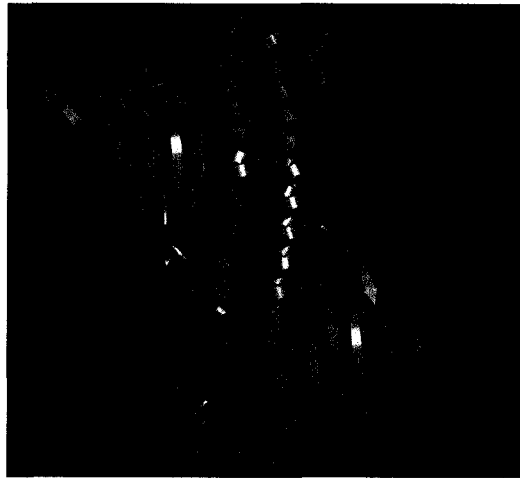
Results

5.2 The CTAD of yNAP1 contributes to the binding affinity of yNAP1 for histones H2A/H2B

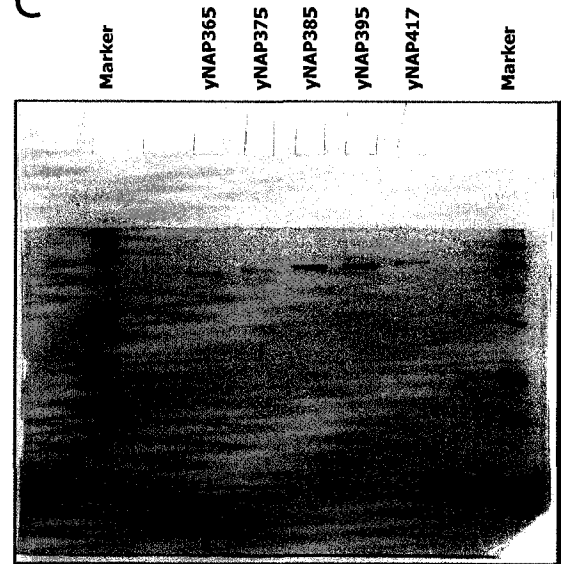
Unpublished structural studies of a truncated version of yNAP1 (amino acids 74 to 365) show that the structure of the yNAP1 core domain remains unchanged upon removal of the CTAD (Park Y-J personal communication), demonstrating that this domain is not required for the structural integrity of yNAP1. This is consistent with previous qualitative findings that the CTAD does not contribute to the key functions of histone binding and nucleosome assembly. Figure 5.1A shows the core domain of yNAP1, the C-terminal acidic tail is denoted by red lines. To investigate the effect of the charge and length of the CTAD on the various functions of yNAP1, we prepared several successive C-terminal truncations of yNAP1 (Fig. 5.1B). The proteins (designated yNAP1₍₁₋₃₉₅₎, yNAP1₍₁₋₃₈₅₎, yNAP1₍₁₋₃₇₅₎, and yNAP1₍₁₋₃₆₅₎, respectively, were expressed and purified as described (Fig. 5.1C) (Fujii Nakata et al., 1992). As expected, the proteins expressed at high yields and were soluble.

Recombinant histone H2A-H2B dimers were incubated with equimolar amounts of the various yNAP1 truncation mutants and the ensuing complexes were analyzed on a 5%

A



C



B

yNAP365 ████████-
 yNAP375 ████████-efefeedeee
 yNAP385 ████████-efefeedeeeadededeed
 yNAP395 ████████-efefeedeeeadededeeedddhgleddg
 yNAP417 ████████-efefeedeeeadededeeedddhgledddgesaeeqddfagrpeqaqackqs

Figure 5.1: C-terminal acidic domain (CTAD) deletion does not affect yNAP1 structure. (A) Crystal structure of yNAP1 74-360. yNAP1 forms a homo-dimer in solution. The C-terminal acidic domain (CTAD) is shown as the red lines. (B) Various yNAP1 truncation constructs shown along with their CTAD composition. The acidic amino acids aspartates and glutamates are shown in red. (C) 15% SDS-PAGE gel of the truncation constructs as indicated on the lane. Low-molecular weight marker is seen on either side of the truncation constructs.

native PAGE gel (Figure 5.2, lanes 2, 4, 8, and 10). Consistent with previous results, all yNAP1 constructs form complexes with WT histone dimers. Since the native gel is sensitive to both size and charge of the particle, the yNAP1₍₁₋₃₆₅₎- H2A/H2B complex runs higher than the rest of the yNAP1 – histone complexes. yNAP1₍₁₋₃₇₅₎ consistently produces a smear, despite the fact that it behaves as a homogenous species on a 15% denaturing SDS-PAGE gel and on native gels in the absence of histones.

To test whether the CTAD affects the affinity of yNAP1 for histone complexes, we designed competition experiments based on our finding that various truncated forms of yNAP1 form easily distinguishable complexes with histone H2A/H2B. We incubated full length yNAP1 and histone H2A-H2B dimers with either yNAP1₍₁₋₃₉₅₎, yNAP1₍₁₋₃₈₅₎, yNAP1₍₁₋₃₇₅₎, and yNAP1₍₁₋₃₆₅₎ at a molar ratio of 1:1:1 (Figure 5.3A). The appearance of the various histone – yNAP1 complexes was monitored by native gel electrophoresis. Wild type yNAP1 easily competes with yNAP₍₁₋₃₆₅₎ and yNAP₍₁₋₃₇₅₎ for the H2A-H2B dimer (Figure 5.3B, lanes 1 and 4), indicating that the removal of the CTAD significantly reduces the affinity of yNAP1 for histones. Competition with yNAP385 also shows a predominant yNAP417- histone complex, but some yNAP385- dimer complex is also formed (Figure 5.3B, lane 7). yNAP395 effectively competes with yNAP417 for H2A-H2B dimer (Figure 5.3B lane 10), indicating that the removal of the last 22 amino acids (including a total of seven acidic residues) has no effect on the stability of the yNAP1 – histone interaction.

To quantify these findings, we determined the binding affinity of yNAP365 and yNAP417 for the histone H2A-H2B dimer using a fluorescence polarization/anisotropy assay. H2B was labeled with Alexa-488 on T112C, and the change in fluorescence upon

| | | | | | | | | | | |
|---------------|---|---|---|---|---|---|---|---|---|---|
| yNAP365 | + | + | | | | | | | | |
| yNAP375 | | | + | + | | | | | | |
| yNAP385 | | | | | + | + | | | | |
| yNAP395 | | | | | | | + | + | | |
| yNAP417 | | | | | | | | | + | + |
| Histone dimer | + | - | + | - | + | - | + | - | + | - |

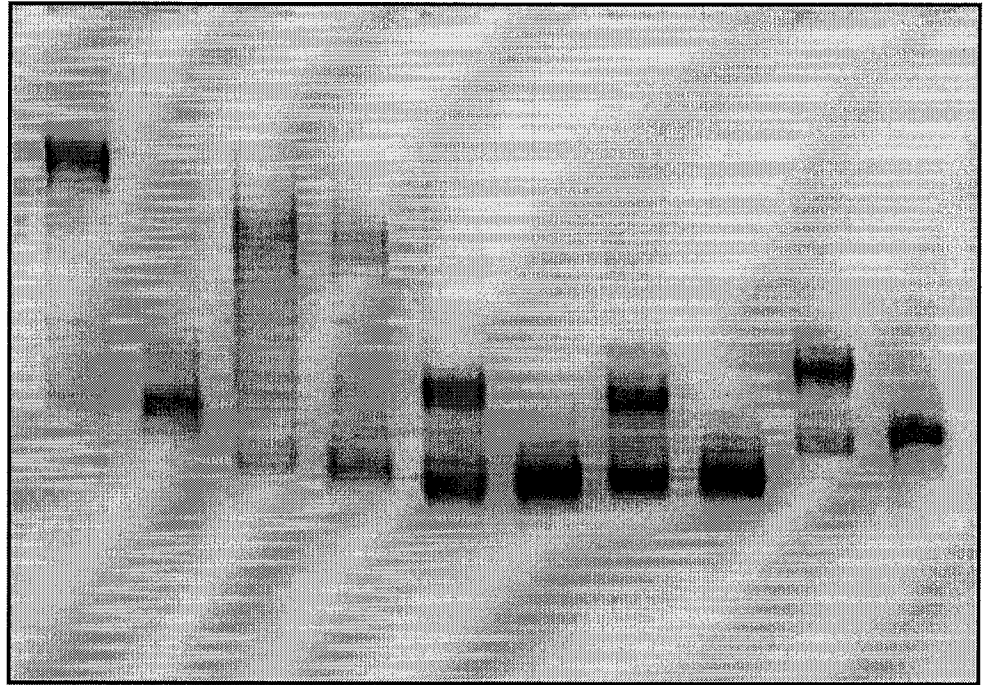


Figure 5.2: NAP deletion constructs can make complexes with histone dimers. 5% native gel showing NAP – Xenopus histone dimer complexes with different deletion yNAP1 constructs. Lane 1, 3, 5, 7, 9 show yNAP365-, yNAP375-, yNAP385-, yNAP395-, and yNAP417-dimer complexes respectively. Lanes 2, 4, 6, 8 and 10 show yNAP365, yNAP375, yNAP385, yNAP395 and yNAP417 respectively.

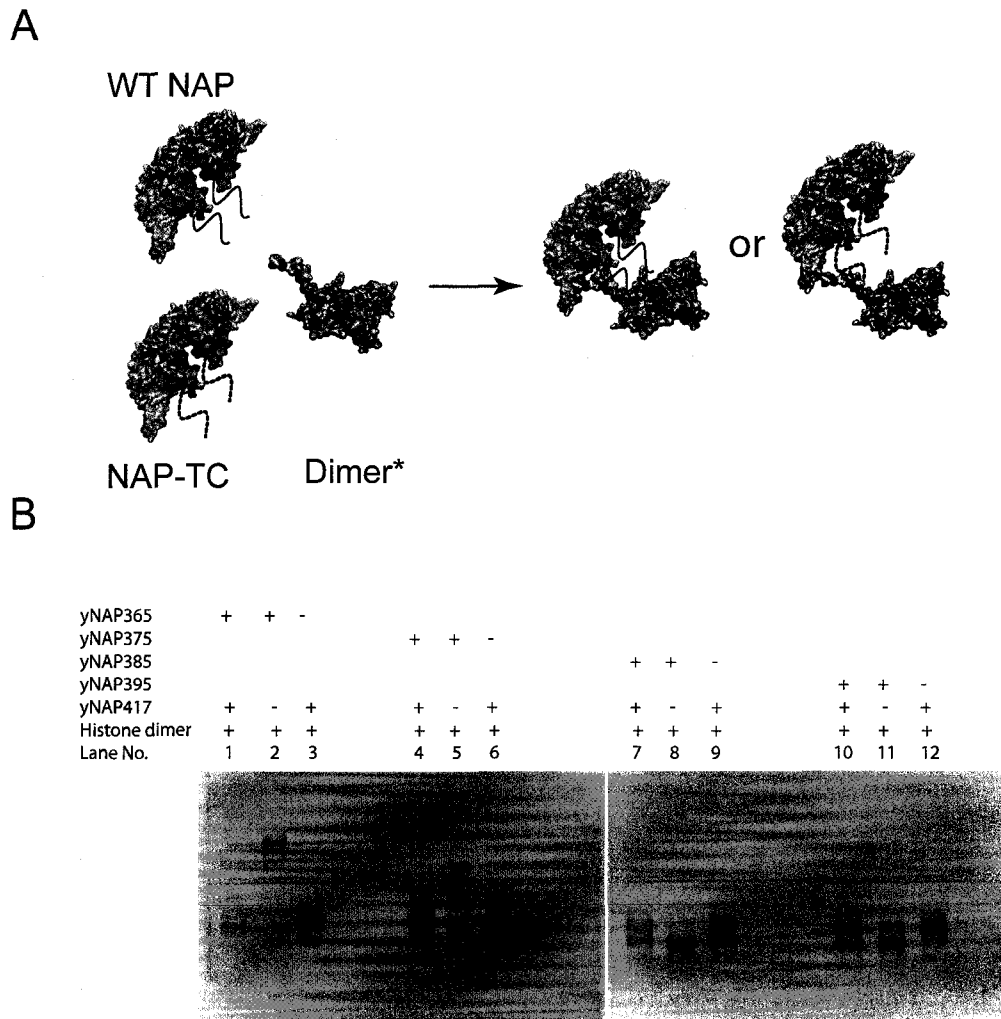


Figure 5.3: CTAD of yNAP1 increases binding affinity of yNAP1 for histone dimer:

(A) Xenopus histone dimers were incubated with a mixture of a yNAP1 truncation construct and yNAP417 (WT) in a molar ratio of 1:1:1. Appearance of either the NAP deletion construct-dimer complex or yNAP417 – dimer complex was monitored on a native 5% gel. (B) 5% native gel of the competition reactions. Lanes 1, 4, 7, 10 show complexes formed by yNAP365, yNAP375, yNAP385, yNAP395 constructs competing with yNAP417 to form a complex with the histone dimer respectively. Lanes 2, 5, 8, 11 shows yNAP365-, yNAP375-, yNAP385-, yNAP395- dimer complexes respectively. Lanes 3, 6, 9, 12 show yNAP417 -dimer complex.

addition of yNAP1 was monitored. Wild type yNAP1 binds H2A/H2B with an affinity of 1.4 nM (data not shown). Confirming our competition studies, the affinity of yNAP1₍₁₋₃₆₅₎ was found to be 3.0 nM (data not shown). To exclude effects of the fluorescent label on H2B on binding affinity, the K_d of wild type yNAP1 for H2A/H2B was determined with an independent assay in which fluorescence quenching of C-terminally labeled yNAP1 was measured as a response to H2A/H2B addition.

5.3 The ability of yNAP1 to exchange histones into nucleosome is a function of its affinity

We have previously shown that yNAP1 exchanges H2A-H2B dimers into preformed nucleosomes. A construct of yNAP1 encompassing amino acids 74-365 was unable to perform this function, whereas removal of only the N-terminal domain had no effect (Park et al., 2005). We repeated these experiments with the four yNAP1 truncations described above. The various constructs were pre-incubated with fluorescently labeled H2A-H2B dimers, and were then mixed with unlabeled purified nucleosomes reconstituted by salt-gradient dialysis (Figure 5.4A). Consistent with earlier studies (Park et al., 2005), yNAP417 exchanges labeled histone dimers into preformed nucleosomes, whereas yNAP1₍₁₋₃₆₅₎ shows no such activity (Figure 5.4B). These experiments directly prove the involvement of the CTAD in histone exchange. The removal of the 22 penultimate amino acids (including seven acidic residues; yNAP1₍₁₋₃₉₅₎) has no effect on the ability of yNAP1 to exchange histones. However, further removal of residues from the CTAD results in an impaired activity (yNAP1₍₁₋₃₈₅₎, yNAP1₍₁₋₃₇₅₎), concomitant with a decreased relative affinity for histones compared to wild type yNAP1 demonstrated in Figures 5.3B.

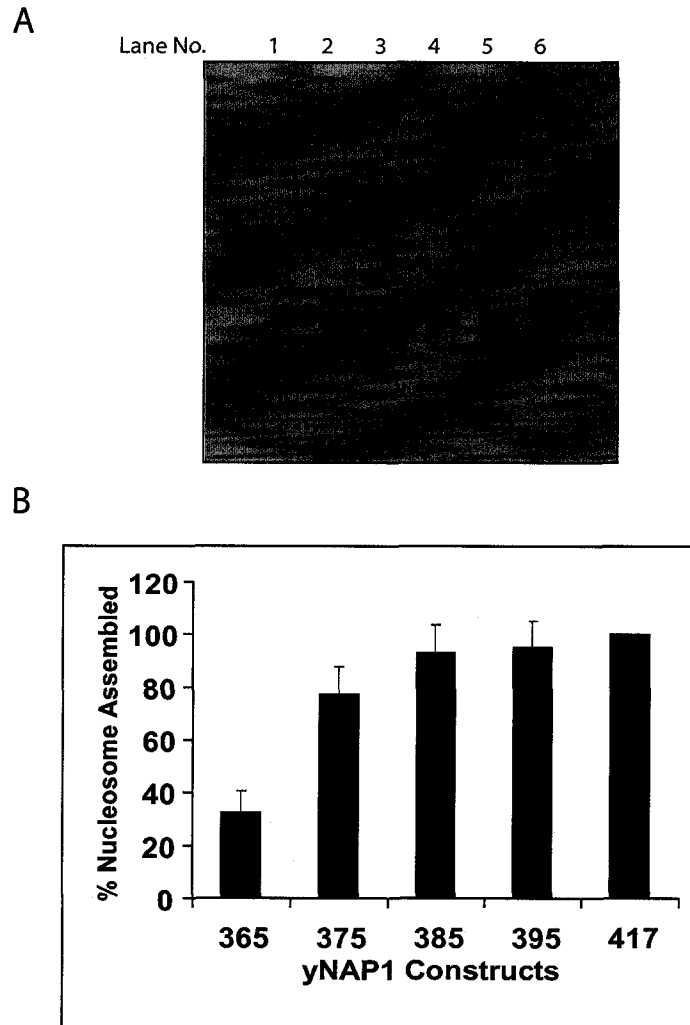


Figure 5.4: CTAD enhances histone dimer exchange into preformed nucleosomes.

(A) Salt-dialyzed unlabeled nucleosomes were incubated with yNAP365, yNAP375, yNAP385, yNAP395 or yNAP417-Alexa 488 labeled dimer complexes at a ratio of 1:4 nucleosome: NAP at 4°C overnight. A 5% native gel was used to check for the formation of labeled nucleosomes due to exchange mediated by NAP. (B) The labeled nucleosome bands were quantified and were plotted as a bar graph. 100% exchange was normalized to the labeled nucleosome band by wt-yNAP1. Error bars represent standard deviations from three separate experiments.

5.4 The CTAD contributes to the efficiency of chromatin assembly

Even though previous experiments have shown that the CTAD of yNAP1 is dispensable for nucleosome assembly, we wanted to investigate the possibility that the CTAD contributes to the efficiency of the process. We incubated equal amounts of purified histone octamer (labeled with Alexa488 on the dimer) and 5S 146mer DNA with a two-fold molar excess of yNAP1₍₁₋₃₉₅₎, yNAP1₍₁₋₃₈₅₎, yNAP1₍₁₋₃₇₅₎, and yNAP1₍₁₋₃₆₅₎, respectively at 4°C for 16 hours. The reconstituted nucleosomes were analyzed on a 5% native PAGE gel and quantified. We have previously shown that this assay is able to distinguish between misformed or alternatively positioned nucleosomes (Dyer et al., 2004). The gel was viewed under UV light at 365nm to observe fluorescence derived from Alexa-488 – labeled H2A, and subsequently stained with ethidium bromide. yNAP1₍₁₋₃₉₅₎ and yNAP1₍₁₋₃₈₅₎ are both as efficient as wild type yNAP1 in assembling high-quality nucleosomes (Fig. 5.5). yNAP1₍₁₋₃₇₅₎, and yNAP1₍₁₋₃₆₅₎ are also competent for assembly, but at a reduced efficiency.

5.5 The CTAD is required for removal of non-specifically bound histones from DNA

Incubation of deliberately overassembled mono-nucleosomes with wild type yNAP1 resulted in a remarkable improvement, most likely due to the ability of wild type yNAP1 to remove excess histones that are bound to nucleosomal DNA non-specifically. As predicted, successive removal of the CTAD resulted in a decreased ability of yNAP1 to rescue overassembled nucleosomes.

We next wanted to test this novel activity of yNAP1 in the more biologically relevant (and easily quantifiable) system of nucleosomal arrays. Nucleosomal arrays were

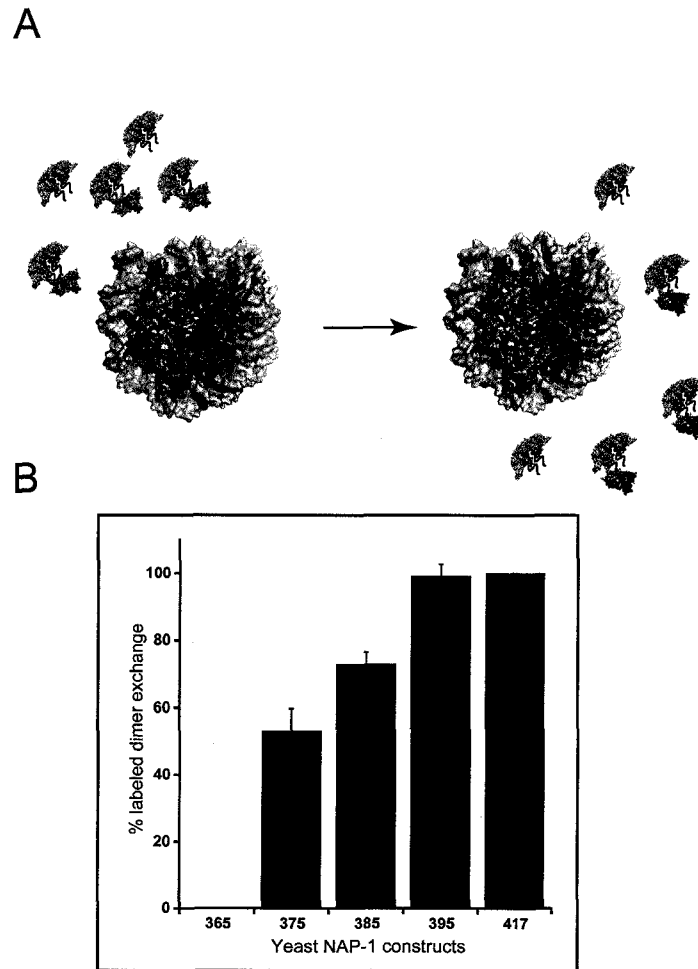


Figure 5.5: CTAD plays a role in nucleosome assembly: (A) H2B labeled with Alexa 488 histone octamers were incubated with DNA and yNAP1 at a molar ratio of 1:1:2 at 4°C for 16 hours. The samples were run on a 5% native PAGE gel and visualized under UV at 365nm for observing the label. Lane 1 shows nucleosomes assembled by yNAP365, lane 2, 3, 4, 5 shows nucleosomes assembled by yNAP375, yNAP385, yNAP395 and yNAP417 respectively. Lane 6 represents the labeled nucleosome assembled through salt gradient dialysis. (B) The labeled nucleosomes formed on the gels were quantified and were plotted as a bar graph. 100% assembly was normalized to the labeled nucleosome band formed by yNAP417. Error bars represent standard deviations from four separate experiments.

reconstituted from 208–12mer DNA and purified core histone octamers using salt dialysis. It has previously been determined that a fully saturated 208-12mer nucleosomal array has a s_{ave} value of $\sim 28S$, which translates to 10 ± 2 nucleosomes per DNA (Tse and Hansen, 1997). For our purposes, we used a 2.5- fold excess octamers to the octamer binding sites available on the DNA. This leads to non-specific binding of histones to linker DNA as well as to nucleosomes, forming heterogeneously supersaturated arrays with an average S value ranging from 45-70S (Figure 5.6). We then added a seven-fold molar excess of yNAP1₍₁₋₃₉₅₎, yNAP1₍₁₋₃₈₅₎ yNAP1₍₁₋₃₇₅₎, and yNAP1₍₁₋₃₆₅₎ dimer per DNA repeat (an 84-fold molar excess of yNAP1 for each array). The reaction was allowed to proceed at 4°C for 16 hours, followed by analysis via sedimentation velocity. Wild type yNAP1 and yNAP1₍₁₋₃₉₅₎ were able to convert these supersaturated arrays into well-behaved 28 S arrays. In contrast, the removal of the remainder of the CTAD resulted in an impaired ability of yNAP1 to rescue overassembled nucleosomal arrays. In particular, the addition of yNAP1₍₁₋₃₆₅₎ had no effect on the sedimentation behavior of the overassembled arrays, consistent with the contribution of the CTAD to histone binding.

We also visualized these experiments using atomic force microscopy to provide an independent assay of this novel yNAP1 function. Dilutions of the same supersaturated arrays as analyzed above were incubated with with a seven-fold excess of wild type yNAP1 or yNAP1₍₁₋₃₆₅₎ per nucleosome positioning sequence and incubated for 16 hours at 4°C. The samples were then placed on glass slides with a cleaved mica sheet treated with APTES (3-Aminopropyl Triethoxysilane), and images were obtained in air using the tapping mode. Figure 5.7a shows the amplitude image of such supersaturated arrays. Excess histones effectively act as glue, promoting nonspecific intra and intermolecular

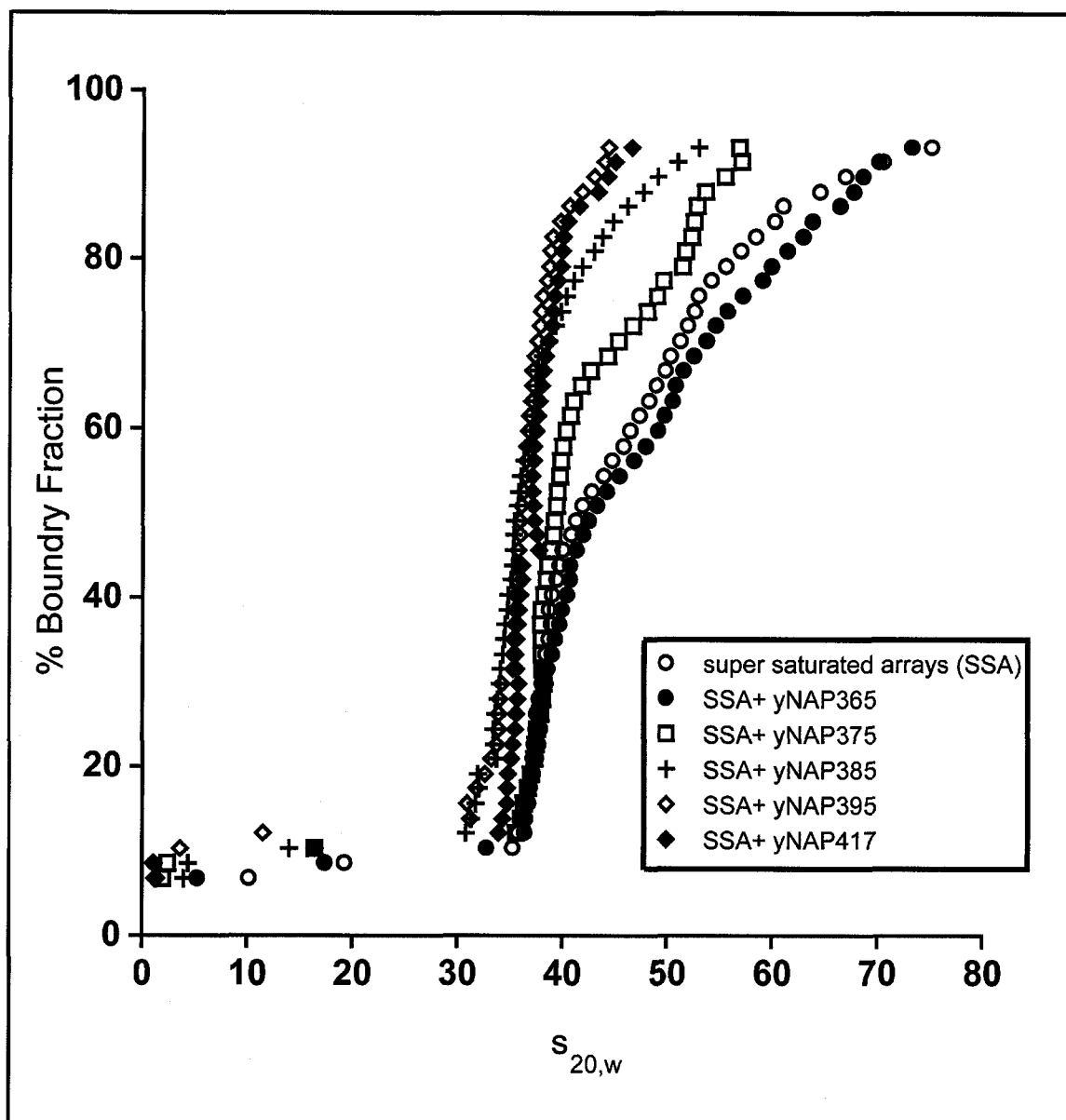
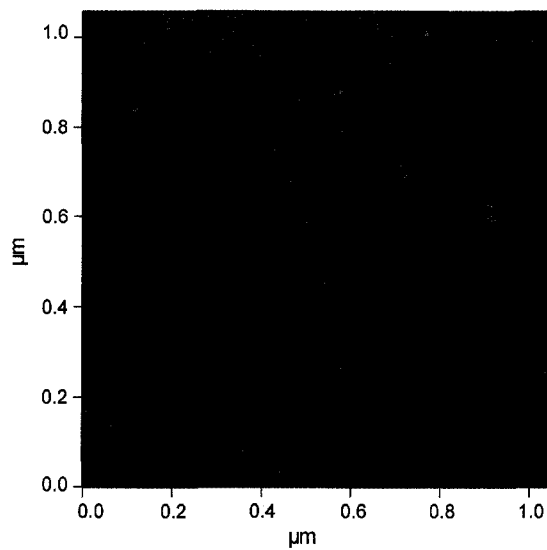


Figure 5.6: CTAD of yNAP1 aids histone scavenging on super-saturated nucleosomal arrays. Nucleosome arrays treated with yNAP1 truncation constructs were characterized by sedimentation velocity in TEN buffer as described under "Experimental Procedures." Shown is the integral distribution of sedimentation coefficients, $G(s)$, for each sample. (○) super saturated arrays (SSA), (●) SSA + yNAP365, (□) SSA + yNAP375, (+) SSA + yNAP385, (◇) SSA + yNAP395, (◆) SSA + yNAP417.

A



B

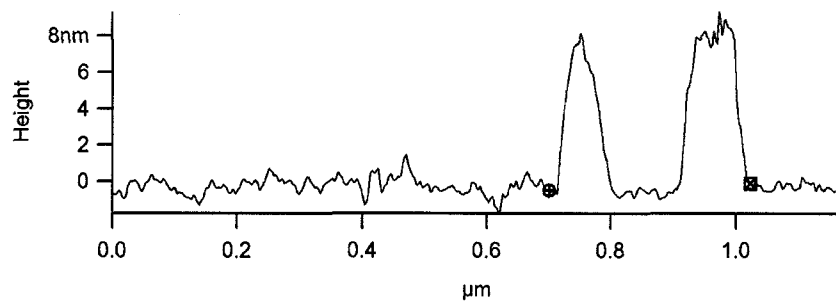
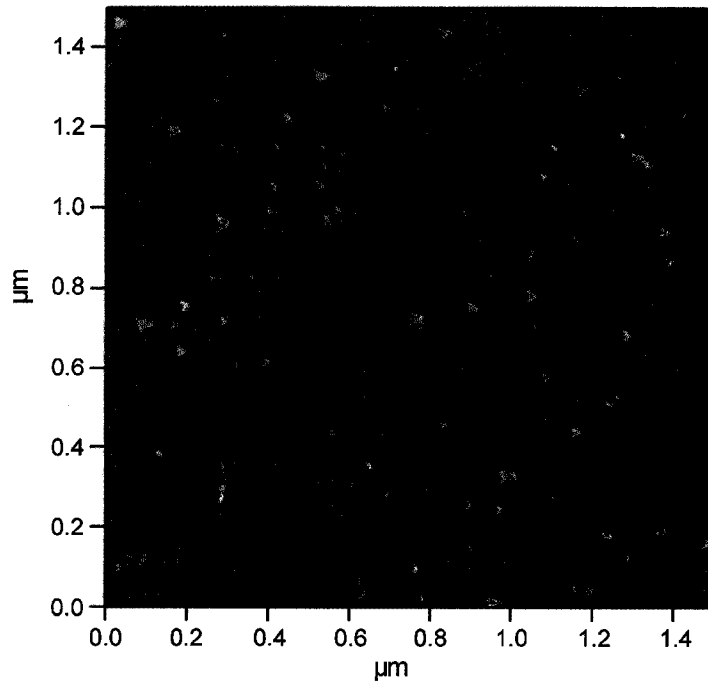


Figure 5.7: Nucleosome scavenging at a single-molecule level: Nucleosomal arrays treated with γ NAP1 truncation constructs were characterized by Atomic force microscopy. (A) Amplitude images of the super saturated arrays. 1.1 μ m X 1.1 μ m scan (B) Height profile of the supersaturated arrays.

C



D

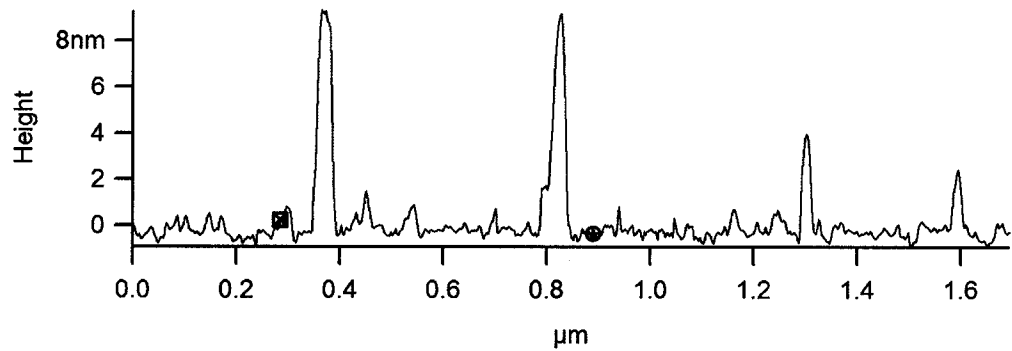


Figure 5.7: Nucleosome scavenging at a single-molecule level: Nucleosomal arrays treated with yNAP1 truncation constructs were characterized by atomic force microscopy. (C) Amplitude images of the super saturated arrays treated with yNAP365. 1.5 μm X 1.5 scan (D) Height profile of the supersaturated array treated with yNAP365.

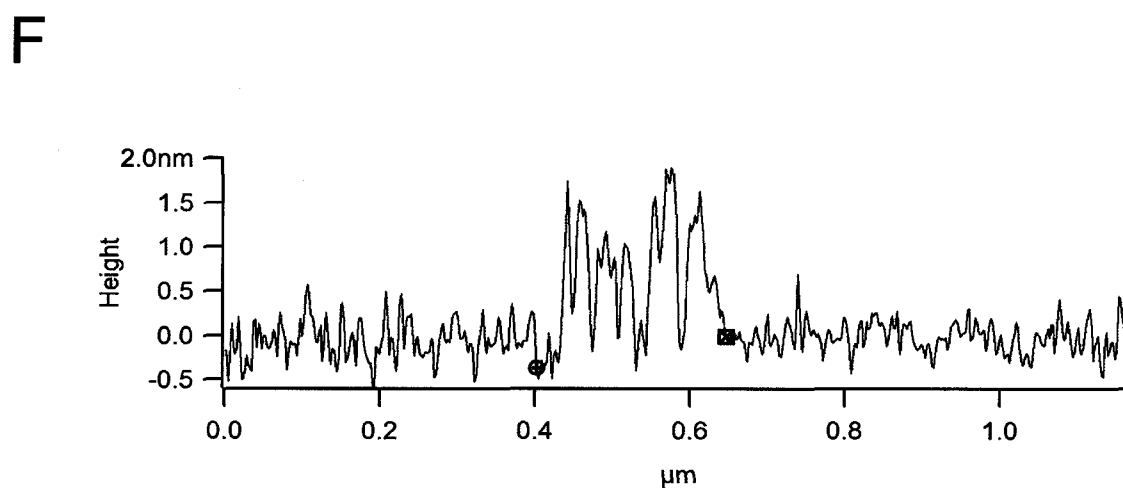
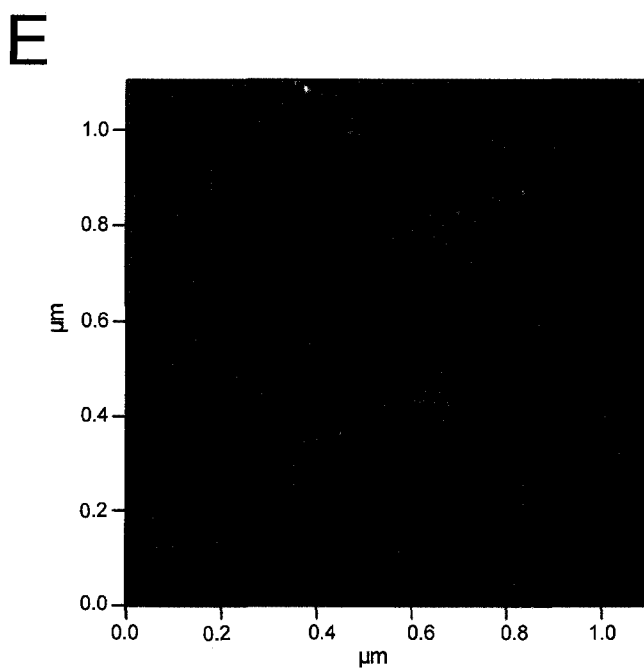


Figure 5.7: Nucleosome scavenging at a single-molecule level: Nucleosomal arrays treated with yNAP1 truncation constructs were characterized by atomic force microscopy. (E) Amplitude images of the super saturated arrays treated with yNAP417. 1.5 μ m X 1.5 scan (F) Height profile of the supersaturated array treated with yNAP417.

interactions of arrays. The resulting large assemblies exhibit an average height profile of around 8nm (Fig. 5.7B). Upon treatment with wild type yNAP1, these aggregates are converted to a beads-on-a-string structure that is typical of correctly assembled 28 S nucleosomal arrays with an average height profile of 2 nm. In contrast, the addition of yNAP1₍₁₋₃₆₅₎ has no effect, consistent with the sedimentation velocity analysis.

5.6 Discussion

The crystal structure of dimeric yNAP1 reveals a novel dome-shaped fold that is dominated by long paired alpha-helices and a β -sheet domain (Park and Luger, 2006b). Although the molecular details of yNAP1 – histone interactions are unknown, the distribution of negative surface potential displayed by yNAP1 suggests that histones interact with the underside of the β -domain (domain II) in the general vicinity of the disordered C-terminal acidic domain (CTAD) (Park and Luger, 2006b). Mutational studies conducted with the related human SET protein, which also contains the NAP1 fold, later supported this interpretation (Muto et al., 2007). The location of the histone binding site within reach of the CTAD is supported by our present findings that deletion of the entire CTAD results in a ~ five-fold reduction in the affinity of yNAP1 for the histone H2A-H2B dimer, and that the contributions of the CTAD appear to directly correlate with the number of acidic amino acids present in the CTAD.

It has been proposed earlier that the nucleosome assembly activity of yNAP1 might be a result of the differences in the affinities between histones and yNAP1 on the one hand, and between histones and DNA or DNA – (H3-H4)₂ tetramer complexes on the

other hand (Nakagawa et al., 2001). We assume that histones that are non-specifically bound to either DNA or assembled nucleosome bind with lower affinity than those histones that are found in legitimate nucleosomes. Our results demonstrate that the CTAD of yNAP1 contributes to the modulation of yNAP1 – histone affinities, and further show that this finely tuned affinity for histones may be responsible for the ability of yNAP1 to remove histones from assembled or over-assembled nucleosomes or chromatin.

We find that the removal of the 22 most C-terminal residues (which contain only seven acidic residues that are mostly clustered within the proximal 8 amino acids; yNAP1₁₋₃₉₅) has no effect on chromatin assembly, histone exchange, and histone removal. This is consistent with the finding that this mutant (whose CTAD retains 23 acidic amino acids) exhibits similar relative affinities for H2A-H2B dimer as wild type yNAP1. It should be pointed out that the CTAD in the human and drosophila homologues contain 25 and 21 acidic amino acids, respectively.

Removal of 10 more amino acids (6 of which are acidic; yNAP1₁₋₃₈₅) results in a slight reduction of affinity for H2A-H2B dimer compared to full length yNAP1, as demonstrated by its decreased fitness in a competition assay with wild type protein. This mutant has no effect on nucleosome assembly, and only very moderate effects on histone removal from over assembled nucleosomal arrays. Intriguingly, this mutant is impaired in its histone exchange activity, a process that requires the removal of a tightly bound H2A-H2B dimer from folded nucleosomes.

yNAP1₁₋₃₇₅ (obtained by the removal of 9 more acidic residues) leaves only 8 acidic residues in the CTAD. While the ability of this protein to bind histones could not be

assessed, it exhibits intermediate activity in all other assays. Finally, removal of the penultimate 8 acidic residues (all of which are still disordered in the structure) results in the complete loss of histone exchange and histone removal activity, and an only 30 % activity in nucleosome assembly. Together, our findings are consistent with the hypothesis that yNAP1 functions in histone exchange and histone removal via a non-invasive mechanism by capturing histones that are temporarily unbound to DNA and chromatin.

It is *a priori* not obvious whether the ability of NAP1 to remove histones from chromatin is an activity that is maintained in other organisms. A comparison of the length and amino acid composition of NAP1 CTADs from various species reveals that with 52 amino acids (30 of which are acidic), the yNAP1 CTAD has the highest negative charge. The CTADs of human and *Drosophila* NAP1 are about five amino acids shorter, and, with 25 and 21 acidic residues, slightly less acidic. However, NAP1 in *Drosophila* and humans is the target of posttranslational polyglutamylation (Regnard et al., 2000), suggesting the exciting possibility that the affinity of NAP1 for histones may be regulated in metazoans. Intriguingly, the presence of an extended CTAD in several (but not all) members of the extended NAP1 family of proteins suggests that the various and diverse functions previously assigned to NAP1 proteins may be at least in part the result of different affinities for histones.

5.7 Materials and Methods

Site-directed Mutagenesis of yNAP1 Vector.

Forward and reverse primers with a single point mutation at amino acids 365, 375, and 395 were used to insert a premature stop codon in the yeast NAP1 sequence. PCR using the mutated primers was used to mutagenize and amplify the yNAP1 gene-containing pTN2 plasmid vector (Ishimi and Kikuchi, 1991). *E. coli* DH5 α cells were transformed with the mutated plasmids and plated on LB-Amp plates. Plasmids were isolated using Qiagen mini-prep DNA isolation protocol. Plasmids were sequenced to check for the mutations.

Expression and Purification of Protein.

The mutated plasmids were transformed into BDP cells for expression. Extraction and purification were conducted as previously described (Fujii Nakata et al., 1992; McBryant et al., 2003). Proteins isolated were pooled and assayed on a 15% SDS-PAGE gel.

Histone dimer exchange reactions.

3 μ M unlabeled NCP was incubated with preincubated yNAP-1-histone dimer mixtures (3 μ M H2A-H2B alexa-488 labeled dimer and 6 μ M yNAP-1 monomer) at 4 °C for 10 h in 100mM NaCl, 10mM Tris pH 7.5, 1mM EDTA, 1mM DTT. Nucleosomes containing fluorescently labeled (H2A-H2BT112C) dimer were prepared as a control. The exchange of fluorescently labeled H2A-H2B dimer was analyzed on a 5% native PAGE. The gel was photographed under UV with a 488 filter using a Chemi-doc XRS

system. Exchange was quantified by integrating the area under the peaks using Scion Image software (www.scioncorp.com). Histone exchange mediated by wt-yNAP1 was considered 100% exchange and the relative exchange by rest of the yNAP1 constructs calculated. The error bars represent standard deviation from four separate experiments.

yNAP1 mediated nucleosome assembly reactions.

Alexa488-labeled histone dimer-containing octamers (labeling of histones as described in (Park et al., 2004)), 5S 146merDNA were incubated with yNAP365, yNAP375, yNAP385, yNAP395 or wt-yNAP1 at a molar ratio of 1:1:2. The reaction was allowed to proceed for 16 hours at 4°C and then run on a 5% native PAGE gel. The gel was viewed under UV at 365nm using a Bio-Rad ChemiDoc XRS system. The percentage of properly formed nucleosomes was calculated from the integrated area under the peaks of the nucleosome bands using Scion Image (www.scioncorp.com). Nucleosome assembly by wt-yNAP1 was considered as 100% assembly and the relative nucleosome assemblies for the other yNAP1s were calculated. The error bars represent standard deviation from four separate experiments.

Preparation of supersaturated nucleosomal arrays.

208-12 mer 5sDNA, histones, and histone octamers were prepared as previously described in (Gordon et al., 2005, Luger et al., 1999). DNA was mixed with 2.5-fold excess of histone octamers to 208mer repeat at 2M NaCl, 10mM Tris pH 7.5 and 0.25 mM EDTA. The mixture was dialyzed against buffers containing 1M NaCl, 0.75M NaCl and 2.5mM NaCl (TEN). For a detailed description refer to (Hansen and Lohr, 1993).

The saturation level of the arrays was tested using sedimentation velocity experiments and EcoRI digestions. For further description see (Tse and Hansen, 1997). Sedimentation velocity experiments were performed in a Beckman XLA or XLI ultracentrifuge. Data was analyzed using Van-Holde Weischet analysis (Ultrascan 7.3 software) (van Holde and Weischet, 1978, Demeler et al., 1997).

yNAP1 Scavenging on nucleosomal arrays using analytical ultracentrifugation.

Supersaturated arrays were incubated with seven-fold excess of yNAP365, yNAP375, yNAP385, yNAP395 or yNAP417 per 208-12mer repeat in TEN for 16 hours at 4°C. Sedimentation velocity experiments were done on the sample at 23000 rpm in a Beckman XLA or XLI ultracentrifuge and the data was analyzed using Van-Holde Weischet analysis (Ultrascan 7.3 software) (van Holde and Weischet, 1978, Demeler et al., 1997).

yNAP1 scavenging of nucleosomal arrays using Atomic Force Microscope.

Slide preparation: A Glass slide with freshly cleaved mica was used as the surface on which the sample is placed. The cleaved mica was then treated with a 1:1000 dilution of 3-Aminopropyltriethoxysilane (APTES). This was allowed to stand for 20 minutes and then washed with 0.22µm-filtered double-distilled water and then dried using air or nitrogen gas.

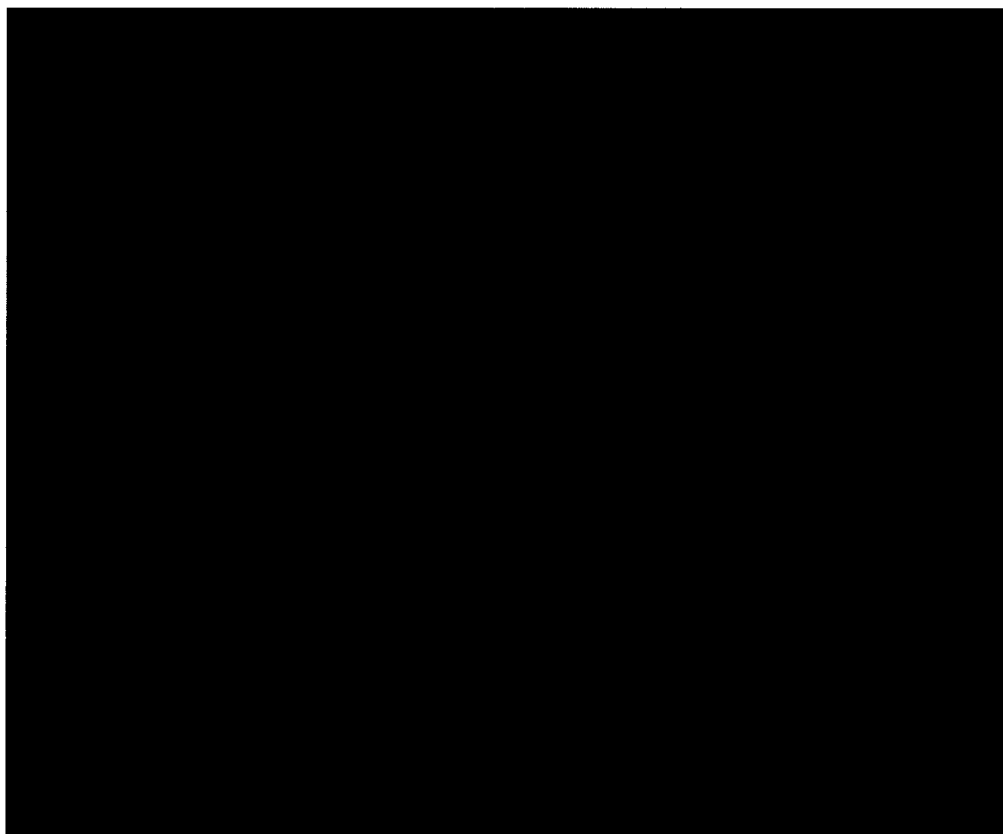
Sample preparation: Supersaturated arrays were treated with a seven-fold excess of yNAP365, yNAP375, yNAP385, yNAP395 or yNAP417 per 208-12mer repeat in TEN

for 16 hours at 4°C. To prevent crowding of the slide with the sample, the samples are diluted to either 1:100 (for supersaturated arrays), or 1:4000 (for yNAP365 or yNAP417 treated arrays) with 0.22µm filtered TEN. The 1:4000 dilution is necessary to prevent the excess yNAP1 from crowding the surface of the mica in case of the yNAP1 treated arrays.

Sample imaging and analysis: Samples were imaged on an Asylum MFP-3D Atomic force microscope with an AC240TS or AC160TS cantilever from Olympus. Images were analyzed using the MFP-3D- Igor Pro software.

CHAPTER VI

Contributions to other publications



(Electron density of LANA peptide)

The following are references and abstracts of the contributions I made to other scientific publications of which I was co-author.

1. **Chodaparambil JV**, Edayathumangalam RS, Bao Y, Park YJ, Luger K. Nucleosome structure and function. Ernst Schering Res Found Workshop. 2006;(57):29-46.

It is now widely recognized that the packaging of genomic DNA, together with core histones, linker histones, and other functional proteins into chromatin profoundly influences nuclear processes such as transcription, replication, DNA repair, and recombination. How chromatin structure modulates the expression of knowledge encoded in eukaryotic genomes, and how these processes take place within the context of a highly complex and compacted genomic chromatin environment remains a major unresolved question in biology. Here we review recent advances in nucleosome structure and dynamics.

2. Chakravarthy S, Park YJ, **Chodaparambil J**, Edayathumangalam RS, Luger K. Structure and dynamic properties of nucleosome core particles. FEBS Lett. 2005; 579:895-8.

It is now widely recognized that the packaging of genomic DNA, together with core histones, linker histones, and other functional proteins into chromatin profoundly influences nuclear processes such as transcription, replication, DNA repair, and

recombination. Whereas earlier structural studies portrayed nucleosomes (the basic repeating unit of chromatin) as monolithic and static macromolecular assemblies, we now know that they are highly dynamic and capable of extensive cross-talk with the cellular machinery. Histone variants have evolved to locally alter chromatin structure, whereas histone chaperones and other cellular factors promote histone exchange and chromatin fluidity. Both of these phenomena likely facilitate interconversion between different chromatin states that show varying degrees of transcriptional activity.

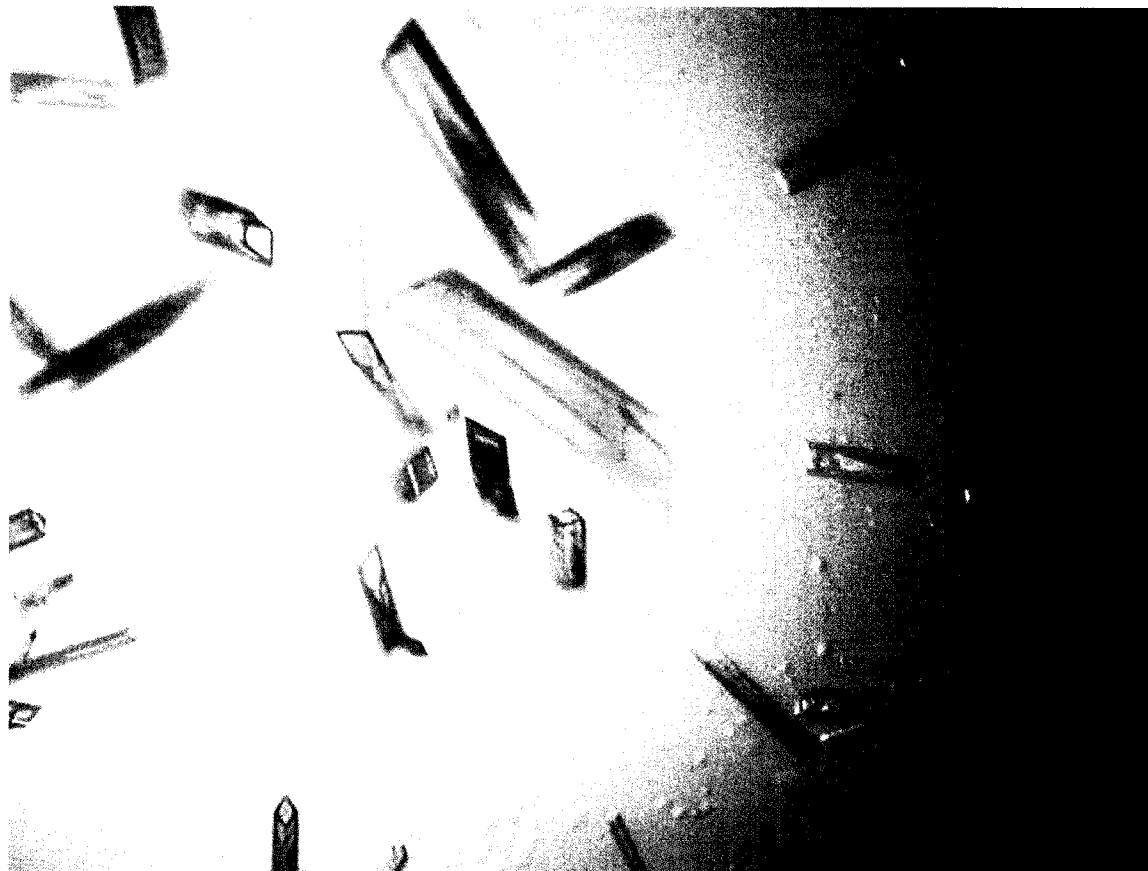
3. Barbera AJ, **Chodaparambil JV**, Kelley-Clarke B, Luger K, Kaye KM. Kaposi's sarcoma-associated herpesvirus LANA hitches a ride on the chromosome. *Cell Cycle*. 2006;5:1048-52. Epub 2006 May 15.

Kaposi's sarcoma-associated herpesvirus (KSHV) latently infects tumor cells and has an etiologic role in Kaposi's sarcoma, primary effusion lymphoma, and multicentric Castleman's disease. Survival in rapidly dividing cells depends on a carefully orchestrated chain of events. The viral genome, or episome, must replicate in concert with cellular genetic material, and then efficiently segregate to progeny nuclei. KSHV achieves this through its latency associated nuclear antigen (LANA), which simultaneously binds to viral DNA and mitotic chromosomes to efficiently partition episomes. LANA's N-terminal region has been shown to be essential for efficient KSHV DNA replication and tethering to mitotic chromosomes. The precise mechanism by which LANA attaches to host chromosomes has been an area of active investigation. We recently reported that this association is mediated by the chromatin components histones H2A and H2B. Binding between LANA and these proteins was demonstrated in vivo and

in vitro, and use of an H2A-H2B-depleted system demonstrated their central role in LANA's chromosome binding. Further, we provided a structural description of the interaction of LANA's N-terminal chromosome association region with the nucleosome using x-ray crystallography. Our data offer further insight into the mechanism of KSHV latency, and also reveal a new concept for a role of the nucleosome as a docking site for other proteins.

CHAPTER VII

Summary and Future directions



(Wild-type Xenopus nucleosome crystals)

The overall goal of this dissertation was to study the structure and function of the nucleosomal surface and nucleosome-binding proteins and how this influences the higher order chromatin compaction. In Chapter II, we for the first time show in molecular detail, the mode of LANA tethering to the host chromosome. We show that the $28,000\text{\AA}^2$ total surface area of the nucleosome could act as a docking station for trans acting proteins. It will be interesting to determine which other proteins bind on the surface of the nucleosome. Studies are underway to look at this. In collaboration with the Kaye lab at Brigham and Young's Women's Hospital, we will try to identify proteins from HeLa cell extracts which bind to the wild-type histone dimer but not to acidic patch mutants (nhs-dimer) by doing pull-down studies. The proteins so identified can further be characterized for their functions. Since LANA binds to the interface formed by the dimerization of H2A and H2B, the effect of LANA binding on the nucleosome stability would also be of interest. This would again throw light on whether the nucleosome can be directly modulated by trans-acting proteins, which might be involved in transcription regulation.

The charged patch region is also the interaction surface for the H4 tail from the adjacent nucleosome in the crystal structure. Richmond and colleagues also showed through cross-linking studies that in solution, the H4 tail could interact with this region. From our studies (chapter III) we see that the H4 tail has multiple binding sites on the nucleosome. To identify these alternative sites, we will crystallize the acidic patch-mutant nucleosome and see whether the H4 tail now makes alternative interactions with the nucleosome and whether they will be visible in the crystal structure. Initial crystallization studies indicate that these mutant nucleosomes do not form stable crystals

under the conditions standardized from wild-type nucleosomes. Further crystal conditions will be screened.

Denu and colleagues have shown that the histone-fold domain of H4 is essential for the Piccolo NuA4 complex to bind and acetylate the H4 tail. It is interesting to note that the charged surface representation of the nucleosome shows a charged region formed by the dimerization of H3 and H4. This region is also close to the H3K79, which gets methylated by the Dot1p methyltransferases. Mutation in this region affects telomeric silencing. In collaboration with Rolf Sternglanz at SUNY, Stony Brook, we could study the effect of another silencing protein called Sir3 binding to the nucleosome. Sternglanz and colleagues have shown that mutations in H3D77, which is an amino acid involved in the charged patch at the H3-H4 interface leads to better binding of the Sir3 protein. We will try to co-crystallize the Sir3 protein with the nucleosome. It will be interesting to see whether Sir3 is another protein, that binds very stereo specifically to the surface of the nucleosome and thereby modulates chromatin function.

In chapter III of this thesis, we used LANA as a tool and studied the effect of LANA binding on chromatin in solution. We found that the surface of the nucleosome plays a critical role in chromatin compaction. We showed that the charged domains formed by the dimerization of the histone dimers act as repulsive domains thereby preventing chromatin compaction. We showed that LANA binding to the charged domain induced better folding. We also showed that the H4 tail could act in trans to mediate the same effects as LANA. Experiments done so far only address the effect of H4 tail in chromatin compaction. Hansen and colleagues have shown that the histone tails act independently and also additively. Further experiments will be done to study the effect of

the other tails in chromatin compaction and see whether these tails might be involved in interacting with the nucleosomal surface or with the DNA. We should also study the effect of the Sir3 binding to the nucleosomal arrays.

In Chapter IV and V we show novel functions for the histone chaperone yeast Nucleosome Assembly Protein (yNAP1). Chapter IV shows that yNAP1 can slide nucleosomes on a longer piece of DNA. We have also shown that for this process to occur, yNAP1 has to remove and exchange the histone dimers. Since yNAP1 is a histone dimer-specific chaperone, it would be very interesting to see whether yNAP1 can exchange the histone dimers in the presence of the LANA peptide. This would show whether trans-acting proteins could affect transcriptional activity by preventing nucleosome from falling apart. An *in vitro* transcriptional activity study would be useful in proving this hypothesis. We can also test whether the binding of LANA to the histone dimer and binding of yNAP1 is mutually exclusive or whether yNAP1 can bind to the dimer in presence of LANA. This would give us a clue to how yNAP1 specifically interacts with the histone dimer. The ability of yNAP1 to bind the acidic patch mutant should also be studied. This would tell us whether yNAP1 can recognize the surface of the nucleosome. We can also use yNAP1 as a tool to study the stability of the mononucleosome in the presence and absence of LANA. The experiments done to show that yNAP1 can exchange dimers into preformed nucleosomes have only been done in mononucleosomes. This study should be extended to nucleosomal arrays. This would determine whether the exchange activity observed in mononucleosomes is biologically relevant.

In Chapter V, we showed that the C-terminal tail acidic domain (CTAD) of yNAP1, which was considered non-essential, is in fact responsible for a “scavenging activity” of yNAP1. We have shown that the binding affinity for yNAP1 is changed in the absence of the CTAD. We further need to do fluorescence polarization studies with all the yNAP1 constructs available to determine the binding constants for yNAP1 truncations to the histone dimers and the acidic patch mutant histone dimers. This would determine whether yNAP1 exchanges/scavenges histone dimers from nucleosomes by either physically removing the histones or by acting as a histone sink with higher binding affinity so that any non-specifically bound histones bind to yNAP1 rather than non-specifically interact with the nucleosome/tetrasome or DNA.

The CTAD of yNAP1 has more glutamates than aspartates. In the case of *Drosophila* NAP1, the CTAD has more aspartates than glutamates. However, in *Drosophila*, an enzyme polyglutamylase adds a 10-13 stretch of glutamates to the C-terminal region. We hypothesize that this post-translational modification could act as a switch to change NAP1 from being a histone chaperone to a histone scavenger. To test this hypothesis in vitro, a domain swap experiment can be done wherein we swap the CTAD of yNAP1 with the CTAD of *Drosophila* NAP1 and vice versa. If the hypothesis regarding the glutamate content is correct, the chimeric *Drosophila* NAP1 should exhibit the exchange/scavenging activity whereas the chimeric yNAP1 shouldn't exhibit the functions described earlier. In vitro polyglutamylation using the purified enzyme polyglutamylase or chemical peptide ligation of a polyglutamate stretch can also be done to identify whether this modification can act as a molecular switch.

In summary, this dissertation has reshaped the way the nucleosomal surface should be viewed. We have shown that the nucleosomal surface can act as a docking station for transcriptional/ viral proteins. We have also shown that by changing the surface, either through point mutations or by ligand binding, we can modulate the higher order chromatin compaction. All these data point to the fact that the nucleosomal core surface is dynamically involved in modulation of the chromatin structure. This work will hopefully lead to studying the surface and its posttranslational modifications in detail in the future. We have also shown that the yeast nucleosomal assembly protein is a multifaceted protein, which can act as a histone exchanger and scavenger of chromatin. Further studies should be done on other histone chaperones to determine whether all the histone chaperones carry these novel functions in addition to their assembly function. These studies hopefully will increase understanding of the complex and intricate world of chromatin.

CHAPTER VIII

References

Adkins, M.W., Howar, S.R., and Tyler, J.K. (2004). Chromatin Disassembly Mediated by the Histone Chaperone Asf1 Is Essential for Transcriptional Activation of the Yeast PHO5 and PHO8 Genes. *Mol Cell* 14, 657-666.

Ahmad, K., and Henikoff, S. (2002). The histone variant H3.3 marks active chromatin by replication- independent nucleosome assembly. *Mol Cell* 9, 1191-1200.

Akey, C.W., and Luger, K. (2003). Histone chaperones and nucleosome assembly. *Curr Opin Struct Biol* 13, 6-14.

Albig, W., Ebentheuer, J., Klobeck, G., Kunz, J., and Doenecke, D. (1996). A solitary human H3 histone gene on chromosome 1. *Hum Genet* 97, 486-491.

Altman, R., and Kellogg, D. (1997). Control of mitotic events by Nap1 and the Gin4 kinase. *J Cell Biol* 138, 119-130.

Arents, G., and Moudrianakis, E.N. (1995). The histone fold: a ubiquitous architectural motif utilized in DNA compaction and protein dimerization. *Proc Natl Acad Sci U S A* 92, 11170-11174.

Asahara, H., Tartare-Deckert, S., Nakagawa, T., Ikehara, T., Hirose, F., Hunter, T., Ito, T., and Montminy, M. (2002). Dual roles of p300 in chromatin assembly and transcriptional activation in cooperation with nucleosome assembly protein 1 in vitro. *Mol Cell Biol* 22, 2974-2983.

Baer, B.W., and Rhodes, D. (1983). Eukaryotic RNA polymerase II binds to nucleosome cores from transcribed genes. *Nature* 301, 482-488.

Ballestas, M.E., Chatis, P.A., and Kaye, K.M. (1999). Efficient persistence of extrachromosomal KSHV DNA mediated by latency-associated nuclear antigen. *Science (New York, NY)* 284, 641-644.

Bannister, A.J., Schneider, R., and Kouzarides, T. (2002). Histone methylation: dynamic or static? *Cell* 109, 801-806.

Bao, Y., Konesky, K., Park, Y.J., Rosu, S., Dyer, P.N., Rangasamy, D., Tremethick, D.J., Laybourn, P.J., and Luger, K. (2004). Nucleosomes containing the histone variant H2A.Bbd organize only 118 base pairs of DNA. *Embo J* 23, 3314-3324.

Barbera, A.J., Ballestas, M.E., and Kaye, K.M. (2004). The Kaposi's sarcoma-associated herpesvirus latency-associated nuclear antigen 1 N terminus is essential for chromosome association, DNA replication, and episome persistence. *J Virol* 78, 294-301.

Barbera, A.J., Chodaparambil, J.V., Kelley-Clarke, B., Joukov, V., Walter, J.C., Luger, K., and Kaye, K.M. (2006). The nucleosomal surface as a docking station for Kaposi's sarcoma herpesvirus LANA. *Science (New York, NY)* 5762, 856-861.

Becker, P.B., and Horz, W. (2002). ATP-dependent nucleosome remodeling. *Annu Rev Biochem* 71, 247-273.

Belotserkovskaya, R., Oh, S., Bondarenko, V.A., Orphanides, G., Studitsky, V.M., and Reinberg, D. (2003). FACT facilitates transcription-dependent nucleosome alteration. *Science (New York, NY)* 301, 1090-1093.

Berndsen, C.E., Selleck, W., McBryant, S.J., Hansen, J.C., Tan, S., and Denu, J.M. (2007). Nucleosome recognition by the Piccolo NuA4 histone acetyltransferase complex. *Biochemistry* 46, 2091-2099.

Boeger, H., Griesenbeck, J., Strattan, J.S., and Kornberg, R.D. (2004). Removal of promoter nucleosomes by disassembly rather than sliding in vivo. *Mol Cell* 14, 667-673.

Boshoff, C., and Weiss, R.A. (1997). Aetiology of Kaposi's sarcoma: current understanding and implications for therapy. *Mol Med Today* 3, 488-494.

Brower-Toland, B., Wacker, D.A., Fulbright, R.M., Lis, J.T., Kraus, W.L., and Wang, M.D. (2005). Specific contributions of histone tails and their acetylation to the mechanical stability of nucleosomes. *J Mol Biol* 346, 135-146.

Bruno, M., Flaus, A., and Owen-Hughes, T. (2004). Site-specific attachment of reporter compounds to recombinant histones. *Methods Enzymol* 375, 211-228.

Bruno, M., Flaus, A., Stockdale, C., Rencurel, C., Ferreira, H., and Owen-Hughes, T. (2003). Histone H2A/H2B dimer exchange by ATP-dependent chromatin remodeling activities. *Mol Cell* 12, 1599-1606.

Burglin, T.R., and De Robertis, E.M. (1987). The nuclear migration signal of *Xenopus laevis* nucleoplasmin. *Embo J* 6, 2617-2625.

Cairns, B.R., Lorch, Y., Li, Y., Zhang, M., Lacomis, L., Erdjument Bromage, H., Tempst, P., Du, J., Laurent, B., and Kornberg, R.D. (1996). RSC, an essential, abundant chromatin-remodeling complex. *Cell* 87, 1249-1260.

Cesarman, E., Chang, Y., Moore, P.S., Said, J.W., and Knowles, D.M. (1995). Kaposi's sarcoma-associated herpesvirus-like DNA sequences in AIDS-related body-cavity-based lymphomas. *The New England journal of medicine* 332, 1186-1191.

Chadwick, B.P., and Willard, H.F. (2001). Histone H2A variants and the inactive X chromosome: identification of a second macroH2A variant. *Hum Mol Genet* 10, 1101-1113.

Chakravarthy, S., Gundimella, S. K., Caron, C., Perche, P. Y., Pehrson, J. R., Khochbin, S., and Luger, K. (2005). Structural characterization of the histone variant macroH2A. *Mol Cell Biol* 25, 7616-7624.

Chang, L., Loranger, S.S., Mizzen, C., Ernst, S.G., Allis, C.D., and Annunziato, A.T. (1997). Histones in transit: cytosolic histone complexes and diacetylation of H4 during nucleosome assembly in human cells. *Biochemistry* 36, 469-480.

Chang, Y., Cesarman, E., Pessin, M.S., Lee, F., Culpepper, J., Knowles, D.M., and Moore, P.S. (1994). Identification of herpesvirus-like DNA sequences in AIDS-associated Kaposi's sarcoma. *Science (New York, NY)* 266, 1865-1869.

Chen, H., Li, B., and Workman, J.L. (1994). A histone-binding protein, nucleoplasmin, stimulates transcription factor binding to nucleosomes and factor-induced nucleosome disassembly. *Embo J* 13, 380-390.

Chodaparambil, J.V., Edayathumangalam, R.S., Bao, Y., Park, Y.J., and Luger, K. (2006). Nucleosome structure and function. *Ernst Schering Res Found Workshop*, 29-46.

Cocklin, R.R., and Wang, M. (2003). Identification of methylation and acetylation sites on mouse histone H3 using matrix-assisted laser desorption/ionization time-of-flight and nano-electrospray ionization tandem mass spectrometry. *J Protein Chem* 22, 327-334.

Costanzi, C., and Pehrson, J.R. (1998). Histone macroH2A1 is concentrated in the inactive X chromosome of female mammals. *Nature* 393.

Cote, J., Quinn, J., Workman, J.L., and Peterson, C.L. (1994). Stimulation of GAL4 derivative binding to nucleosomal DNA by the yeast SWI/SNF complex. *Science (New York, NY)* 265, 53-60.

Cotter, M.A., 2nd, and Robertson, E.S. (1999). The latency-associated nuclear antigen tethers the Kaposi's sarcoma-associated herpesvirus genome to host chromosomes in body cavity-based lymphoma cells. *Virology* 264, 254-264.

Davey, C.A., and Richmond, T.J. (2002). DNA-dependent divalent cation binding in the nucleosome core particle. *Proc Natl Acad Sci U S A* 99, 11169-11174.

Davey, C.A., Sargent, D.F., Luger, K., Maeder, A.W., and Richmond, T.J. (2002). Solvent mediated interactions in the structure of the nucleosome core particle at 1.9 Å resolution. *J Mol Biol* 319, 1097-1113.

Decker, L.L., Shankar, P., Khan, G., Freeman, R.B., Dezube, B.J., Lieberman, J., and Thorley-Lawson, D.A. (1996). The Kaposi sarcoma-associated herpesvirus (KSHV) is present as an intact latent genome in KS tissue but replicates in the peripheral blood mononuclear cells of KS patients. *The Journal of experimental medicine* 184, 283-288.

DeLano, W.L. (2002). *The PyMOL User's Manual* (DeLano Scientific, San Carlos, CA, USA.).

Demeler, B., Saber, H., and Hansen, J.C. (1997). Identification and interpretation of complexity in sedimentation velocity boundaries. *Biophys J* 72, 397-407.

Dingwall, C., Dilworth, S.M., Black, S.J., Kearsley, S.E., Cox, L.S., and Laskey, R.A. (1987). Nucleoplasmin cDNA sequence reveals polyglutamic acid tracts and a cluster of sequences homologous to putative nuclear localization signals. *Embo J* 6, 69-74.

Dong, F., Hansen, J.C., and van Holde, K.E. (1990). DNA and protein determinants of nucleosome positioning on sea urchin 5S rRNA gene sequences in vitro. *Proc Natl Acad Sci U S A* 87, 5724-5728.

Dong, F., and van Holde, K.E. (1991). Nucleosome positioning is determined by the (H3-H4)₂ tetramer. *Proc Natl Acad Sci U S A* 88, 10596-10600.

Dorigo, B., Schalch, T., Bystricky, K., and Richmond, T.J. (2003). Chromatin fiber folding: requirement for the histone H4 N-terminal tail. *J Mol Biol* 327, 85-96.

Dorigo, B., Schalch, T., Kulangara, A., Duda, S., Schroeder, R.R., and Richmond, T.J. (2004). Nucleosome arrays reveal the two-start organization of the chromatin fiber. *Science (New York, NY)* 306, 1571-1573.

Dorigo, B., Schalch, T., Bystricky, K., Richmond, T.J. (2003). Chromatin fiber folding: requirement for the histone H4 N-terminal tail. *Journal of Molecular Biology* 327, 85-96.

Dyer, P.N., Edayathumangalam, R.S., White, C.L., Bao, Y., Chakravarthy, S., Muthurajan, U.M., and Luger, K. (2004). Reconstitution of nucleosome core particles from recombinant histones and DNA. *Methods Enzymol* 375, 23-44.

Emre, N.C., Ingvarsdottir, K., Wyce, A., Wood, A., Krogan, N.J., Henry, K.W., Li, K., Marmorstein, R., Greenblatt, J.F., Shilatifard, A., *et al.* (2005). Maintenance of low histone ubiquitylation by Ubp10 correlates with telomere-proximal Sir2 association and gene silencing. *Mol Cell* 17, 585-594.

Fan, J.Y., Gordon, F., Luger, K., Hansen, J.C., and Tremethick, D.J. (2002). The essential histone variant H2A.Z regulates the equilibrium between different chromatin conformational states. *Nat Struct Biol* 19, 172-176.

Fan, J.Y., Rangasamy, D., Luger, K., and Tremethick, D.J. (2004). H2A.Z Alters the Nucleosome Surface to Promote HP1 α -Mediated Chromatin Fiber Folding. *Mol Cell* 16, 655-661.

Finch, J.T., and Klug, A. (1976). Solenoidal model for superstructure in chromatin. *Proc Natl Acad Sci U S A* 73, 1897-1901.

Fischle, W., Tseng, B.S., Dormann, H.L., Ueberheide, B.M., Garcia, B.A., Shabanowitz, J., Hunt, D.F., Funabiki, H., and Allis, C.D. (2005). Regulation of HP1-chromatin binding by histone H3 methylation and phosphorylation. *Nature* 438, 1116-1122.

Flaus, A., Luger, K., Tan, S., and Richmond, T.J. (1996). Mapping nucleosome position at single base-pair resolution by using site-directed hydroxyl radicals. *Proc Natl Acad Sci U S A* *93*, 1370-1375.

Flaus, A., and Owen-Hughes, T. (2001). Mechanisms for ATP-dependent chromatin remodelling. *Curr Opin Genet Dev* *11*, 148-154.

Fletcher, T.M., and Hansen, J.C. (1996). The nucleosomal array: structure/function relationships. *Crit Rev Eukaryot Gene Expr* *6*, 149-188.

Freitas, M.A., Sklenar, A.R., and Parthun, M.R. (2004). Application of mass spectrometry to the identification and quantification of histone post-translational modifications. *J Cell Biochem* *92*, 691-700.

Friborg, J., Jr., Kong, W., Hottiger, M.O., and Nabel, G.J. (1999). p53 inhibition by the LANA protein of KSHV protects against cell death. *Nature* *402*, 889-894.

Fry, C.J., Norris, A., Cosgrove, M., Boeke, J.D., and Peterson, C.L. (2006). The LRS and SIN domains: two structurally equivalent but functionally distinct nucleosomal surfaces required for transcriptional silencing. *Mol Cell Biol* *26*, 9045-9059.

Fujii Nakata, T., Ishimi, Y., Okuda, A., and Kikuchi, A. (1992). Functional analysis of nucleosome assembly protein, NAP-1. The negatively charged COOH-terminal region is not necessary for the intrinsic assembly activity. *J Biol Chem* *267*, 20980-20986.

Fyodorov, D.V., and Kadonaga, J.T. (2003). Chromatin assembly in vitro with purified recombinant ACF and NAP-1. *Methods Enzymol* *371*, 499-515.

Ganem, D. (1997). KSHV and Kaposi's sarcoma: the end of the beginning? *Cell* *91*, 157-160.

Garcia-Ramirez, M., Dong, F., and Ausio, J. (1992). Role of the histone "tails" in the folding of oligonucleosomes depleted of histone H1. *J Biol Chem* 267, 19587-19595.

Gardner, R.G., Nelson, Z.W., and Gottschling, D.E. (2005). Ubp10/Dot4p regulates the persistence of ubiquitinated histone H2B: distinct roles in telomeric silencing and general chromatin. *Mol Cell Biol* 25, 6123-6139.

Gautier, T., Abbott, D.W., Molla, A., Verdel, A., Ausio, J., and Dimitrov, S. (2004). Histone variant H2ABbd confers lower stability to the nucleosome. *EMBO Rep* 5, 715-720.

Geiman, T.M., and Robertson, K.D. (2002). Chromatin remodeling, histone modifications, and DNA methylation-how does it all fit together? *J Cell Biochem* 87, 117-125.

Gordon, F., Luger, K., and Hansen, J.C. (2005). The core histone N-terminal tail domains function independently and additively during salt-dependent oligomerization of nucleosomal arrays. *J Biol Chem* 280, 33701-33706.

Guan, K.L., and Dixon, J.E. (1991). Eukaryotic proteins expressed in *Escherichia coli*: an improved thrombin cleavage and purification procedure of fusion proteins with glutathione S-transferase. *Analytical biochemistry* 192, 262-267.

Gwack, Y., Baek, H.J., Nakamura, H., Lee, S.H., Meisterernst, M., Roeder, R.G., and Jung, J.U. (2003). Principal role of TRAP/mediator and SWI/SNF complexes in Kaposi's sarcoma-associated herpesvirus RTA-mediated lytic reactivation. *Mol Cell Biol* 23, 2055-2067.

Hansen, J.C. (2002). CONFORMATIONAL DYNAMICS OF THE CHROMATIN FIBER IN SOLUTION: Determinants, Mechanisms, and Functions. *Annu Rev Biophys Biomol Struct* 31, 361-392.

Hansen, J.C., Ausio, J., Stanik, V.H., and van Holde, K.E. (1989). Homogeneous reconstituted oligonucleosomes, evidence for salt-dependent folding in the absence of histone H1. *Biochemistry* 28, 9129-9136.

Hansen, J.C., and Lohr, D. (1993). Assembly and structural properties of subsaturated chromatin arrays. *J Biol Chem* 268, 5840-5848.

Hansen, J.C., van Holde, K.E., and Lohr, D. (1991). The mechanism of nucleosome assembly onto oligomers of the sea urchin 5 S DNA positioning sequence. *J Biol Chem* 266, 4276-4282.

Harauz, G., Borland, L., Bahr, G.F., Zeitler, E., and van Heel, M. (1987). Three-dimensional reconstruction of a human metaphase chromosome from electron micrographs. *Chromosoma* 95, 366-374.

Harp, J.M., Hanson, B.L., Timm, D.E., and Bunick, G.J. (2000). Asymmetries in the nucleosome core particle at 2.5 Å resolution. *Acta Crystallogr D Biol Crystallogr* 56 Pt 12, 1513-1534.

Hassa, P.O., Haenni, S.S., Elser, M., and Hottiger, M.O. (2006). Nuclear ADP-ribosylation reactions in mammalian cells: where are we today and where are we going? *Microbiol Mol Biol Rev* 70, 789-829.

Hirano, T., and Mitchison, T.J. (1994). A heterodimeric coiled-coil protein required for mitotic chromosome condensation in vitro. *Cell* 79, 449-458.

Horowitz, R.A., Agard, D.A., Sedat, J.W., and Woodcock, C.L. (1994). The three-dimensional architecture of chromatin in situ: electron tomography reveals fibers composed of a continuously variable zig-zag nucleosomal ribbon. *J Cell Biol* 125, 1-10.

Hudson, D.F., Vagnarelli, P., Gassmann, R., and Earnshaw, W.C. (2003). Condensin is required for nonhistone protein assembly and structural integrity of vertebrate mitotic chromosomes. *Dev Cell* 5, 323-336.

Hung, S.C., Kang, M.S., and Kieff, E. (2001). Maintenance of Epstein-Barr virus (EBV) oriP-based episomes requires EBV-encoded nuclear antigen-1 chromosome-binding domains, which can be replaced by high-mobility group-I or histone H1. *Proc Natl Acad Sci U S A* 98, 1865-1870.

Hyland, E.M., Cosgrove, M.S., Molina, H., Wang, D., Pandey, A., Cottee, R.J., and Boeke, J.D. (2005). Insights into the role of histone H3 and histone H4 core modifiable residues in *Saccharomyces cerevisiae*. *Mol Cell Biol* 25, 10060-10070.

Ishimi, Y., and Kikuchi, A. (1991). Identification and molecular cloning of yeast homolog of nucleosome assembly protein I which facilitates nucleosome assembly in vitro. *J Biol Chem* 266, 7025-7029.

Ishimi, Y., Kojima, M., Yamada, M., and Hanaoka, F. (1987). Binding mode of nucleosome-assembly protein (AP-I) and histones. *Eur J Biochem* 162, 19-24.

Ito, T., Bulger, M., Kobayashi, R., and Kadonaga, J.T. (1996a). *Drosophila* NAP-1 is a core histone chaperone that functions in ATP-facilitated assembly of regularly spaced nucleosomal arrays. *Mol Cell Biol* 16, 3112-3124.

Ito, T., Ikehara, T., Nakagawa, T., Kraus, W.L., and Muramatsu, M. (2000). p300-mediated acetylation facilitates the transfer of histone H2A-H2B dimers from nucleosomes to a histone chaperone. *Genes Dev* 14, 1899-1907.

Ito, T., Tyler, J.K., Bulger, M., Kobayashi, R., and Kadonaga, J.T. (1996b). ATP-facilitated chromatin assembly with a nucleoplasmin-like protein from *Drosophila melanogaster*. *J Biol Chem* 271, 25041-25048.

Jackson, V. (1990). In vivo studies on the dynamics of histone-DNA interaction: evidence for nucleosome dissolution during replication and transcription and a low level of dissolution independent of both. *Biochemistry* 29, 719-731.

Janke, C., Rogowski, K., Wloga, D., Regnard, C., Kajava, A.V., Strub, J.M., Temurak, N., van Dijk, J., Boucher, D., van Dorsselaer, A., *et al.* (2005). Tubulin polyglutamylase enzymes are members of the TTL domain protein family. *Science (New York, NY)* 308, 1758-1762.

Jones, S., and Thornton, J.M. (1996). Principles of protein-protein interactions. *Proc Natl Acad Sci U S A* 93, 13-20.

Jones, T.A., Zou, J.Y., Cowan, S.W., and Kjeldgaard, M. (1991). Improved methods for building protein models in electron density maps and the location of errors in these models. *Acta Cryst A* 47, 110-119.

Ju, B.G., Lunyak, V.V., Perissi, V., Garcia-Bassets, I., Rose, D.W., Glass, C.K., and Rosenfeld, M.G. (2006). A topoisomerase IIbeta-mediated dsDNA break required for regulated transcription. *Science (New York, NY)* 312, 1798-1802.

Kamakaka, R.T., and Biggins, S. (2005). Histone variants: deviants? *Genes Dev* 19, 295-310.

Kan, P.Y., Lu, X., Hansen, J.C., and Hayes, J.J. (2007). The H3 tail domain participates in multiple interactions during folding and self-association of nucleosome arrays. *Mol Cell Biol*.

Kapoor, P., Shire, K., and Frappier, L. (2001). Reconstitution of Epstein-Barr virus-based plasmid partitioning in budding yeast. *Embo J* 20, 222-230.

- Kaufman, P. D., Cohen, J. L., and Osley, M. A. (1998). Hir Proteins Are Required for Position-Dependent Gene Silencing in *Saccharomyces cerevisiae* in the Absence of Chromatin Assembly Factor I. *Mol Cell Biol* *18*, 4793-4806.
- Kedes, D.H., Lagunoff, M., Renne, R., and Ganem, D. (1997). Identification of the gene encoding the major latency-associated nuclear antigen of the Kaposi's sarcoma-associated herpesvirus. *J Clin Invest* *100*, 2606-2610.
- Kellam, P., Boshoff, C., Whitby, D., Matthews, S., Weiss, R.A., and Talbot, S.J. (1997). Identification of a major latent nuclear antigen, LNA-1, in the human herpesvirus 8 genome. *J Hum Virol* *1*, 19-29.
- Kellogg, D.R., Kikuchi, A., Fujii-Nakata, T., Turck, C.W., and Murray, A.W. (1995). Members of the NAP/SET family of proteins interact specifically with B-type cyclins. *J Cell Biol* *130*, 661-673.
- Kepert, J.F., Mazurkiewicz, J., Heuvelman, G.L., Toth, K.F., and Rippe, K. (2005). NAP1 modulates binding of linker histone H1 to chromatin and induces an extended chromatin fiber conformation. *J Biol Chem* *280*, 34063-34072.
- Khorasanizadeh, S. (2004). The nucleosome: from genomic organization to genomic regulation. *Cell* *116*, 259-272.
- Kimura, H., and Cook, P.R. (2001). Kinetics of core histones in living human cells: little exchange of H3 and H4 and some rapid exchange of H2B. *J Cell Biol* *153*, 1341-1353.
- Kireeva, M.L., Walter, W., Tchernajenko, V., Bondarenko, V., Kashlev, M., and Studitsky, V.M. (2002). Nucleosome Remodeling Induced by RNA Polymerase II. Loss of the H2A/H2B Dimer during Transcription. *Mol Cell* *9*, 541-552.

Kobor, M.S., Venkatasubrahmanyam, S., Meneghini, M.D., Gin, J.W., Jennings, J.L., Link, A.J., Madhani, H.D., and Rine, J. (2004). A Protein Complex Containing the Conserved Swi2/Snf2-Related ATPase Swr1p Deposits Histone Variant H2A.Z into Euchromatin. *PLoS Biol* 2, E131.

Korber, P., and Horz, W. (2004). SWRred not shaken; mixing the histones. *Cell* 117, 5-7.
Kornberg, R.D., and Lorch, Y. (1991). Irresistible force meets immovable object: transcription and the nucleosome. *Cell* 67, 833-836.

Kouzarides, T. (2007). Chromatin modifications and their function. *Cell* 128, 693-705.
Krithivas, A., Fujimuro, M., Weidner, M., Young, D.B., and Hayward, S.D. (2002). Protein interactions targeting the latency-associated nuclear antigen of Kaposi's sarcoma-associated herpesvirus to cell chromosomes. *J Virol* 76, 11596-11604.

Krithivas, A., Young, D.B., Liao, G., Greene, D., and Hayward, S.D. (2000). Human herpesvirus 8 LANA interacts with proteins of the mSin3 corepressor complex and negatively regulates Epstein-Barr virus gene expression in dually infected PEL cells. *J Virol* 74, 9637-9645.

Krogan, N.J., Keogh, M.C., Datta, N., Sawa, C., Ryan, O.W., Ding, H., Haw, R.A., Pootoolal, J., Tong, A., Canadien, V., *et al.* (2003). A Snf2 family ATPase complex required for recruitment of the histone H2A variant Htz1. *Mol Cell* 12, 1565-1576.

Krude, T., and Keller, C. (2001). Chromatin assembly during S phase: contributions from histone deposition, DNA replication and the cell division cycle. *Cell Mol Life Sci* 58, 665-672.

Kruger, W., Peterson, C.L., Sil, A., Coburn, C., Arents, G., Moudrianakis, E.N., and Herskowitz, I. (1995). Amino acid substitutions in the structured domains of histones H3 and H4 partially relieve the requirement of the yeast SWI/SNF complex for transcription. *Genes Dev* 9, 2770-2779.

Lacoste, N., Utley, R.T., Hunter, J.M., Poirier, G.G., and Cote, J. (2002). Disruptor of Telomeric Silencing-1 Is a Chromatin-specific Histone H3 Methyltransferase. *J Biol Chem* 277, 30421-30424.

Ladoux, B., Quivy, J.P., Doyle, P., du Roure, O., Almouzni, G., and Viovy, J.L. (2000). Fast kinetics of chromatin assembly revealed by single-molecule videomicroscopy and scanning force microscopy. *Proc Natl Acad Sci U S A* 97, 14251-14256.

Langst, G., and Becker, P.B. (2001). Nucleosome mobilization and positioning by ISWI-containing chromatin-remodeling factors. *J Cell Sci* 114, 2561-2568.

Lankenau, S., Barnickel, T., Marhold, J., Lyko, F., Mechler, B.M., and Lankenau, D.H. (2003). Knockout targeting of the *Drosophila* nap1 gene and examination of DNA repair tracts in the recombination products. *Genetics* 163, 611-623.

Lee, K.-M., and Hayes, J.J. (1997). The N-terminal tail of histone H2A binds to two distinct sites within the nucleosome core. *PNAS* 94, 8959-8964.

Levchenko, V., and Jackson, V. (2004). Histone release during transcription: NAP1 forms a complex with H2A and H2B and facilitates a topologically dependent release of H3 and H4 from the nucleosome. *Biochemistry* 43, 2359-2372.

Lewis, E.A., DeBuysere, M.S., and Rees, A.W. (1976). Configuration of unsheared nucleohistone. Effects of ionic strength and of histone F1 removal. *Biochemistry* 15, 186-192.

Lim, C., Choi, C., and Choe, J. (2004). Mitotic chromosome-binding activity of latency-associated nuclear antigen 1 is required for DNA replication from terminal repeat sequence of Kaposi's sarcoma-associated herpesvirus. *J Virol* 78, 7248-7256.

Lim, C., Lee, D., Seo, T., Choi, C., and Choe, J. (2003). Latency-associated nuclear antigen of Kaposi's sarcoma-associated herpesvirus functionally interacts with heterochromatin protein 1. *J Biol Chem* 278, 7397-7405.

Loyola, A., and Almouzni, G. (2004). Histone chaperones, a supporting role in the limelight. *Biochim Biophys Acta* 1677, 3-11.

Luger, K., Maeder, A.W., Richmond, R.K., Sargent, D.F., and Richmond, T.J. (1997). Crystal structure of the nucleosome core particle at 2.8 Å resolution. *Nature* 389, 251-259.

Luger, K., Rechsteiner, T.J., and Richmond, T.J. (1999). Preparation of nucleosome core particle from recombinant histones. *Methods Enzymol* 304, 3-19.

Luger, K., and Richmond, T.J. (1998a). DNA binding within the nucleosome core. *Current Opinion in Structural Biology* 8, 33-40.

Luger, K., and Richmond, T.J. (1998b). The histone tails of the nucleosome. *Curr Opin Genet Dev* 8, 140-146.

Macdonald, N., Welburn, J.P., Noble, M.E., Nguyen, A., Yaffe, M.B., Clynes, D., Moggs, J.G., Orphanides, G., Thomson, S., Edmunds, J.W., *et al.* (2005). Molecular basis for the recognition of phosphorylated and phosphoacetylated histone h3 by 14-3-3. *Mol Cell* 20, 199-211.

Malik, H.S., and Henikoff, S. (2003). Phylogenomics of the nucleosome. *Nat Struct Biol* 10, 882-891.

Margueron, R., Trojer, P., and Reinberg, D. (2005). The key to development: interpreting the histone code? *Curr Opin Genet Dev* 15, 163-176.

Matsubara, K., Sano, N., Umehara, T., and Horikoshi, M. (2007). Global analysis of functional surfaces of core histones with comprehensive point mutants. *Genes Cells* 12, 13-33.

Mazurkiewicz, J., Kepert, J. F., and Rippe, K. (2006). On the mechanism of nucleosome assembly by histone chaperone NAP1. *J Biol Chem* 281, 16462-16472.

McBryant, S.J., Park, Y.J., Abernathy, S.M., Laybourn, P.J., Nyborg, J.K., and Luger, K. (2003). Preferential binding of the histone (H3-H4)₂ tetramer by NAP1 is mediated by the amino-terminal histone tails. *J Biol Chem* 278, 44574-44583.

McBryant, S.J., and Peersen, O.B. (2004). Self-Association of the Yeast Nucleosome Assembly Protein 1. *Biochemistry In Press*.

McQuibban, G.A., Commisso-Cappelli, C.N., and Lewis, P.N. (1998). Assembly, Remodeling, and Histone Binding Capabilities of Yeast Nucleosome Assembly Protein 1. *Biol Chem* 273, 6582-6590.

Mersfelder, E.L., and Parthun, M.R. (2006). The tale beyond the tail: histone core domain modifications and the regulation of chromatin structure. *Nucleic Acids Res* 34, 2653-2662.

Miyaji-Yamaguchi, M., Kato, K., Nakano, R., Akashi, T., Kikuchi, A., and Nagata, K. (2003). Involvement of nucleocytoplasmic shuttling of yeast Nap1 in mitotic progression. *Mol Cell Biol* 23, 6672-6684.

Mizuguchi, G., Shen, X., Landry, J., Wu, W.H., Sen, S., and Wu, C. (2004). ATP-driven exchange of histone H2AZ variant catalyzed by SWR1 chromatin remodeling complex. *Science (New York, NY)* 303, 343-348.

Moore, P.S., and Chang, Y. (1995). Detection of herpesvirus-like DNA sequences in Kaposi's sarcoma in patients with and without HIV infection. *The New England journal of medicine* 332, 1181-1185.

Mosammaparast, N., Guo, Y., Shabanowitz, J., Hunt, D.F., and Pemberton, L.F. (2002). Pathways mediating the nuclear import of histones H3 and H4 in yeast. *J Biol Chem* 277, 862-868.

Mullinger, A.M., and Johnson, R.T. (1987). Disassembly of the mammalian metaphase chromosome into its subunits: studies with ultraviolet light and repair synthesis inhibitors. *J Cell Sci* 87 (*Pt 1*), 55-69.

Murray, A.W. (1991). Cell cycle extracts. *Methods in cell biology* 36, 581-605.

Muthurajan, U.M., Park, Y.J., Edayathumangalam, R.S., Suto, R.K., Chakravarthy, S., Dyer, P.N., and Luger, K. (2003). Structure and dynamics of nucleosomal DNA. *Biopolymers* 68, 547-556.

Muto, S., Senda, M., Akai, Y., Sato, L., Suzuki, T., Nagai, R., Senda, T., and Horikoshi, M. (2007). Relationship between the structure of SET/TAF-Ibeta/INHAT and its histone chaperone activity. *Proc Natl Acad Sci U S A* 104, 4285-4290.

Nakagawa, T., Bulger, M., Muramatsu, M., and Ito, T. (2001). Multistep chromatin assembly on supercoiled plasmid DNA by nucleosome assembly protein-1 and ATP-utilizing chromatin assembly and remodeling factor. *J Biol Chem* 276, 27384-27391.

Nathan, D., Ingvarsdottir, K., Sterner, D.E., Bylebyl, G.R., Dokmanovic, M., Dorsey, J.A., Whelan, K.A., Krsmanovic, M., Lane, W.S., Meluh, P.B., *et al.* (2006). Histone sumoylation is a negative regulator in *Saccharomyces cerevisiae* and shows dynamic interplay with positive-acting histone modifications. *Genes Dev* 20, 966-976.

Ng, H.H., Feng, Q., Wang, H., Erdjument-Bromage, H., Tempst, P., Zhang, Y., and Struhl, K. (2002). Lysine methylation within the globular domain of histone H3 by Dot1 is important for telomeric silencing and Sir protein association. *Genes Dev* 16, 1518-1527.

Nicholls, A., Sharp, K.A., and Honig, B. (1991). Protein folding and association: insights from the interfacial and thermodynamic properties of hydrocarbons. *Proteins* 11, 281-296.

Nussenzweig, A., Chen, C., da Costa Soares, V., Sanchez, M., Sokol, K., Nussenzweig, M.C., and Li, G.C. (1996). Requirement for Ku80 in growth and immunoglobulin V(D)J recombination. *Nature* 382, 551-555.

Ohkuni, K., Shirahige, K., and Kikuchi, A. (2003). Genome-wide expression analysis of NAP1 in *Saccharomyces cerevisiae*. *Biochem Biophys Res Commun* 306, 5-9.

Old, R.W., Woodland, H.R., Ballantine, J.E., Aldridge, T.C., Newton, C.A., Bains, W.A., and Turner, P.C. (1982). Organization and expression of cloned histone gene clusters from *Xenopus laevis* and *X. borealis*. *Nucleic Acids Res* 10, 7561-7580.

Orphanides, G., LeRoy, G., Chang, C.H., Luse, D.S., and Reinberg, D. (1998). FACT, a factor that facilitates transcript elongation through nucleosomes. *Cell* 92, 105-116.

Otwinowski, Z., and Minor, W. (1997). Processing of X-ray diffraction data collected in oscillation mode, Vol 276, *Macromolecular Crystallography, part A* (New York, Academic Press).

Park, J.H., Cosgrove, M.S., Youngman, E., Wolberger, C., and Boeke, J.D. (2002). A core nucleosome surface crucial for transcriptional silencing. *Nat Genet* 16, 16.

Park, Y.J., Chodaparambil, J.V., Bao, Y., McBryant, S.J., and Luger, K. (2005). Nucleosome assembly protein 1 exchanges histone H2A-H2B dimers and assists nucleosome sliding. *J Biol Chem* 280, 1817-1825.

Park, Y.J., Dyer, P.N., Tremethick, D.J., and Luger, K. (2004). A New Fluorescence Resonance Energy Transfer Approach Demonstrates That the Histone Variant H2AZ Stabilizes the Histone Octamer within the Nucleosome. *J Biol Chem* 279, 24274-24282.

Park, Y.J., and Luger, K. (2006a). Structure and function of nucleosome assembly proteins. *Biochem Cell Biol* 84, 549-558.

Park, Y.J., and Luger, K. (2006b). The structure of nucleosome assembly protein 1. *Proc Natl Acad Sci U S A* 103, 1248-1253.

Pavri, R., Zhu, B., Li, G., Trojer, P., Mandal, S., Shilatifard, A., and Reinberg, D. (2006). Histone H2B monoubiquitination functions cooperatively with FACT to regulate elongation by RNA polymerase II. *Cell* 125, 703-717.

Pehrson, J.R., and Fried, V.A. (1992). MacroH2A, a core histone containing a large nonhistone region. *Science (New York, NY)* 257, 1398-1400.

Philpott, A., and Leno, G.H. (1992). Nucleoplasmin remodels sperm chromatin in *Xenopus* egg extracts. *Cell* 69, 759-767.

Philpott, A., Leno, G.H., and Laskey, R.A. (1991). Sperm decondensation in *Xenopus* egg cytoplasm is mediated by nucleoplasmin. *Cell* 65, 569-578.

Piolo, T., Tramier, M., Coppey, M., Nicolas, J.C., and Marechal, V. (2001). Close but distinct regions of human herpesvirus 8 latency-associated nuclear antigen 1 are responsible for nuclear targeting and binding to human mitotic chromosomes. *J Virol* 75, 3948-3959.

Radkov, S.A., Kellam, P., and Boshoff, C. (2000). The latent nuclear antigen of Kaposi sarcoma-associated herpesvirus targets the retinoblastoma-E2F pathway and with the oncogene Hras transforms primary rat cells. *Nat Med* 6, 1121-1127.

Rainbow, L., Platt, G.M., Simpson, G.R., Sarid, R., Gao, S.J., Stoiber, H., Herrington, C.S., Moore, P.S., and Schulz, T.F. (1997). The 222- to 234-kilodalton latent nuclear protein (LNA) of Kaposi's sarcoma-associated herpesvirus (human herpesvirus 8) is encoded by orf73 and is a component of the latency-associated nuclear antigen. *J Virol* 71, 5915-5921.

Rattner, J.B., and Lin, C.C. (1985). Radial loops and helical coils coexist in metaphase chromosomes. *Cell* 42, 291-296.

Redon, C., Pilch, D., Rogakou, E., Sedelnikova, O., Newrock, K., and Bonner, W. (2002). Histone H2A variants H2AX and H2AZ. *Curr Opin Genet Dev* 12, 162-169.

Rehtanz, M., Schmidt, H.M., Warthorst, U., and Steger, G. (2004). Direct interaction between nucleosome assembly protein 1 and the papillomavirus E2 proteins involved in activation of transcription. *Mol Cell Biol* 24, 2153-2168.

Reinke, H., and Horz, W. (2003). Histones are first hyperacetylated and then lose contact with the activated PHO5 promoter. *Mol Cell* 11, 1599-1607.

Renne, R., Barry, C., Dittmer, D., Compitello, N., Brown, P.O., and Ganem, D. (2001). Modulation of cellular and viral gene expression by the latency-associated nuclear antigen of Kaposi's sarcoma-associated herpesvirus. *J Virol* 75, 458-468.

Rhoades, A.R., Ruone, S., and Formosa, T. (2004). Structural features of nucleosomes reorganized by yeast FACT and its HMG box component, Nhp6. *Mol Cell Biol* 24, 3907-3917.

Rice, L.M., Shamoo, Y., and Brunger, A.T. (1998). Phase improvement by multi-start simulated annealing refinement and structure-factor averaging. *J Appl Cryst* *31*, 798-805.

Robinson, P.J., and Rhodes, D. (2006). Structure of the '30 nm' chromatin fibre: a key role for the linker histone. *Curr Opin Struct Biol* *16*, 336-343.

Rodriguez, P., Pelletier, J., Price, G.B., and Zannis-Hadjopoulos, M. (2000). NAP-2: histone chaperone function and phosphorylation state through the cell cycle. *J Mol Biol* *298*, 225-238.

Schalch, T., Duda, S., Sargent, D.F., and Richmond, T.J. (2005). X-ray structure of a tetranucleosome and its implications for the chromatin fibre. *Nature* *436*, 138-141.

Schwam, D.R., Luciano, R.L., Mahajan, S.S., Wong, L., and Wilson, A.C. (2000). Carboxy terminus of human herpesvirus 8 latency-associated nuclear antigen mediates dimerization, transcriptional repression, and targeting to nuclear bodies. *J Virol* *74*, 8532-8540.

Schwarz, P.M., Felthauer, A., Fletcher, T.M., and Hansen, J.C. (1996). Reversible oligonucleosome self-association: dependence on divalent cations and core histone tail domains. *Biochemistry* *35*, 4009-4015.

Schwarz, P.M., and Hansen, J.C. (1994). Formation and stability of higher order chromatin structures. Contributions of the histone octamer. *J Biol Chem* *269*, 16284-16289.

Sears, J., Ujihara, M., Wong, S., Ott, C., Middeldorp, J., and Aiyar, A. (2004). The amino terminus of Epstein-Barr Virus (EBV) nuclear antigen 1 contains AT hooks that facilitate the replication and partitioning of latent EBV genomes by tethering them to cellular chromosomes. *J Virol* *78*, 11487-11505.

Shi, Y., Lan, F., Matson, C., Mulligan, P., Whetstone, J.R., Cole, P.A., Casero, R.A., and Shi, Y. (2004). Histone demethylation mediated by the nuclear amine oxidase homolog LSD1. *Cell* 119, 941-953.

Shikama, N., Chan, H.M., Krstic-Demonacos, M., Smith, L., Lee, C.W., Cairns, W., and La Thangue, N.B. (2000). Functional interaction between nucleosome assembly proteins and p300/CREB-binding protein family coactivators. *Mol Cell Biol* 20, 8933-8943.

Shinohara, H., Fukushi, M., Higuchi, M., Oie, M., Hoshi, O., Ushiki, T., Hayashi, J., and Fujii, M. (2002). Chromosome binding site of latency-associated nuclear antigen of Kaposi's sarcoma-associated herpesvirus is essential for persistent episome maintenance and is functionally replaced by histone H1. *J Virol* 76, 12917-12924.

Shogren-Knaak, M., Ishii, H., Sun, J.M., Pazin, M.J., Davie, J.R., and Peterson, C.L. (2006). Histone H4-K16 acetylation controls chromatin structure and protein interactions. *Science* (New York, NY) 311, 844-847.

Simpson, R.T., and Stafford, D.W. (1983). Structural features of a phased nucleosome core particle. *Proc Natl Acad Sci U S A* 80, 51-55.

Simpson, R.T., Thoma, F., and Brubaker, J.M. (1985). Chromatin reconstituted from tandemly repeated cloned DNA fragments and core histones: a model system for study of higher order structure. *Cell* 42, 799-808.

Smythe, C., and Newport, J.W. (1991). Systems for the study of nuclear assembly, DNA replication, and nuclear breakdown in *Xenopus laevis* egg extracts. *Methods in cell biology* 35, 449-468.

Soulier, J., Grollet, L., Oksenhendler, E., Cacoub, P., Cazals-Hatem, D., Babinet, P., d'Agay, M.F., Clauvel, J.P., Raphael, M., Degos, L., *et al.* (1995). Kaposi's sarcoma-

associated herpesvirus-like DNA sequences in multicentric Castleman's disease. *Blood* 86, 1276-1280.

Steer, W.M., Abu-Daya, A., Brickwood, S.J., Mumford, K.L., Jordanaires, N., Mitchell, J., Robinson, C., Thorne, A.W., and Guille, M.J. (2003). Xenopus nucleosome assembly protein becomes tissue-restricted during development and can alter the expression of specific genes. *Mech Dev* 120, 1045-1057.

Strahl Bolsinger, S., Hecht, A., Luo, K., and Grunstein, M. (1997). SIR2 and SIR4 interactions differ in core and extended telomeric heterochromatin in yeast. *Genes Dev* 11, 83-93.

Sullivan, S., Sink, D.W., Trout, K.L., Makalowska, I., Taylor, P.M., Baxevanis, A.D., and Landsman, D. (2002). The Histone Database. *Nucleic Acids Res* 30, 341-342.

Sullivan, S.A., Aravind, L., Makalowska, I., Baxevanis, A.D., and Landsman, D. (2000). The histone database: a comprehensive WWW resource for histones and histone fold-containing proteins. *Nucleic Acids Res* 28, 320-322.

Suto, R.K., Clarkson, M.J., Tremethick, D.J., and Luger, K. (2000). Crystal structure of a nucleosome core particle containing the variant histone H2A.Z. *Nat Struct Biol* 7, 1121-1124.

Swedlow, J.R., and Hirano, T. (2003). The making of the mitotic chromosome: modern insights into classical questions. *Mol Cell* 11, 557-569.

Takahashi, T.S., Yiu, P., Chou, M.F., Gygi, S., and Walter, J.C. (2004). Recruitment of Xenopus Scc2 and cohesin to chromatin requires the pre-replication complex. *Nature cell biology* 6, 991-996.

Taniguchi, T., and Takayama, S. (1986). High-order structure of metaphase chromosomes: evidence for a multiple coiling model. *Chromosoma* 93, 511-514.

Tetsuka, T., Higuchi, M., Fukushi, M., Watanabe, A., Takizawa, S., Oie, M., Gejyo, F., and Fujii, M. (2004). Visualization of a functional KSHV episome-maintenance protein LANA in living cells. *Virus genes* 29, 175-182.

Thoma, F., Koller, T., and Klug, A. (1979). Involvement of histone H1 in the organization of the nucleosome and of the salt-dependent superstructures of chromatin. *J Cell Biol* 83, 403-427.

Tong, A.H., Lesage, G., Bader, G.D., Ding, H., Xu, H., Xin, X., Young, J., Berriz, G.F., Brost, R.L., Chang, M., *et al.* (2004). Global mapping of the yeast genetic interaction network. *Science (New York, NY)* 303, 808-813.

Tse, C., and Hansen, J.C. (1997). Hybrid trypsinized nucleosomal arrays: identification of multiple functional roles of the H2A/H2B and H3/H4 N-termini in chromatin fiber compaction. *Biochemistry* 36, 11381-11388.

Tyler, J.K. (2002). Chromatin assembly. *Eur J Biochem* 269, 2268-2274.

Tyler, J.K., Adams, C.R., Chen, S.R., Kobayashi, R., Kamakaka, R.T., and Kadonaga, J.T. (1999). The RCAF complex mediates chromatin assembly during DNA replication and repair. *Nature* 402, 555-560.

Van Holde, K.E. (1988). *Chromatin* (New York, Springer-Verlag).

van Holde, K.E., and Weischet, W.O. (1978). Boundary analysis of sedimentation-velocity experiments with monodisperse and paucidisperse solutes. *Biopolymers* 17, 1387-1403.

van Leeuwen, F., Gafken, P.R., and Gottschling, D.E. (2002). Dot1p modulates silencing in yeast by methylation of the nucleosome core. *Cell* 109, 745-756.

Verreault, A., Kaufman, P.D., Kobayashi, R., and Stillman, B. (1996). Nucleosome assembly by a complex of CAF-1 and acetylated histones H3/H4. *Cell* 87, 95-104.

Viejo-Borbolla, A., Kati, E., Sheldon, J.A., Nathan, K., Mattsson, K., Szekely, L., and Schulz, T.F. (2003). A Domain in the C-terminal region of latency-associated nuclear antigen 1 of Kaposi's sarcoma-associated Herpesvirus affects transcriptional activation and binding to nuclear heterochromatin. *J Virol* 77, 7093-7100.

Walter, J., and Newport, J.W. (1997). Regulation of replicon size in *Xenopus* egg extracts. *Science* (New York, NY) 275, 993-995.

Walter, J.C. (2000). Evidence for sequential action of cdc7 and cdk2 protein kinases during initiation of DNA replication in *Xenopus* egg extracts. *J Biol Chem* 275, 39773-39778.

Walter, P.P., Owen-Hughes, T.A., Cote, J., and Workman, J.L. (1995). Stimulation of transcription factor binding and histone displacement by nucleosome assembly protein 1 and nucleoplasmin requires disruption of the histone octamer. *Mol Cell Biol* 15, 6178-6187.

Wang, H., Zhai, L., Xu, J., Joo, H.Y., Jackson, S., Erdjument-Bromage, H., Tempst, P., Xiong, Y., and Zhang, Y. (2006). Histone H3 and H4 ubiquitylation by the CUL4-DDB-ROC1 ubiquitin ligase facilitates cellular response to DNA damage. *Mol Cell* 22, 383-394.

West, M. H., and Bonner, W. M. (1980). Histone 2A, a heteromorphous family of eight protein species. *Biochemistry* 19, 3238-3245.

White, C.L., Suto, R.K., and Luger, K. (2001). Structure of the yeast nucleosome core particle reveals fundamental changes in internucleosome interactions. *Embo J* 20, 5207-5218.

Witt, O., Albig, W., and Doenecke, D. (1996). Testis-specific expression of a novel human H3 histone gene. *Exp Cell Res* 229, 301-306.

Wong, L.Y., Matchett, G.A., and Wilson, A.C. (2004). Transcriptional activation by the Kaposi's sarcoma-associated herpesvirus latency-associated nuclear antigen is facilitated by an N-terminal chromatin-binding motif. *J Virol* 78, 10074-10085.

Woodcock, C.L., and Dimitrov, S. (2001). Higher-order structure of chromatin and chromosomes. *Curr Opin Genet Dev* 11, 130-135.

Xu, F., Zhang, K., and Grunstein, M. (2005). Acetylation in histone H3 globular domain regulates gene expression in yeast. *Cell* 121, 375-385.

Yates, J.L., Warren, N., and Sugden, B. (1985). Stable replication of plasmids derived from Epstein-Barr virus in various mammalian cells. *Nature* 313, 812-815.

Yoon, H.W., Kim, M.C., Lee, S.Y., Hwang, I., Bahk, J.D., Hong, J.C., Ishimi, Y., and Cho, M.J. (1995). Molecular cloning and functional characterization of a cDNA encoding nucleosome assembly protein 1 (NAP-1) from soybean. *Mol Gen Genet* 249, 465-473.

You, J., Croyle, J.L., Nishimura, A., Ozato, K., and Howley, P.M. (2004). Interaction of the bovine papillomavirus E2 protein with Brd4 tethers the viral DNA to host mitotic chromosomes. *Cell* 117, 349-360.

Zhang, L., Eugeni, E.E., Parthun, M.R., and Freitas, M.A. (2003). Identification of novel histone post-translational modifications by peptide mass fingerprinting. *Chromosoma* 112, 77-86.

Zhu, B., Zheng, Y., Pham, A.D., Mandal, S.S., Erdjument-Bromage, H., Tempst, P., and Reinberg, D. (2005). Monoubiquitination of human histone H2B: the factors involved and their roles in HOX gene regulation. *Mol Cell* 20, 601-611.